NSF/CEE-82053

UILU-ENG-82-2011

CIVIL ENGINEERING STUDIES

STRUCTURAL RESEARCH SERIES NO. 501

PB83-143917

SEISMIC ENERGY ABSORPTION IN SIMPLE STRUCTURES

by

T. F. ZAHRAH

and

W. J. HALL

A Technical Report of
Research Supported by the
NATIONAL SCIENCE FOUNDATION
under Grant Nos. ENV 77-07190
and
PFR 80-02582

DEPARTMENT OF CIVIL ENGINEERING
UNIVERSITY OF ILLINOIS
AT URBANA-CHAMPAIGN
URBANA, ILLINOIS

JULY 1982

INFORMATION RESOURCES
NATIONAL SCIENCE FOUNDATION

50272-101

REPORT DOCUMENTATION PAGE	1. REPORT NO. NSF/CEE-82053	2.	3. Recipient's Accession No. PB83 143917
4. Title and Subtitle: Seismic Energy Absorption in Simple Structures			5. Report Date: July 1982
			6.
7. Author(s): T.F. Zahrah, W.J. Hall			8. Performing Organization Rept. No.
9. Performing Organization Name and Address: University of Illinois at Urbana-Champaign, Department of Civil Engineering, Urbana, IL 61801			10. Project/Task/Work Unit No.
			11. Contract(C) or Grant(G) No. (C) (G) ENV7707190 PFR8002582
12. Sponsoring Organization Name and Address: Directorate for Engineering (ENG), National Science Foundation, 1800 G Street, N.W., Washington, DC 20550			13. Type of Report & Period Covered
			14.

15. Supplementary Notes: Submitted by: Communications Program (OPRM), National Science Foundation, Washington, DC 20550

16. Abstract (Limit: 200 words)

The energy absorption in, and the inelastic behavior of, simple structures during strong earthquake excitation are investigated to determine each structure's response to various types of ground motion and to identify the factors that influence structural deformation and damage. The investigation focuses on the total amount of energy imparted to a structure, the amount of energy dissipated in the structure by inelastic deformation and by damping, the displacement ductility the structure experiences, and the number of yield excursions and reversal the structure goes through during the excitation. The effects of duration of ground motion on earthquake response are also investigated and, based on the amount of energy imparted to structures, a possible effective motion criterion is defined. Two methods of scaling ground motion records for equal damage potential are examined. The inverse of the scale factors may be used as reduction factors to modify elastic response spectra for design purposes.

17. Document Analysis a. Descriptors

Earthquakes
Earthquake resistant structures
Dynamic response
Ductility
Damping
Energy absorption

b. Identifiers/Open-Ended Terms

Ground motion
Response spectra
Energy spectra
W.J. Hall, /PI

c. COSATI Field/Group

18. Availability Statement	19. Security Class (This Report)	21. No. of Pages
NTIS	20. Security Class (This Page)	22. Price

SEISMIC ENERGY ABSORPTION IN SIMPLE STRUCTURES

by

TONY F. ZAHRAH

and

WILLIAM J. HALL

A Report on a Research Project Sponsored by the

NATIONAL SCIENCE FOUNDATION

Research Grants Nos. ENV 77-07190 and PFR 80-02582

UNIVERSITY OF ILLINOIS

Urbana, Illinois

July 1982

ACKNOWLEDGMENT

This report was prepared as a doctoral dissertation by Mr. Tony F. Zahrah and was submitted to the Graduate College of the University of Illinois at Urbana-Champaign in partial fulfillment of the requirements for the degree of Doctor of Philosophy in Civil Engineering. The thesis was completed under the supervision of Professor William J. Hall.

The investigation was a part of a research program sponsored by the National Science Foundation under Grants ENV 77-07190, Engineering Design For Natural Hazards and PFR 80-02852, Earthquake Engineering Design Investigations. Any opinions, findings, and conclusions or recommendations expressed in this publication are those of the authors and do not necessarily reflect the views of the National Science Foundation.

The numerical results presented in this report were obtained with the use of the CDC Cyber 175; most of the figures were prepared using the Zeta 1453B plotting device. These facilities are supported by the Computing Services Office (CSO) of the University of Illinois. Partial computer service funding was provided by the Research Board of the Graduate College of the University of Illinois.

The authors wish to thank Professors D. A. W. Pecknold, W. L. Gamble, J. E. Stallmeyer, and D. E. Carlson for their constructive comments. The authors are also grateful for the assistance of S. Sengenberger, P. Griffis and K. Tengler in typing this manuscript.

TABLE OF CONTENTS

CHAPTER Page

LIST OF TABLES

TABLE Page

TABLE Page

LIST OF FIGURES

FIGURE Page

FIGURE Page

FIGURE Page

FIGURE Page

FIGURE Page

FIGURE Page

FIGURE Page

FIGURE Page

FIGURE Page

CHAPTER 1

INTRODUCTION

1.1 Background and Motivation

When a structure is subjected to earthquake ground motion, energy is imparted to it. The energy input is dissipated in part by damping and, in part, by yielding or inelastic deformations in all the components of the structure (structural and nonstructural). Well designed and well constructed buildings should be able to absorb and dissipate the energy imparted to them with no loss of life and with the least possible amount of damage.

The amount of energy imparted to a structure and the manner by which it is dissipated depends on several factors. Some of these factors are related to the characteristics of the ground motion, such as its amplitude and frequency content, and others are related to the properties of the structure, such as its natural period, damping and resistance (or load-deformation) properties.

A parameter widely employed to characterize the severity of ground shaking that may occur at a given site is the peak ground acceleration. Although it is a relatively easy quantity to estimate, peak gound acceleration is a poor measure of the amount of energy imparted to a structure and of the damage potential of an earthquake ground motion (30). Observations of earthquake damage in areas where large amplitude, high frequency components of acceleration were recorded suggest that damage does not correlate well with peak ground acceleration (15). These observations have led to the concept of effective acceleration which may be defined as the acceleration that is most closely related to the damage potential of an earthquake. The effective acceleration is smaller than the recorded peak ground acceleration and is, in part, based on the observation that a single high-frequency spike of

acceleration normally contributes less to structural deformation and damage than repetitive shaking with somewhat less severe ground shaking (43).

The structural response parameter most widely employed to evaluate the performance of structures subjected to ground motion is the displacement ductility which may be simply defined as the ratio of the maximum to yield displacements. The displacement ductility, however, does not account for the cumulative damage that may occur as a result of reversed inelastic deformations. The focusing on the maximum displacement ultimately ignores any relationship that exists between the time-history of the response and the ground motion.

Recently major efforts are being devoted to better understand the structural and ground motion parameters that influence the earthquake response of engineering structures. This particular study complements, and parallels to some small degree, a current research project sponsored by the U.S. Nuclear Regulatory Commission through Woodward-Clyde Consultants and Structural Mechanics Associates (54).

The purpose of this study is to investigate the nonlinear response of simple structures and the damage potential of an earthquake ground motion as measured in terms of the amount of energy imparted to a structure, the amount of energy dissipated in it by inelastic deformations and by damping, the displacement ductility of the structure, and the number of yield excursions and reversals it goes through during the excitation. The effects of duration of ground motion on earthquake response also are investigated, and based on the amount of energy imparted to structures a possible effective motion criterion is defined.

1.2 Previous Work

Lateral design forces obtained from an elastic response spectrum for strong earthquake ground motion are, in general, much higher than those specified by code regulations (3,61). Obviously then during severe earthquake ground motion part of the energy imparted to a structure is dissipated by inelastic deformations. This phenomenon has been recognized for some time, and the inelastic behavior of, and energy absorption in, structures subjected to strong earthquake ground motion have been studied to some extent by various investigators over the years.

One of the earliest studies on energy approaches to the aseismic design of structures was undertaken by Housner (24) in 1956. This limit design approach was based on (a) the amount of energy fed to a structure, and (b) the ability of the structure to dissipate that energy. The energy imparted to a structure was estimated as being equal to the product of one half the mass of the structure times the square of the maximum velocity of the mass relative to the base. The latter value is obtained from the velocity spectrum (with the appropriate damping value) for the design ground motion and corresponds to the fundamental frequency of the structure. The ability of the structure to dissipate energy is based on its resistance-deformation properties. With this approach the structure should be designed such that it will behave elastically during a moderate earthquake, and should have sufficient energy absorbing capacity against collapse during a strong earthquake.

In 1960 Blume (8,9) introduced a procedure called the reserve energy technique. This procedure utilizes the energy absorption capacity of all building elements in a structure, as represented by the lateral force-deflection diagram of the whole structure, and takes into account the change in the natural period, damping and permanent set. The method provides

a means of reconciling the energy capacity of a structure with the energy demand.

Berg (6,7) studied to some extent the inelastic deformation of, and the energy dissipation in, single-degree-of-freedom structures. It was pointed out that a decrease in yield level will usually not increase the maximum displacement unless the yield level drops below some threshold value, a result found by Veletsos and Newmark (62). At the same time, a decrease in yield level will usually decrease the amount of energy imparted to the structure. The design procedure that was suggested by Berg for simple structures is essentially the same as that of Housner's plus an additional requirement that the restoring force at yield level be at least equal to 5 percent of the weight of the structure in order to avoid excessive drift.

Further investigation of the energy absorption in simple structures was undertaken by Jennings (29) in 1965. The study was conducted on a class of yielding structures, represented by the Ramberg-Osgood structural model, which includes the linear, the elastoplastic and the bilinear hysteretic structures. The response of this class of structures to a set of eight artificial earthquakes was studied. Among the calculated response quantities were the total energy imparted to a structure normalized by its elastic strain energy at the yield point and the energy dissipation ratio (the amount of energy dissipated by viscous damping or the amount of energy dissipated by yielding over the total amount of energy dissipated in the structure). The total energy imparted to a yielding structure was found to be approximately the same as that imparted to a linear structure with the same natural period. As the strength of the earthquake, as characterized by the root-mean square acceleration (27), increased the proportion of energy dissipated by yielding was noted to increase.

More recently McKevitt et al. (34) investigated the energy absorption in single-degree-of-freedom systems, and Nagahashi (37) examined the effects of ground motion duration on the earthquake response of simple structures. Both studies examined in a limited way the amount of energy imparted to a structure and the amount of energy dissipated in it by yielding.

The inelastic behavior and the energy absorption capacity of multi-degree-of-freedom structures also were investigated to some degree: Penzien (45) and Veletsos and Vann (63) have undertaken studies on elastoplastic shear-beam type models with several degrees of freedom. Goel (20) examined the behavior of unbraced, moment-resisting frames. Workman (65), and Goel and Hanson (21) examined the behavior of multistory braced frame structures. The ductility demand and energy absorption by the various members of a frame were examined. Montgomery and Hall (35) studied to some degree the behavior of low-rise steel buildings during earthquake excitation and presented some guidelines for the design of this type of structures.

The most recent study on the damage potential of an earthquake ground motion and the nonlinear behavior of structures was undertaken by Structural Mechanics Associates (54). In the latter study, the effects of duration of ground motion and peak ground acceleration on nonlinear behavior of nuclear power plant safety category structures, and a new technique for modifying elastic response spectra to design response spectra with an acceptable level of inelastic deformation were investigated. The effective duration of ground motion T_D, or the duration of the record which causes peak structural response, was found to be characterized best by

$$T_D = t_{0.75} - t_{0.05}$$

where $t_{0.05}$ and $t_{0.75}$ correspond respectively to the time at which 5 percent

and 75 percent of the energy of the accelerogram is fed to the structure. The total energy of an accelerogram is assumed, as suggested by Arias (4), to be proportional to the integral $\int_0^{t_f} a(t)^2\,dt$ where a(t) is the ground acceleration at time t and t_f is the total duration of the record. It was found that short duration records, $T_D < 2.5$ sec, have a narrow frequency content but can greatly influence the response of structures with natural frequencies equal to about 1.4 to 2.0 times the predominant frequency of the record. Long duration records, $T_D > 9.0$ sec, have a broad frequency content response spectra. On the other hand peak ground acceleration was found to be a poor measure of the damage potential of an earthquake. A more appropriate acceleration A_D' to anchor a design response spectrum for a consistent damage potential was defined by Kennedy (30) as

$$A_D' = 3.5 * \text{rms} * \sqrt{T_D/20}$$

where rms, the root-mean square acceleration (27), is given by

$$\text{rms} = \sqrt{\frac{1}{T_D}\int_{t_0}^{t_0 + T_D} a(t)^2\,dt}$$

In the SMA study a hysteresis model, similar to the Takeda model (55) except for shear pinching and strength degradation, was used to model the type of structures considered, and the displacement ductility was chosen as an appropriate measure of damage. All ground motion records were first scaled to obtain the same elastic spectral acceleration at the structural model elastic period. The resulting records were then multiplied by a scale factor in order for a given structure to reach a specified displacement ductility. The scale factors were found to depend on the shape of the elastic response spectra, the duration of strong motion and the target displacement ductility. For

structures with frequencies equal to or less than the predominant frequency of the ground motion record, the short duration records must be scaled to higher levels than the long duration records for structures to achieve the same level of nonlinear response.

1.3 Purpose and Outline of the Study

In this study the energy absorption in, and the inelastic behavior of, simple structures during strong earthquake excitation are investigated. The purpose of this investigation is to better identify than at present the factors that influence structural deformation and damage, and to evaluate the performance of structures and the damage potential of various ground motions.

Attention is given to the time-history response in addition to the maximum response quantities. The investigation focuses on (a) the amount of energy imparted to a structure, (b) the amount of energy dissipated in the structure by inelastic deformations (or hysteretic energy), (c) the amount of energy dissipated in it by damping (or damping energy), (d) the duration of strong motion and its effect on damage, and (e) the number of yield excursions and reversals a structure undergoes during the entire duration of ground motion.

In Chapter 2 a brief review of the experimental work on the hysteretic behavior of structural steel systems is presented with the purpose of defining the resistance functions employed in this study. A discussion of the damping values available from measurements and recommended for design is also included in this chapter.

The analytical procedure used for the time-history analysis is described in Chapter 3. A definition for the various energy terms and the manner in which they are calculated are presented.

In chapter 4 the input ground motion records used in this investigation, and the energy absorption in, and the inelastic behavior of, single-degree-of-freedom structures are examined. The results are discussed, and observations regarding the influence of various parameters on the structural response are made. Response spectra and energy spectra for the various ground motions are presented, and an effective motion corresponding to the free-field ground motion is defined. In this case the definition is based on the amount of energy imparted to structures when they are subjected to the free-field ground motion.

Two methods of scaling ground motion records for equal damage potential are described in Chapter 5. One method is based on the assumption that equal displacement ductility will result in equal damage. The other is based on the assumption that equal energy dissipation by inelastic deformations will result in equal damage. The results are discussed, and then employed to modify elastic response spectra for design purposes.

In Chapter 6 the earthquake response of two-story, shear-beam type structures is considered. The mass and stiffness of the structures considered are varied, and the energy dissipated at each story level and the associated drift (or maximum relative displacement) are investigated. A modal analysis employing modified (inelastic) response spectrum of the structures considered is undertaken and the results are reported along with the results of the time-history analyses for comparison purposes.

Chapter 7 contains a summary of the major observations of the study.

1.4 Notation

The symbols used in the text are defined where they are first introduced. For reference purposes they are also defined here. A dot above a symbol indicates one differentiation with respect to time. A Greek delta, Δ ,

prefixed to a symbol indicates an incremental quantity.

A_g = maximum ground acceleration

C = damping coefficient for a single-degree-of-freedom-structure

$[C]$ = damping matrix for a multi-degree-of-freedom structure

D_n = spectral displacement in the n-th mode of vibration

E = modulus of elasticity of steel

E_D^* = total energy dissipated by damping in a structure or total damping energy

E_D = damping energy per unit mass dissipated in a structure

E_H^* = total energy dissipated by yielding in a structure or total hysteretic energy

E_H = hysteretic energy per unit mass dissipated in a structure

E_I^* = total energy imparted to a structure or total energy input

E_I = energy input per unit mass imparted to a structure

E_K^* = total kinetic energy stored in a structure

E_K = kinetic energy per unit mass stored in a structure

E_S^* = total strain energy stored in a structure

E_S = strain energy per unit mass stored in a structure

f = frequency of vibration in cycles per second for a single-degree-of-freedom structure

F = scale factor

F_d = scale factor based on equal displacement ductility

F_e = scale factor based on equal hysteretic energy

$[F]$ = resisting-force vector due to structural stiffness

I = moment of inertia

K = initial or elastic stiffness for a single-degree-of-freedom structure

K_S = strain-hardening stiffness of a bilinear load-deformation resistance relationship

$[K(t)]$ = tangent stiffness matrix at time t for a multi-degree-of-freedom structure

$[K^*(t)]$ = pseudostatic stiffness matrix at time t for a multi-degree-of-freedom structure

L = length of a member

M = mass of a single-degree-of-freedom structure

M_Y = yield moment capacity of a member

$[M]$ = mass matrix for a multi-degree-of-freedom structure

N = equivalent number of yield cycles

$\{P\}$ = residual load vector

$\{Q(t)\}$ = pseudostatic load vector at time t

R^* = total resistance or restoring force for a single-degree-of-freedom structure

R = resistance or restoring force per unit mass for a single-degree-of-freedom structure

R_Y = yield resistance per unit mass for a single-degree-of-freedom structure

$\{R(t)\}$ = residual load vector at time t

S = scale factor

S_a = spectral acceleration

S_d = spectral displacement

S_v = spectral velocity

$t_{e_{0.05}}$ = time by which 5 percent of the energy imparted to a structure is dissipated

$t_{e_{0.75}}$ = time by which 75 percent of the energy imparted to a structure is dissipated

$t_{e_{0.90}}$ = time by which 90 percent of the energy imparted to a structure is dissipated

T = period of vibration for a single-degree-of-freedom structure

T_e = effective duration of ground motion in seconds

U = relative displacement of the mass with respect to the ground for a single-degree-of-freedom structure

$\{U(t)\}$ = story displacement vector at time t

U_e = elastic or recoverable relative displacement for a single-degree-of-freedom structure

U_m = maximum relative displacement of the mass relative to the ground for a single-degree-of-freedom structure

U_Y = yield displacement for a single-degree-of-freedom structure

Y = ground displacement

α = constant

β = percent of critical damping for a single-degree-of-freedom structure

β_n = percent of critical damping in the n-th mode of vibration for a multi-degree-of-freedom structure

ω = undamped circular frequency for a single-degree-of-freedom structure

ω_n = undamped circular frequency of the n-th mode of vibration for a multi-degree-of-freedom structure

μ = displacement ductility

Δ_Y = yield displacement for a structural member

$\{1\}$ = unit vector

$\{\ \}^T$ = vector transposed

CHAPTER 2

BEHAVIOR OF STRUCTURES UNDER CYCLIC LOADING AND STRUCTURAL MODELS USED IN THIS STUDY

2.1 Introduction

In the past twenty years, studies to identify the several types of hysteretic loops governing the behavior of real structures under severe dynamic motion were undertaken by various investigators (13,49). The experimental studies included tests on materials, members and structural subassemblages. In addition tests have been conducted on real structures (22), and measurements have been obtained during actual earthquakes from instrumented buildings (5). While the amount of information has increased greatly in the last ten years, the nonlinear response of actual buildings to a severe earthquake is not yet well understood.

This chapter contains a brief review of the experimental work on the hysteretic behavior of structural steel systems as well as a description of the analytical models used in this study. A summary of damping values obtained from actual measurements and of values recommended for design purposes also is included.

2.2 Behavior of Structural Steel Systems under Cyclic Loading

Results from experiments on the material behavior of structural steel under cyclic loading illustrate the excellent properties of this material which are particularly relevant to earthquake resistant design. As shown in Fig. 2.1, structural steel material exhibits stable hysteretic loops and large ductility. For a structure to exhibit good energy dissipation characteristics, a ductile behavior is needed in the members, joints and structural frames.

Almuti and Hanson (2) studied to some extent the behavior of a structural steel beam in a frame under large cyclic deformation. The beams tested showed very little deterioration and the hysteretic loops remained constant in shape after a large number of load reversals and a relatively large displacement ductility, up to about 5.7.

Under severe earthquake motion connections might be subjected to a large number of load reversals into the inelastic range. While the failure of one connection is not likely to be critical for the behavior of the entire structure, properly designed beam-column joints are essential for the ductile behavior of a structural frame. Popov and Pinkney (48) investigated the behavior of connections under cyclically reversed loading. The hysteretic loops for bolted connections were unique in shape as shown in Fig. 2.2, and clearly show the slippage that takes place under reversed loading. Similar tests on wide-flange section cantilever beams connected to a column stub fixed to a reaction frame were undertaken (49). Results from these experiments show stable load-deflection hysteretic loops for welded connections that are very much like the hysteretic curves for the material itself, Fig. 2.3. The hysteretic loops are highly reproducible during repetitive load applications and, in the absence of slip, can be modeled best by the Ramberg-Osgood curves. Most of the tested specimens failed by local buckling of the flanges at loads higher than those predicted on the basis of the plastic yield moment. These tests show that properly designed and fabricated steel connections have the ability to withstand repeated and reversed loading with little or no deterioration , and can be counted upon to absorb and dissipate a large amount of energy.

The behavior of several types of steel frames under cyclic loading has also been investigated to some extent. Carpenter and Lu (13) studied the behavior of moment-resisting frames under relatively high vertical loads and lateral cyclic loading. As illustrated in Fig. 2.4, in general this type of steel frame exhibited an excellent ductile behavior and good energy dissipation characteristic provided ductile connections were achieved. In the absence of the P-delta effect which is causing the negative slope in the load deformation curve, Fig. 2.4b, the hysteretic loops are stable and the load carrying capacity of the frame increases with higher lateral loads as a result of strain hardening of the steel, Fig. 2.4a.

The behavior of X-braced frames subjected to cyclic lateral loading is illustrated in Fig. 2.5. The hysteretic diagram shows a good deal of pinching and represents the behavior of braces that act only in tension. This type of braced frame has poor energy absorption and dissipation characteristics when compared with moment-resisting type steel frames. The cyclic behavior of K-braced frames is illustrated in Fig. 2.6. The hysteretic loops show some pinching but they are stable.

Finally a new bracing system has been developed (52) in order to balance between strength, stiffness, and energy dissipation. The bracing members of this eccentrically braced frame were designed so that they would remain elastic at all times and, thus, energy is dissipated through cyclic shear deformation in the girders. The hysteretic loops for this braced frame are repetetive and do not exhibit any pinching effect like the other types of braced frames, Fig. 2.7. This frame has a sound energy dissipation capability under strong ground shaking but the local floor damage might be quite severe.

2.3 Structural Models Considered

2.3.1 Single-Degree-of-Freedom Structures -- Before the behavior of a sructure can be examined analytically, it is necessary to establish an appropriate model for the force-displacement relationship either for each element of the structure or for the structure as a whole. In general the model used is based on the results of experimental investigations of the material, members and structural assemblages. The accuracy of the calculated response quantities depends on how closely the model approximates the behavior of the actual structure and on the solution technique used to solve the governing equations of motion. The solution procedure employed in this investigation is presented in the next chapter. The structural models selected were intended to satisfy the following criteria: (a) they should approximate the overall behavior of the structural system rather than that of individual members. This criterium is based on the assumption that in general the failure of one member will not affect the response of the structure as a whole; (b) the models should be capable of approximating the overall behavior of a relatively broad range of structures; and (c) they should be relatively simple to use in the proposed method of solving the equations of motion.

Based on the above, the nonlinear models employed in this study have (a) an elastoplastic hysteretic force-displacement relationship, and (b) a bilinear relationship. The second slope in the bilinear model accounts for the strain-hardening that might occur in structural steel frames. It is herein taken equal to 2 or 5 percent of the first or initial slope. The bilinear model is substituted for the curvilinear model because the bilinear one is easier to use, although a curvilinear model, as for example the Ramberg-Osgood model, more closely approximates the behavior of the actual structural system. Both elastoplastic and bilinear models represent a

ductile, non-deteriorating structural system. From the discussion in the previous section it is apparent that these models cover a fairly wide range of steel structures. Besides these models have been widely used in the past, and results from this study may be compared with those from previous investigations (51,63). The two nonlinear models are shown in Fig. 2.8.

2.3.2 Multi-Degree-of-Freedom Structures -- While a single-degree-of-freedom system gives an estimate of the total energy absorbed and dissipated in a structure, a multi-degree-of-freedom system gives an insight on how the absorbed energy is dissipated at different story levels, and the effect of stiffness and mass distributions on the ductility and energy dissipation in the structure. Only shear-beam type structures with two degrees of freedom are considered in this study. The member behavior is modeled first by an elastic and then by an elastoplastic bending moment-end rotation relationship. This model has been widely used in the dynamic analysis of multi-degree-of-freedom structures (45,63).

2.4 Structural Damping

During earthquake excitation the energy losses include energy feedback into the ground, and energy dissipation by damping and inelastic deformation in the structure. The energy fedback into the ground is in part lost by radiation of waves from the base of the structure into the surrounding soil, and in part transformed into heat due to internal damping in the ground-- a phenomenon termed material damping. The energy lost by radiation of waves is called radiation or spatial damping and depends on such factors as the amplitude and frequency content of the earthquake excitation, the site conditions and the configuration of the structure. It is best accounted for in a dynamic analysis, whenever pertinent, by using a soil-structure

interaction technique. The interaction effects are especially important for massive, lightly damped structures.

The energy absorbed by a structure is dissipated in part by inelastic deformation in various components of the structure (structural and non-structural), and in part by internal damping in the structure. In the former case the energy dissipated by inelastic deformation is incorporated in a dynamic analysis by the use of a nonlinear model which best approximates the actual behavior of the structure under study. The latter type of energy dissipation is called structural damping and depends on the structural material, the type and condition of the structure, the level of stress, and the intensity and type of the ground motion. The structural damping is mainly due to friction at the grain boundaries in most structural materials. For analysis purposes it is assumed to be viscous in nature (velocity dependent) and is included in a structural model as a number of dashpots in parallel with the flexible elements of the structure. The damping value is generally expressed as a percentage of the critical damping coefficient which is defined as the least damping value required to prevent oscillation of the system.

Dynamic testing of full-scale structures provides an estimate of the damping values to be used in the seismic analysis of various structural systems. Portillo and Ang (50) summarized damping values from tests on full-scale reinforced concrete structures. The average damping values ranged from 1.2 percent of critical under man-excited vibrations to 3.5 percent under natural earthquakes to 5.7 percent under blast type loading. In each category the coefficient of variation of the data was on the order of 50 percent.

Hart *et al.* (22) summarized the data available from tests on full-scale nuclear reactor facilities. The damping values ranged from one to ten percent of critical depending on the type of structure, and the level and type of

excitation.

Another source of information regarding the damping characteristics of engineering structures is measurements obtained during actual earthquakes. The 1971 San Fernando earthquake resulted in numerous records for the response of a variety of structures. Based on these measurements, Hart and Vasudevan (23) provided estimates of the damping factors for a number of reinforced concrete and steel buildings located throughout the Los Angeles area. The peak ground acceleration recorded in the basement of these buildings ranged from 0.10g to 0.27g, and the estimated damping ratio for the fundamental mode ranged from 1.9 percent of critical to 16.4 percent for reinforced concrete, and from 3.2 to 11.3 percent of critical for steel structures. The corresponding mean values for steel and concrete are 10.4 and 12.2 percent of critical, respectively. The highest damping values were obtained in the buildings which experienced the highest intensity of ground motion. The higher mode damping values showed no appreciable difference in magnitude from those of the fundamental mode.

Newmark and Hall (41) recommended damping values to be employed in the design of structures. These values depend on the stress level, and the type and condition of the structure and are shown in Table 2.1. They range from 2 up to 7 percent of critical for welded steel structures and from 3 up to 10 percent for reinforced concrete structures.

From the above brief summary of recommended and calculated damping values, it is clear that a great deal of judgement is involved in the choice of a damping value to be used in a dynamic analysis. In this study damping values of 2, 5 and 10 percent of critical are used with the elastic and the elastoplastic models. The intermediate value of 5 percent was arbitrarily chosen to be used with the bilinear and the multi-degree-of-freedom models.

CHAPTER 3

EQUATIONS OF MOTION AND ENERGY EXPRESSIONS

3.1 Introduction

This chapter contains a description of the equations of motion governing the dynamic behavior of simple structures and the numerical integration procedure used to solve these equations. It is divided into two major parts: the first part deals with single-degree-of-freedom structures and the second deals with multi-degree-of-freedom structures.

Also included in this chapter are a definition and a detailed description of the various energy terms, namely, energy input, kinetic energy, strain energy, hysteretic energy (or energy dissipated by inelastic deformations) and damping energy (or energy dissipated by viscous damping). In each case the equations needed to compute the numerical value of the item are derived.

3.2 Single-Degree-of-Freedom Structures

3.2.1 Equation of Motion -- The equation of motion for a single-degree-of-freedom structure subjected to an earthquake ground excitation, Fig. 3.1, can be written as follows:

$$M\ddot{U}(t) + C\dot{U}(t) + R^{*}(U) = -M\ddot{Y}(t) \qquad (3.1)$$

where M is the mass of the structure, C is its damping coefficient, $\ddot{Y}(t)$ is the ground acceleration, and U is the relative displacement of the mass with respect to the ground. The dots represent differentiation with respect to time. $R^{*}(U)$ is the restoring force for the structure; it is proportional to the relative displacement U for a linear elastic model and varies according to the inelastic behavior of the material under cyclic loading conditions for a

nonlinear model.

The undamped circular frequency ω and the fraction of critical damping β are given by

$$\omega = \sqrt{\frac{K}{M}} \tag{3.2}$$

and

$$\beta = \frac{C}{2\omega M} = \frac{C}{\sqrt{2KM}} \tag{3.3}$$

where K is the initial elastic stiffness of the load-deformation model. The circular frequency is related to the natural frequency f and the period T as follows:

$$\omega = 2\pi f = \frac{2\pi}{T} \tag{3.4}$$

The fraction of critical damping β is assumed herein to be constant during the entire ground motion for linear as well as nonlinear models.

The equation of motion, Eq. 3.1, may be rewritten using Eqs. 3.2 and 3.3 as

$$\ddot{U}(t) + 2\beta\omega \dot{U}(t) + R(U) = -\ddot{Y}(t) \tag{3.5}$$

where R(U) represents the resistance per unit mass of the structure. It is equal to ω^2 U for a linear elastic model.

3.2.2 Energy Expressions -- When a structure is subjected to a base excitation, energy is imparted to it. During the ground motion, part of the absorbed energy is stored temporarily in the structure in the form of kinetic and strain energy, and the rest is dissipated by damping and inelastic deformation in all the components of the structure (structural and non structural). Ultimately, all the energy imparted to a structure should be

dissipated. Accordingly one may assume that the degree of damage, as represented by the maximum deformation and the number of yield excursions, sustained by a structure depends to at least some major extent on the amount of energy imparted to that structure. In the following, the equations needed to calculate the various energy quantities are derived.

For a single-degree-of-freedom structure with a fixed-base and subjected to a horizontal force of magnitude $- M \ddot{Y}(t)$, Fig. 3.2, the governing equation of motion is that given by Eq. 3.1. The energy imparted to that structure E_I^*, assuming it is initially at rest, is given by

$$E_I^* = - \int_0^U M \ddot{Y}(t) \, dU = -M \int_0^U \ddot{Y}(t) \, dU \tag{3.6}$$

The energy absorbed in the structure by the various behavioral mechanisms must be equal to the energy imparted to it. Integration of the differential equation of motion, Eq. 3.1, with respect to the displacement U yields

$$E_I^* = \int_0^U M \ddot{U}(t) \, dU + \int_0^U C \dot{U}(t) \, dU + \int_0^U R^*(U) \, dU \tag{3.7}$$

As can be seen from Eq. 3.5 for a single-degree-of-freedom oscillator, once the force-displacement relationship, damping and input ground motion are specified, its displacement-, velocity- and acceleration-time histories can be calculated independently of the values of its mass. It follows then that the value of the integral $\int_0^U \ddot{Y}(t) \, dU$ also is independent of the mass of the oscillator and is equal to a constant for a given oscillator subjected to ground excitation. As a result, the ratio E_I^* / M or the energy input per unit mass E_I, rather than the total energy input E_I^*, may be employed as a characteristic of a single-degree-of-freedom structure. Hereafter, unless otherwise mentioned, the term energy input refers to the <u>energy input per unit mass</u>. The same holds for the other energy quantities, namely, the kinetic

energy, the strain energy, the damping energy and the hysteretic energy, as defined later, refer to these quantities per unit mass of the structure.

The energy input to the structure E_I may be redefined, from Eq. 3.6, by

$$E_I = -\int_0^{U} \ddot{Y}(t)\, dU \tag{3.8}$$

and likewise Eq. 3.7 can be written as

$$E_I = \int_0^{U} \ddot{U}(t)\, dU + 2\beta\omega \int_0^{U} \dot{U}(t)\, dU + \int_0^{U} R(U)\, dU \tag{3.9}$$

In order to simplify the numerical integration, the integrals in Eq. 3.9 can be taken with respect to time by using the relationship $dU = \dot{U}\, dt$,

$$E_I = \int_0^{t} \ddot{U}(t)\, \dot{U}(t)\, dt + 2\beta\omega \int_0^{t} \dot{U}(t)^2\, dt + \int_0^{t} R(U)\, \dot{U}(t)\, dt \tag{3.10}$$

and Eq. 3.8 yields

$$E_I = -\int_0^{t} \ddot{Y}(t)\, \dot{U}(t)\, dt \tag{3.11}$$

The first term on the right hand side of Eq. 3.10 represents the kinetic energy E_K of the structure considered,

$$E_K = \int_0^{t} \ddot{U}(t)\, \dot{U}(t)\, dt = \frac{1}{2}\left(\dot{U}(t)^2 - \dot{U}(0)^2\right) \tag{3.12}$$

where $\dot{U}(t)$ is the relative velocity of the structure at time t, and $\dot{U}(0)$ is its initial velocity. Since the structure is initially at rest, $\dot{U}(0)=0$. If the integration is carried long enough, the final velocity of the structure becomes vanishingly small. In the present study the integration is carried for the duration of the ground motion plus a time equal to one half the period of free vibration of the structure. At this time the relative velocity is, in general, small and the kinetic energy may be considered negligible when

compared to the other energy quantities.

The second term on the right hand side of Eq. 3.10 represents the damping energy E_D or the energy dissipated by viscous damping,

$$E_D = 2\beta\omega \int_0^t \dot{U}(t)^2 \, dt \tag{3.13}$$

The third term represents the sum of the hysteretic energy E_H or the energy dissipated by inelastic deformations from the onset of the base motion until time t, plus the strain energy E_S of the structure at that time,

$$E_H + E_S = \int_0^t R(U) \, \dot{U}(t) \, dt \tag{3.14}$$

The equation for the energy input E_I may be cast in yet another form which can aid with a physical interpretation. Integration by parts of Eq. 3.11 yields

$$E_I = \left(\dot{U}(0) \, \dot{Y}(0) - \dot{U}(t) \, \dot{Y}(t) \right) + \int_0^t \dot{Y}(t) \, \ddot{U}(t) \, dt \tag{3.15}$$

Since the initial and final ground velocities are zero, $\dot{Y}(0) = \dot{Y}(t_f) = 0$, the energy input E_I at the end of the motion is given by

$$E_I = \int_0^{t_f} \dot{Y}(t) \, \ddot{U}(t) \, dt \tag{3.16}$$

For an undamped structure, the relative acceleration $\ddot{U}(t)$ is given by

$$\ddot{U}(t) = -\ddot{Y}(t) - R(U) \tag{3.17}$$

Substitution of the value of $\ddot{U}(t)$ in Eq. 3.16 yields

$$E_I = - \int_0^{t_f} R(U) \, \dot{Y}(t) \, dt = - \frac{1}{M} \int_0^{t_f} R^*(U) \, \dot{Y}(t) \, dt \tag{3.18}$$

In the form of Eq. 3.18, the energy input at time $t = t_f$ may be interpreted as

the integral over time (from the outset of the base motion) of the product of the resistance R^* (which is equivalent to the base shear) and the ground velocity divided by the mass of the structure. The same equation holds for a damped structure provided the force, $C\dot{U}$, in the dashpot is added to the value of the resistance, R^*.

The equation of motion and the energy equations derived above may be used to calculate the response quantities of interest for a structure subjected to ground excitation. Once the results are obtained, the response quantities for a structure with similar properties (natural frequency, damping and displacement ductility) subjected to the same ground motion scaled by a certain factor can be obtained from those already available. Two special cases that will be used later in this study are considered. For a linear elastic structure, the restoring force R^* is equal to the product of the stiffness, K, and the displacement, U. The equation of motion ,Eq. 3.1, becomes

$$\ddot{U}(t) + 2\beta\omega\,\dot{U}(t) + \omega^2\,U(t) = -\ddot{Y}(t) \tag{3.19}$$

and Eq. 3.10 yields

$$E_I = \frac{1}{2}\,\dot{U}(t)^2 + 2\beta\omega \int_0^t \dot{U}(t)^2\,dt + \frac{1}{2}\,\omega^2\,U(t)^2 \tag{3.20}$$

From the ordinary differential equation, Eq. 3.19, it can be seen that the relative displacement, velocity and acceleration are directly proportional to the ground motion given by $\ddot{Y}(t)$; i.e., if the input ground motion is scaled by a factor S, the response quantities U, $\dot{U}$ and $\ddot{U}$ will be multiplied by the same factor. The energy input, given by Eq. 3.20, is proportional to the square of the relative displacement and velocity, and as a result it will be multiplied by the square of the scale factor of the ground motion. The above observation

is strictly valid for a linear elastic system to which Eq. 3.19 applies.

In a similar manner, for a nonlinear structural model, as for example the type used in this study, Eq. 3.5 may be normalized by U_Y, the yield displacement of the model,

$$\frac{\ddot{U}(t)}{U_Y} + 2\beta\omega \frac{\dot{U}(t)}{U_Y} + \frac{1}{U_Y} R(U) = - \frac{\ddot{Y}(t)}{U_Y} \tag{3.21}$$

From the above equation, it is apparent that if the input ground motion and the yield displacement are multiplied by the same factor, the right hand side of the equation remains constant. It follows then that the value of the response quantity U_m/U_Y where U_m is the maximum relative displacement remains also a constant. As a result, if the input ground motion is multiplied by a factor S, the yield displacement of the structure should be multiplied by the same factor S in order for the structure to experience the same displacement ductility which is numerically equal to the ratio U_m/U_Y. The response quantities U, $\dot{U}$ and $\ddot{U}$ are thus multiplied by S, and the energy imparted to the structure, as well as other energy quantities, will be multiplied by S^2.

3.2.3 Solution Procedure -- A step by step numerical integration in the time domain may be used to solve the governing equation of motion and to calculate the various energy quantities. Newmark's Beta-method (38) with Beta equal to 1/6 corresponding to a linear variation of the response acceleration $\ddot{U}$ is employed herein. The equations relating the velocity and displacement at two consecutive time steps t and t+Δt can be written as follows

$$\dot{U}(t+\Delta t) = \dot{U}(t) + \frac{\Delta t}{2}\left(\ddot{U}(t) + \ddot{U}(t+\Delta t)\right)$$

and (3.22)

$$U(t+\Delta t) = U(t) + \Delta t\, \dot{U}(t) + \frac{\Delta t^2}{3} \ddot{U}(t) + \frac{\Delta t^2}{6} \ddot{U}(t+\Delta t)$$

The time step Δt used in this study was uniform throughout the integration. It is equal to the digitized time interval of the ground motion if the latter is equal to or smaller than 1/20 of the undamped period of free vibration of the structure. Otherwise, the digitized time interval is divided into equal time steps less than or equal to T/20 and the ground acceleration is obtained by linear interpolation between the known values at the digitized time steps.

The energy quantities defined in the previous section can be easily calculated by using Eqs. 3.22 and assuming that the ground acceleration varies linearly between two consecutive time steps. The amount of energy imparted to a structure between times t and $t+\Delta t$, or the incremental energy input, is equal to

$$\Delta E_I = -\left[\dot{U}(t)\,\ddot{Y}(t) + \frac{1}{2}\dot{U}(t)\,\Delta\ddot{Y} + \frac{1}{3}\Delta\dot{U}\,\Delta\ddot{Y} + \frac{1}{2}\Delta\dot{U}\,\ddot{Y}(t)\right]\Delta t + \left[\frac{1}{2}\Delta\ddot{U}\,\Delta\ddot{Y} + \Delta\ddot{U}\,\ddot{Y}(t)\right]\frac{\Delta t^2}{12} \tag{3.23a}$$

The incremental kinetic energy is equal to

$$\Delta E_K = \dot{U}(t)\,\Delta\dot{U} + \frac{1}{2}(\Delta\dot{U})^2 \tag{3.23b}$$

The amount of energy dissipated by viscous damping during a time increment of Δt, or incremental damping energy, is given by

$$\Delta E_D = 2\beta\omega\left[\left(\dot{U}(t)^2 + \dot{U}(t)\,\Delta\dot{U} + \frac{1}{2}(\Delta\dot{U})^2\right)\Delta t - \frac{1}{6}\left(\dot{U}(t)\,\Delta\ddot{U} + \frac{1}{2}\Delta\dot{U}\,\Delta\ddot{U}\right)\Delta t^2 + \frac{1}{120}(\Delta\ddot{U})^2\,\Delta t^3\right] \tag{3.23c}$$

The amount of energy dissipated by yielding and the strain energy are best evaluated depending on the shape of the load-deformation model. For an elastoplastic model, the strain energy E_S at time t is equal to $1/2\ \omega^2\ U_e^2$ where U_e is the elastic or recoverable relative displacement as shown in Fig. 3.3. The amount of energy dissipated by yielding during a time

increment Δt or incremental hysteretic energy ΔE_H is equal to zero if the structure remains elastic during this increment of time. It is equal to $\omega^2 U_Y$ times the incremental plastic displacement if the structure has yielded.

Finally, the energy at time $t+\Delta t$ is obtained by adding the incremental energy quantities calculated above to the values at the beginning of the time step t,

$$\begin{aligned} E_I\ (t+\Delta t) &= E_I(t) + \Delta E_I \\ E_K\ (t+\Delta T) &= E_K(t) + \Delta E_K \\ E_D\ (t+\Delta t) &= E_D(t) + \Delta E_D \\ E_H\ (t+\Delta t) &= E_H(t) + \Delta E_H \end{aligned} \tag{3.24}$$

It should be noted that the kinetic energy as calculated by Eqs. 3.23 and 3.24 is the same as

$$E_K\ (t+\Delta t) = \frac{1}{2}\ \dot{U}(t+\Delta t)^2 \tag{3.25}$$

namely, the kinetic energy at any given time is governed by the instantaneous relative velocity, U(t).

The numerical integration proceeds as follows. At time t the relative displacement U(t), the relative velocity $\dot{U}(t)$ and the relative acceleration $\ddot{U}(t)$ are known quantities. A value for the acceleration $\ddot{U}(t+\Delta t)$ is assumed and Eq. 3.22 is used to calculate $U(t+\Delta t)$ and $\dot{U}(t+\Delta t)$. From the force-deformation model the value of the restoring force R corresponding to the displacement $U(t+\Delta t)$ is obtained. Finally, substitution of the values of $\dot{U}$ and R in Eq. 3.5 yields an estimate of $\ddot{U}$. If the calculated acceleration agrees with the assumed value to within a certain tolerance, the integration proceeds to the next time step. Otherwise another iteration is performed with

the calculated acceleration used as the new assumed value. When convergence is achieved, each energy term is calculated separately using Eqs. 3.23 and 3.24. As a checking procedure at any given time t, the sum of the kinetic energy, the strain energy and the energy dissipated (from t = 0) by yielding and damping should be equal to the value of the energy input at that time t, namely,

$$E_I(t) = E_K(t) + E_S(t) + E_H(t) + E_D(t) \tag{3.26}$$

A qualitative estimate of the error involved in the solution procedure may be obtained from Figs. 3.4 and 3.5. In these figures, the resistance-relative displacement hysteretic loops for two different structures are shown. The solid line corresponds to the actual numerical solution while the dotted line corresponds to the "exact" solution which may be obtained if one employs a very tiny time step. It can be seen that the magnitude of the error is larger for structures with a high frequency than it is for structures with a low frequency. The reason is that for a low frequency (long period) structure, the value of the time step Δt used in the solution procedure is equal to the digitized time interval of the ground motion record. Therefore if the record is digitized at a 0.02 sec interval, for a structure with a frequency of 0.1 cps Δt is equal to T/1000. As a result, for this structure the actual and "exact" solutions are about the same.

One other point of interest related to the solution procedure is the iterative method used to calculate the yield displacement for a target ductility value. Initially the maximum displacement U_m for an elastic structure subjected to ground motion is calculated. Thereafter a yield displacement smaller than U_m is used and the displacement ductility for the structure is calculated. If the calculated value is smaller than the target

value, then the yield displacement is decreased, and vice versa, until the calculated and target values agree to within one percent. While this is a general rule, there are cases in which a decrease in yield level is coupled with a decrease in the maximum displacement ductility. These special cases are discussed in detail in Sect. 5.3.

3.3 Multi-Degree-of-Freedom Structures

3.3.1 Equations of Motion -- For a multi-degree-of-freedom structure subjected to ground excitation, the equations of motion are similar to those of a single-degree-of-freedom structure with the exception that the mass, stiffness and damping scalar quantities should be replaced by their corresponding matrix quantities. The governing equations of motion can thus be written as follows

$$[M]\{\ddot{U}(t)\} + [C]\{\dot{U}(t)\} + [K(t)]\{U(t)\} = -[M]\{1\}\ddot{Y}(t) \qquad (3.27)$$

where

$[M]$ = mass matrix
$[C]$ = damping matrix
$[K(t)]$ = tangent stiffness matrix at time t
$\{U(t)\}$ = story displacement vector at time t

and $\{1\}$ = unit vector

In incremental form, the above equations become

$$[M]\{\Delta\ddot{U}\} + [C]\{\Delta\dot{U}\} + [K(t)]\{\Delta U\} = -[M]\{1\}\ddot{Y}(t) + \{R(t)\} \qquad (3.28)$$

where {R(t)} is the residual load vector at time t. Equations 3.22 can also be written in incremental form

$$\{\Delta\dot{U}\} = \Delta t\{\ddot{U}(t)\} + \frac{\Delta t}{2}\{\Delta\ddot{U}\} \qquad (3.29)$$

and

$$\left\{\Delta U\right\} = \Delta t \left\{\dot{U}(t)\right\} + \frac{\Delta t^2}{2}\left\{\ddot{U}(t)\right\} + \frac{\Delta t^2}{6}\left\{\Delta\ddot{U}\right\} \tag{3.29}$$

At time t, the velocity vector $\{\dot{U}(t)\}$ and the displacement vector $\{U(t)\}$ are known quantities. Therefore, if the incremental displacement vector $\{\Delta U(t)\}$ is taken as the unknown quantity, the above equations yield the following expressions for the incremental velocity and acceleration vectors

$$\left\{\Delta\dot{U}\right\} = \frac{3}{\Delta t}\left\{\Delta U\right\} - 3\left\{\dot{U}(t)\right\} - \frac{\Delta t}{2}\left\{\ddot{U}(t)\right\}$$

and (3.30)

$$\left\{\Delta\ddot{U}\right\} = \frac{6}{\Delta t^2}\left\{\Delta U\right\} - \frac{6}{\Delta t}\left\{\dot{U}(t)\right\} - 3\left\{\ddot{U}(t)\right\}$$

Substitution of these equations in the equations of motion, Eq. 3.28, yields

$$\left[K^*(t)\right]\left\{\Delta U\right\} = \left\{Q(t)\right\} \tag{3.31}$$

where

$$\left[K^*(t)\right] = \left[K(t)\right] + \frac{6}{\Delta t^2}\left[M\right] + \frac{3}{\Delta t}\left[C\right]$$

and

$$\left\{Q(t)\right\} = \left[M\right]\left(\frac{6}{\Delta t}\left\{\dot{U}(t)\right\} + 3\left\{\ddot{U}(t)\right\} - \left\{1\right\}\Delta\ddot{Y}\right) + \left[C\right]\left(3\left\{\dot{U}(t)\right\} + \frac{\Delta t}{2}\left\{\ddot{U}(t)\right\}\right) + \left\{R(t)\right\}$$

$\left[K^*(t)\right]$ is called the pseudostatic stiffness matrix and $\{Q(t)\}$ the pseudostatic load vector.

3.3.2 Energy Expressions -- Just as in the case of a single-degree-of-freedom structure, the energy quantities are calculated by integration of the equation of motion, Eq. 3.27. The only difference is that the mass M should be replaced by the mass matrix $\left[M\right]$ and the displacement, velocity and acceleration should be replaced by the displacement, velocity and acceleration vectors, respectively. The total energy input is thus equal to

$$E_I^* = -\int_0^t \left\{\dot{U}(t)\right\}^T \left[M\right]\left\{1\right\}\ddot{Y}(t)\,dt \tag{3.32}$$

The total kinetic energy is given by

$$E_K^* = \int_0^t \left\{\dot{U}(t)\right\}^T \left[M\right] \left\{\ddot{U}(t)\right\} dt \tag{3.33}$$

The total energy dissipated by viscous damping is given by

$$E_D^* = \int_0^t \left\{\dot{U}(t)\right\}^T \left[C\right] \left\{\dot{U}(t)\right\} dt \tag{3.34}$$

The total energy dissipated by hysteretic behavior from the beginning of the ground motion until time t, plus the strain energy stored in the structure at that time is given by

$$E_H^* + E_S^* = \int_0^t \left\{\dot{U}(t)\right\}^T \left[K(t)\right] \left\{U(t)\right\} dt \tag{3.35}$$

The energy per unit mass is obtained by dividing each of the above quantities by the total mass of the structure.

3.3.3 Solution Procedure -- Preparatory to discussing the solution procedure, it is important to first reiterate the assumptions included in the derivation of the equations of motion.

Mass Matrix -- In this study, only shear-beam type structures were investigated; i.e., floors were considered to be rigid (no rotation). The structure has only one-degree-of-freedom (translation) per floor. The masses are lumped at the floor levels and associated with the horizontal translation. This assumption results in a diagonal mass matrix (nonzero terms only along the diagonal) and has been widely used in time-history dynamic analyses (20,63).

Damping Matrix -- The damping matrix is assumed to be linearly proportional to the mass matrix, namely,

$$\left[C\right] = \alpha \left[M\right] \tag{3.36}$$

where α is a constant and is chosen such that there is a certain percentage of critical viscous damping β in the fundamental mode of vibration of the structure. For the higher modes, β_n is given by

$$\beta_n = \frac{\alpha}{2\omega_n} \tag{3.37}$$

Once α is chosen, the above equation shows that the higher modes of vibration of the structure are damped less strongly than the fundamental mode.

Element Stiffness -- A one-component beam element, as defined by Giberson (19), was used herein to model each structural element. In this model, the bending moment-end rotation relationship is assumed to be elastoplastic. A plastic hinge, capable of sustaining the plastic moment capacity of the member, is assumed to form at either end of the member whenever the moment at this end exceeds the yield moment. As a result, four states of yield are possible for this beam element:

State (a) - elastic state, no plastic hinges at either end.

State (b) - a plastic hinge at the left end, elastic at the right end.

State (c) - elastic at the left end, a plastic hinge at the right end.

State (d) - plastic hinges at both ends.

The numerical integration proceeds as follows. Equations 3.31 represent a set of simultaneous algebraic equations which can be solved for the incremental displacement vector by Gaussian elimination. The incremental velocity and acceleration vectors are then calculated using Eqs. 3.30. Thereafter the displacement, velocity and acceleration vectors at time $t+\Delta t$ are obtained by adding the increment values obtained above to the response quantities at the beginning of the time step.

The above procedure which is equivalent to the Initial Stress Method (66) can be used, provided no changes in the stiffness matrix occur during a given time step. In case any yielding or hardening takes place during a time increment, the stiffness matrix $\left[K(t)\right]$ changes and a successive correction approach (1) is used. In this procedure, the quantity $\left[K(t)\right]\{\Delta U\}$ is replaced by

$$\left\{\Delta F\right\} = \left[K(t)\right] \left\{\Delta U\right\} - \left\{\Delta P\right\} \tag{3.38}$$

where $\{\Delta F\}$ is the actual incremental resisting force of the structure and $\{\Delta P\}$ is the residual load vector. The incremental displacement and residual forces between time t and $t+\Delta t$ are approximated by successive corrections,

$$\begin{aligned} \left\{\Delta U\right\} &= \left\{\Delta U\right\}^0 + \left\{\Delta U\right\}^1 + \ldots + \left\{\Delta U\right\}^n \\ \left\{\Delta P\right\} &= \left\{\Delta P\right\}^0 + \left\{\Delta P\right\}^1 + \ldots + \left\{\Delta P\right\}^n \end{aligned} \tag{3.39}$$

The corrections for $\{\Delta U\}$ are calculated by solving the following equations

$$\begin{aligned} \left[K^*(t)\right] \left\{\Delta U\right\}^0 &= \left\{Q(t)\right\} \\ \left[K^*(t)\right] \left\{\Delta U\right\}^1 &= \left\{\Delta P\right\}^0 \\ \left[K^*(t)\right] \left\{\Delta U\right\}^n &= \left\{\Delta P\right\}^{n-1} \end{aligned} \tag{3.40}$$

The tangent stiffness matrix applicable at the beginning of the time increment is used for all cycles of iteration. The incremental residual forces are found from consideration of the end moment-rotation model of the structural element. For a flexural element in the inelastic state, there is no unique relationship between the rotation and end moment: the moment at one end is affected by the moment at the other end and vice versa depending on the state of yield of the member. Half the incremental moment at one end is carried to the far end if the latter is elastic, otherwise no adjustment is necessary.

The iteration is continued for a specified number of cycles or until $\{\Delta P(t)\}^n$ is smaller than a specified tolerance. The final increment $\{\Delta P(t)\}^n$ becomes the residual force vector $\{R(t)\}$ for the next time step. Before proceeding to the next time increment, the stiffness matrix $\left[K(t)\right]$ is updated to account for any yielding or hardening in any member of the structure and the incremental energy quantities are calculated.

The total energy input is calculated using Eq. 3.32 which can also be written as follows

$$E_I^* = -\int_0^t \left(\dot{U}_1(t)\, m_1 + \dot{U}_2(t)\, m_2 + \ldots \right) \ddot{Y}(t)\, dt \qquad (3.41a)$$

Each term in the above equation is evaluated using the equation derived for a single-degree-of-freedom structure, Eq. 3.23a, multiplied by the corresponding mass. Similarly, Eq. 3.33 for the total kinetic energy can be written as

$$E_K^* = -\int_0^t \left(\dot{U}_1(t)\, m_1\, \ddot{U}_1(t) + \dot{U}_2(t)\, m_2\, \ddot{U}_2(t) + \ldots \right) dt \qquad (3.41b)$$

The total energy dissipated by viscous damping, Eq. 3.34, can be written as

$$E_D^* = \int_0^t \left(C_1\, \dot{U}_1(t)^2 + C_2\, \dot{U}_2(t)^2 + \ldots \right) dt \qquad (3.41c)$$

Each term is calculated using Eq. 3.23c multiplied by its corresponding mass. For this particular model, the total energy dissipated by inelastic deformations in each member is equal to the product of the sum of the cumulative inelastic hinge rotations at both ends times the yield moment of the member.

CHAPTER 4

ENERGY ABSORPTION IN SDF STRUCTURES AND EARTHQUAKE DAMAGE POTENTIAL

4.1 Introduction

In this chapter the earthquake response of a single-degree-of-freedom structure and the damage potential of ground motion are investigated, especially from the standpoint of energy considerations. The chapter begins with a description of the ground motion records employed in this study. Thereafter the response of a structure is evaluated in terms of (a) the amount of energy imparted to the structure, (b) the displacement ductility that the structure experiences, and (c) the number of yield excursions and reversals that the structure goes through when it is subjected to the various ground motions.

As part of the investigation, among the topics receiving detailed attention were the amount of energy dissipated by yielding or hysteretic energy E_H and the amount of energy dissipated by viscous damping or damping energy E_D. An index called equivalent number of yield cycles is defined in order to compare the damage potential of different ground motions and to evaluate the use of the displacement ductility as a measure of damage. An effective motion also is defined. The latter definition is based on the amount of energy imparted to structures when they are subjected to ground excitation.

4.2 Ground Motion Records

Eight earthquake records are selected as input ground motion. For the earthquake sources of these records the local magnitude, M_L, ranges between 4.7 and 7.7, and the epicentral distance between 6 and 31.9 Km. All records

have a peak acceleration greater than 0.10g which can be considered a reasonably high acceleration. Additional characteristics regarding earthquake events, fault mechanisms, site characteristics, instrument location and the duration of motion employed are given in Tables 4.1 and 4.2.

The records selected were intended to cover at least two types of ground motion, namely, (a) near-field, short duration, impulsive type ground motion, as for example that represented by the Melendy Ranch record, and (b) far-field, long duration, relatively severe and symmetric type cyclic excitation, as for example that represented by the Taft record. Five of the records chosen are the same as those used in the study undertaken by Structural Mechanics Associates (54) and another two are different components for the same earthquake events. In the study just indicated, eleven records were used and considerable effort was spent in their selection in order to cover a wide range of ground motions.

All records used are standard corrected accelerograms published by either the California Institute of Technology (17) or the U. S. Geological Survey (11,12,59). All were corrected by employing a filtering technique developed at Caltech and were digitized at a time increment of 0.02 sec, except two records (Bonds Corner and Coyote Lake) which were digitized at a 0.01 sec interval.

As a result of the balancing technique, and since the early part of the ground motion required to trigger the recording instrument is lost, all records have non-zero initial conditions. A two-second acceleration pulse, as described by Pecknold and Riddell (44), was prefixed to each ground motion in order to avoid any difficulty with the initial excitation conditions. Once the pulse is prefixed to the ground motion record the structure may be assumed to be at rest initially. The resulting accelerogram time-histories are shown

in Figs. 4.1 to 4.8.

The initial ground velocity, displacement, and the maximum ground acceleration, as well as the time at which it occurs, for the records employed in this study are presented in Table 4.3.

4.3 Time-History Response

Valuable information may be obtained by studying the time-history response of structural systems when they are subjected to various ground motions. In this section the focus is on some of the factors thought to be important in understanding the earthquake response and the amount of damage structures may suffer during an excitation. Two quantities of particular interest are the number of yield excursions and the number of yield reversals that a structure with a certain damping and displacement ductility (for a particular ground motion) goes through during the entire motion. The number of yield excursions is equal to the number of times the structure is in a yield state. The latter is defined whenever the internal force R in the structure attains the yield resistance R_Y . It is apparent from the yield sequence shown in Fig. 4.9a that the duration of each yield excursion is slightly different. The number of yield reversals is equal to the number of times the structure yields in opposite directions consecutively. For example the structure shown in Fig. 4.9a undergoes 7 yield excursions in one direction, 9 yield excursions in the other and 8 yield reversals.

Another quantity of interest is the duration of ground motion (or portion of the record) during which most or all inelastic deformations take place in the structure. This quantity may be obtained from the energy time-history response of the structure and may be used as one technique for classification of ground motion records.

In the following the response of single-degree-of-freedom systems over the whole range of frequencies from very low, 0.05 cps, to very high, 35 cps, is considered. Since previous studies showed differences in the earthquake response of a structure depending on its natural frequency, first the earthquake response of structures with low frequency and then that of structures with high frequency is studied. Unless otherwise mentioned, the nonlinear model referred to is the one with an elastoplastic force-displacement relationship.

4.3.1 Low-Frequency Structures -- The time-history response of single-degree-of-freedom structures with a low natural frequency (0.1 or 0.2 cps) and subjected to various ground motions is shown in Figs. 4.9 to 4.13. In these figures the displacement-time history, the yield sequence (or the yield excursions and reversals) and the resistance-displacement hysteretic loops are shown. The energy imparted to a structure and the energy dissipated (by damping and inelastic deformations) as a function of time also are shown. The difference at any time, t, between the curves for the energy input and the total energy dissipated represents the stored energy in the structure. The latter is equivalent to the sum of the strain and kinetic energy at time t. At the end of the motion, the stored energy becomes vanishingly small; i.e., the energy dissipated in the structure becomes almost equal to the energy imparted to it.

The response of structures with f = 0.1 cps, a damping value of 5 percent of critical and subjected to the El-Centro, the Pacoima Dam and the Parkfield ground motions, respectively, is shown in Figs. 4.9 to 4.11. For this structure to experience a displacement ductility of 3 when it is subjected to the Parkfield ground motion, it needs to have a yield displacement U_Y equal to 3.94 in. This structure will yield twice in each direction and goes through

two yield reversals. For the structure to experience the same ductility when it is subjected to the Pacoima Dam ground motion, it needs a yield displacement U_Y = 5.05 in., but it will yield four times in the positive direction and five times in the negative direction resulting in four yield reversals. Similarly, when the structure is subjected to the El-Centro ground motion it should have a U_Y = 2.46 in. and will yield seven times in one direction and nine times in the other resulting in eight yield reversals. A design based only on displacement ductility disregards the number of yield excursions and reversals which may be valuable in understanding the amount of damage sustained by structures after an earthquake excitation. It should also be noted that the yield displacements in the examples given above are large since they correspond to relatively long-period structures.

The energy time-history curves, such as those shown in Figs. 4.9 to 4.11, reflect the type of motion to which the structure is subjected. Under the El-Centro ground motion, the energy input curve has a large number of peaks and troughs as compared to two or three major peaks when the structure is subjected to the Parkfield ground motion which is of shorter duration. Those peaks result from the fact that for low-frequency (long-period) structures a large proportion of the energy imparted to the structure is stored in the form of strain and kinetic energy, and each peak corresponds to a strong cycle of earthquake input excitation which may or may not have a significant influence on the response. As a result the number of peaks in the energy input curve increases as the duration of strong motion increases.

If all the energy imparted to the structure can be stored as strain and kinetic energy, then no inelastic deformation will take place and the structure will suffer no structural damage. The input energy in long-period structures is slowly dissipated, and the maximum displacement experienced by

the structure is more likely to occur towards the end of the excitation rather than coincide with the strong motion part. The same type of general response occurs for structures with a fundamental frequency up to about 0.2 cps when they are subjected to different ground motions, such as the Taft and the Melendy Ranch records, as shown in Figs. 4.12 and 4.13.

4.3.2 High-Frequency Structures -- The time-history response of single-degree-of-freedom structures with f = 5 cps and subjected to various ground motions is shown in Figs. 4.14 to 4.17. As in the case of low-frequency structures, those with high frequency and with the same displacement ductility undergo a greater number of yield excursions and reversals under a severe, symmetric type excitation, such as the El-Centro record, than under an impulsive type motion, such as the Parkfield record. As shown in Figs. 4.14 to 4.16, for a structure with f = 5 cps and damping of 5 percent of critical to experience a displacement ductility of 3, it should have a yield displacement equal to 0.152, 0.136 and 0.378 in. when it is subjected to the Parkfield, the Melendy Ranch and the Pacoima Dam ground motions, respectively. At the same time the structure will undergo respectively 4, 7 and 21 yield excursions under the above ground motions.

From the energy time-history curves it is apparent that the stored energy represents a small proportion of the energy imparted to the structure. The latter is dissipated almost immediately (by damping and yielding), and the maximum displacement coincides in general with the strong motion part of the excitation. For a structure subjected to a ground motion with a high-frequency acceleration spike, such as the Parkfield ground motion, the energy input curve shows a sudden jump at about the same time the peak ground acceleration occurs, and most inelastic deformations in the structure take place around that time.

The times by which 5, 75 and 90 percent of the energy absorbed in a structure is dissipated are given in Table 4.4. They will be referred to as $t_{e_{0.05}}$, $t_{e_{0.75}}$ and $t_{e_{0.90}}$, respectively. Before $t_{e_{0.05}}$ and after $t_{e_{0.90}}$ most or all energy imparted to a structure is dissipated by damping and is associated with little or no damage in the structure.

The times given in Table 4.4 are for structures with a frequency equal to 2.0 cps, a damping of 5 percent of critical and a displacement ductility of 3 under the various ground motions. The amount of damping and the value of the displacement ductilty have a small effect on the times given in Table 4.4. For structures with a frequency greater than 2 cps, the amount of energy dissipated by $t_{e_{0.75}}$ is larger than 75 percent of the energy imparted to the structure. For example 89 percent of the energy input is dissipated by t = 4.6 sec for a structure with f = 5 cps when it is subjected to the Melendy Ranch ground motion, and no yielding occurs after that time.

The difference between $t_{e_{0.75}}$ and $t_{e_{0.05}}$ corresponds to the portion of the ground motion during which most or all inelastic deformations occur in the structure. It is denoted herein as effective duration, T_e, and may be used as one technique for classification of ground motion records. The records employed in this study may be classified in three groups as follows: (1) the Coyote Lake, the Parkfield, the Gavilan College and the Melendy Ranch records with $T_e < 3.5$ sec will be referred to as short duration records; (2) the Bonds Corner and the Pacoima Dam records with $3.5 < T_e < 7.5$ sec will be referred to as moderate duration records; and (3) the Taft and the El-Centro records with $T_e > 7.5$ sec will be referred to as long duration records.

The effects of type of ground motion and properties of a structure (its frequency, damping and displacement ductility) on the number of yield excursions and reversals it goes through during an excitation are summarized

next. On the basis of the findings shown in Figs. 4.18 through 4.22, the following observations may be made.

(1) On the average, structures with frequencies between about 0.3 and 5 cps experience the largest number of yield excursions provided all other factors (damping, ductility and ground motion) are the same. As may be seen in all the figures, the number of yield excursions decreases for long period structures and is lowest for short period (stiff) structures.

(2) The input ground motion has a great effect on the number of yield excursions. Over the whole frequency range, structures with a given damping and displacement ductility undergo in general a larger number of yield excursions when they are subjected to long duration motion, such as the Taft record, than when they are subjected to a short duration motion, such as the Melendy Ranch record (Figs. 4.18 through 4.20).

(3) Besides the type of ground motion, the displacement ductility has a major influence on the number of yield excursions that structures undergo during an excitation. As shown in Figs. 4.19 and 4.20, the number of yield excursions greatly increases as the displacement ductility of the structure increases, especially when the structure is subjected to long duration motion.

(4) The effect of damping is to lower the number of yield excursions structures experience during ground motion. For example as shown in Fig. 4.21, structures with a displacement ductility of 5 when they are subjected to the El-Centro ground motion will experience up to 15 percent reduction in the number of yield excursions if the damping is increased from 2 to 5 percent of critical.

(5) The second slope in the force-displacement relationship has a small effect on the number of yield excursions structures undergo during an excitation. As shown in Fig. 4.22, the number of yield excursions is about

the same for structures with the same properties (initial stiffness, damping and displacement ductility) irrespective of whether they have elastoplastic or bilinear force-deformation resistance relationship.

4.4 Response and Energy Spectra

For single-degree-of-freedom systems, the maximum response quantities are obtained by solving the equation of motion, Eq. 3.1, and the various energy quantities are obtained by solving Eqs. 3.23 and 3.24. The response quantities of interest are the maximum relative displacement U_m for linear elastic systems and the yield displacement U_Y for a specified displacement ductility for nonlinear systems. The energy quantities of interest are the amount of energy imparted to a structure or energy input E_I, the amount of energy dissipated by viscous damping or damping energy E_D and the amount of energy dissipated by inelastic deformations or hysteretic energy E_H. The results are shown in the form of response and energy spectra.

A response spectrum for a linear elastic single-degree-of-freedom oscillator may be presented as a tripartite logarithmic plot of the maximum response quantities (spectral displacement S_d, spectral velocity S_v and spectral acceleration S_a) as a function of the natural frequency and damping of the structure. These response quantities are related to each other in the following way:

$$S_v = \omega S_d \tag{4.1}$$

$$S_a = \omega S_v = \omega^2 S_d \tag{4.2}$$

The spectral displacement is exactly equal to the maximum relative displacement U_m in the spring over the whole range of frequencies. The spectral velocity, S_v, or pseudovelocity, is nearly equal to the maximum relative velocity for systems with moderate or high frequencies but may differ

substantially from the maximum relative velocity for very low-frequency systems. The product 1/2 S_v^2 is equivalent to the maximum strain energy stored in the system.

The spectral acceleration, S_a , or pseudoacceleration, is exactly equal to the maximum absolute acceleration for systems with no damping and is not greatly different from the maximum acceleration for systems with moderate amounts of damping, over the whole range of frequencies. The product of the mass times the pseudoacceleration represents the maximum internal resistance force in the structure.

An energy spectrum may be presented as a logarithmic plot of the numerical value of the energy per unit mass E_I imparted to a linear elastic structure at the end of the ground motion as a function of its natural frequency and damping. For a nonlinear structure, an energy spectrum may be presented as a logarithmic plot of the numerical value of either the energy input E_I or the hysteretic energy E_H at the end of the motion as a function of its natural frequency, damping and displacement ductility. The value of the energy input is equal to the total energy dissipated in the structure by damping and inelastic deformations (if any occurs); at the end of the motion the stored energy (kinetic plus strain) becomes vanishingly small.

4.4.1 Linear Elastic Model -- The response and energy input spectra for linear elastic systems with a damping of 2, 5 and 10 percent of critical and subjected to the ground motions employed in this study are shown in Figs. 4.23 through 4.30. The following observations regarding these spectra may be made.

(1) Long duration records, such as the El-Centro and the Taft records, have broad response and energy input spectra. They are thus effective over a wide range of frequencies.

(2) Short duration records, such as the Parkfield and the Melendy Ranch records, have narrow response and energy input spectra. Their spectra peak over a narrow frequency range and drop sharply for frequencies below the predominant frequencies. For example, as shown in Figs. 4.24 and 4.26, the spectra for the Melendy Ranch record peak in the frequency range of 3 to 10 cps, and the spectra for the Parkfield record peak for frequencies between 0.5 and 2.0 cps. While both records have a maximum acceleration of about 0.50g, structures with natural frequencies less than 3 cps will experience higher maximum relative displacements when subjected to the Parkfield ground motion than when subjected to the Melendy Ranch ground motion. The opposite is true for structures with frequencies greater than 3 cps.

(3) Response spectra and energy input spectra for structures with the same properties and subjected to the same ground motion are similar in shape; their peaks and troughs occur at the same frequencies.

(4) The effect of increasing the amount of damping in a structure is to reduce its maximum response, especially for structures with frequencies between about 0.2 and 10 cps.

(5) The amount of damping in a structure has little or no effect on the amount of energy imparted to that structure.

(6) The product of one half times the square of the spectral velocity for a structure with no damping and subjected to ground motion represents, in general, a good estimate of the amount of energy per unit mass imparted to the structure (Fig. 4.31).

(7) The product of one half times the square of the spectral velocity S_v for a structure with some damping and subjected to ground motion will, in general, underestimate the amount of energy per unit mass imparted to the structure. As shown in Fig. 4.32, the difference between the values of

$1/2\ S_v^2$ and E_I increases as the percent of critical damping in the structure increases.

Response and energy spectra for linear elastic systems are thus useful to determine the frequency range over which a ground motion is most effective and to estimate the amount of energy imparted to a structure.

4.4.2 Nonlinear Models -- Two types of nonlinear models, shown in Fig. 2.8, were investigated as a part of this study. The first model has an elastoplastic and the second has a bilinear force-deformation resistance relationship. In the latter model, the second slope is equal to 2 or 5 percent of the first or initial slope.

For each model, the yield displacement U_Y for various conditions (frequency, damping, displacement ductility and ground motion) was computed first as described in the previous chapter. Then those yield values were used to calculate the energy quantities of interest, i.e., energy input E_I, damping energy E_D and hysteretic energy E_H. The results are shown in Figs. 4.33 through 4.37 in the form of energy spectra for structures with damping of 2 and 5 percent of critical and displacement ductilities of 1.5, 2, 3 and 5 when subjected to different ground motions. The following observations can be made as to the effect of damping and ductility on the amount of energy imparted to a structure and on the amount of energy dissipated by viscous damping and that dissipated by inelastic deformations.

(1) As in the case of a linear elastic structure, damping has little or no effect on the amount of energy imparted to a structure by ground motion, Figs. 4.33 and 4.34.

(2) The amount of energy absorbed in a structure when it is subjected to ground motion is slightly affected by its displacement ductility. As shown in Fig. 4.35 through 4.38, in general, as the displacement ductility of a

structure increases, the amount of energy imparted to it decreases if its natural frequency is smaller than about 2 cps and increases if its natural frequency is higher.

(3) While damping and ductility have a small effect on the amount of energy imparted to a structure, they greatly influence the manner in which that energy is dissipated. As shown in Fig. 4.39, for a structure with some damping, the proportion of energy input dissipated by yielding increases as its displacement ductility increases. The same is true if the damping in the structure decreases.

(4) For a structure with some damping and low displacement ductility (about 2), as shown in Fig. 4.40, the percent of energy input dissipated by yielding is, in general, higher for impulsive type motion, such as the Parkfield record, than it is for symmetric type motion, such as the Taft record. However, as the displacement ductility increases, the type of motion becomes less important.

(5) The energy input spectra for a bilinear system are compared with those of an elastoplastic system with the same damping and ductility and subjected to the same ground motion in Fig. 4.41. It is apparent that the amount of energy imparted to a structure is about the same irrespective of whether its load-deformation function is elastoplactic or bilinear. The differences in the energy spectra increase with the ductility and the second slope but remain very small.

The energy spectra for nonlinear systems are very similar to those of linear systems. Their peaks and troughs occur at the same frequencies, and the amount of energy input, in general, is about the same for linear and nonlinear systems (with moderate displacement ductility) with the same natural frequency. A study of nonlinear systems provides, however , information on

the amount of energy dissipated in the structure by damping and that dissipated by yielding in addition to information on other factors that influence damage, as for example displacement ductility and number of yield excursions and reversals.

4.5 Earthquake Damage Potential

There is no unique way of evaluating the damage potential of an earthquake ground motion. The displacement ductility has been a commonly used factor to measure (or limit) damage (51,54). However, the focus on one factor such as displacement ductility does not account for cumulative damage that may occur as a result of reversed cyclic deformations.

A structure with a natural frequency of 5 cps and a damping of 2 percent of critical will undergo 15 yield excursions and 9 reversals if it is designed to experience a displacement ductility equal to 2 when it is subjected to the El-Centro ground motion which has a 0.35g peak acceleration. The amount of energy per unit mass imparted to it is 285 $(in./sec)^2$ of which 116 $(in./sec)^2$ is dissipated by inelastic deformations. Another structure with the same properties (mass, stiffness and damping) and designed to experience the same ductility of 2 when it is subjected to the Parkfield ground motion which has a 0.49g peak acceleration will undergo 5 yield excursions and 4 yield reversals. Under this ground motion, the structure will dissipate by yielding 97 $(in./sec)^2$ of the 144 $(in./sec)^2$ imparted to it.

Although the above structures have the same properties and are designed to experience the same displacement ductility, the first structure would sustain more damage than the second structure as measured by a larger amount of energy imparted to it, a larger amount of energy dissipated by yielding and a greater number of yield excursions and reversals. The last factor was discussed in Sect. 4.2. In the following, the damage potential of a ground motion is

evaluated in terms of the amount of energy imparted to structures and the amount of energy dissipated by yielding in these structures in addition to their displacement ductilty. Based on the amount of energy imparted to structures, a possible effective motion criterion is defined.

4.5.1 Equivalent Number of Yield Cycles -- A useful comparative index of the severity of ground shaking is the equivalent number of yield cycles, N. This index is numerically equal to the ratio of the total energy dissipated by yielding, E_H, in a structure when subjected to ground motion to the area under the resistance-displacement curve for the structure when it is loaded monotonically until it reaches the same maximum displacement it experiences during the excitation, Fig. 4.42, namely,

$$N = \frac{E_H}{\omega^2 U_Y^2 (\mu-1)} \tag{4.3}$$

The smallest value N can have is 1; in this case, the structure yields only in one direction and reaches its maximum displacement. In the previous example, the value of N is equal to 2.9 and 2.5 when the structure is subjected to the El-Centro and Parkfield ground motions, respectively.

The equivalent number of yield cycles is different from the number of yield excursions. The former is based on the amount of energy dissipated by yielding in a structure while the latter is numerically equal to the number of times the structure reaches a yield state independently of the duration yield. The index N is useful to evaluate the strength or damage potential of an earthquake excitation in the sense that the stronger or more severe a ground motion is, the larger the amount of energy imparted to a structure when it is subjected to that excitation. This in turn will cause an increase in the amount of energy dissipated by yielding in a structure, and thus an increase in the value of N. At the same time, an increase in the amount of energy

dissipated by yielding in a structure is accompanied by an increase in the number of yield excursions and reversals it goes through during the excitation. As a result, the damage sustained by the structure increases.

Comparisons of the values of N for the various types of ground motion employed in this study and for structures with different properties (frequency, damping and displacement ductility) are shown in Figs. 4.43 through 4.45. From these figures, the following observations may be drawn.

(1) The value of N is highest for structures with natural frequencies in the intermediate frequency range (between about 0.2 and 2.0 cps) of a response spectrum. As a result, structures with frequencies in the above region will experience more yielding than those with frequencies outside that region.

(2) In general, the value of N for a structure subjected to ground motion increases as the displacement ductility of the structure increases. Namely, the amount of energy dissipated by yielding increases and the yield level of a structure decreases as the ductility increases; both factors will contribute to an increase in the value of N as given by Eq. 4.3.

(3) For structures with the same displacement ductility, the value of N is, in general, higher for a long duration ground motion, such as that represented by the El-Centro record, than it is for a short duration ground motion, such as that represented by the Parkfield record. As shown in Figs. 4.43 through 4.45, the differences are largest for structures with frequencies in the velocity region of the response spectrum.

(4) The differences in the values of N mentioned above are accentuated by an increase in the displacement ductility. This implies that as the displacement ductility increases, it becomes less appropriate to be used as a measure of damage especially for structures subjected to long duration ground motions.

From the above, it can be seen that the value of N in addition to the displacement ductility provides a good measure of the cyclic deformations of structures from which the damage sustained by these structures may be inferred.

4.5.2 Effective Motion -- Peak ground acceleration and response spectra are not always good descriptors of the damage potential of an earthquake ground motion (25,30). The spectrum intensity defined as the area under the velocity spectrum also was found not to be easily related to the damage potential of a ground motion (26). Newmark (39) and Page (43) noted that an earthquake excitation with a short duration and a single peak of intense motion may be less damaging to structures than might be inferred from its maximum acceleration. This has led several investigators (30,42) to define a new quantity called effective acceleration or effective motion which is most closely related to the damage potential of a ground motion. Newmark and Hall (42) defined effective acceleration in the following manner:

> It is that acceleration which is most closely related to structural response and to damage potential of an earthquake. It differs from and is less than the peak free-field ground acceleration. It is a function of the size of the loaded area, the frequency content of the excitation, which in turn depends on the closeness to the source of the earthquake, and to the weight, embedment, damping characteristic, and stiffness of the structure and its foundation.

As a result of this study, effective motion might be defined in terms of the damage potential as characterized by the amount of energy imparted to structures when they are subjected to that ground motion. In order to obtain the effective motion corresponding to a free-field ground motion, first a reference ground motion, characterized as a ground motion whose effective

acceleration as defined above may be assumed equal to its peak acceleration, is chosen. The reference motion is then multiplied by a factor S, which can be either greater or smaller than one, such that the energy input spectra of the resulting motion match those of the free-field ground motion. The scaled reference motion thus represents the effective motion corresponding to the free-field ground motion considered.

When scaling ground motion records in order to compare their energy input spectra, it is not possible in general to match these spectra over the whole range of frequencies. This is especially true for short duration ground motions since their energy spectra peak over a narrow frequency range. Therefore, the energy input spectra should be matched over the frequency range of interest. Herein the main focus is on structures with frequencies in the amplified acceleration region of a response spectrum (frequency between about 2 and 10 cps).

The North-South component of the El-Centro record, 1940 Imperial Valley earthquake, has several cycles of strong motion, near-peak acceleration, and the damage reported in the area where it was recorded may be considered as consistent with its peak acceleration of 0.35g. The effective acceleration for this ground motion can thus be taken equal to its peak acceleration. As a result, this ground motion may be employed as a reference motion.

Another accelerogram with similar characteristics to that of the El-Centro record is the S69E component of the Taft record, 1952 Kern County earthquake, which has a 0.18g peak acceleration. This record multiplied by a factor of two will have a peak acceleration of 0.36g which is about the same as that of the El-Centro record. The energy spectra (energy input E_I and hysteretic energy E_H) for the resulting Taft record and the El-Centro record, shown in Fig. 4.46, are very similar over a wide range of frequencies; i.e., the amount

of energy imparted to and dissipated by yielding in structures with the same mass and frequency when subjected to either the El-Centro record or the Taft record scaled by a factor of two are essentially the same under similar conditions of damping and displacement ductility. As a result, both ground motions may be employed as reference motions.

The results of scaling the energy spectra for the various ground motion records used in this study are shown in Figs. 4.47 through 4.50. The following observations regarding these results may be made.

(1) From Fig. 4.47, it can be seen that the energy input spectra of the El-Centro record multiplied by a factor of four, which is equivalent to multiplying the record by a factor of two, represent a good approximation to that of the Bonds Corner record. It may thus be assumed that a 0.70g El-Centro motion is as damaging to structures with frequencies between about 2 and 10 cps as the Bonds Corner ground motion. However, the latter motion is much less damaging than can be inferred from the maximum acceleration of 0.70g for structures with frequencies less than 2 cps.

(2) The energy input spectra for the El-Centro record scaled to a 0.70g peak acceleration represent a good approximation to those of the Pacoima Dam record, which has a 1.17g maximum acceleration, for frequencies less than 2 cps, as shown in Fig. 4.48a. The energy input spectra for the El-Centro record scaled to 0.80g and for the Pacoima Dam record are shown in Fig. 4.48b. It can be seen that these spectra are similar in the frequency range of interest (between about 2 and 10 cps). A reference motion scaled to a 0.80g maximum acceleration may thus be taken as the effective motion corresponding to the Pacoima Dam ground motion.

(3) The energy input spectra for the El-Centro, the Parkfield and the Melendy Ranch records which have 0.35g, 0.49g and 0.52g peak acceleration, respectively, are shown in Fig. 4.49. The damage potential of the Parkfield ground motion may be approximated by that of the El-Centro ground motion for its effect on stiff structures (frequency greater than about 3 cps). The latter motion will, however, slightly underestimate the damage potential of the Parkfield ground motion on structures with frequencies between 0.4 and 3 cps. On the other hand, the same ground motion will greatly overestimate the damage potential of the Melendy Ranch ground motion on structures with frequencies less than 5 cps, but it is appropriate for structures with higher frequencies.

(4) From Fig. 4.50, it can be seen that the spectra for the Taft record scaled to a 0.27g maximum acceleration will closely approximate that of the Coyote Lake which has 0.42g peak acceleration for frequencies greater than 2 cps. The resulting Taft record will, however, overestimate the damage effect of this ground motion on structures with frequencies less than 2 cps.

(5) From Fig. 4.24b, it is apparent that the damage potential of the Gavilan College ground motion on structures with frequencies less than 10 cps is much smaller than might be inferred from its peak acceleration of 0.14g. A reference motion with 0.05g maximum acceleration may be taken as a good measure of the damage potential of this ground motion.

The maximum accelerations for the free-field ground motion records and their corresponding effective motions are summarized in Table 4.5. From this table, it is apparent that the maximum acceleration of an effective motion is equal to that of its corresponding free-field ground motion for long duration motion which normally occurs at some distance from the epicenter, as for example the El-centro record. It is smaller than the maximum acceleration of

the free-field ground motion for moderate and short duration motions, as for example the Pacoima Dam and the Coyote Lake records. It should also be remembered that the response and energy spectra corresponding to moderate and short duration records peak over a narrow frequency range. As a result, the damage potential of these ground motions on structures with frequencies outside that range is in general less than might be inferred from the maximum acceleration of either the free-field ground motion or its corresponding effective motion.

CHAPTER 5

SCALING GROUND MOTION RECORDS FOR EQUAL DAMAGE POTENTIAL

5.1 Introduction

In this chapter two methods of scaling ground motion records for equal damage potential are described. The two methods differ in the manner in which damage is measured. Structures with the same properties (initial stiffness, damping and yield resistance) and subjected to ground motion are assumed to sustain the same amount of damage after an excitation when they either experience the same displacement ductility or dissipate the same amount of energy by yielding.

The displacement ductility has been widely employed for years in structural dynamic research (in both analytical and experimental work) to evaluate the response of structures (or structural members) when they are subjected to cyclic loading. From the results shown in the previous chapter, it is apparent that structures which experience the same displacement ductility under various ground motions may sustain different amounts of damage depending on the number of yield excursions and the amount of energy input.

Herein, the method of using the displacement ductility as a measure of damage is further examined, and another method based on an energy concept is investigated. In the latter method, similar structures are assumed to sustain the same amount of damage after different earthquake excitations if the amount of energy dissipated by yielding in these structures is the same.

5.2 Structural Models

A single-degree-of-freedom structural model with an elastoplastic, hysteretic load-deformation relationship is employed to demonstrate the two scaling procedures. As discussed in Chapter 2, this model may be used to represent the nonlinear behavior of moment-resisting, non-deteriorating steel frame structures.

The model frequencies selected fall in the velocity and amplified acceleration regions of a response spectrum. A small number of examples was employed in order to keep the cost of computations down while still clearly demonstrating how the methods work. The model frequencies selected are 0.5, 1.0, 1.5, 2.0, 3.5, 5.0 and 8.5 cps. The damping is assumed to be equal to 5 percent of critical throughout.

Each structural model is assumed to have a yield displacement equal to the spectral displacement obtained from a smooth elastic response spectrum at the model's natural frequency. The smooth response spectrum is constructed as recommended by Newmark and Hall (41) and anchored to a 0.15g ground acceleration. The latter is only a reference (or intermediate) value selected for illustrative purposes and has no effect on the observations to be made.

The resulting response spectrum is shown in Fig. 5.1, and the yield displacement U_Y and the yield resistance R_Y ($= \omega^2 U_Y$) for the various structural models are given in Table 5.1.

5.3 Scaling Ground Motions for Equal Damage

Herein ground motion records are scaled such that structures with the same properties (initial stiffness, yield displacement and damping) and subjected to any ground motion will either experience the same displacement ductility or dissipate the same amount of energy by yielding.

The first step in both methods is to scale the ground motion records, shown in Table 4.1, such that at each model frequency the maximum relative displacement of the structural model when it is subjected to any ground motion is equal to its yield displacement. Two examples are shown in Figs. 5.2 and 5.3. In Fig. 5.2 the elastic response spectrum for the Taft record is multiplied by 1.15 such that it intersects the smooth elastic response spectrum at a frequency of 2 cps. The two spectra may or may not intersect at other frequencies. Similarly, in Fig. 5.3 the elastic response spectrum for the Coyote Lake record is multiplied by 0.58 such that it intersects the smooth spectrum at a frequency of 5 cps. The factor by which the ground motion is multiplied, such as 0.58 in the previous example, is called the scale factor and denoted as S. It should be noted that such a scaling procedure does not alter the frequency content of a given ground motion. It is useful as a means for raising or lowering the intensity of an excitation at a given frequency.

The scale factors depend on the frequency of the structure and the ground motion record. They can be either smaller or greater than one depending on whether or not the maximum displacement at a model frequency and under a particular ground motion is larger or smaller than the yield displacement of the structure. Since for elastic response no yielding occurs in the structure, each scale factor at yield may be obtained from the ratio of the yield displacement U_Y of the structural model to the spectral displacement S_d (which is equivalent to U_m) obtained from the elastic response spectrum of the ground motion record before any scaling, namely, $S = U_Y / U_m$. In a sense, this step of the scaling procedure may be considered equivalent to the normalization that is performed in a statistical analysis of response spectra.

The spectral displacement before any scaling and the scale factor for each model frequency are shown in Tables 5.2 and 5.3. Since the response spectra corresponding to moderate and short duration records have narrow frequency content, the scale factors are high at the model frequencies outside that range, as can be seen from the values shown in Table 5.3. For example, the scale factors for the Melendy Ranch record are higher than 2.5 for frequencies lower than 2 cps and smaller than one for frequencies equal to or greater than 3.5 cps.

At this point, the stucture responds elastically and additional scaling is needed to cause yielding. In the following step, the "normalized" ground motion records are multiplied by a scale factor, F, such that when similar structures are subjected to any of the resulting records they will sustain the same amount of damage however defined.

The procedure described above is illustated in Figs. 5.4 and 5.5. Initially the Taft record is multiplied by 1.15 such that the elastic response spectrum for the resulting record intersects the smooth elastic response spectrum at a frequency of 2 cps; this step is labeled (a) in Fig. 5.4, and the scale factor is denoted as S. Next the resulting record (and thus the response spectrum) is multiplied by 2.14 in order for the structural model with f = 2 cps to experience a displacement ductility equal to three; this step is labeled (b) in Fig. 5.4, and the scale factor is denoted as F. Similarly, the two main steps of the scaling procedure for the Coyote Lake record at a frequency of 5 cps are illustrated in Fig. 5.5.

5.3.1 Equal Displacement Ductility -- In this particular method the displacement ductility is selected as the appropriate measure of damage sustained by structures. The ground motion records are multiplied by a scale factor, F_d, such that a structural model will experience the same

displacement ductility when it is subjected to any of the scaled ground motions.

The first step is to pick a target displacement ductility. In this study two ductility values were chosen. One value is 3 and corresponds to structures which experience low to average inelastic deformation; the other value is 5 and corresponds to structures which experience high inelastic deformation. These values may be compared to those employed in building codes (3,61) for ductile type structures, namely about 3 to 6.

The second step in the scaling procedure is to find the scale factor, F_d, by which a ground motion record should be multiplied in order for the structural model to reach the target ductility. This scale factor depends on the frequency of the structural model, the input ground motion and the target ductility value. It is always greater than one since in the latter case no inelastic deformation occurs in the structure and a higher intensity ground motion is needed to cause yielding. This scaling procedure is illustrated in Fig. 5.4.

A trial and error procedure is employed to calculate at a given frequency the scale factor, F_d, for a target displacement ductility. Initially an arbitrary factor greater than one is used, and the displacement ductility for a given structural model is calculated. Thereafter if the calculated displacement ductility is higher than its target value, a lower scale factor is used in the next iteration and vice versa. This procedure is repeated until the calculated and target values for the displacement ductility agree to within one percent.

While the procedure described above is general, there are some cases in which increasing the scale factor will decrease, rather than increase, the displacement ductility. One such case is shown in Fig. 5.6. This special

case may be explained as follows. When a structure is subjected to ground motion, the maximum relative displacement it experiences in one direction is in general different from that it experiences in the other direction. The displacement ductility is thus different in opposite directions, but the structure is assumed to have a ductility equal to the maximum absolute value of the displacement ductility it experiences in either direction. In some cases, such as the one considered, an increase in the scale factor will cause a decrease in the displacment ductility in one direction and an increase in the opposite direction, rather than an increase in both directions. As a result, the maximum displacement ductility of the structure decreases such as between points a and b in Fig. 5.6a.

However from the standpoint of energy, it should be noted that an increase in the scale factor will always result in a higher intensity ground motion which should cause more yielding in the structure. As shown in Fig. 5.6b, the hysteretic energy increases monotonically with an increase in the scale factor independently of whether or not the displacement ductility increases.

Once the scale factor for a target ductility is found, the amount of energy dissipated in the structure by inelastic deformations or E_H can be caluclated. The latter quantity is expressed in terms of the equivalent number of yield cycles or N as given by Eq. 4.3. For a certain structural model and target ductility value, the product $\omega^2 U_Y^2 (\mu - 1)$ is equal to a constant and the value of N is directly proportional to E_H : the higher the amount of energy dissipated by yielding in a structure when it is subjected to ground motion, the higher the value of N.

The scaling factor and the value of N calculated for the various ground motion records at each model frequency are shown in Tables 5.4 and 5.5. In order to compare these results with those of other studies, the mean or

average scale factor $\bar{F}$, the standard deviation σ and the coefficient of variation Ω at each model frequency may be calculated, respectively, as follows:

$$\bar{F}(f) = \frac{1}{n} \sum_{i=1}^{n} F_i(f) \tag{5.1}$$

$$\sigma\left[F(f)\right] = \sqrt{\frac{1}{n}\left(\sum_{i=1}^{n} F_i(f)^2 - n\,\bar{F}(f)^2\right)} \tag{5.2}$$

$$\Omega\left[F(f)\right] = \frac{\sigma\left[F(f)\right]}{\bar{F}(f)} \tag{5.3}$$

where n is the number of ground motion records. The results are also shown in Tables 5.4 and 5.5.

5.3.2 Equal Hysteretic Energy -- In this particular method the amount of energy dissipated by yielding or hysteretic energy E_H is selected as an appropriate measure of damage sustained by structures. The ground motion records are multiplied by a scale factor, F_e, such that a structure will dissipate the same amount of energy by yielding when it is subjected to any of the resulting records.

The first step is to calculate the amount of energy that should be dissipated by yielding in each structural model or target E_H. From Eq. 4.3, the value of E_H is equal to the product of the value of N times $\omega^2 U_Y^2$ $(\mu - 1)$. For a structural model the circular frequency ω and the yield displacement U_Y are known quantities.

In order to calculate E_H, the values of N and the displacement ductility are selected (or estimated). The latter is assumed to be equal to 3. From the results shown in the previous chapter, the value of N depends on the natural frequency of the structure, its damping and its displacement

ductility. It is highest generally for structures with frequencies in the velocity region of the response spectrum and decreases for those with frequencies in the acceleration region. The assumed value for N and the target value for hysteretic energy at each model frequency are shown in Table 5.6. It should be noted that the assumed values for the displacement ductility μ and the equivalent number of yield cycles N are used in an intermediate step to help estimate the amount of energy dissipated by yielding in a structure. Their assumed and final values need not be the same.

The next step in the scaling procedure is to find the scale factor by which a ground motion record should be multiplied such that the amount of energy dissipated by yielding in a structure is equal to the target value. As in the previous method, this scale factor depends on the frequency of the structural model and the ground motion record. It is also always greater than one.

A procedure similar to that employed in the previous method is employed to calculate the scale factors. Initially an arbitrary factor greater than one is used, and the amount of energy dissipated by yielding is calculated. Thereafter if the caluclated value for E_H is smaller than the target value, the scale factor is increased and vice versa. As shown in Fig. 5.4b, the amount of energy dissipated by yielding always increases as the intensity of ground motion increases. The iteration procedure is continued until the calculated value for E_H agrees with its target value to within one percent.

Once the scale factor for the target E_H value is obtained, the displacement ductility of the structural model can be calculated. The results (scale factors and displacement ductility values) are shown in Table 5.7. The mean value, the standard deviation and the coefficient of variation for the scale factors and ductility values at each model frequency may be calculated

using Eqs. 5.1 to 5.3 and are also shown in the above table.

5.4 Discussion of Results

Under severe earthquake excitation, structures will experience one or several excursions into the inelastic range depending on the type of ground motion and on the properties of the structure itself. Although the displacement ductility is very useful and has been widely employed to evaluate the earthquake response of a structure, this factor does not give the entire picture of the amount of damage sustained by the structure after the excitation. From the results shown in Tables 5.4b and 5.5b, it can be seen that the value of N and the amount of energy dissipated by yielding in a structure is, in general, higher when the structure is subjected to long duration motion than when it is subjected to short duration motion. For example, the value of N for a structure with a frequency of 3.5 cps is equal to 5.94 under the El-Centro record and to 2.08 under the Parkfield record. The differences in the values of N increase as the displacement ductility of the structure increases. For a displacement ductility of five, the coefficent of variation of the values of N may be as high as 0.75, as shown in Table 5.5b.

The results of scaling ground motion records for equal damage potential based on equal hysteretic energy are shown in Table 5.7. It can be seen that if the amount of energy dissipated by yielding in the structure is known (or estimated), its displacement ductility can be predicted within acceptable limits. The C.O.V. for the displacement ductility values varies between 0.27 and 0.31, and that for the scale factors varies between 0.13 and 0.30. The above statistical values should be carefully interpreted since a relatively small number of ground motion records was employed in the analysis.

The scale factors shown in Tables 5.4, 5.5 and 5.7 may also be interpreted as reduction factors. In other words, instead of scaling a ground motion record by a factor F in order for a structure with a yield displacement U_Y to either experience a specified displacement ductility or dissipate a specified amount of hysteretic energy, the yield displacement may be reduced by 1/F and the structure will still either experience the same displacement ductility or dissipate the same amount of hysteretic energy. These reduction factors may be employed to derive a modified response spectrum from an elastic response spectrum for use in inelastic analysis by multiplying the ordinates of the latter by 1/F.

The reduction factors, 1/F, may be compared with those suggested by Newmark and Hall (40) and those obtained by Riddell and Newmark (51). Newmark and Hall suggested that an inelastic response spectrum for elastoplastic single-degree-of-freedom systems be derived from an elastic response spectrum by reducing the ordinates of the latter by a factor of $1/\mu$ in the displacement and velocity regions of the spectrum and by $1/\sqrt{2\mu-1}$ in the acceleration region independently of the amount of damping in the structure. The reduction factors obtained by Riddell and Newmark were derived from a statistical analysis of the response of nonlinear systems subjected to ten earthquake ground motions. They are based on displacement ductility and account for the amounts of damping in the structure.

In order to do such comparisons, the overall average of the scaling factors for structures with frequencies between 0.5 and 2.0 cps (velocity region of a response spectrum) and for structures with frequencies between 3.5 and 8.5 cps (acceleration region) are calculated. The results are shown in Table 5.8.

It can be seen that the reduction factors obtained in the various studies are relatively close. This is in part the result of employing intermediate values for the damping and displacement ductility, namely 5 and 3 respectively. The C.O.V. for the reduction factors calculated in this study is smaller than that calculated by Riddell and Newmark in the velocity region of a response spectrum. However, the opposite is true in the amplified acceleration region.

It should be remembered that the scale factors derived herein are for structures with a damping equal to 5 percent of critical. For a different value of damping, the maximum displacement experienced by the structure and the amount of energy dissipated by yielding vary. As a result, the scaling factor, F, for a given ground motion varies depending on the amount of damping in the structure.

CHAPTER 6

EARTHQUAKE RESPONSE AND ENERGY ABSORPTION IN TWO-STORY STRUCTURES

6.1 Introduction

In this chapter a limited pilot study of the earthquake response and energy absorption in two-story, shear-beam type structures is presented. The chapter begins with a description of the structural models and the input ground motions employed in this part of the study. Thereafter the earthquake response and energy absorption in these structures are investigated. This second part is divided into two major sections: one section deals with the response of linear elastic structural models, and the other deals with the response of nonlinear structural models. Finally a modal analysis employing modified (inelastic) response spectra of the two-degree-of-freedom structures examined is presented along with time-history analyses for comparison purposes.

6.2 Structural Models and Input Ground Motions

Four types of structural models, each with two-degree-of-freedom (only horizontal translation), are considered. These models are shown in Fig. 6.1 and will be referred to as follows: (a) Type I -- uniform stiffness and uniform mass distributions, (b) Type II -- uniform stiffness and nonuniform mass distributions, (c) Type III -- nonuniform stiffness and nonuniform mass distributions, and (d) Type IV -- nonuniform stiffness and uniform mass distributions. In the case of nonuniform (either stiffness or mass) distribution, the value at the second story level of the quantity referred to is equal to half its corresponding value at the first story level.

The structural models selected are intended to cover a fairly wide range of low-rise, stick-type model structures. At the same time, a small number of examples are employed in order to keep the cost of computations down. As a result, general rules (or conclusions) on the earthquake response of this type of structures may not be reached, but it is hoped this pilot study will lead to a better understanding than at present of their response.

The fundamental frequencies of the models selected fall in the velocity and amplified acceleration regions of a response spectrum. These frequencies are 0.5, 1.0, 2.0 and 5.0 cps. Only one damping value equal to 5 percent of critical is used in the analysis. Additional information regarding the elastic frequencies of vibration and the mode shapes for the various structural models are presented in Table 6.1.

Two earthquake records are used as input ground motions. One is the El-Centro record and corresponds to a long duration motion. The other is the Parkfield record and corresponds to a short duration motion.

6.3 Time-History Analysis

The response of the structural models described above to the El-Centro and the Parkfield ground motions is studied. The focus of this portion of the investigation is on the amount of energy imparted to the structure, and the amount of energy dissipated (by damping and inelastic deformations), the drift (or maximum relative displacement) and the displacement ductility at each story level. The displacement ductility is herein defined as the ratio of drift to yield displacement. In the following, first the response of linear elastic structural models, then that of nonlinear structural models is considered.

6.3.1 Linear Elastic Models -- The structural models are assumed to respond elastically when they are subjected to the El-Centro and the Parkfield ground motions. In this case no yielding occurs in the structure and all energy imparted to it is dissipated by viscous damping. The results of the time-history analyses for these structural models are shown in Tables 6.2 through 6.4.

The amount of energy per unit mass imparted to the various structural models is shown in Tables 6.2a and 6.2b. Also shown in the above tables is the value of E_I obtained from the energy input spectra for the El-Centro and the Parkfield records at a frequency equal to the fundamental frequency of the structural models considered. It can be seen that the amount of energy per unit mass imparted to a structure is essentially independent of the stiffness and mass distributions in that structure. It depends on the input ground motion and the fundamental frequency of the structure, and is about the same as that imparted to a single-degree-of-freedom oscillator with a natural frequency and damping equal to the fundamental frequency and damping of the original structure.

Since no yielding takes place in the structure, all the energy imparted to it is dissipated by damping, i.e., $E_D = E_I$. The percentage of the damping energy dissipated at each story level is shown in Tables 6.3a and 6.3b when the structures are subjected to the El-Centro and the Parkfield ground motions, respectively. This percentage is essentially independent of the ground motion and the fundamental frequency of the structure, except for Type IV model, but it depends on the stiffness and mass distributions in the structure. The percent of energy dissipated in the first story is highest for the model with uniform stiffness and nonuniform mass distribution and decreases as the second story becomes more flexible than the first story.

The maximum relative displacement at each story level is shown in Tables 6.4a and 6.4b. It can be seen that the maximum relative displacement occurs at the first story level for the models with uniform stiffness (Types I and II), and in general at the second story level for the models with nonuniform stiffness (Types III and IV).

The maximum relative displacements for the structural models with a fundamental frequency equal to 1.0 and 5.0 cps and the amount of energy imparted to them are, in general, higher when they are subjected to the El-Centro ground motion than when they are subjected to the Parkfield ground motion. The above may be predicted once the response and energy input spectra of both records are examined. The ordinates of the spectra for the El-Centro record are higher than those of the Parkfield record at a frequency equal to 1.0 and 5.0 cps. The opposite is true at a frequency equal to 0.5 and 2.0 cps.

6.3.2 Nonlinear Models -- In this case yielding is allowed to occur at the end of any member (herein column) whenever the bending moment at this end reaches the yield moment capacity M_Y of the member. It is appropriate that in a balanced structural frame, yielding may occur at the ends or along the beams, but this case is not considered herein. The yield moment M_Y is assumed to be proportional to the elastic stiffness of the member and may be computed as follows

$$M_Y = \frac{6EI}{L^2} \Delta_Y \tag{6.1}$$

where I and L are the moment of inertia and length of the member respectively, E is the modulus of elasticity of steel, and Δ_Y is the yield displacement. For the models with a fundamental frequency equal to 0.5, 1.0 and 2.0 cps, Δ_Y is arbitrarily assumed to be equal to one half the maximum relative

displacement experienced by the structural model in the elastic case whether this maximum displacement occured at the first or the second story level. The use of the same assumption for the yield displacement for the structural model with a fundamental frequency equal to 5 cps led to a displacement ductility as high as 20 in some cases. Since this value for the ductility factor is considered unrealistic, a yield displacement equal to 3/4 of the maximum relative displacement in the elastic case was employed.

The results of the time-history analyses for the various structural models are shown in Tables 6.5 through 6.8. The amount of energy per unit mass imparted to these models when they are subjected to the El-Centro and the Parkfield ground motions is shown in Tables 6.5a and 6.5b. Also shown in these tables is the value of E_I obtained from the energy input spectra for the El-Centro and the Parkfield records for structures with a displacement ductility equal to two. The actual displacement ductility experienced by the various structural models varies between about 1.5 and 4. The value of two herein employed is an average value. As in the elastic case, the amount of energy per unit mass imparted to a structure depends on the ground motion and the fundamental frequency of the structure, but it is essentially independent of the stiffness and mass distributions. It may also be approximated by the value of E_I obtained from the energy input spectrum for the ground motion considered. Except for the structural models with a fundamental frequency equal to 5 cps and subjected to the Parkfield ground motion, the value of E_I for the inelastic models is within 20 percent of that for the elastic models.

Since yielding is permitted to occur in the structural model, the energy imparted to it is dissipated in part by inelastic deformations and in part by viscous damping. The percent of the energy dissipated by yielding for the

various structural models and that for a single-degree-of-freedom structure with $\mu = 2$ are shown in Table 6.6. As for the energy input, the amount of energy dissipated by yielding in a structure depends on its fundamental frequency and the ground motion to which it is subjected. It is essentially independent of the stiffness and mass distributions, and is about the same as that for a single-degree-of-freedom structure with the same frequency, damping and displacement ductility as shown in Tables 6.6a and 6.6b.

The proportion of the hysteretic energy dissipated at each story level, however, depends on the stiffness and mass distributions in the structure. As shown in Tables 6.7a and 6.7b, for the models with uniform stiffness (Types I and II) most or all yielding occurs in the first story. For the models with nonuniform stiffness (Types III and IV) yielding takes place in both stories, and the maximum displacement ductility is more likely to occur at the second story level. Type III model which has nonuniform mass and stiffness distributions showed the best response as characterized by the most balanced energy dissipation and the closest displacement ductility values at the two story levels.

The amount of energy dissipated by damping is equal to the difference between that imparted to the structure and that dissipated by yielding. The percentage of damping energy dissipated in each story is shown in Table 6.8. It is about the same whether or not yielding occurs in the structure.

6.4 Modal Analysis

This section contains (a) a summary of the modal method for dynamic analysis of structures and (b) a comparison of the results obtained using this method with those of the time-history analyses.

6.4.1 Modal Method -- This method is well known (16,56) and only a brief review of the various steps involved in the solution procedure is herein included.

The set of simultaneous equations of motion governing the dynamic behavior of a multi-degree-of-freedom structure can be uncoupled if the normal modes of vibration are used as generalized coordinates. Each of the resulting independent differential equations is similar to the equation of motion of a single-degree-of-freedom oscillator and corresponds to one mode of vibration of the structure. The dynamic response may be obtained by solving each equation separately and then superposing the results.

The equation of motion of a structure with N degrees of freedom, Eq. 3.27, may be written as

$$\left[M\right]\left\{\ddot{U}(t)\right\} + \left[C\right]\left\{\dot{U}(t)\right\} + \left[K\right]\left\{U(t)\right\} = -\left[M\right]\left\{1\right\}\ddot{Y}(t) \tag{6.2}$$

For undamped free-vibration, the above matrix equation can be reduced to

$$\left[M\right]\left\{\ddot{U}(t)\right\} + \left[K\right]\left\{U(t)\right\} = \left\{0\right\} \tag{6.3}$$

If it is assumed that the free-vibration motion is simple harmonic

$$\left\{U(t)\right\} = \left\{\phi_n\right\}\sin(\omega_n t + \theta) \tag{6.4}$$

where $\{\phi_n\}$ represents the mode shape, ω_n represents the natural circular frequency and θ is a phase angle, then Eq. 6.3 reduces to

$$\left(\left[K\right] - \omega_n^2\left[M\right]\right)\left\{\phi_n\right\} = \left\{0\right\} \tag{6.5}$$

Equation 6.5 is called an eigenvalue equation and can be solved for the frequencies ω_n and their corresponding mode shapes $\{\phi_n\}$. It can be shown that the mode shapes satisfy the following orthogonality relationships

$$\left\{\phi_n\right\}^T\left[M\right]\left\{\phi_m\right\} = 0 \qquad m \neq n$$
$$\left\{\phi_n\right\}^T\left[K\right]\left\{\phi_m\right\} = 0 \qquad (6.6)$$

In order to uncouple the equations of motion, Eq. 6.2, the total displacements are written as the sum of modal components

$$\left\{U\right\} = \sum_{n=1}^{N}\left\{\phi_n\right\} q_n \qquad (6.7)$$

where N is equal to the number of degrees of freedom in the structure and q_n are the generalized coordinates. If Eq. 6.7 is substituted into Eq. 6.3 and the resulting equation premultiplied by $\{\phi_n\}^T$, the equation of motion for the n-th mode of vibration becomes

$$\ddot{q}_n + 2\xi_n\omega_n\dot{q}_n + \omega_n^2 q_n = -\gamma_n\ddot{Y} \qquad (6.8)$$

where ξ_n represents the amount of critical viscous damping in the n-th mode and γ_n denotes the participation factor which is given by

$$\gamma_n = \frac{\left\{\phi_n\right\}^T\left[M\right]\left\{1\right\}}{\left\{\phi_n\right\}^T\left[M\right]\left\{\phi_n\right\}} \qquad (6.9)$$

In the derivation of Eq. 6.8, it was assumed that the damping matrix satisfies the orthogonality condition $\{\phi\}^T\left[C\right]\{\phi\} = 0$ for m=n.

Equation 6.8 is similar to that of a single-degree-of-freedom oscillator vibrating with the frequency of the n-th mode. As a result, the maximum value of the displacement, denoted as D_n, can be obtained from a response spectrum and the maximum value of the n-th generalized coordinate is thus equal to

$$q_n = \gamma_n D_n \qquad (6.10)$$

The maximum displacements in the n-th mode are therefore, from Eq. 6.7,

$$\left\{U_n\right\} = \gamma_n\left\{\phi_n\right\} D_n \qquad (6.11)$$

Once the response for each mode has been determined, the results can be superposed to obtain an estimate of the structural displacements {U} . An upper limit to the story displacements can be obtained by taking the sum of the absolute values of the modal maxima, namely,

$$\left\{U\right\}_{max} = \sum_{n=1}^{N} \left| \gamma_n \left\{\phi_n\right\} D_n \right| \tag{6.12}$$

Another estimate of the maximum story displacements, based on the observation that the modal maxima do not occur in general at the same time, can be obtained by taking the square root of the sum of the squares of the modal responses, namely ,

$$\left\{U\right\}_{max} \doteq \sum_{n=1}^{N} (\gamma_n \left\{\phi_n\right\} D_n)^2 \tag{6.13}$$

Other response parameters such as inertial forces can be estimated in a manner similar to that used to evaluate the displacements.

6.4.2 Comparison of Results -- The modal method, summarized above, is based on superposition and therefore applies only to linear elastic systems. It may, however, be employed to obtain an estimate of the response quantities of interest for nonlinear systems. Accordingly one may use a modified (inelastic) instead of an elastic response spectrum to estimate the maximum response in each mode of vibration and then superpose the results.

In order to compare the results of the modal and time-history analyses, the smooth response spectrum used in the modal analysis was anchored to a 0.35g ground acceleration. This acceleration is equal to the maximum acceleration of the effective motion corresponding to the El-Centro and the Parkfield ground motions which were employed in the time-history analyses. The smooth spectra (elastic and inelastic) are constructed as recommended by

Newmark and Hall (41). First an elastic spectrum is drawn. The ordinates of this spectrum are then reduced by $1/\mu$ in the displacement and velocity regions of the response spectrum and by $1/\sqrt{2\mu-1}$ in the amplified acceleration region. The displacement values obtained from the resulting response spectrum correspond to the yield displacements and they should be multiplied by the ductility value μ to obtain the maximum displacements. The ductility value used to construct the inelastic spectrum is equal to 3 and may be compared to the values of about 2 to 4 obtained in the time-history analyses. The resulting spectra, shown in Fig. 6.2, are then used in the modal analysis.

The maximum displacements for the various structural models obtained from the modal analyses along with those of the time-history analyses are shown in Tables 6.9 and 6.10. The following observations regarding these results may be made.

(1) The modal method used in conjunction with an elastic response spectrum gave a conservative estimate of the maximum displacements obtained from an elastic time-history analysis, as can be seen from Table 6.9, except for the structural models with a fundamental frequency of 0.5 and 2.0 cps when subjected to Parkfield ground motion. This is expected since an effective motion with a 0.35g maximum acceleration represents an underestimate of the effect of the Parkfield motion on structures with frequencies between about 0.5 and 3 cps as noted earlier herein.

(2) The maximum displacements at the first story level obtained from a modal analysis using a modified (inelastic) response spectrum gave conservative estimates of the maximum displacements obtained by inelatic time-history analyses except in 8 out of 32 cases considered. The difference between the "exact" and the approximate values varied between 3 and 27 percent of the exact value. It was largest when yielding was concentrated in the

first story and the displacement ductility was higher than three which is the value employed in the construction of the modified response spectrum.

(3) The maximum displacements at the second story level obtained from a modal analysis using a modified (inelastic) response spectrum gave conservative estimates of the "exact" maximum displacements except in 2 out of 32 cases considered. In one case the maximum displacement was 6 percent less and in the other 27 percent less than the exact value. In the latter case, the maximum displacement ductility in the structure was four as compared to three which is the value employed in the construction of the inelastic response spectrum.

From the results of this limited pilot study it may be concluded that the displacements computed using modal analysis in conjunction with a modified (inelastic) response spectrum are within 20 percent of those obtained using time-history analysis for structurse with moderate displacement ductility (up to about five). They are within 10 percent of those obtained using time-history analyses for structures which experience "balanced" yielding as may be achieved in structures with a decreasing story shear strength in the upper stories.

TABLE 5.1 YIELD DISPLACEMENT AND YIELD RESISTANCE OBTAINED FROM A SMOOTH ELASTIC RESPONSE SPECTRUM ANCHORED TO A 0.15g MAXIMUM ACCELERATION

Frequency (cps)	Yield Displ. U_Y (in.)	Yield Resistance R_Y (g)
0.5	5.284	0.135
1.0	2.642	0.27
1.5	1.738	0.40
2.0	0.978	0.40
3.5	0.319	0.40
5.0	0.156	0.40
8.5	0.054	0.40

TABLE 5.2 ACTUAL SPECTRAL DISPLACEMENT BEFORE ANY SCALING

Ground Motion Record	Maximum Displacement U_m (in.)						
	f=0.5*	f=1.0*	f=1.5*	f=2.0*	f=3.5*	f=5.0*	f=8.5*
PACOIMA DAM	19.040	11.92	3.040	4.075	1.545	0.918	0.2160
BONDS CORNER	6.696	4.368	4.821	3.067	1.550	0.915	0.2510
MELENDY RANCH	2.010	0.780	0.560	0.366	0.520	0.578	0.1320
PARKFIELD	14.180	4.882	6.659	3.372	0.585	0.205	0.0820
COYOTE LAKE	5.851	5.493	3.575	1.743	0.509	0.271	0.0624
EL-CENTRO	6.851	5.051	3.016	1.880	0.580	0.260	0.0845
TAFT	3.263	1.545	1.276	0.850	0.294	0.171	0.0311
GAVILAN COLLEGE	0.210	0.116	0.128	0.203	0.100	0.090	0.0398

*f is in cps

TABLE 5.3 SCALE FACTOR FOR MAXIMUM DISPLACEMENT TO BE EQUAL TO YIELD DISPLACEMENT - ELASTIC RESPONSE

Ground Motion Record	Scale Factor $S(=U_Y/U_m)$						
	f=0.5*	f=1.0*	f=1.5*	f=2.0*	f=3.5*	f=5.0*	f=8.5*
PACOIMA DAM	0.28	0.22	0.57	0.24	0.21	0.17	0.25
BONDS CORNER	0.79	0.61	0.36	0.32	0.21	0.17	0.21
MELENDY RANCH	2.63	3.39	3.10	2.67	0.61	0.27	0.41
PARKFIELD	0.37	0.54	0.26	0.29	0.55	0.76	0.66
COYOTE LAKE	0.90	0.49	0.49	0.56	0.63	0.58	0.87
EL-CENTRO	0.77	0.52	0.58	0.52	0.58	0.60	0.64
TAFT	1.62	1.71	1.36	1.15	1.09	0.91	1.74
GAVILAN COLLEGE	25.16	22.74	13.61	4.83	3.19	1.73	1.36

*f is in cps

TABLE 5.4a SCALE FACTOR F FOR EQUAL DISPLACEMENT DUCTILITY OF THREE

Ground Motion Record	Scale Factor F for μ = 3						
	f=0.5*	f=1.0*	f=1.5*	f=2.0*	f=3.5*	f=5.0*	f=8.5*
PACOIMA DAM	3.53	4.00	1.66	3.52	2.33	2.29	1.55
BONDS CORNER	4.13	2.54	2.65	2.40	2.60	3.30	2.68
MELENDY RANCH	4.14	2.47	2.54	2.16	4.00	4.36	2.24
PARKFIELD	2.83	2.58	3.00	3.38	1.56	1.29	1.33
COYOTE LAKE	2.74	2.75	3.28	3.25	1.83	2.36	1.45
EL-CENTRO	4.41	4.17	3.55	3.65	3.11	1.86	1.55
TAFT	3.45	3.19	2.83	2.14	2.11	2.00	1.42
GAVILAN COLLEGE	2.93	2.40	3.54	4.48	2.12	2.15	2.93
Mean, $\bar{F}$	3.52	3.01	2.88	3.12	2.46	2.45	1.89
Std. Dev., σ	0.61	0.66	0.58	0.77	0.73	0.89	0.59
C. O. V., Ω	0.17	0.22	0.20	0.25	0.30	0.36	0.31

*f is in cps

TABLE 5.4b VALUE OF N FOR MODELS WITH DISPLACEMENT DUCTILITY EQUAL TO THREE

Ground Motion Record	Value of N for μ = 3						
	f=0.5*	f=1.0*	f=1.5*	f=2.0*	f=3.5*	f=5.0*	f=8.5*
PACOIMA DAM	2.17	3.34	3.11	4.23	3.73	3.15	1.46
BONDS CORNER	1.38	5.28	3.99	4.66	2.69	4.93	5.43
MELENDY RANCH	3.49	1.12	1.69	1.29	3.76	2.92	3.93
PARKFIELD	1.16	2.71	1.56	2.73	2.08	2.00	1.33
COYOTE LAKE	1.00	1.29	2.03	3.08	1.66	2.71	1.86
EL-CENTRO	5.17	3.96	5.41	6.99	5.94	2.29	1.08
TAFT	3.63	6.42	2.67	2.06	5.06	2.79	1.26
GAVILAN COLLEGE	2.37	2.06	3.92	3.25	1.15	1.02	4.43
Mean, $\bar{N}$	2.55	3.27	3.05	3.54	3.26	2.73	2.60
Std. Dev., σ	1.36	1.76	1.25	1.65	1.56	1.04	1.61
C.O.V., Ω	0.53	0.54	0.41	0.47	0.48	0.38	0.62

*f is in cps

TABLE 5.5a SCALE FACTOR F FOR EQUAL DISPLACEMENT DUCTILITY OF FIVE

Ground Motion Record	Scale Factor F For $\mu = 5$						
	f=0.5*	f=1.0*	f=1.5*	f=2.0*	f=3.5*	f=5.0*	f=8.5*
PACOIMA DAM	5.19	5.38	2.27	4.45	2.83	2.76	1.72
BONDS CORNER	4.89	5.49	5.25	3.27	4.30	4.22	3.36
MELENDY RANCH	7.72	4.08	3.77	3.00	6.88	7.79	3.57
PARKFIELD	5.44	3.23	4.31	4.46	1.81	1.37	1.45
COYOTE LAKE	5.07	4.08	4.37	3.94	2.20	2.91	1.56
EL-CENTRO	5.59	5.89	4.35	6.47	3.47	3.24	1.77
TAFT	5.34	3.81	4.42	4.19	2.47	3.25	1.74
GAVILAN COLLEGE	3.73	3.32	5.14	7.49	2.85	3.03	4.62
Mean, $\bar{F}$	5.37	4.41	4.24	4.66	3.35	3.57	2.47
Std. Dev.,	1.04	0.97	0.87	1.44	1.52	1.76	1.12
C.O.V.,	0.19	0.22	0.20	0.31	0.45	0.49	0.45

*f is in cps

TABLE 5.5b VALUE OF N FOR MODELS WITH DISPLACEMENT DUCTILITY EQUAL TO FIVE

Ground Motion Record	Value of N For $\mu = 5$						
	f=0.5*	f=1.0*	f=1.5*	f=2.0*	f=3.5*	f=5.0*	f=8.5*
PACOIMA DAM	2.17	2.72	4.07	3.57	3.42	3.00	1.51
BONDS CORNER	4.36	10.50	7.06	4.49	4.80	5.46	6.08
MELENDY RANCH	4.07	1.93	2.14	1.69	4.78	3.72	5.26
PARKFIELD	1.68	2.42	1.43	2.26	2.08	1.90	1.42
COYOTE LAKE	1.38	1.22	1.74	2.40	2.20	3.40	2.07
EL-CENTRO	4.33	3.86	4.41	11.70	4.60	7.89	1.18
TAFT	4.09	4.59	4.23	6.47	4.04	8.05	2.44
GAVILAN COLLEGE	1.87	2.18	3.48	3.56	1.31	1.29	6.38
Mean, $\bar{N}$	2.99	3.68	3.57	4.52	3.40	4.34	3.29
Std. Dev., σ	1.24	2.77	1.72	3.06	1.29	2.40	2.08
C.O.V., Ω	0.41	0.75	0.48	0.68	0.38	0.55	0.63

* f is in cps

Table 5.6 TARGET VALUE FOR HYSTERETIC ENERGY E_H

Frequency (cps)	Yield Displ. U_Y (in.)	Displ. Ductility μ	N^*	E_H $(in./sec)^2$
0.5	5.284	3.0	3.0	1650.
1.0	2.642	3.0	3.0	1650.
1.5	1.738	3.0	3.0	1650.
2.0	0.978	3.0	2.0	604.
3.5	0.319	3.0	2.0	197.
5.0	0.156	3.0	2.0	96.1
8.5	0.054	3.0	1.5	25.1

$$^*N = \frac{E_H}{\omega^2 U_Y^2(\mu-1)}$$

TABLE 5.7a SCALE FACTOR FOR EQUAL HYSTERETIC ENERGY E_H

Ground Motion Record	Scale Factor F For Equal E_H						
	f=0.5*	f=1.0*	f=1.5*	f=2.0*	f=3.5*	f=5.0*	f=8.5*
PACOIMA DAM	4.13	3.73	1.66	2.66	2.00	2.05	1.62
BONDS CORNER	1.58	2.04	2.35	1.80	2.32	2.46	1.88
MELENDY RANCH	3.71	3.67	3.17	2.49	2.91	3.57	1.71
PARKFIELD	5.00	2.69	4.38	2.85	1.56	1.29	1.36
COYOTE LAKE	5.35	4.50	4.02	2.74	1.87	2.12	1.41
EL-CENTRO	3.48	3.79	2.81	2.24	2.32	1.90	1.64
TAFT	3.14	2.35	2.92	2.14	1.68	1.81	1.45
GAVILAN COLLEGE	3.28	2.79	2.99	3.32	2.57	2.73	1.98
Mean, $\bar{F}$	3.71	3.20	3.04	2.53	2.15	2.24	1.63
Std. Dev., σ	1.10	0.79	0.81	0.44	0.43	0.64	0.21
C.O.V., Ω	0.30	0.25	0.27	0.17	0.20	0.29	0.13

*f is in cps

TABLE 5.7b DISPLACEMENT DUCTILITY FOR MODELS WHICH DISSIPATE THE SAME AMOUNT OF HYSTERETIC ENERGY

Ground Motion Record	Displacement Ductility μ						
	f=0.5*	f=1.0*	f=1.5*	f=2.0*	f=3.5*	f=5.0*	f=8.5*
PACOIMA DAM	3.73	2.67	3.00	2.13	2.20	2.30	3.90
BONDS CORNER	2.21	2.23	2.82	1.63	2.75	2.05	1.64
MELENDY RANCH	2.88	4.42	4.03	4.00	2.65	2.10	2.26
PARKFIELD	4.74	3.24	5.12	2.30	3.00	3.00	3.30
COYOTE LAKE	5.27	5.43	4.33	2.94	3.28	2.48	2.37
EL-CENTRO	2.30	2.75	2.20	1.84	2.10	3.10	3.60
TAFT	2.66	2.39	3.17	2.96	1.66	2.40	3.28
GAVILAN COLLEGE	3.85	3.91	2.45	2.35	4.35	4.49	1.77
Mean, $\bar{\mu}$	3.46	3.38	3.39	2.52	2.75	2.74	2.77
Std. Dev., σ	1.06	1.05	0.94	0.71	0.78	0.75	0.81
C.O.V., Ω	0.31	0.31	0.28	0.28	0.28	0.27	0.29

*f is in cps

TABLE 5.8a COMPARISON OF RESULTS FOR EQUAL DISPLACEMENT DUCTILITY WITH THOSE OF OTHER STUDIES

Reference	Displ. Ductility μ	Velocity Region		Acceleration Region	
		Reduction Factor	Coefficient of Variation	Reduction Factor	Coefficient of Variation
Present Study	3.0	0.319	0.22	0.441	0.35
Newmark & Hall (40)	3.0	0.333	--	0.446	--
Riddell & Newmark (51)	3.0	0.328	0.35	0.455	0.17
Present Study	5.0	0.214	0.25	0.319	0.50
Newmark & Hall (39)	5.0	0.200	--	0.333	--
Riddell & Newmark (51)	5.0	0.229	0.36	0.342	0.17

TABLE 5.8b COMPARISON OF RESULTS FOR EQUAL HYSTERETIC ENERGY WITH THOSE OF OTHER STUDIES

Reference	Velocity Region			Acceleration Region		
	Displ. Ductility	Reduction Factor	C.O.V.	Displ. Ductility	Reduction Factor	C.O.V.
Present Study	3.18	0.321	0.30	2.75	0.500	0.27
Newmark & Hall (39)*	3.18	0.314	--	2.75	0.471	--
Riddell & Newmark (51)*	3.18	0.321	0.35	2.75	0.450	0.17

*Results based on equal displacement ductility

TABLE 6.1 NATURAL FREQUENCIES AND MODE SHAPES OF ELASTIC VIBRATION

Structure type		I	II	III	IV
f_2/f_1*		2.617	2.414	2.000	2.414
Mode	Story				
1	2	1.000	1.000	1.000	1.000
	1	0.618	0.707	0.500	0.414
2	2	-0.618	-1.000	-1.000	-0.414
	1	1.000	0.707	1.000	1.000

* f_1 is the fundamental frequency and f_2 is the second frequency of elastic vibration.

TABLE 6.2a ENERGY INPUT $(IN/SEC)^2$ FOR STRUCTURES SUBJECTED TO EL-CENTRO - ELASTIC RESPONSE

Structural Model	f_1 = 0.5 (cps)	f_1 = 1.0 (cps)	f_1 = 2.0 (cps)	f_1 = 5.0 (cps)
Type I	567.	979.	1088.	243.
Type II	579.	990.	1110.	249.
Type III	588.	1004.	1056.	231.
Type IV	686.	948.	1010.	221.
SDF*	586.	1070.	1165.	250.

* E_I for a single-degree-of-freedom structure with β = 5% and subjected to El-Centro (may be obtained from energy spectrum).

TABLE 6.2b ENERGY INPUT $(IN/SEC)^2$ FOR STRUCTURES SUBJECTED TO PARKFIELD - ELASTIC RESPONSE

Structural Model	f_1 = 0.5 (cps)	f_1 = 1.0 (cps)	f_1 = 2.0 (cps)	f_1 = 5.0 (cps)
Type I	1603.	915.	1205.	50.
Type II	1575.	916.	1236.	51.
Type III	1477.	961.	1136.	47.
Type IV	1546.	875.	1093.	45.
SDF*	1575.	995.	1110.	52.

* E_I for a single-degree-of-freedom structure with β = 5% and subjected to Parkfield (may be obtained from energy spectrum).

TABLE 6.3a PERCENT OF DAMPING ENERGY DISSIPATED IN THE FIRST STORY* FOR STRUCTURES SUBJECTED TO EL-CENTRO - ELASTIC RESPONSE

Structural Model	f_1 = 0.5 (cps)	f_1 = 1.0 (cps)	f_1 = 2.0 (cps)	f_1 = 5.0 (cps)
Type I	31.	28.	28.	28.
Type II	49.	49.	50.	50.
Type III	41.	35.	34.	34.
Type IV	35.	20.	17.	15.

* The percent of E_D dissipated at the second story level is equal to 100 minus that dissipated at the first story level.

TABLE 6.3b PERCENT OF DAMPING ENERGY DISSIPATED IN THE FIRST STORY* FOR STRUCTURES SUBJECTED TO PARKFIELD - ELASTIC RESPONSE

Structural Model	f_1 = 0.5 (cps)	f_1 = 1.0 (cps)	f_1 = 2.0 (cps)	f_1 = 5.0 (cps)
Type I	31.	28.	28.	28.
Type II	50.	49.	50.	51.
Type III	35.	35.	34.	34.
Type IV	24.	49.	15.	16.

* The percent of E_D dissipated at the second story level is equal to 100 minus that dissipated at the first story level.

TABLE 6.4a MAXIMUM RELATIVE DISPLACEMENT (IN) FOR STRUCTURES SUBJECTED TO EL-CENTRO - ELASTIC RESPONSE

Structural Model	Story	f_1 = 0.5 cps	f_1 = 1.0 cps	f_1 = 2.0 cps	f_1 = 5.0 cps
Type I	1	5.43	3.89	1.49	0.19
	2	3.43	2.58	1.00	0.12
Type II	1	6.14	4.26	1.73	0.22
	2	3.77	1.91	0.80	0.10
Type III	1	5.18	3.33	1.47	0.18
	2	6.14	3.75	1.71	0.17
Type IV	1	5.34	2.63	1.05	0.13
	2	7.54	3.83	1.60	0.19

TABLE 6.4b MAXIMUM RELATIVE DISPLACEMENT (IN) FOR STRUCTURES SUBJECTED TO PARKFIELD - ELASTIC RESPONSE

Structural Model	Story	f_1 = 0.5 cps	f_1 = 1.0 cps	f_1 = 2.0 cps	f_1 = 5.0 cps
Type I	1	10.52	3.81	2.63	0.15
	2	9.32	2.60	1.53	0.08
Type II	1	11.36	4.23	3.08	0.18
	2	6.83	2.02	1.20	0.06
Type III	1	8.96	3.68	2.44	0.15
	2	12.72	4.31	2.27	0.12
Type IV	1	7.74	2.97	1.89	0.12
	2	13.66	4.04	2.40	0.13

TABLE 6.5a ENERGY INPUT $(IN/SEC)^2$ FOR STRUCTURES SUBJECTED TO EL-CENTRO - INELASTIC RESPONSE

Structural Model	f_1 = 0.5 (cps)	f_1 = 1.0 (cps)	f_1 = 2.0 (cps)	f_1 = 5.0 (cps)
Type I	475.	1039.	1220.	243.
Type II	470.	1019.	1236.	250.
Type III	540.	1036.	1171.	231.
Type IV	667.	1053.	1158.	217.
SDF*	483.	950.	1256.	255.

* E_I for a single-degree-of-freedom structure with β = 5% μ = 2 and subjected to El-Centro (may be obtained from energy spectrum).

TABLE 6.5b ENERGY INPUT $(IN/SEC)^2$ FOR STRUCTURES SUBJECTED TO PARKFIELD - INELASTIC RESPONSE

Structural Model	f_1 = 0.5 (cps)	f_1 = 1.0 (cps)	f_1 = 2.0 (cps)	f_1 = 5.0 (cps)
Type I	1240.	1210.	1539.	180.
Type II	1203.	1361.	1582.	171.
Type III	1344.	1191.	1447.	162.
Type IV	1544.	1248.	1221.	84.
SDF*	1230.	1360.	1542.	110.

* E_I for a single-degree-of-freedom structure with β = 5%, μ = 2 and subjected to Parkfield (may be obtained from energy spectrum).

TABLE 6.6a PERCENT OF HYSTERETIC ENERGY FOR STRUCTURES SUBJECTED TO EL-CENTRO

Structural Model	f_1 = 0.5 (cps)	f_1 = 1.0 (cps)	f_1 = 2.0 (cps)	f_1 = 5.0 (cps)
Type I	33.	36.	37.	11.
Type II	36.	36.	39.	12.
Type III	35.	39.	30.	11.
Type IV	41.	37.	35.	6.
SDF*	36.	48.	46.	17.

* Percent of E_H for a single-degree-of-freedom structure with β = 5%, μ = 2 and subjected to El-Centro.

TABLE 6.6b PERCENT OF HYSTERETIC ENERGY FOR STRUCTURES SUBJECTED TO PARKFIELD

Structural Model	f_1 = 0.5 (cps)	f_1 = 1.0 (cps)	f_1 = 2.0 (cps)	f_1 = 5.0 (cps)
Type I	47.	58.	61.	66.
Type II	49.	51.	60.	65.
Type III	40.	48.	59.	67.
Type IV	46.	50.	54.	42.
SDF*	48.	50.	65.	48.

* Percent of E_H for a single-degree-of-freedom structure with β = 5%, μ = 2 and subjected to Parkfield.

TABLE 6.7a PERCENT OF HYSTERETIC ENERGY AND DISPLACEMENT DUCTILITY AT EACH STORY LEVEL FOR STRUCTURES SUBJECTED TO EL-CENTRO

Structural Model	Story	f_1 = 0.5 cps		f_1 = 1.0 cps		f_1 = 2.0 cps		f_1 = 5.0 cps	
		% E_H	μ	% E_H	μ	% E_H	μ	% E_H	μ
Type I	1	98.	2.13	100.	1.76	100.	1.79	100.	1.92
	2	2.	1.04	0.	0.98*	0.	1.00	0.	0.84*
Type II	1	100.	2.27	100.	1.57	100.	1.76	100.	1.86
	2	0.	0.70*	0.	0.59*	0.	0.68*	0.	0.55*
Type III	1	32.	1.32	43.	1.67	85.	2.17	61.	1.48
	2	68.	1.72	57.	1.82	15.	1.39	39.	1.82
Type IV	1	27.	1.31	7.	1.11	15.	1.36	0.	0.84*
	2	73.	1.46	93.	2.64	85.	2.94	100.	1.71

* μ less than 1.0 corresponds to elastic response at the corresponding story level.

TABLE 6.7b PERCENT OF HYSTERETIC ENERGY AND DISPLACEMENT DUCTILITY AT EACH STORY LEVEL FOR STRUCTURES SUBJECTED TO PARKFIELD

Structural Model	Story	f_1 = 0.5 cps		f_1 = 1.0 cps		f_1 = 2.0 cps		f_1 = 5.0 cps	
		% E_H	μ	% E_H	μ	% E_H	μ	% E_H	μ
Type I	1	93.	2.41	97.	2.81	100.	2.43	100.	4.57
	2	7.	1.11	3.	1.09	0.	0.85*	0.	0.73*
Type II	1	100.	2.30	100.	3.00	100.	2.12	100.	3.79
	2	0.	0.67	0.	0.71*	0.	0.62*	0.	0.50*
Type III	1	60.	1.48	16.	1.26	74.	1.98	95.	4.62
	2	40.	1.61	84.	2.51	26.	1.43	5.	1.29
Type IV	1	9.	1.08	2.	1.02	5.	1.05	33.	1.61
	2	91.	2.27	98.	4.22	95.	2.43	67.	2.38

*μ less than 1.0 corresponds to elastic response at the corresponding story level.

TABLE 6.8a PERCENT OF DAMPING ENERGY DISSIPATED IN THE FIRST STORY* FOR STRUCTURES SUBJECTED TO EL-CENTRO

Structural Model	f_1 = 0.5 (cps)	f_1 = 1.0 (cps)	f_1 = 2.0 (cps)	f_1 = 5.0 (cps)
Type I	33.	29.	31.	28.
Type II	49.	50.	51.	50.
Type III	43.	36.	35.	34.
Type IV	41.	24.	18.	15.

* The percent of E_D dissipated at the second story level is equal to 100 minus that dissipated at the first story level.

TABLE 6.8b PERCENT OF DAMPING ENERGY DISSIPATED IN THE FIRST STORY* FOR STRUCTURES SUBJECTED TO PARKFIELD

Structural Model	f_1 = 0.5 (cps)	f_1 = 1.0 (cps)	f_1 = 2.0 (cps)	f_1 = 5.0 (cps)
Type I	36.	29.	32.	30.
Type II	53.	51.	52.	51.
Type III	36.	33.	35.	36.
Type IV	26.	20.	18.	16.

* The percent of E_D dissipated at the second story level is equal to 100 minus that dissipated at the first story level.

TABLE 6.9a COMPARISON OF VALUES OF MAXIMUM DISPLACEMENT (IN) OBTAINED USING MODAL AND TIME-HISTORY ANALYSES - ELASTIC RESPONSE

Structural Model	Story	f_1 = 0.5 cps			f_1 = 1.0 cps		
		Modal*	El-Centro	Parkfield	Modal*	El-Centro	Parkfield
Type I	1	10.19	5.43	10.52	4.82	3.89	3.81
	2	15.20	7.74	17.68	7.43	5.77	5.65
Type II	1	11.24	6.14	11.36	5.48	4.26	4.23
	2	15.90	3.77	18.18	7.75	6.17	6.02
Type III	1	10.25	5.18	8.96	4.87	3.33	3.68
	2	18.44	9.26	20.42	8.97	6.77	6.74
Type IV	1	8.70	5.34	7.74	3.87	2.63	2.97
	2	15.90	8.50	18.18	7.75	6.17	6.02

* Maximum displacements are obtained by the sum of the absolute values of the modal maxima.

TABLE 6.9b COMPARISON OF VALUES OF MAXIMUM DISPLACEMENT (IN) OBTAINED USING MODAL AND TIME-HISTORY ANALYSES - ELASTIC RESPONSE

Structural Model	Story	f_1 = 2.0 cps			f_1 = 5.0 cps		
		Modal*	El-Centro	Parkfield	Modal*	El-Centro	Parkfield
Type I	1	1.77	1.49	2.63	0.28	0.19	0.15
	2	2.77	2.42	4.16	0.44	0.30	0.23
Type II	1	2.04	1.73	3.08	0.32	0.22	0.18
	2	2.88	2.51	4.27	0.46	0.31	0.24
Type III	1	1.74	1.47	2.44	0.28	0.18	0.15
	2	3.29	2.88	4.71	0.53	0.33	0.26
Type IV	1	1.36	1.05	1.89	0.21	0.13	0.12
	2	2.88	2.51	4.27	0.46	0.31	0.24

* Maximum displacements are obtained by the sum of the absolute values of the modal maxima.

TABLE 6.10a COMPARISON OF VALUES OF MAXIMUM DISPLACEMENT (IN) OBTAINED USING MODAL AND TIME-HISTORY ANALYSES - INELASTIC RESPONSE

Structural Model	Story	f_1 = 0.5 cps			f_1 = 1.0 cps		
		Modal*	El-Centro	Parkfield	Modal*	El-Centro	Parkfield
Type I	1	10.20	5.80	12.68	4.95	3.44	5.37
	2	15.21	8.00	13.94	7.50	4.56	6.70
Type II	1	11.25	6.97	13.03	5.55	3.35	6.14
	2	15.90	8.28	14.70	7.86	4.49	7.13
Type III	1	10.25	4.05	9.39	5.13	3.12	2.72
	2	18.45	7.76	16.19	9.24	5.89	6.04
Type IV	1	8.70	4.94	7.36	4.14	2.12	2.06
	2	15.90	7.30	17.00	7.86	5.43	9.87

* Maximum displacements are obtained by the sum of the absolute values of the modal maxima.

TABLE 6.10b COMPARISON OF VALUES OF MAXIMUM DISPLACEMENT (IN) OBTAINED USING MODAL AND TIME-HISTORY ANALYSES - INELASTIC RESPONSE

Structural Model	Story	f_1 = 2.0 cps			f_1 = 5.0 cps		
		Modal*	El-Centro	Parkfield	Modal*	El-Centro	Parkfield
Type I	1	2.37	1.34	3.20	0.38	0.27	0.52
	2	3.72	1.77	3.57	0.61	0.36	0.60
Type II	1	2.73	1.53	3.26	0.45	0.30	0.51
	2	3.87	1.92	3.65	0.63	0.37	0.57
Type III	1	2.34	1.85	2.41	0.39	0.20	0.51
	2	4.41	2.60	4.08	0.73	0.42	0.58
Type IV	1	1.83	1.90	1.26	0.29	0.12	0.16
	2	3.87	2.57	3.53	0.63	0.36	0.37

* Maximum displacements are obtained by the sum of the absolute values of the modal maxima.

FIGURES

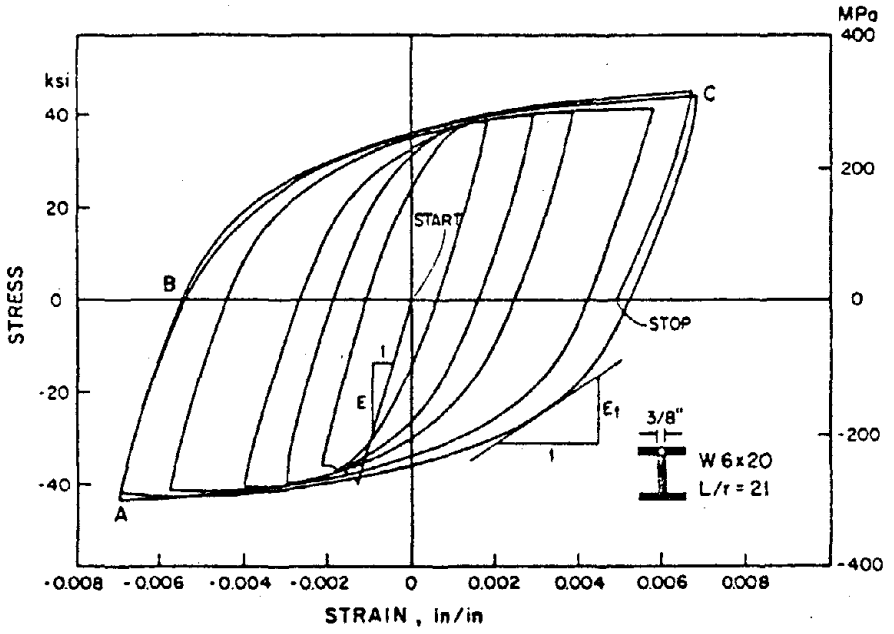

FIG. 2.1 UNIAXIAL HYSTERETIC LOOPS. AFTER POPOV AND PETERSON (47).

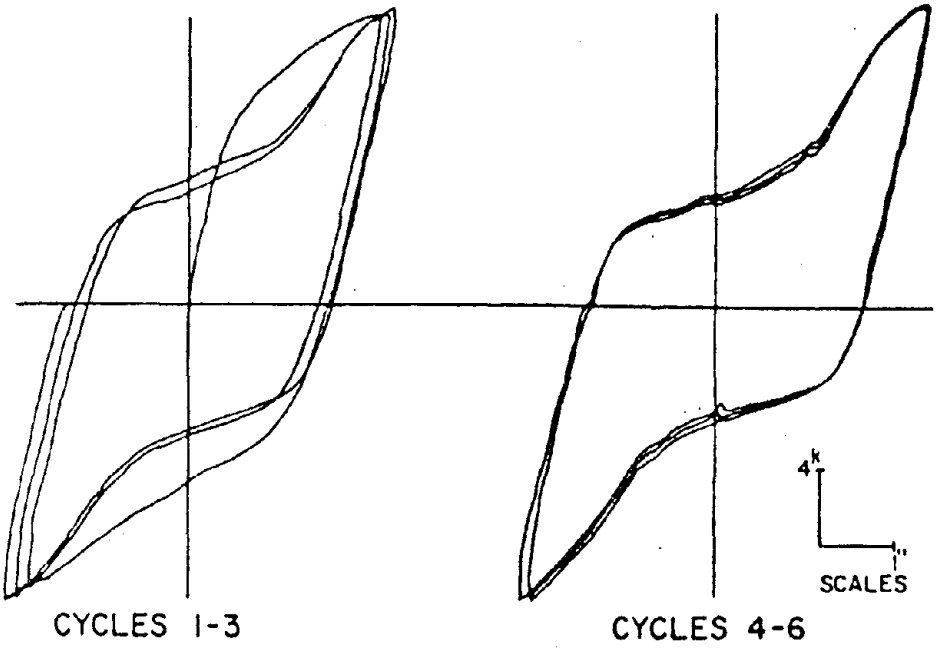

FIG. 2.2 HYSTERETIC LOOPS FOR CANTILEVER WITH BOLTED CONNECTION. AFTER POPOV AND PINKNEY (48).

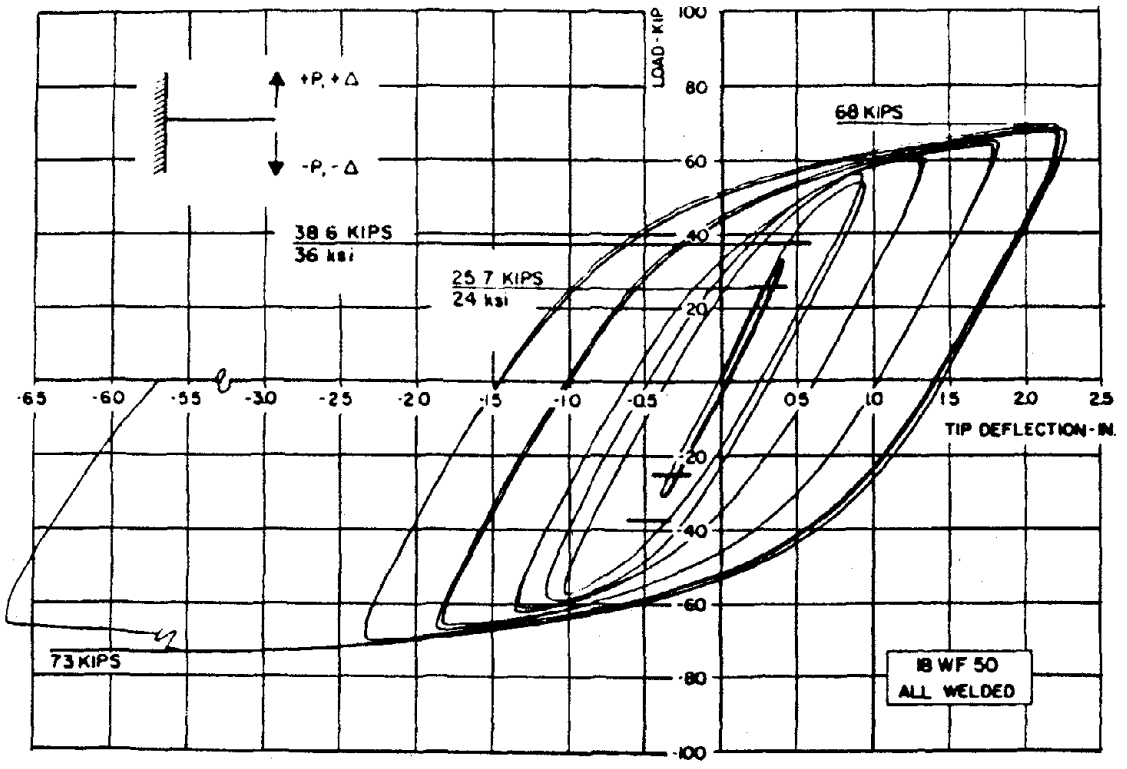

FIG. 2.3 HYSTERETIC LOOPS FOR CANTILEVER WITH WELDED CONNECTION. AFTER POPOV AND STEPHEN (49).

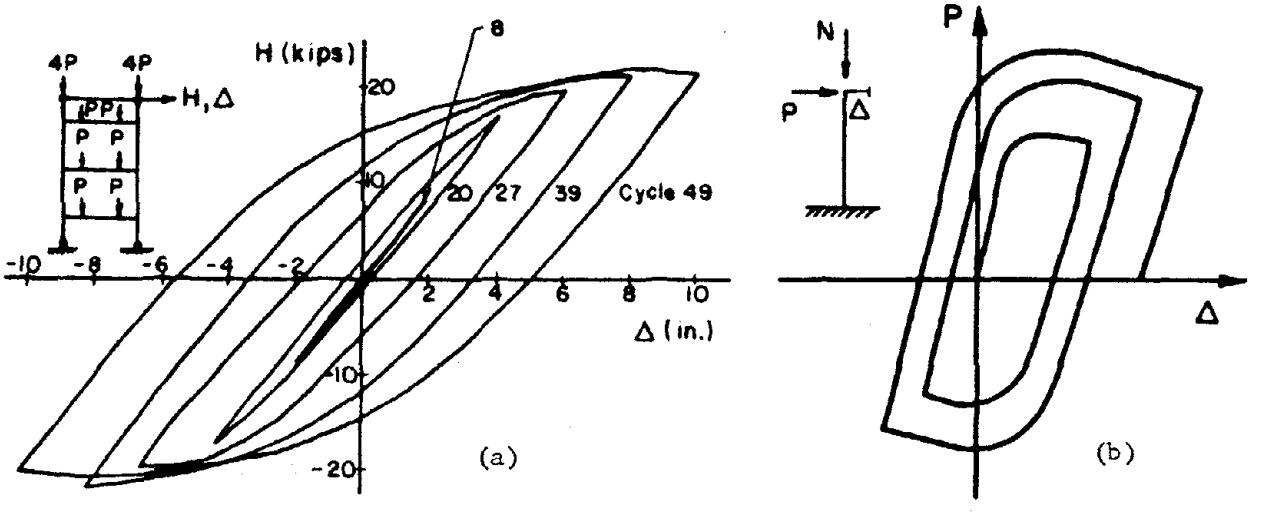

FIG. 2.4 HYSTERETIC LOOPS FOR MOMENT-RESISTING UNBRACED STEEL FRAME. AFTER CARPENTER AND LU (13).

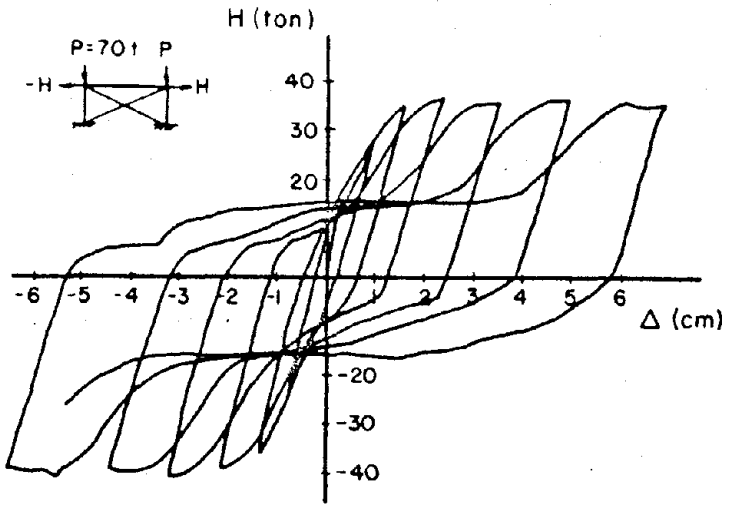

FIG. 2.5 HYSTERETIC LOOPS FOR X-BRACED STEEL FRAME. AFTER WAKABAYASHI (64).

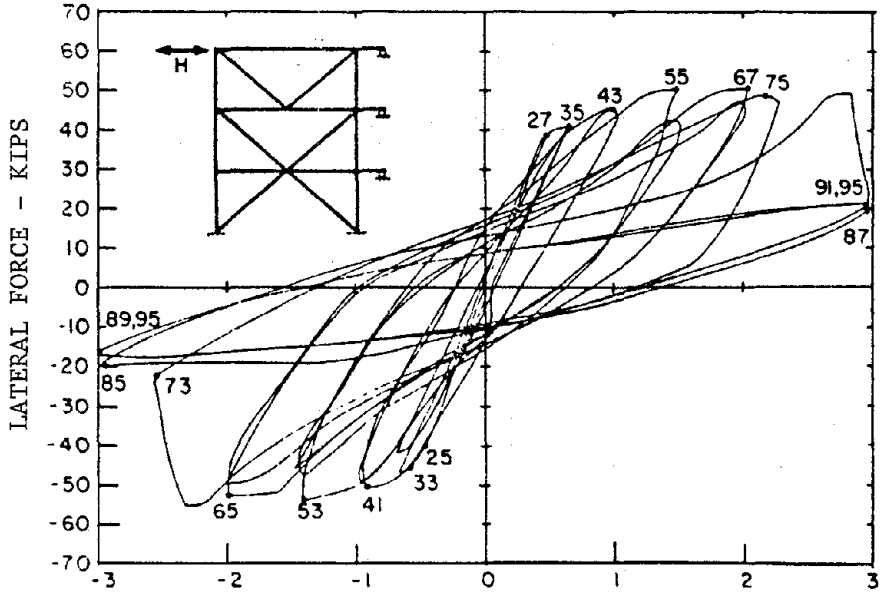

LATERAL DISPLACEMENT - IN.

FIG. 2.6 HYSTERTIC LOOPS FOR K-BRACED STEEL FRAME. AFTER MAISON AND POPOV (33).

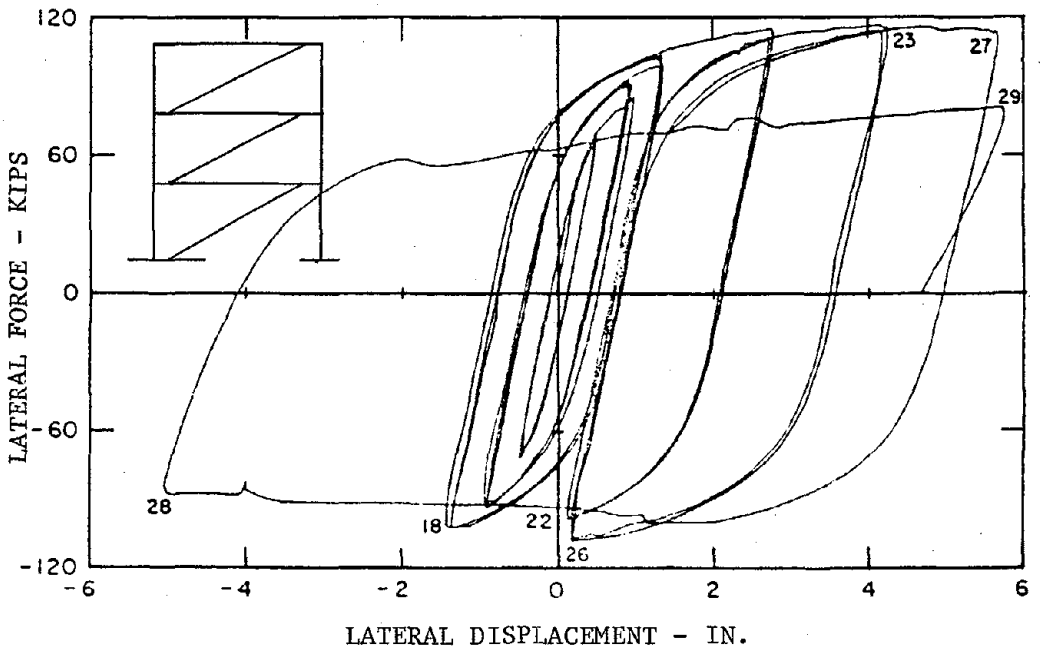

FIG. 2.7 HYSTERETIC LOOPS FOR ECCENTRICALLY BRACED STEEL FRAME. AFTER ROEDER AND POPOV (52).

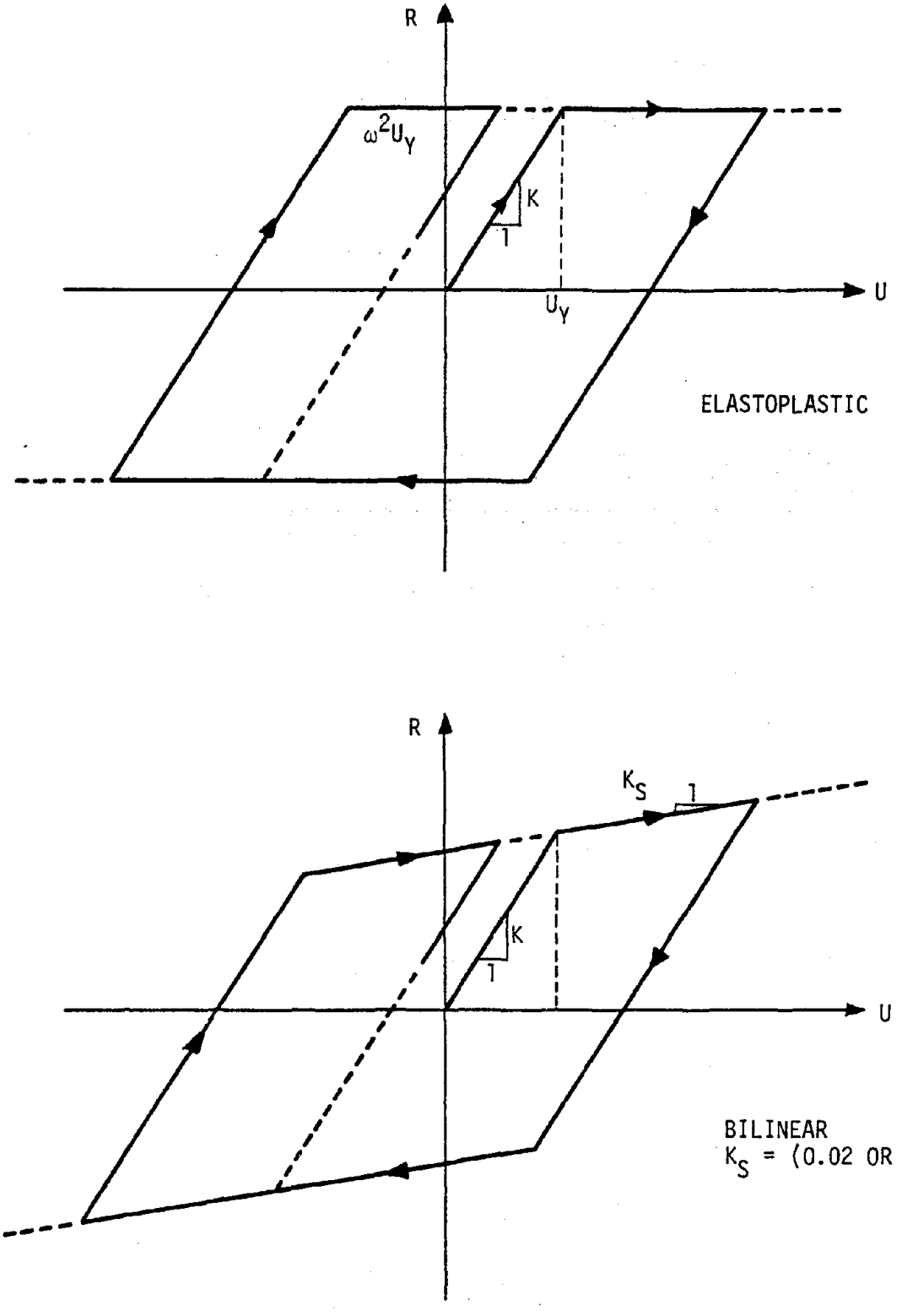

FIG. 2.8 NONLINEAR MODELS USED IN THIS STUDY

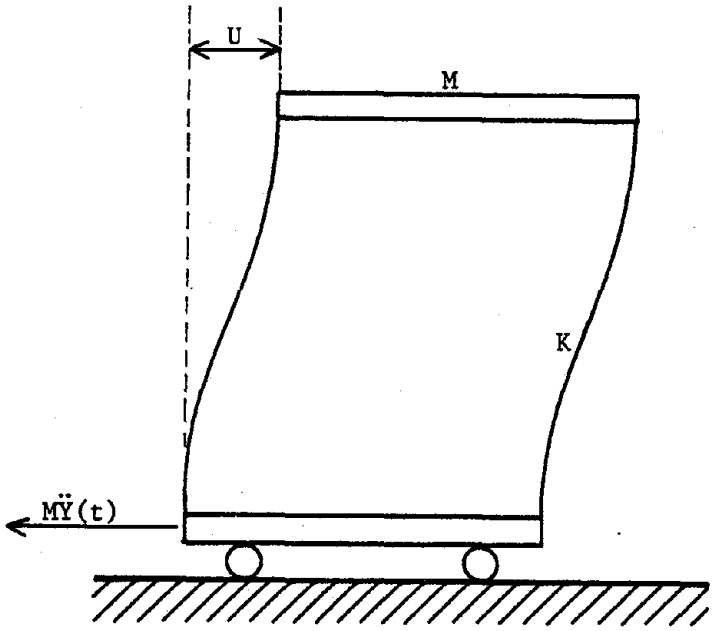

FIG. 3.1 SINGLE-DEGREE-OF-FREEDOM STRUCTURE SUBJECTED TO A BASE EXCITATION $\ddot{Y}(t)$

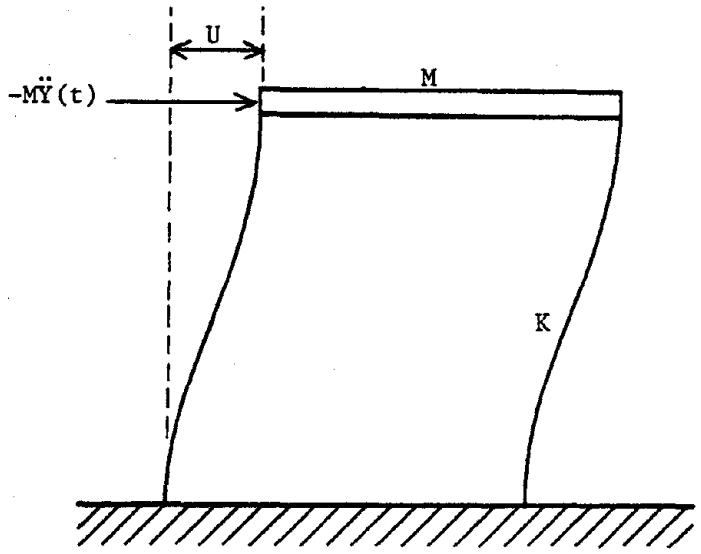

FIG. 3.2 SINGLE-DEGREE-OF-FREEDOM STRUCTURE SUBJECTED TO A LATERAL FORCE OF MAGNITUDE $-M\ddot{Y}(t)$

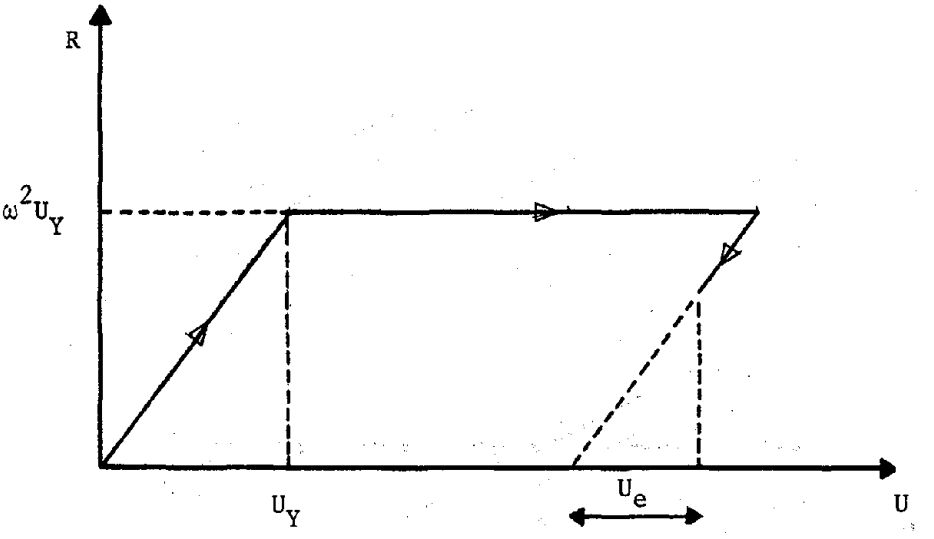

$$E_S = \frac{1}{2}\omega^2 U_e^2$$

FIG. 3.3 INTERNAL RESISTANCE PER UNIT MASS VS. RELATIVE DISPLACEMENT

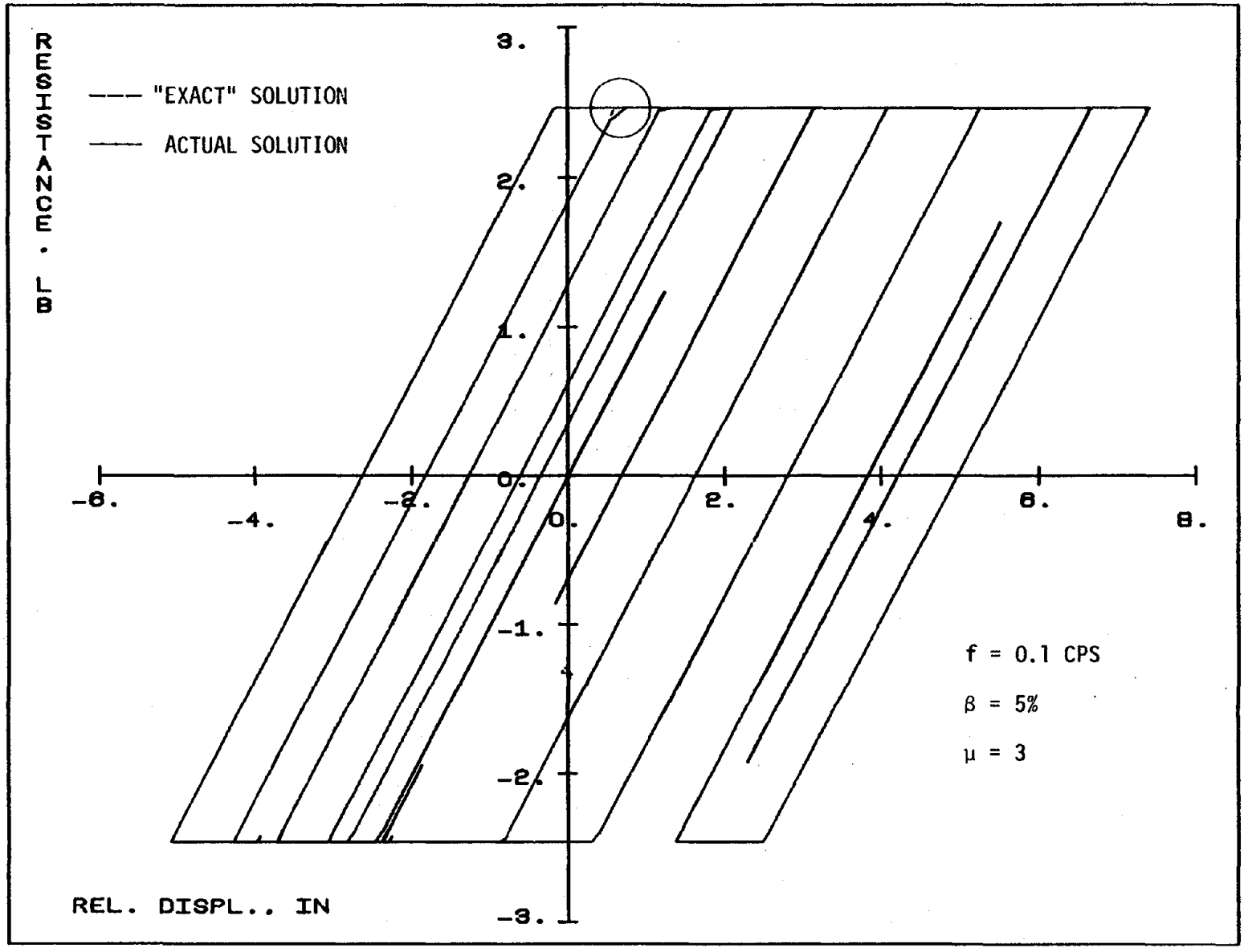

FIG. 3.4 INTERNAL FORCE VS. DEFORMATION FOR A STRUCTRUE SUBJECTED TO EL-CENTRO

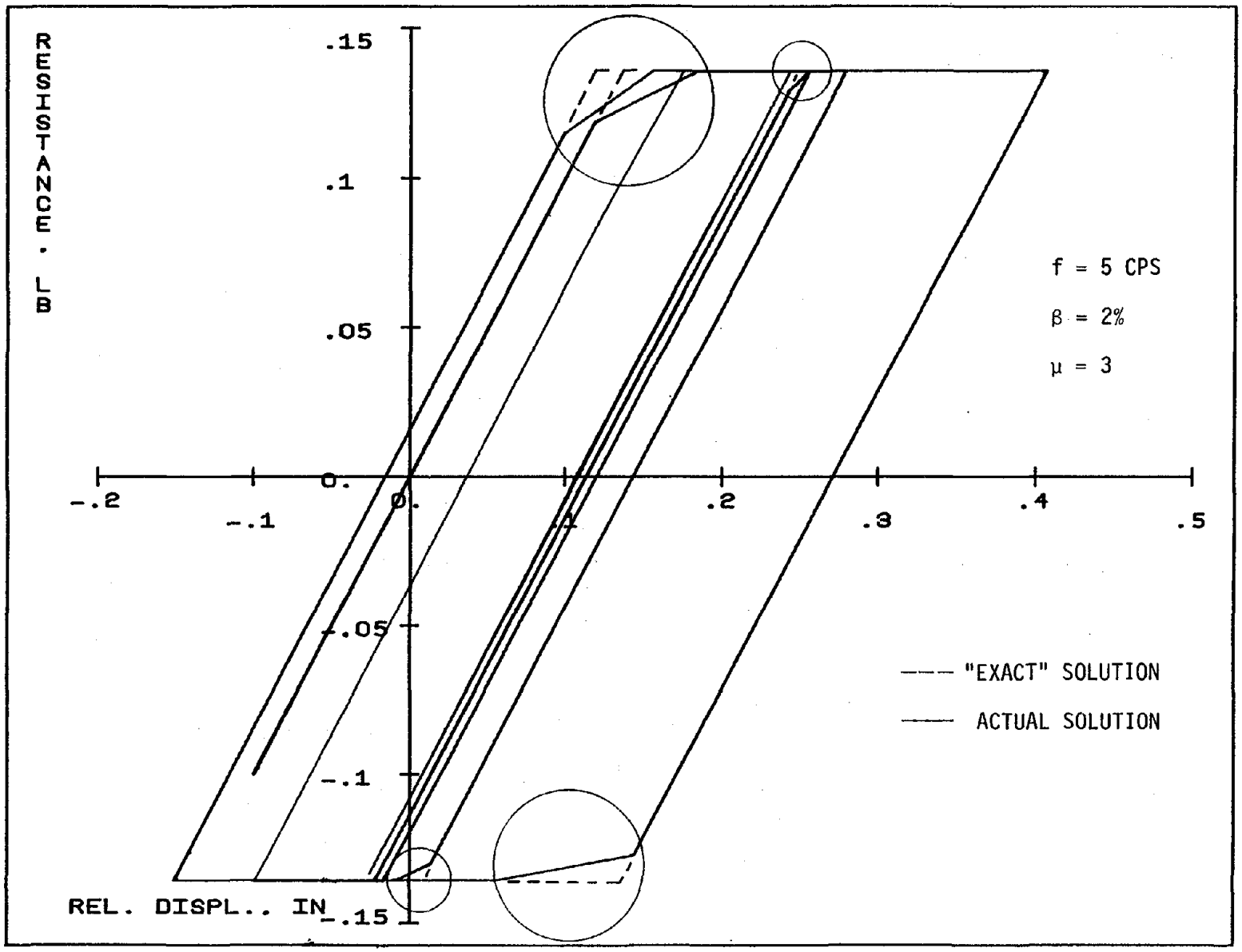

FIG. 3.5 INTERNAL FORCE VS. DEFORMATION FOR A STRUCTURE SUBJECTED TO MELENDY RANCH

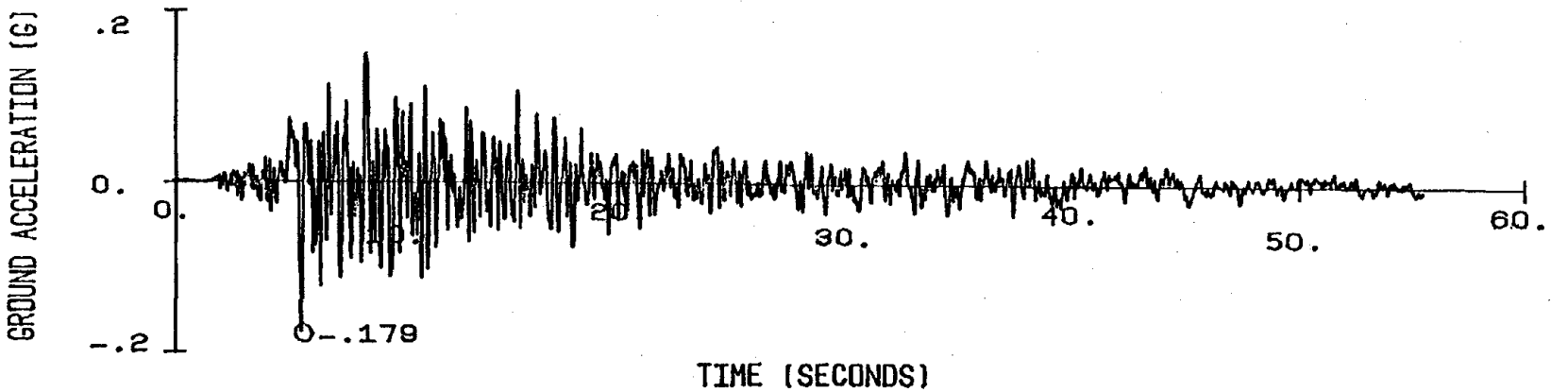

FIG. 4.1 GROUND MOTION FOR THE TAFT-LINCOLN SCHOOL RECORD, KERN COUNTY EARTHQUAKE OF JULY 21, 1952, S69E COMPONENT

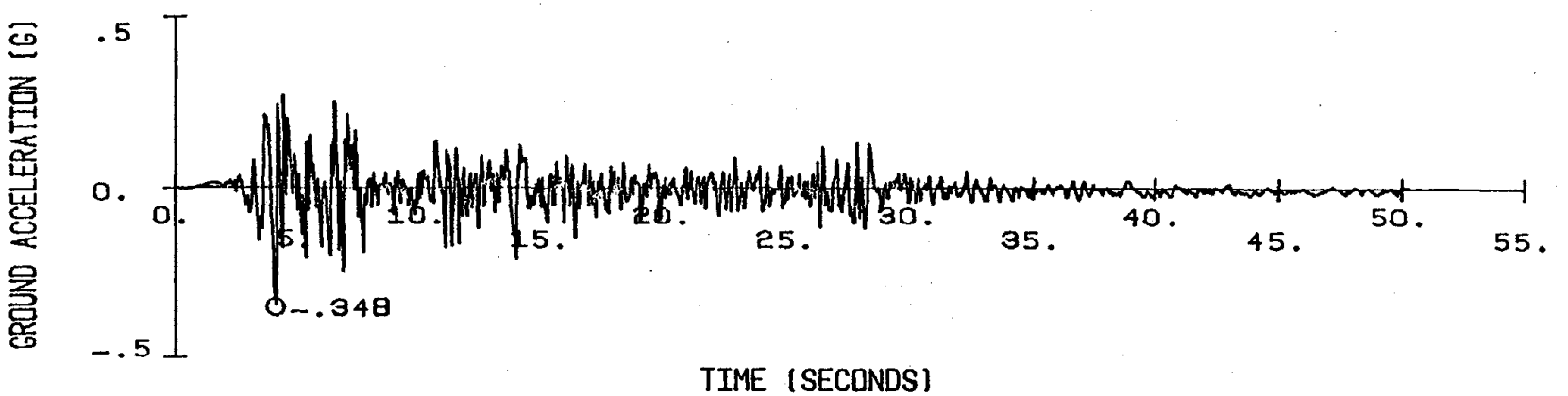

FIG. 4.2 GROUND MOTION FOR THE EL-CENTRO RECORD, IMPERIAL VALLEY EARTHQUAKE OF MAY 18, 1940, S00E COMPONENT

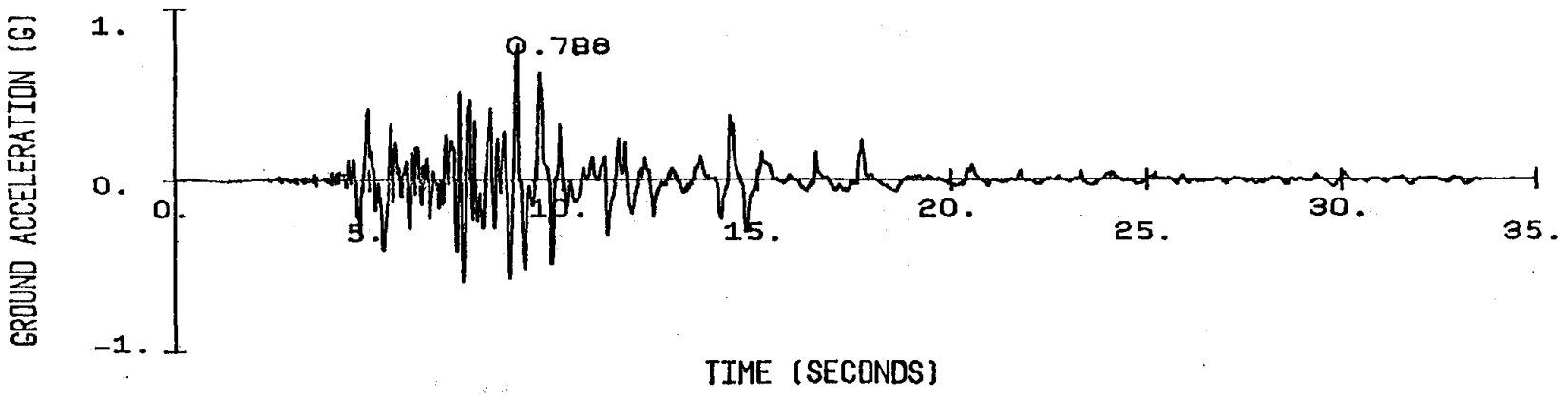

FIG 4.3 GROUND MOTION FOR THE BONDS CORNER RECORD, IMPERIAL VALLEY EARTHQUAKE OF OCT. 15, 1979, 230° COMPONENT

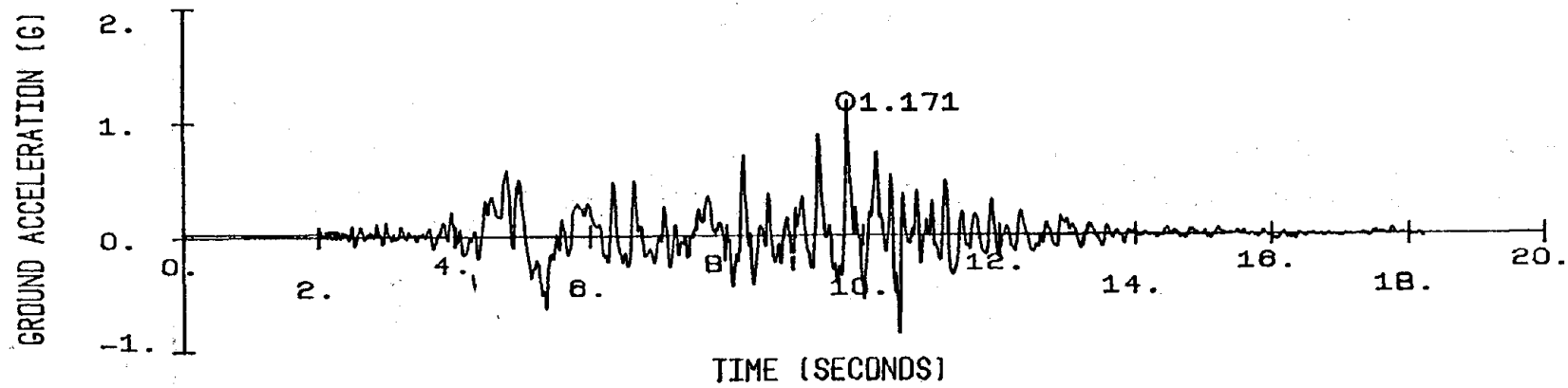

FIG. 4.4 GROUND MOTION FOR THE PACOIMA DAM RECORD, SAN FERNANDO EARTHQUAKE OF FEB. 9, 1971, S16E COMPONENT

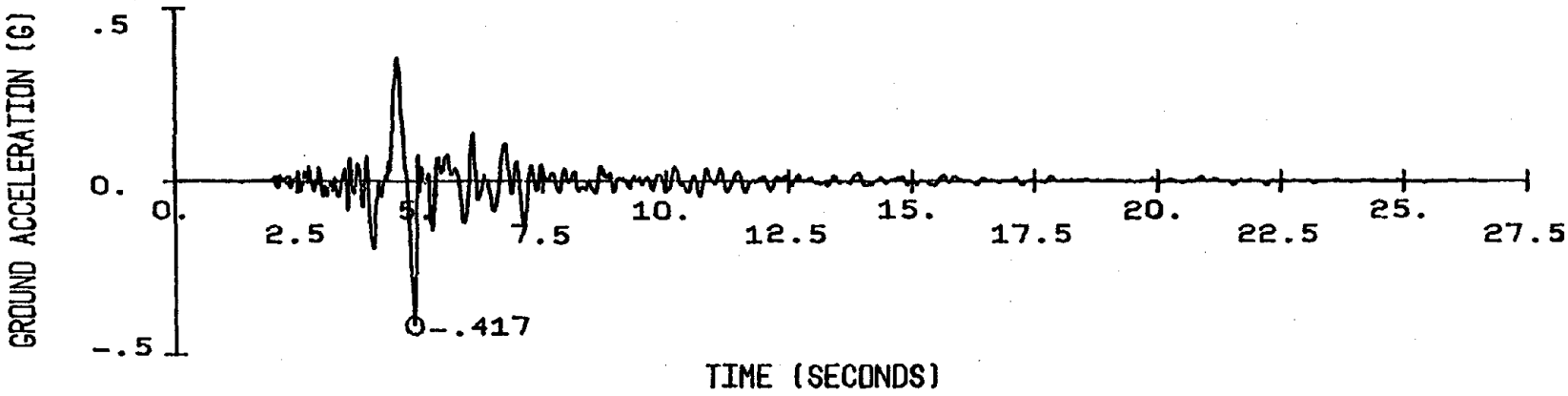

FIG. 4.5 GROUND MOTION FOR THE GILROY ARRAY NO. 6 RECORD, COYOTE LAKE EARTHQUAKE OF AUG. 6, 1979, 230° COMPONENT

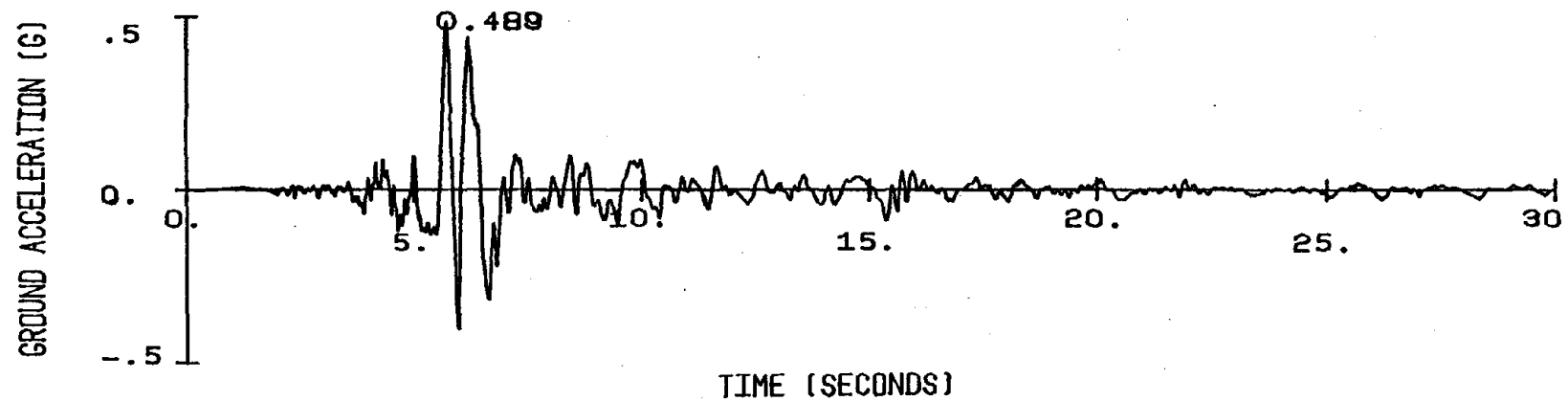

FIG. 4.6 GROUND MOTION FOR THE CHOLANE-SHANDON NO. 2 RECORD, PARKFIELD EARTHQUAKE OF JUNE 27, 1966, N65E COMPONENT

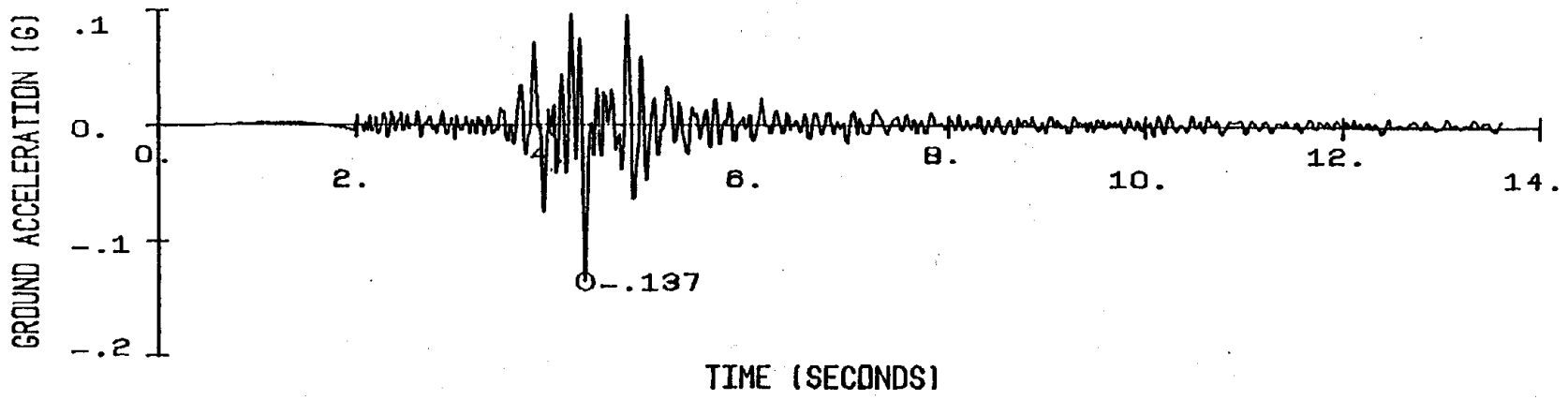

FIG. 4.7 GROUND MOTION FOR THE GAVILAN COLLEGE RECORD, HOLLISTER EARTHQUAKE OF NOV. 28, 1974, S67W COMPONENT

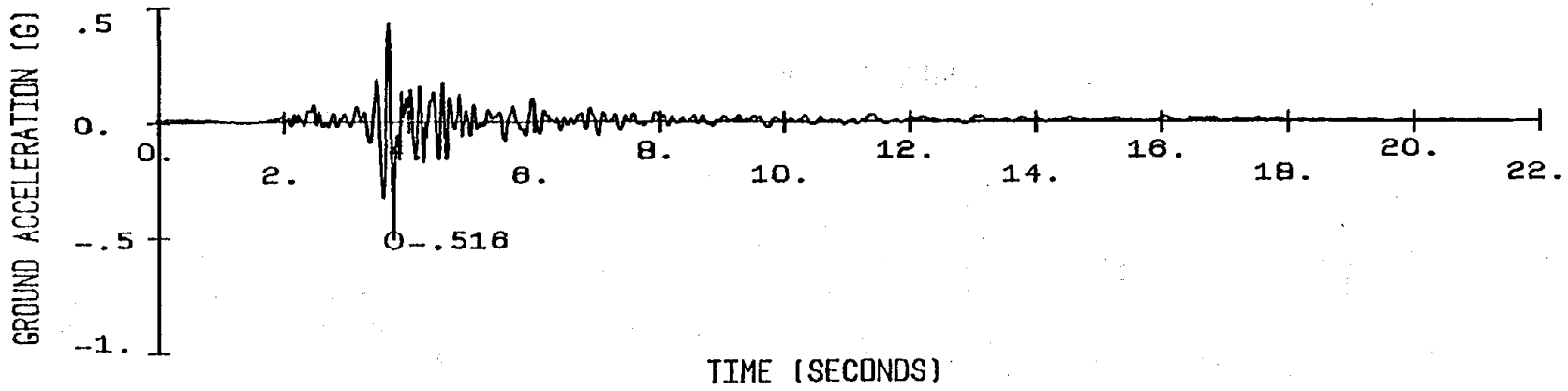

FIG. 4.8 GROUND MOTION FOR THE MELENDY RANCH BARN RECORD, BEAR VALLEY EARTHQUAKE OF SEPT. 4, 1972, N29W COMPONENT

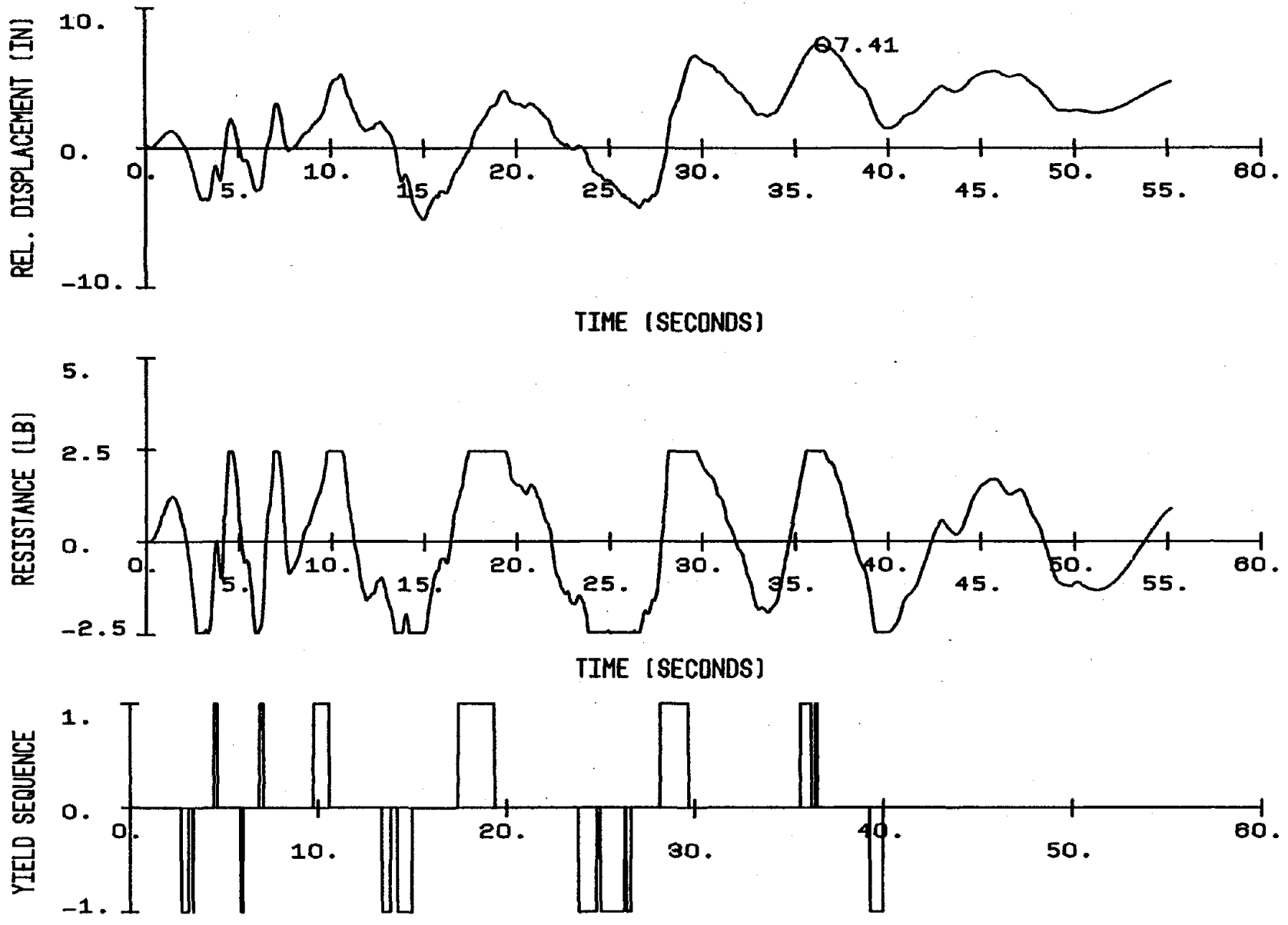

FIG. 4.9a RESPONSE TO EL-CENTRO FOR A STRUCTURE WITH f = 0.1 CPS, β = 5% AND μ = 3

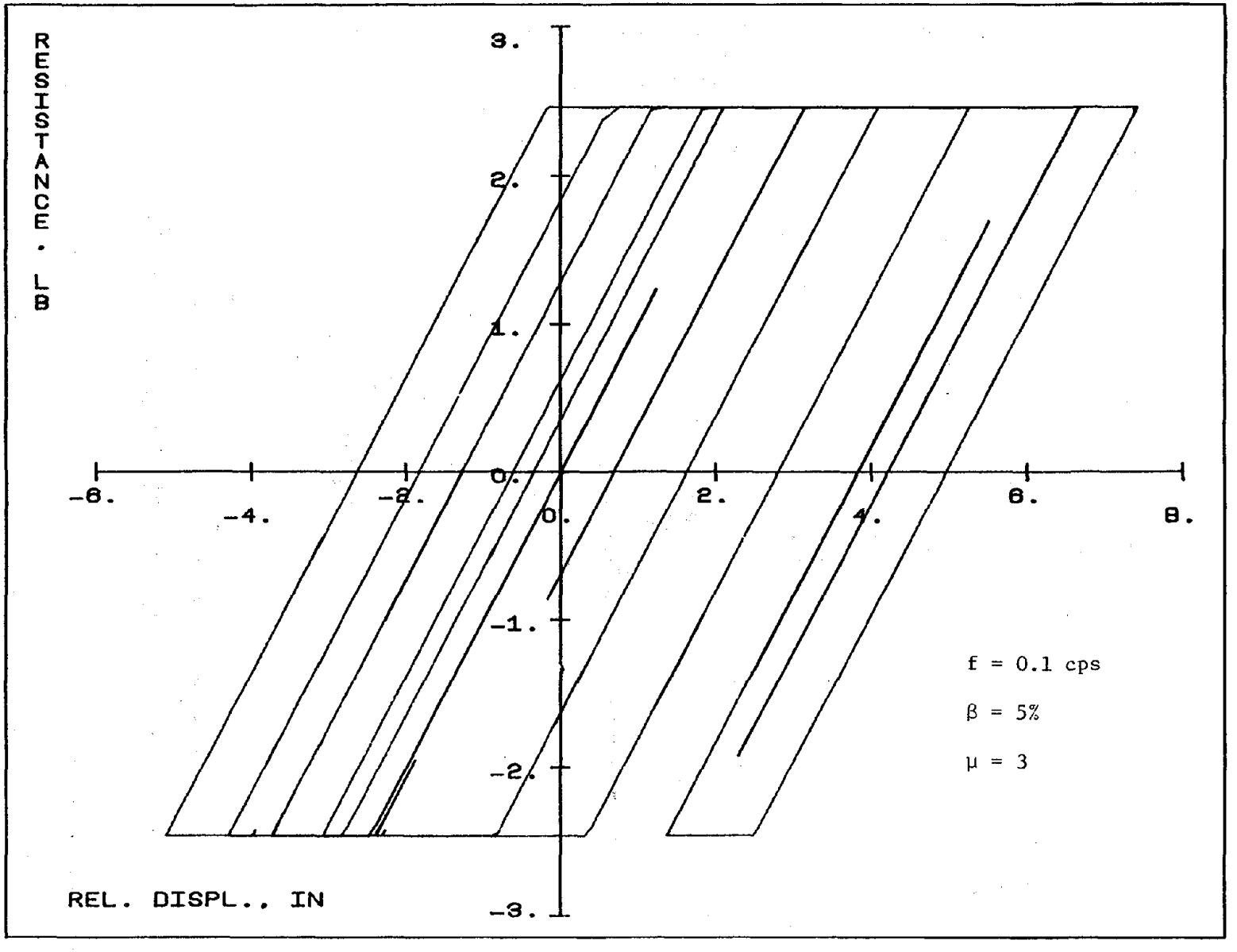

FIG. 4.9b INTERNAL FORCE VS. DEFORMATION FOR A STRUCTURE SUBJECTED TO EL-CENTRO

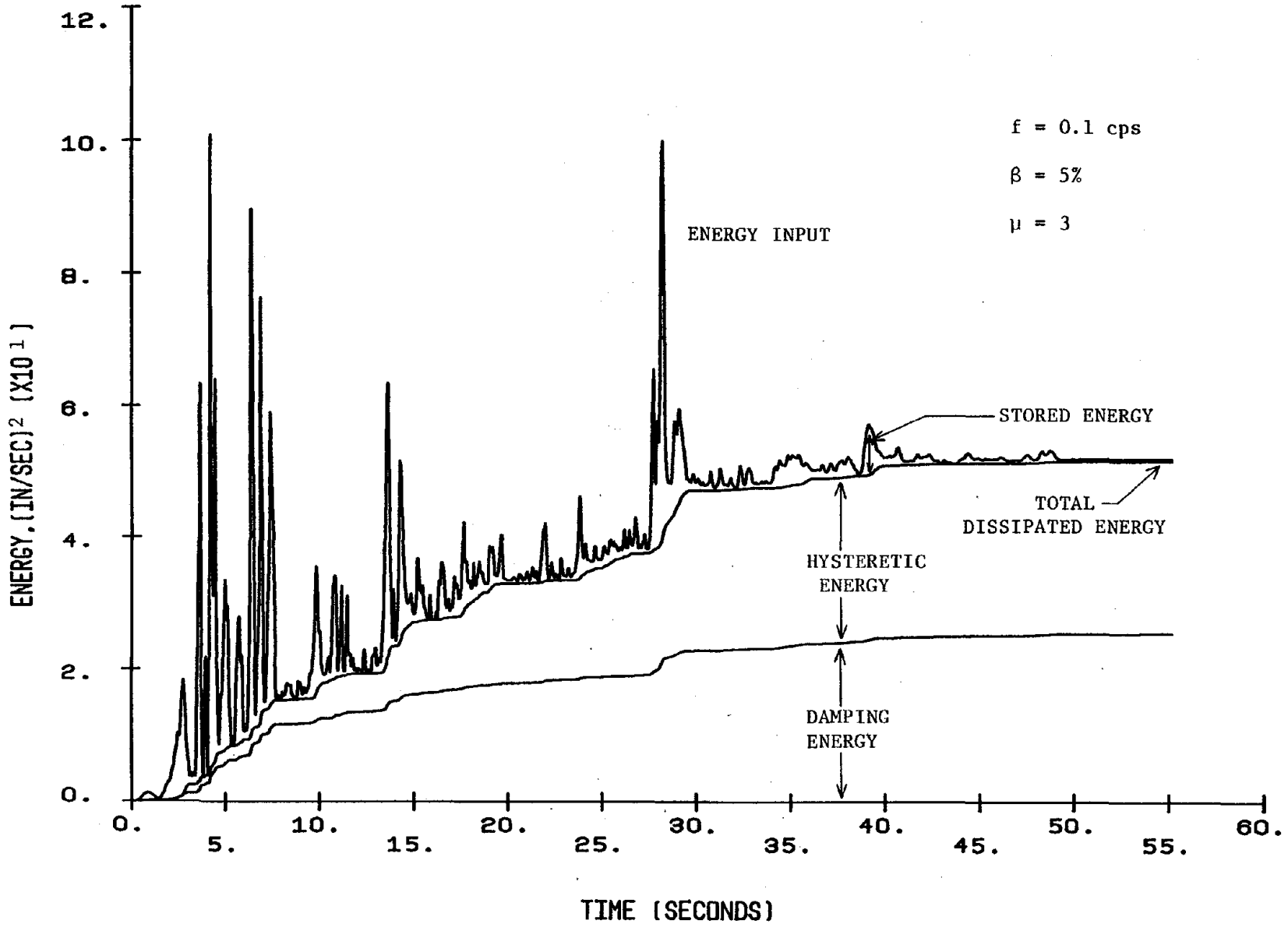

FIG. 4.9c ENERGY VS. TIME FOR A STRUCTURE SUBJECTED TO EL-CENTRO

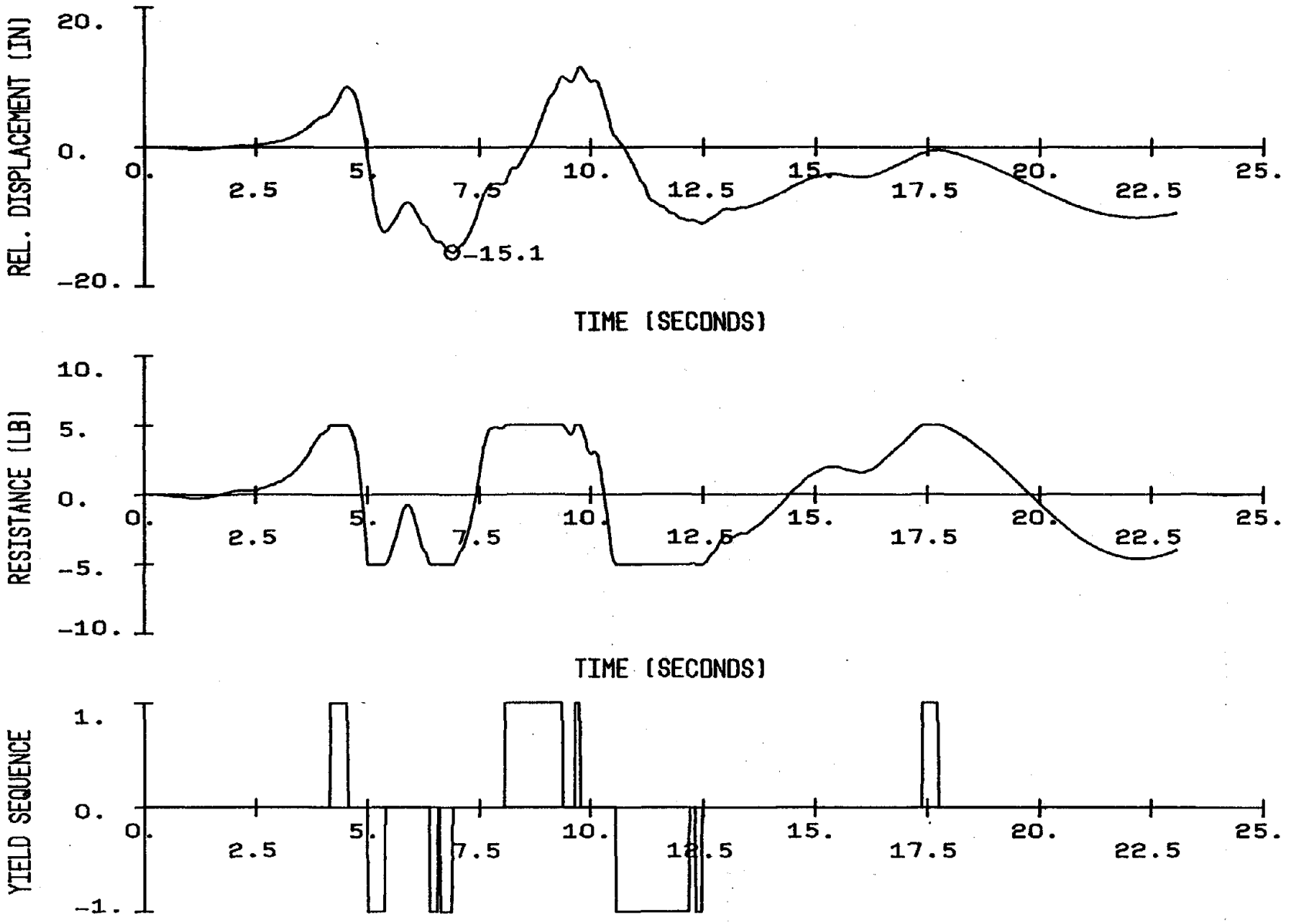

FIG. 4.10a RESPONSE TO PACOIMA DAM FOR A STRUCTURE WITH f = 0.1 CPS, β = 5% AND μ = 3

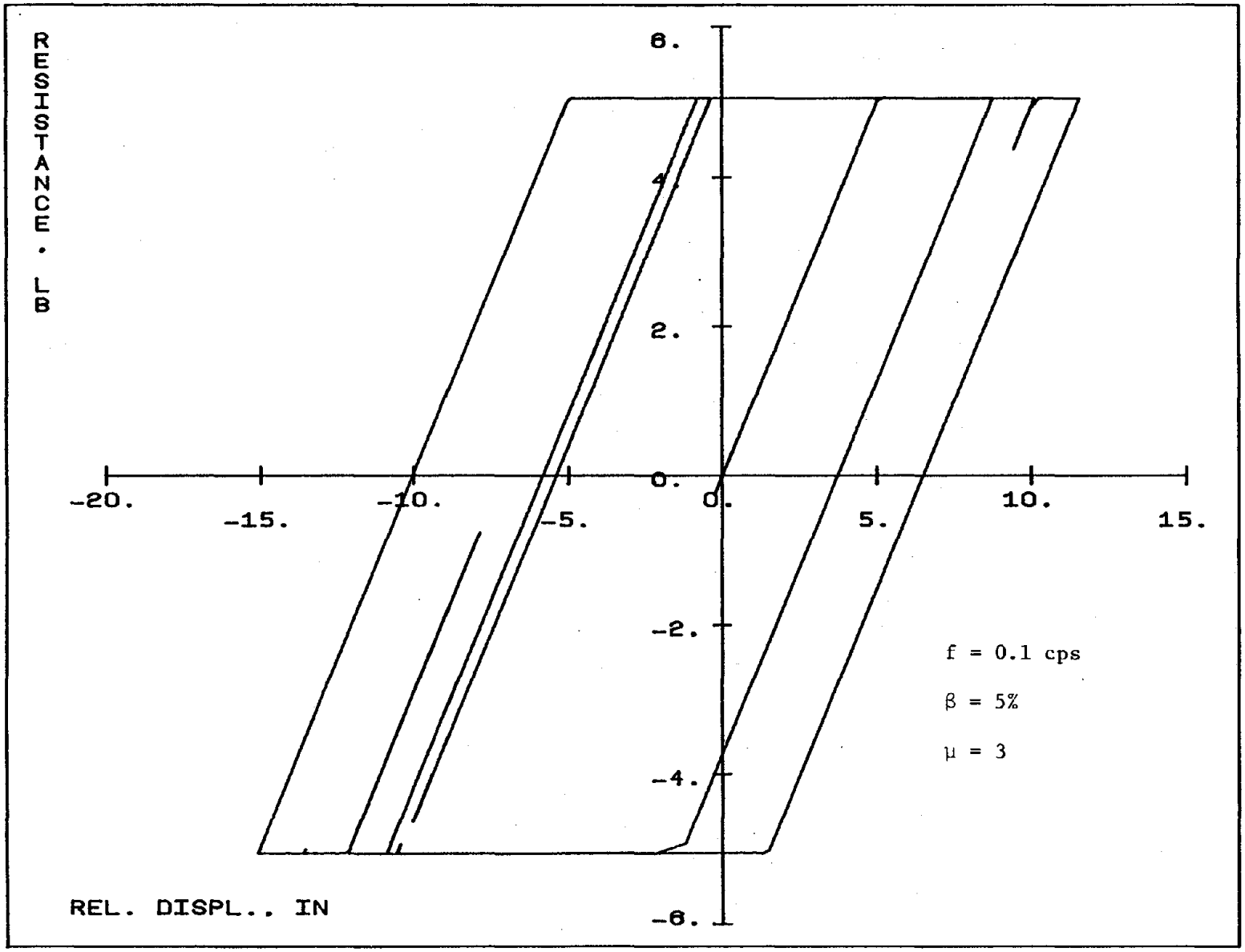

FIG. 4.10b INTERNAL FORCE VS. DEFORMATION FOR A STRUCTURE SUBJECTED TO PACOIMA DAM

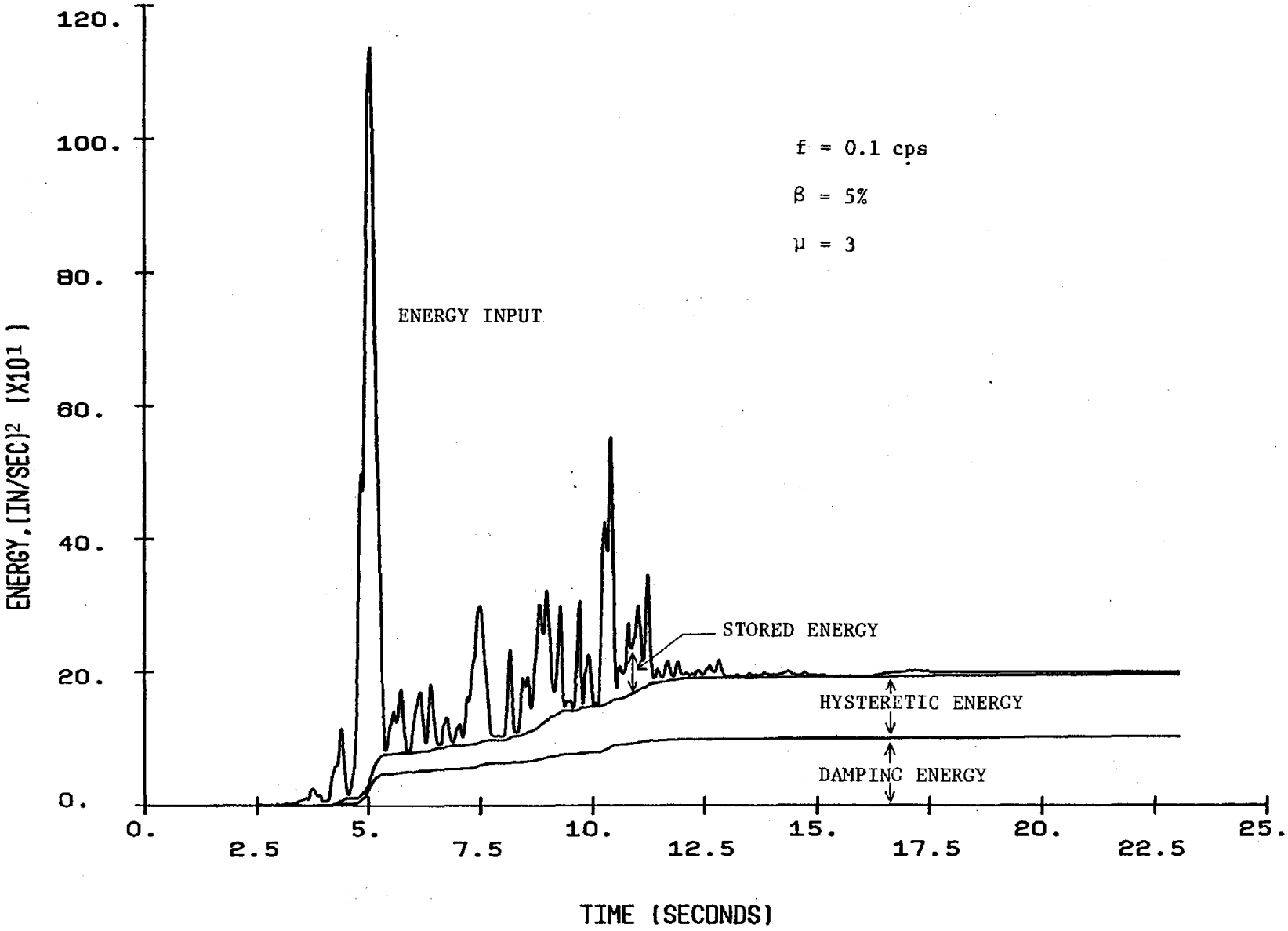

FIG. 4.10c ENERGY VS. TIME FOR A STRUCTURE SUBJECTED TO PACOIMA DAM

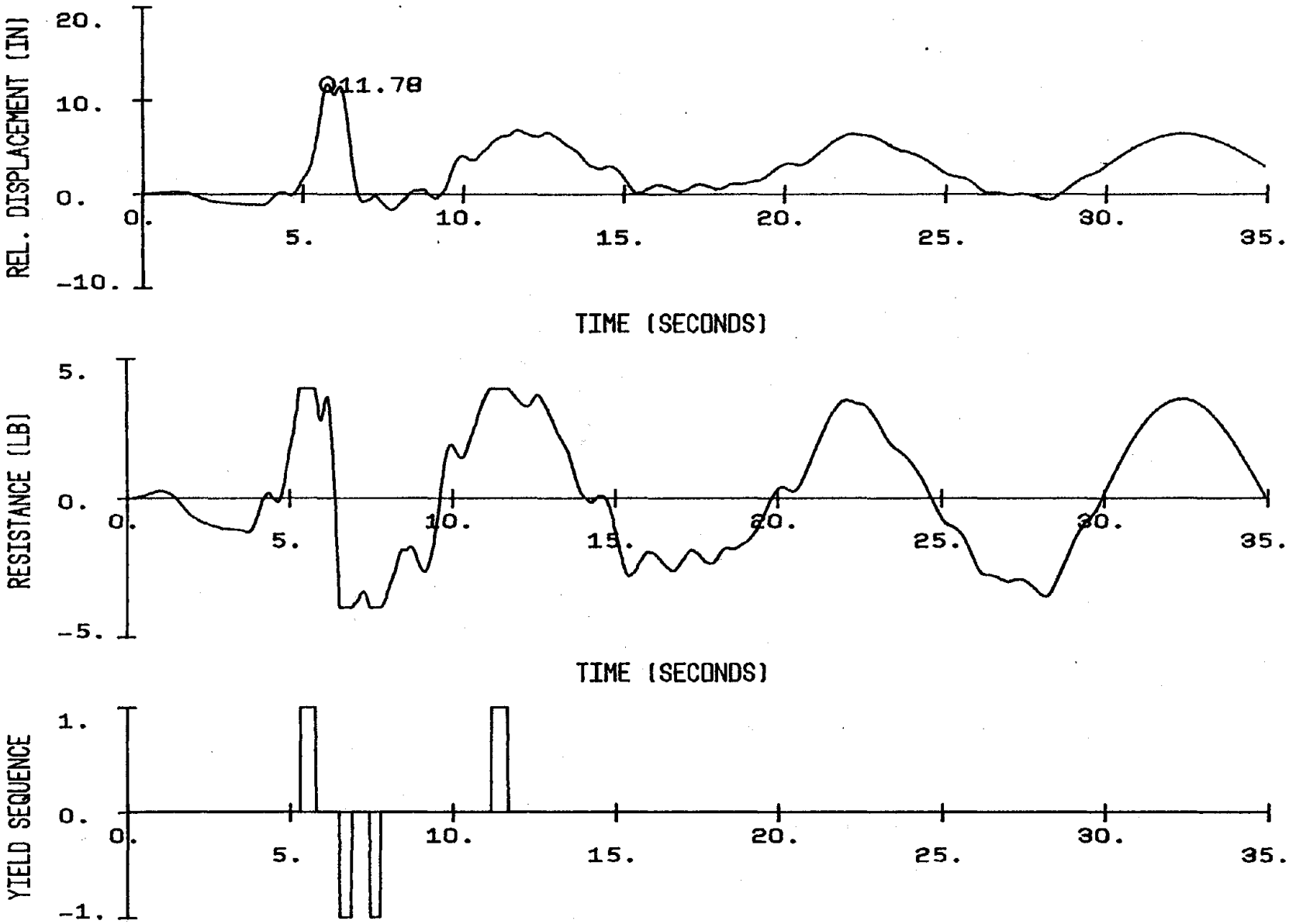

FIG. 4.11a RESPONSE TO PARKFIELD FOR A STRUCTURE WITH f = 0.1 CPS, β = 5% AND μ = 3

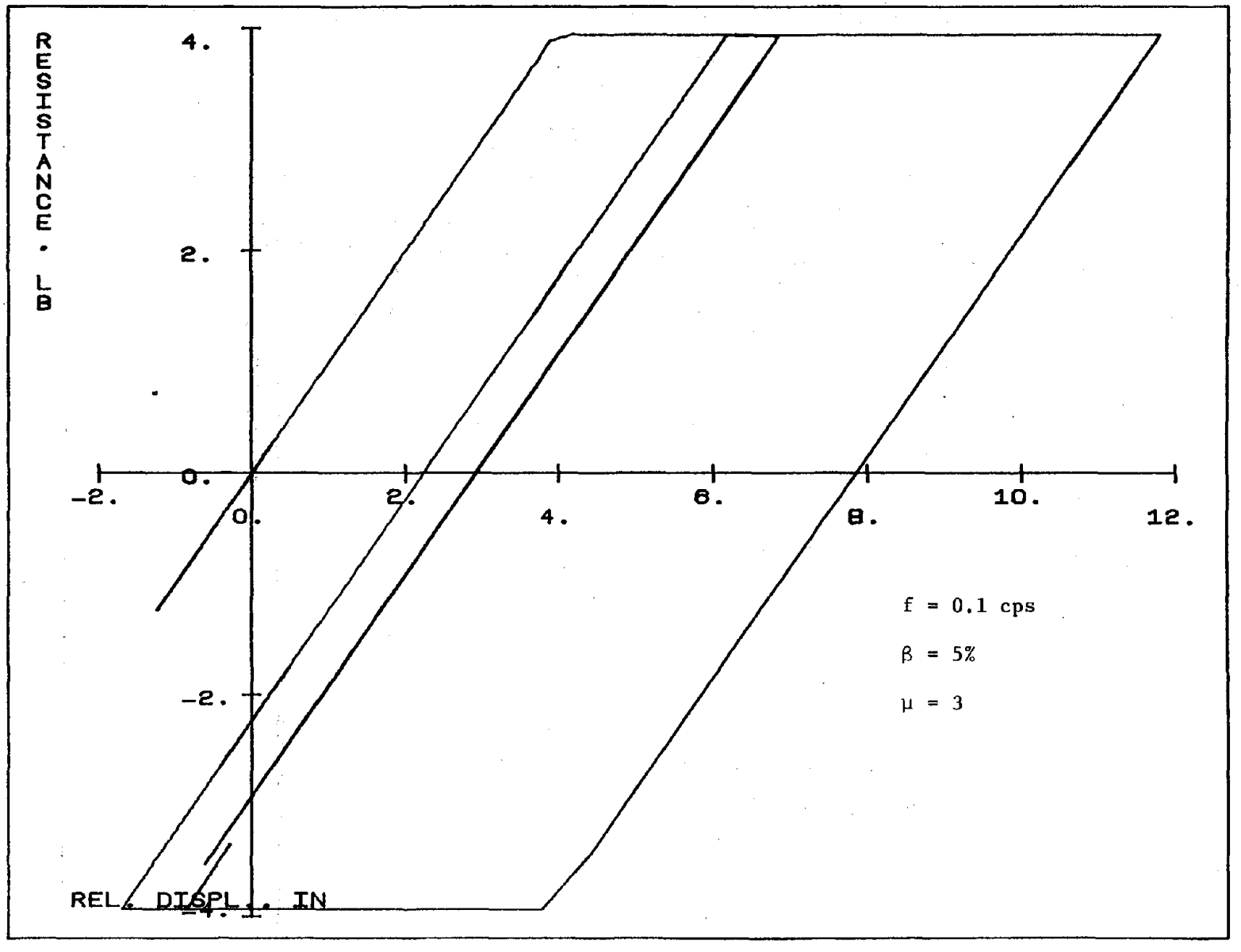

FIG. 4.11b INTERNAL FORCE VS. DEFORMATION FOR A STRUCTURE SUBJECTED TO PARKFIELD

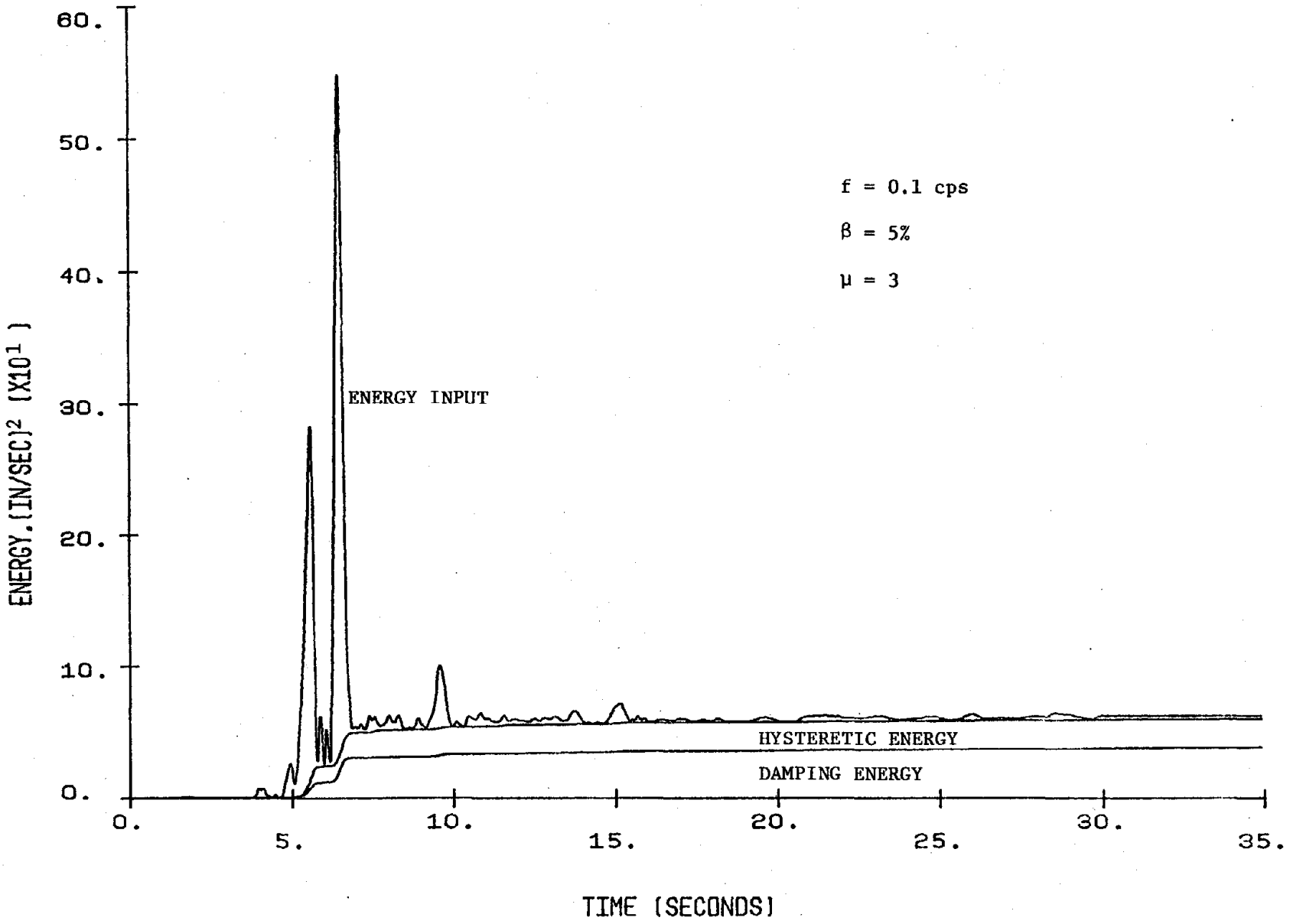

FIG. 4.11c ENERGY VS. TIME FOR A STRUCTURE SUBJECTED TO PARKFIELD

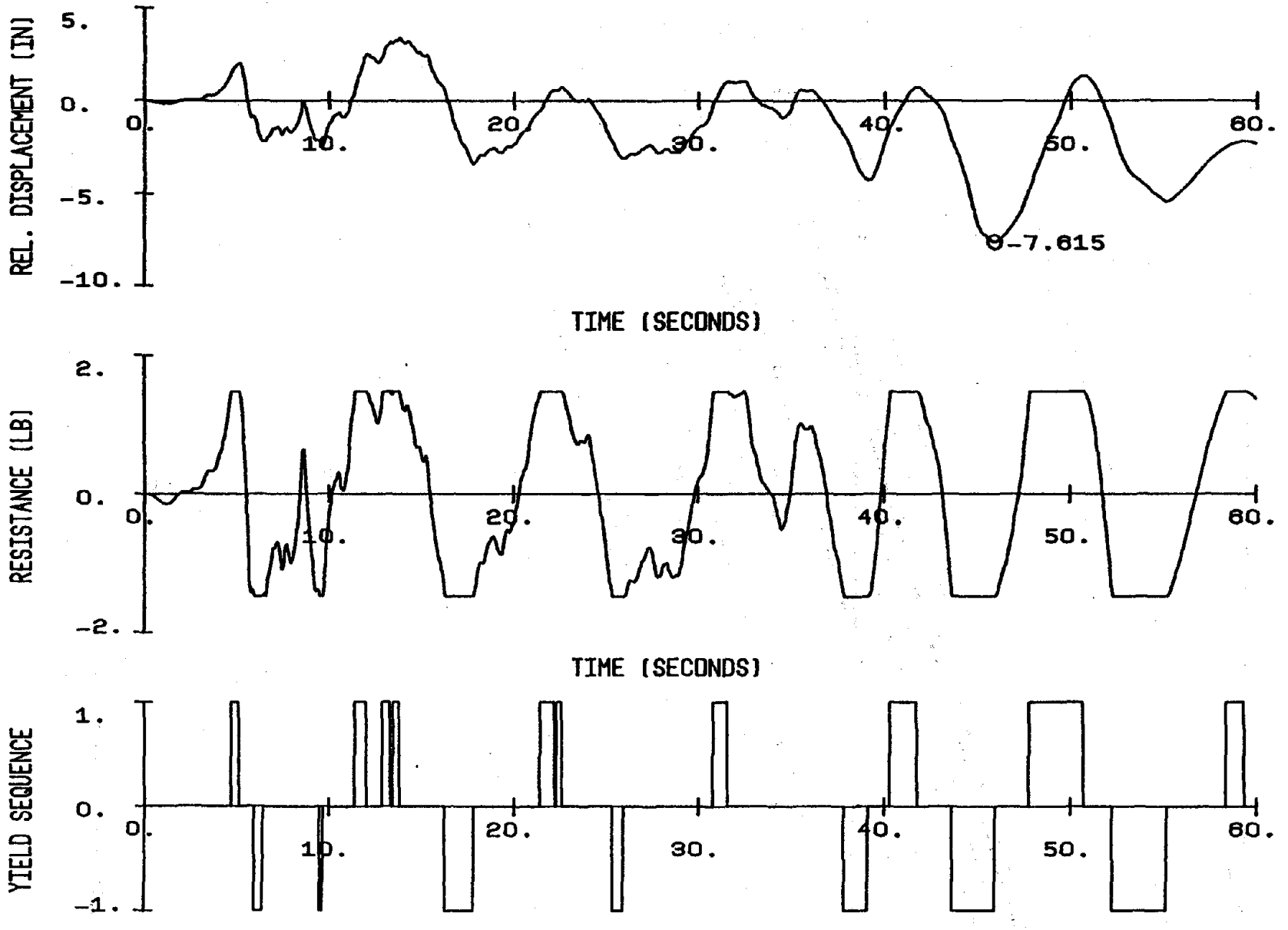

FIG. 4.12a RESPONSE TO TAFT FOR A STRUCTURE WITH f = 0.1 CPS, β = 5% AND μ = 5

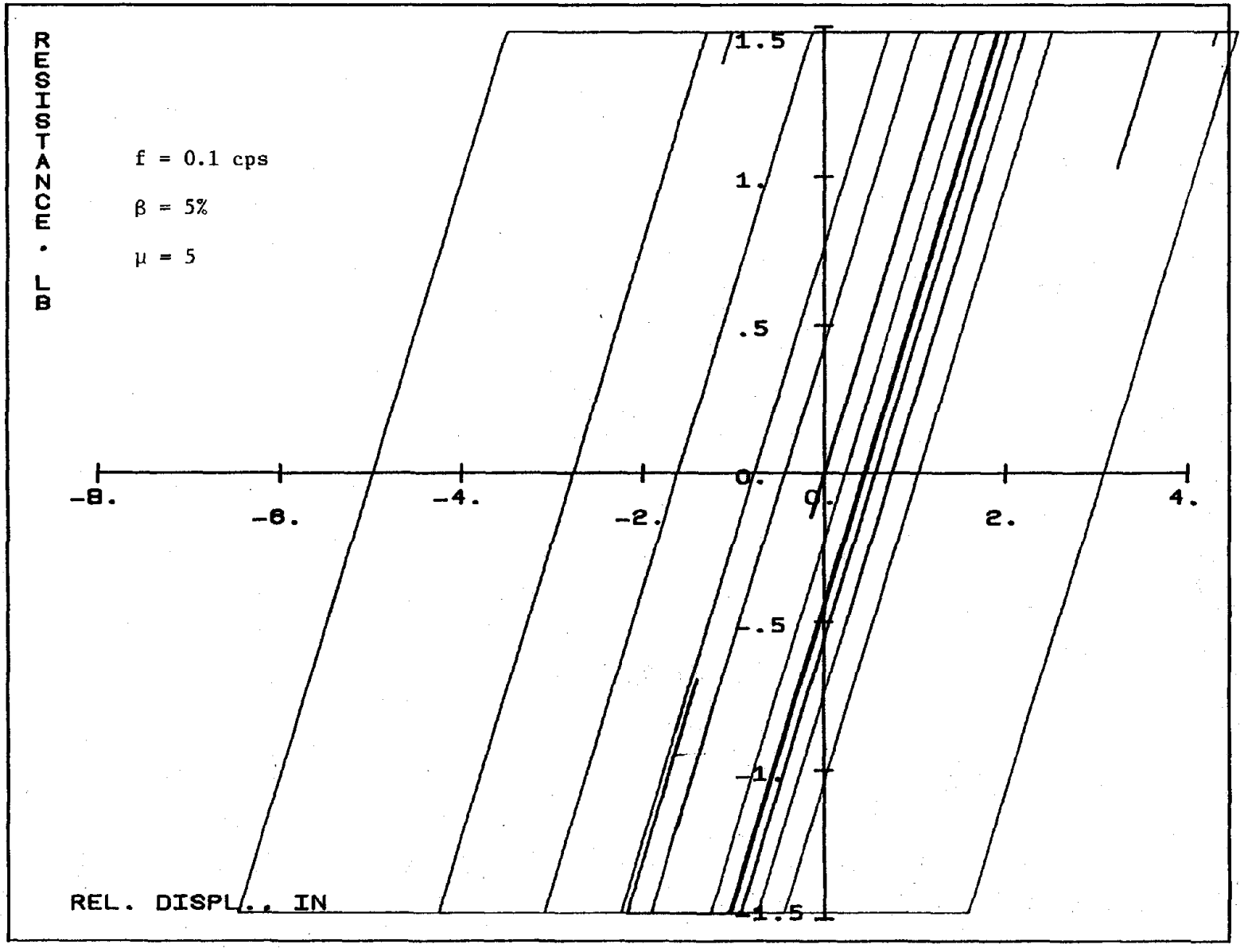

FIG. 4.12b INTERNAL FORCE VS. DEFORMATION FOR A STRUCTURE SUBJECTED TO TAFT

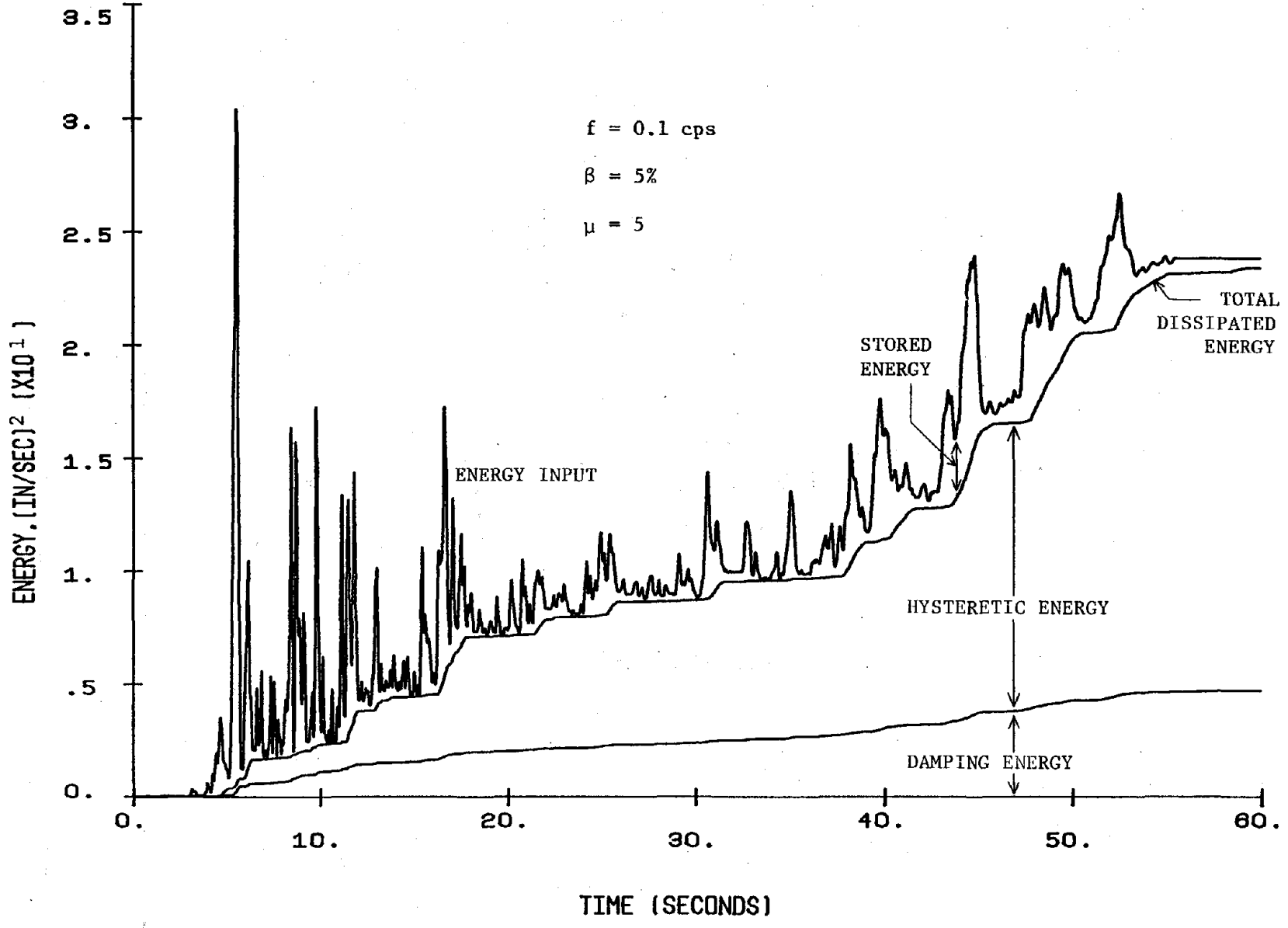

FIG. 4.12c ENERGY VS. TIME FOR A STRUCTURE SUBJECTED TO TAFT

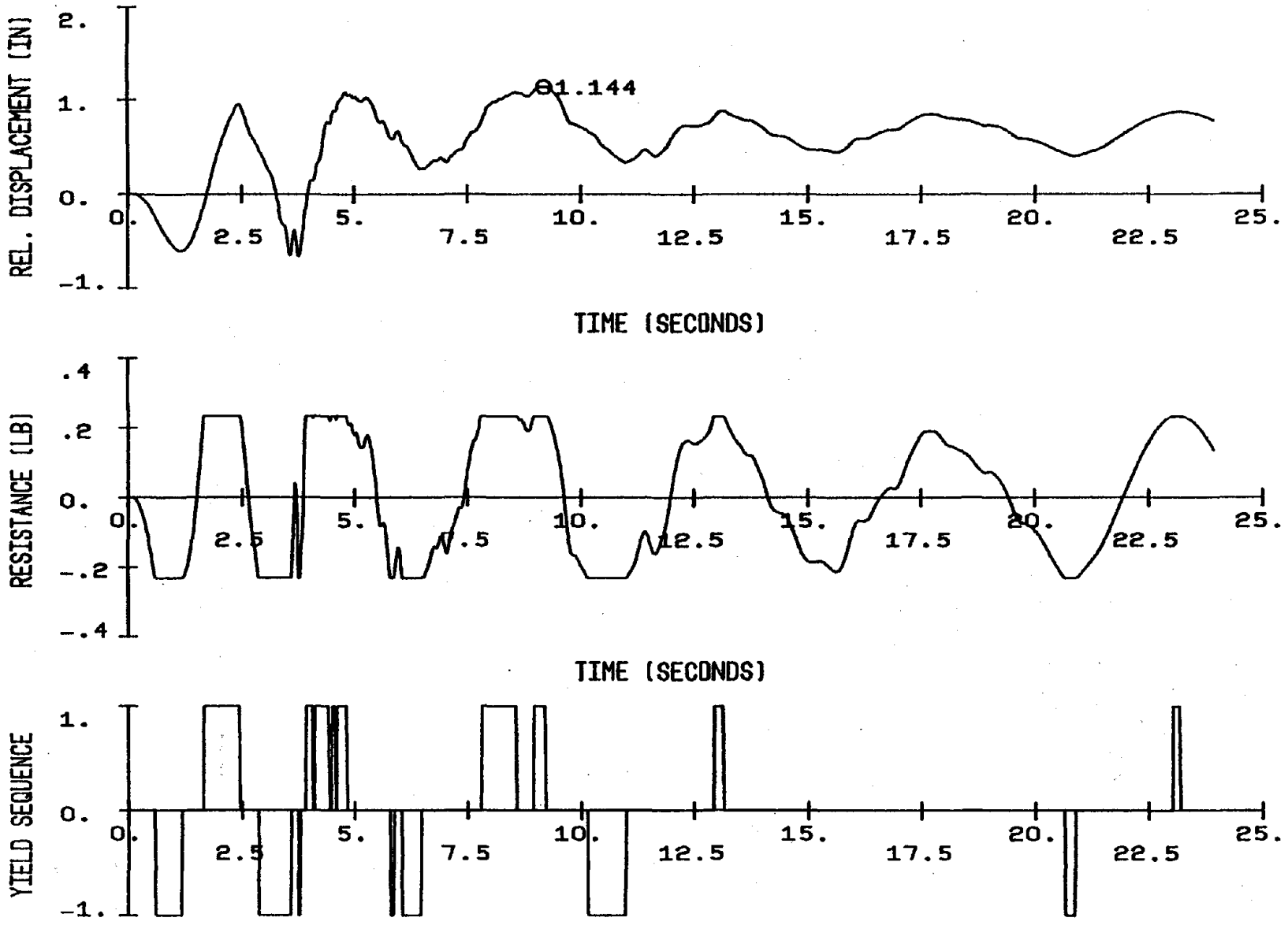

FIG. 4.13a RESPONSE TO MELENDY RANCH FOR A STRUCTURE WITH f = 0.2 CPS, β = 2% AND μ = 5

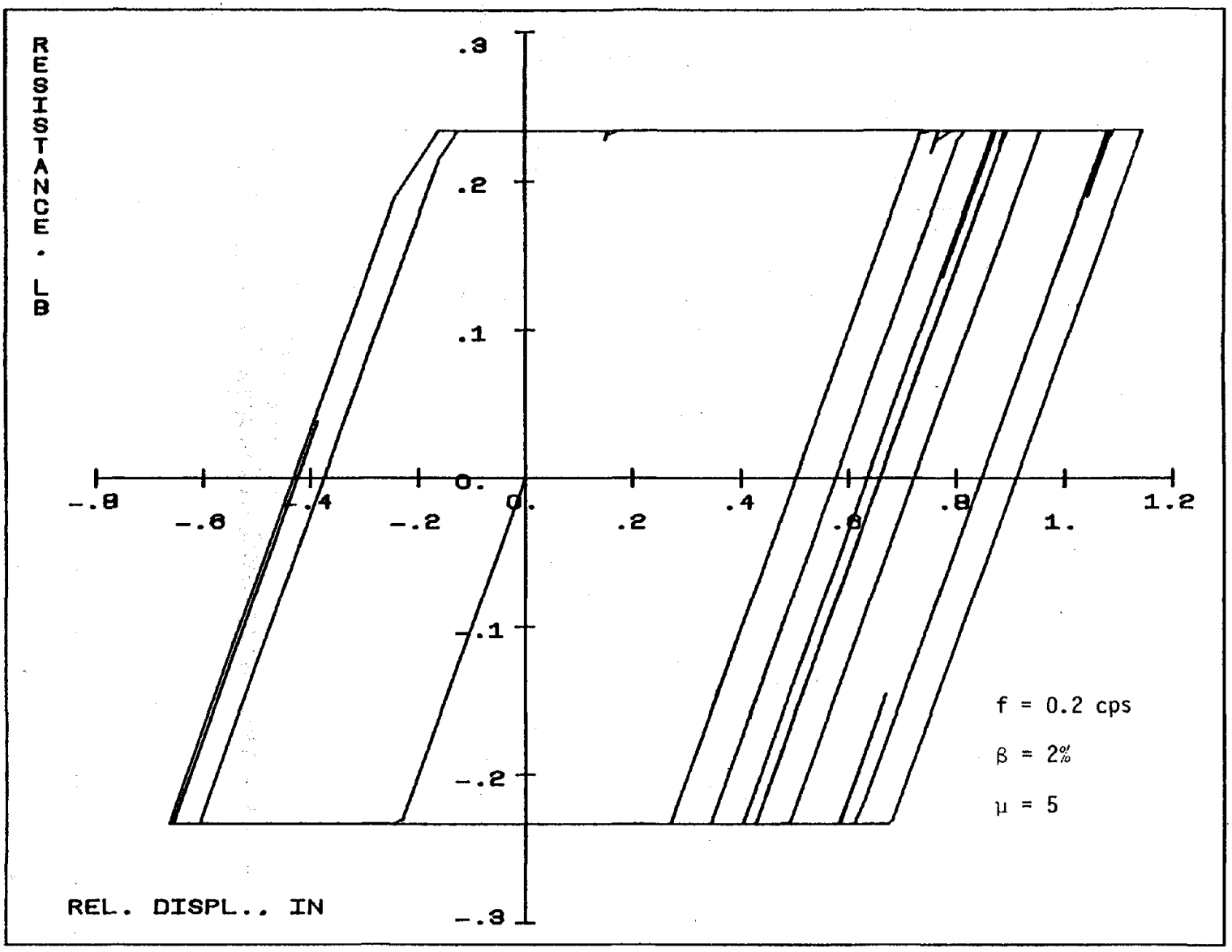

FIG. 4.13b INTERNAL FORCE VS. DEFORMATION FOR A STRUCTURE SUBJECTED TO MELENDY RANCH

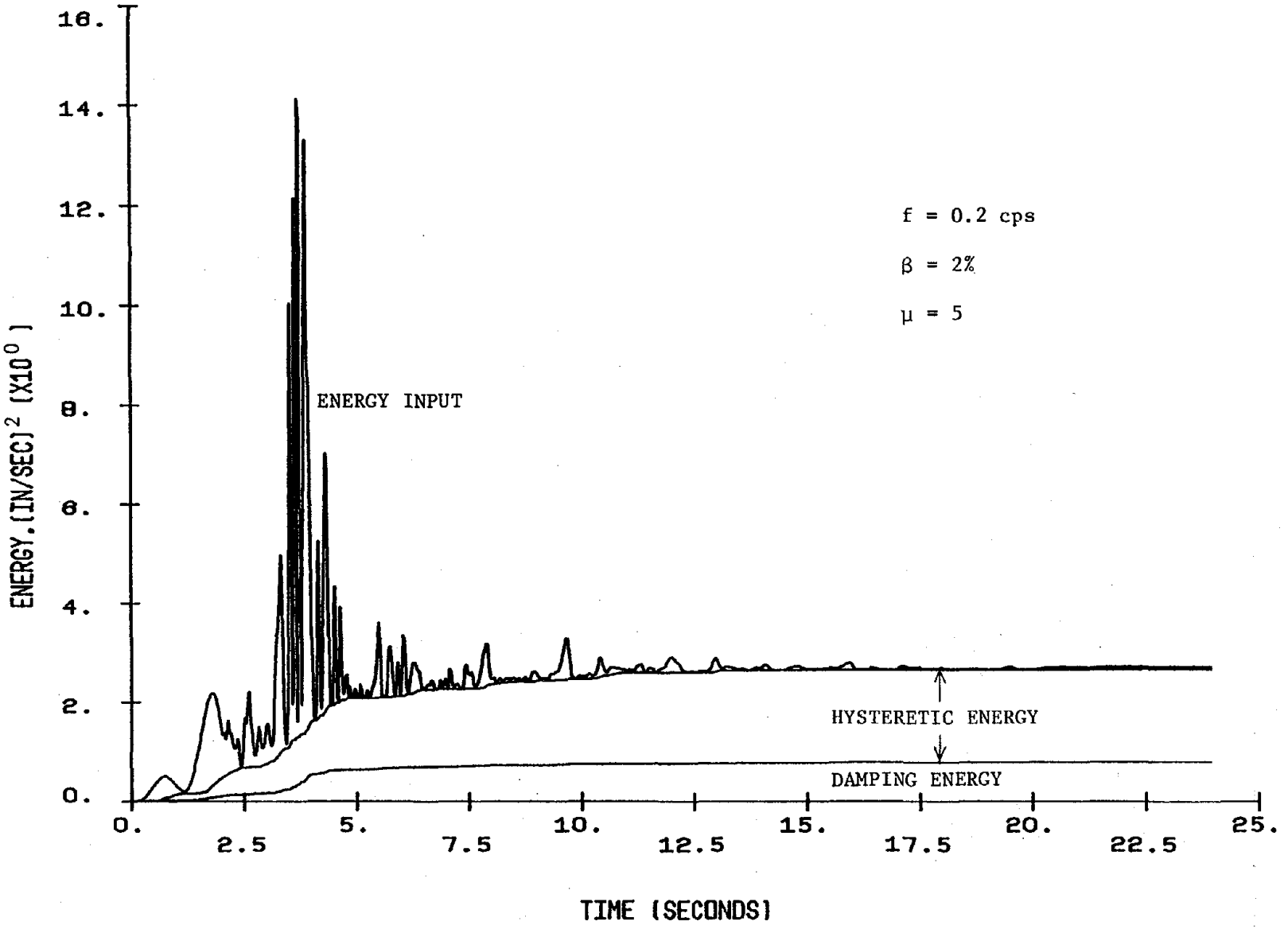

FIG. 4.13c ENERGY VS. TIME FOR A STRUCTURE SUBJECTED TO MELENDY RANCH

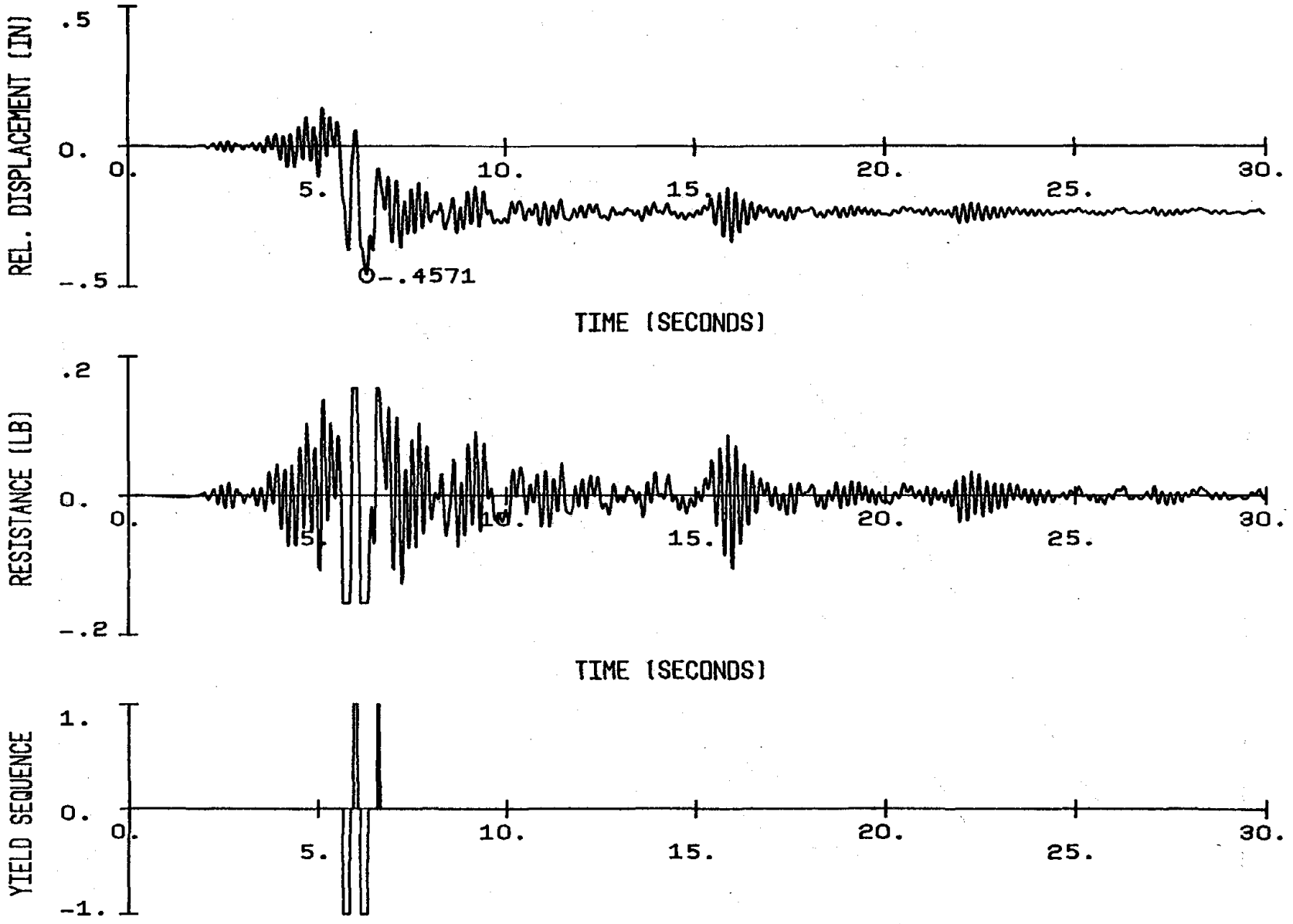

FIG. 4.14a RESPONSE TO PARKFIELD FOR A STRUCTURE WITH f = 5 CPS, β = 5% AND μ = 3

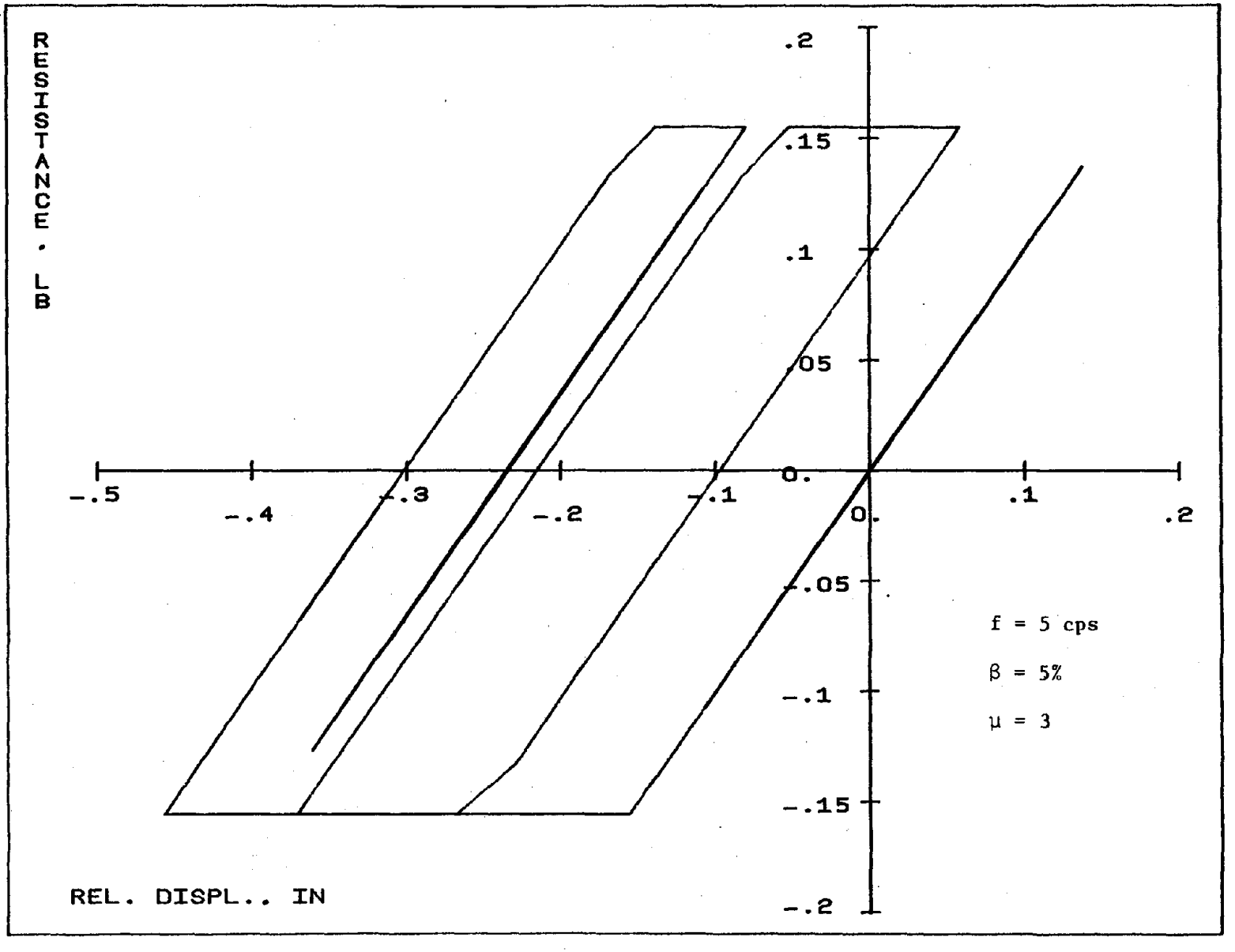

FIG. 4.14b INTERNAL FORCE VS. DEFORMATION FOR A STRUCTURE SUBJECTED TO PARKFIELD

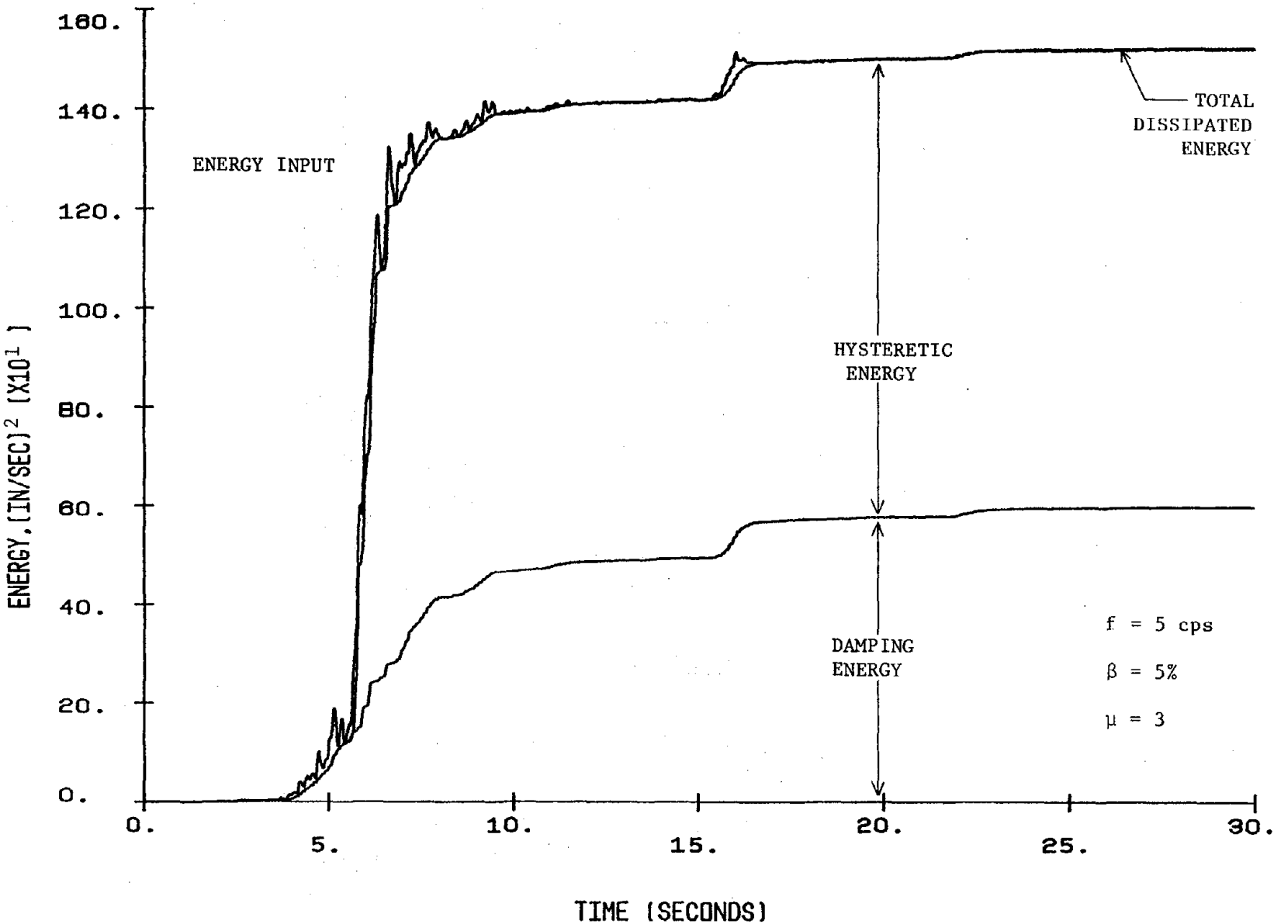

FIG. 4.14c ENERGY VS. TIME FOR A STRUCTURE SUBJECTED TO PARKFIELD

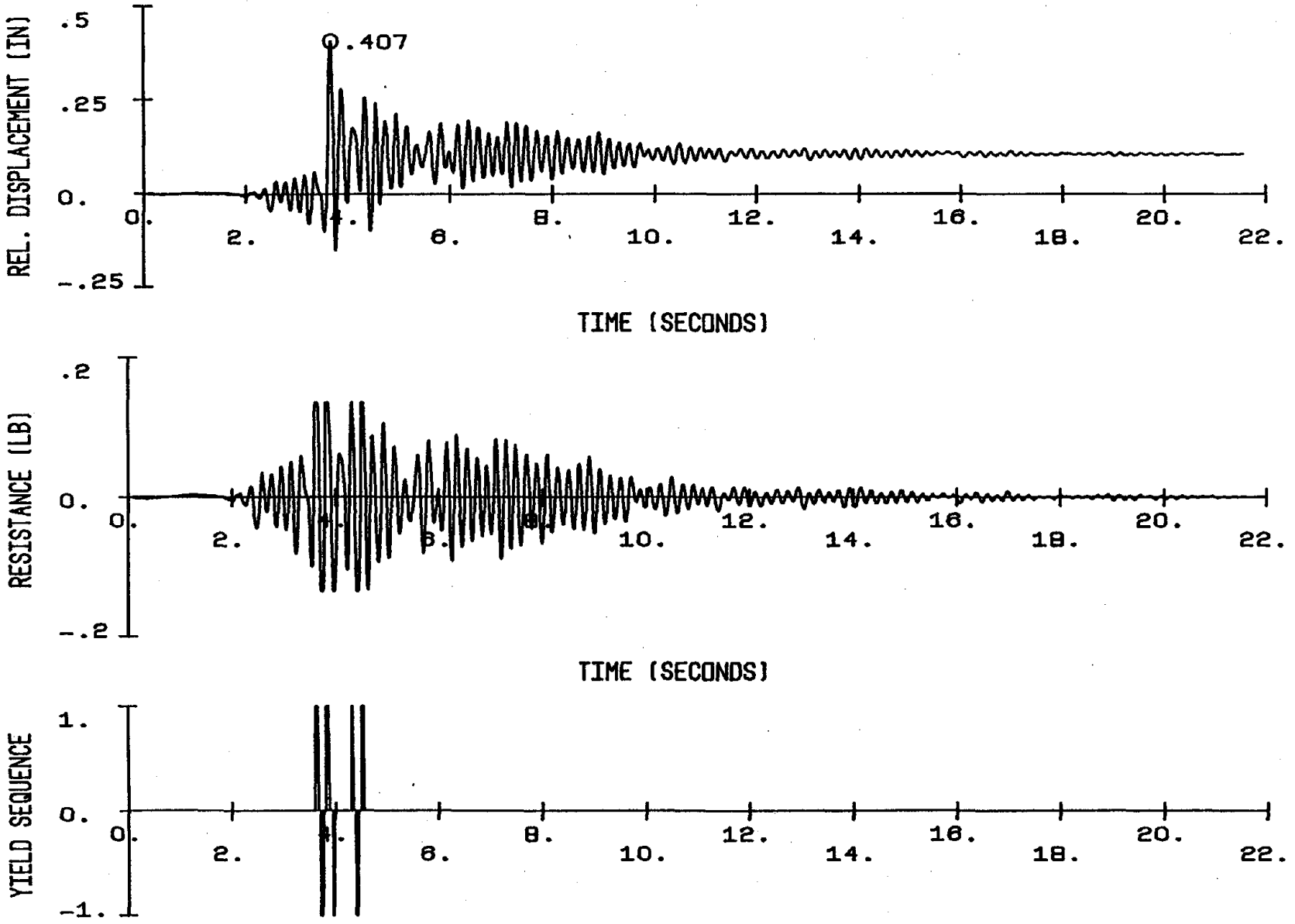

FIG. 4.15a RESPONSE TO MELENDY RANCH FOR A STRUCTURE WITH f = 5 CPS, β = 2% AND μ = 3

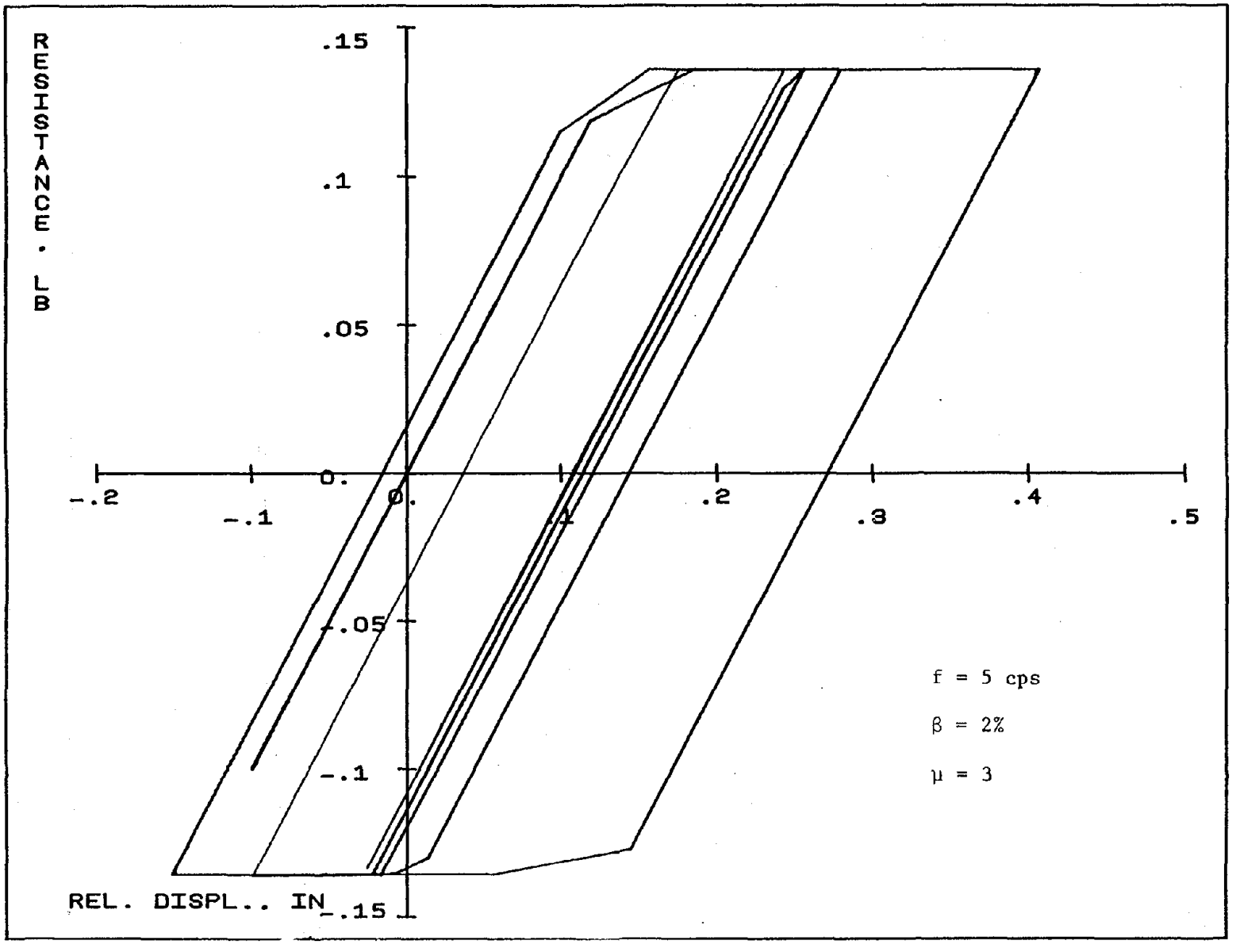

FIG. 4.15b INTERNAL FORCE VS. DEFORMATION FOR A STRUCTURE SUBJECTED TO MELENDY RANCH

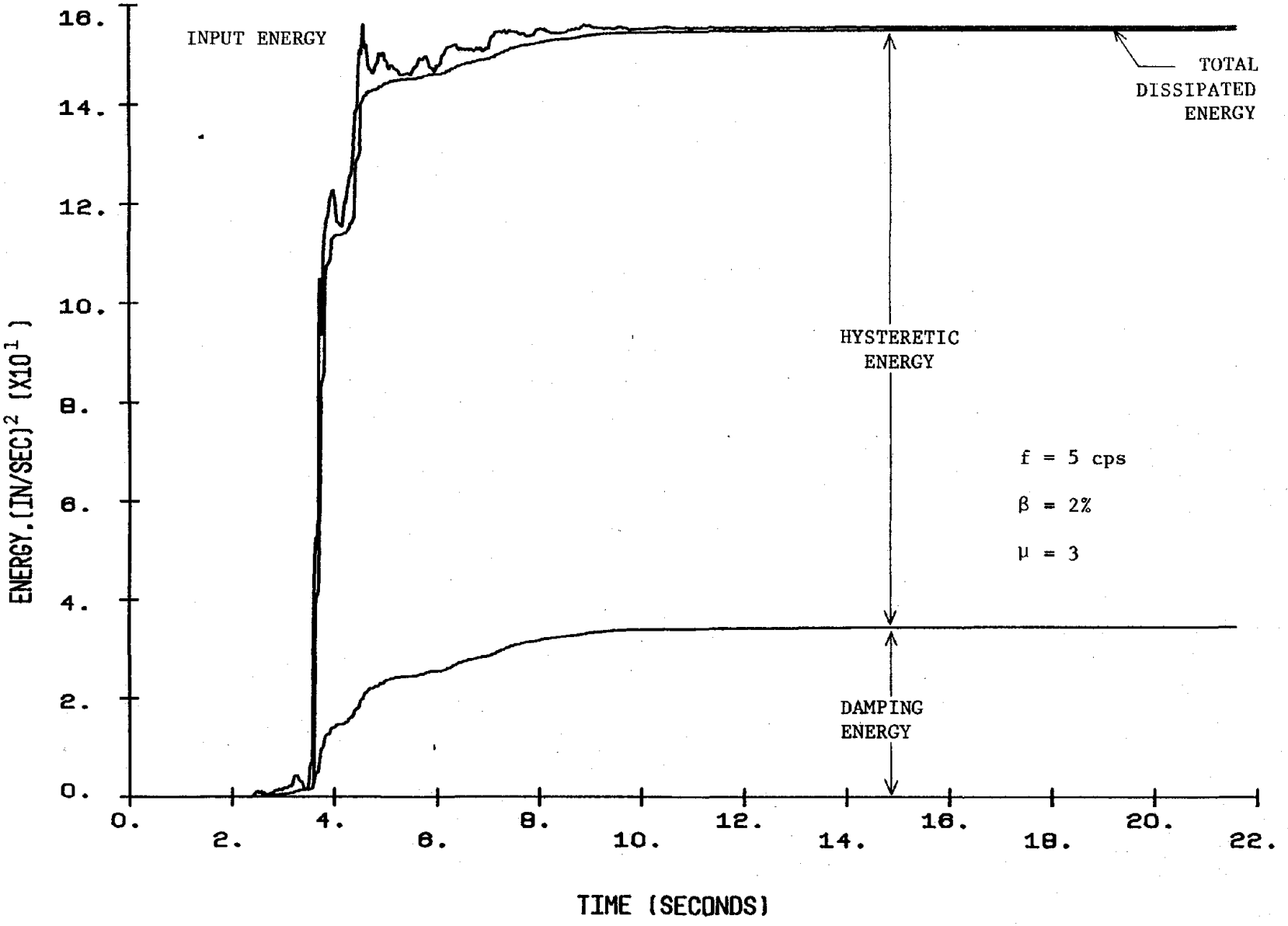

FIG. 4.15c ENERGY VS. TIME FOR A STRUCTURE SUBJECTED TO MELENDY RANCH

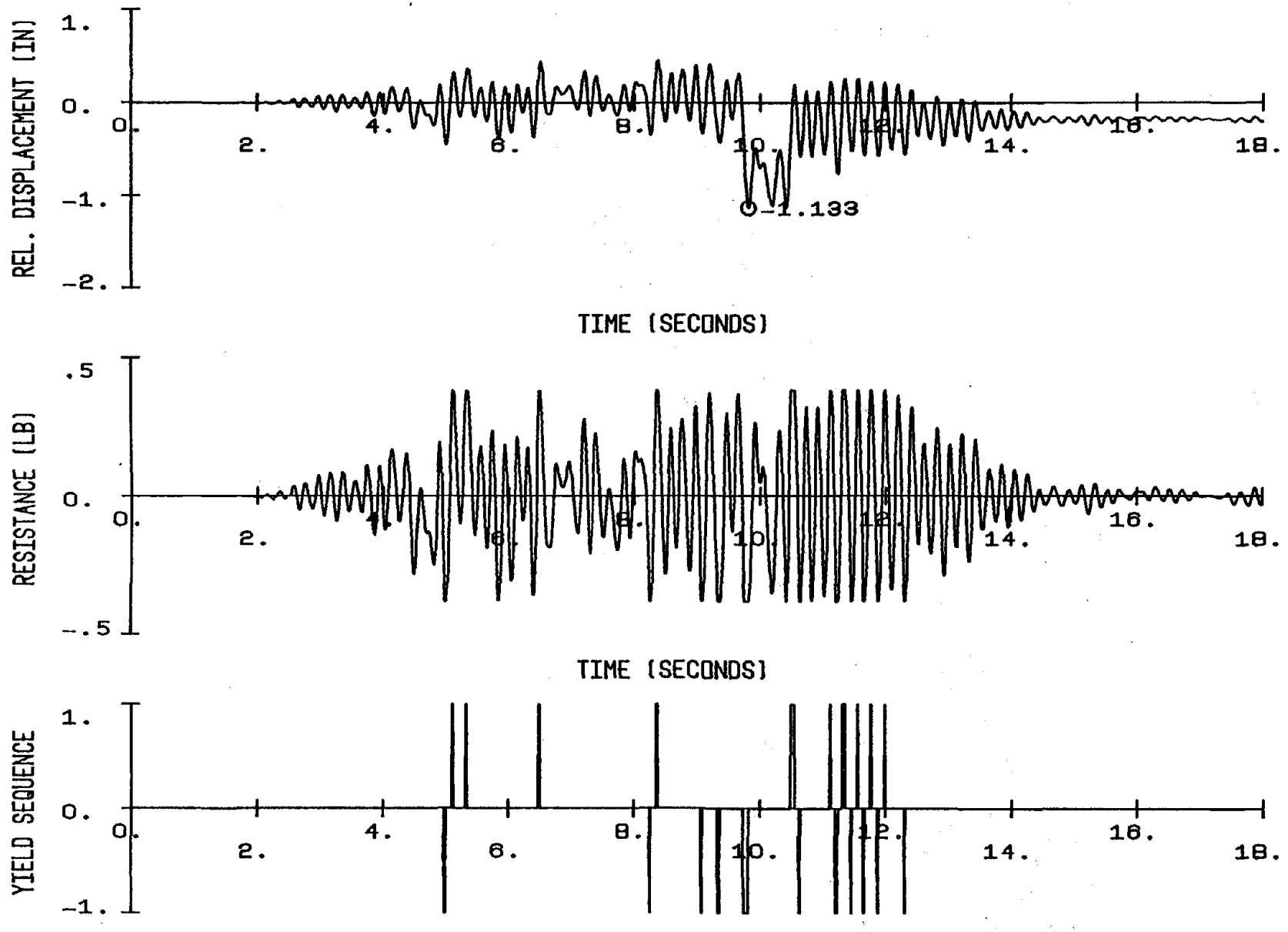

FIG. 4.16a RESPONSE TO PACOIMA DAM FOR A STRUCTURE WITH f = 5 CPS, β = 5% AND μ = 3

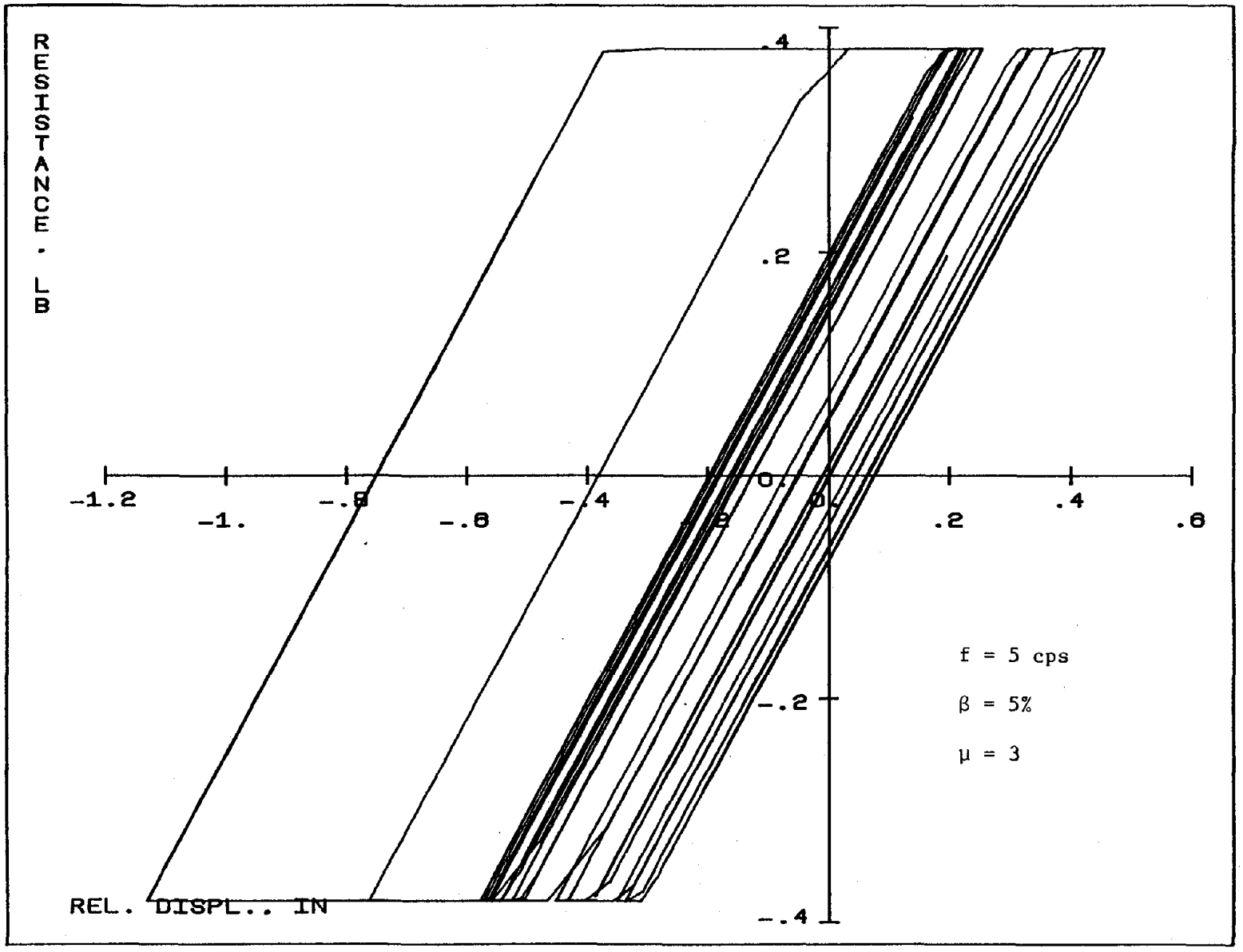

FIG. 4.16b INTERNAL FORCE VS. DEFORMATION FOR A STRUCTURE SUBJECTED TO PACOIMA DAM

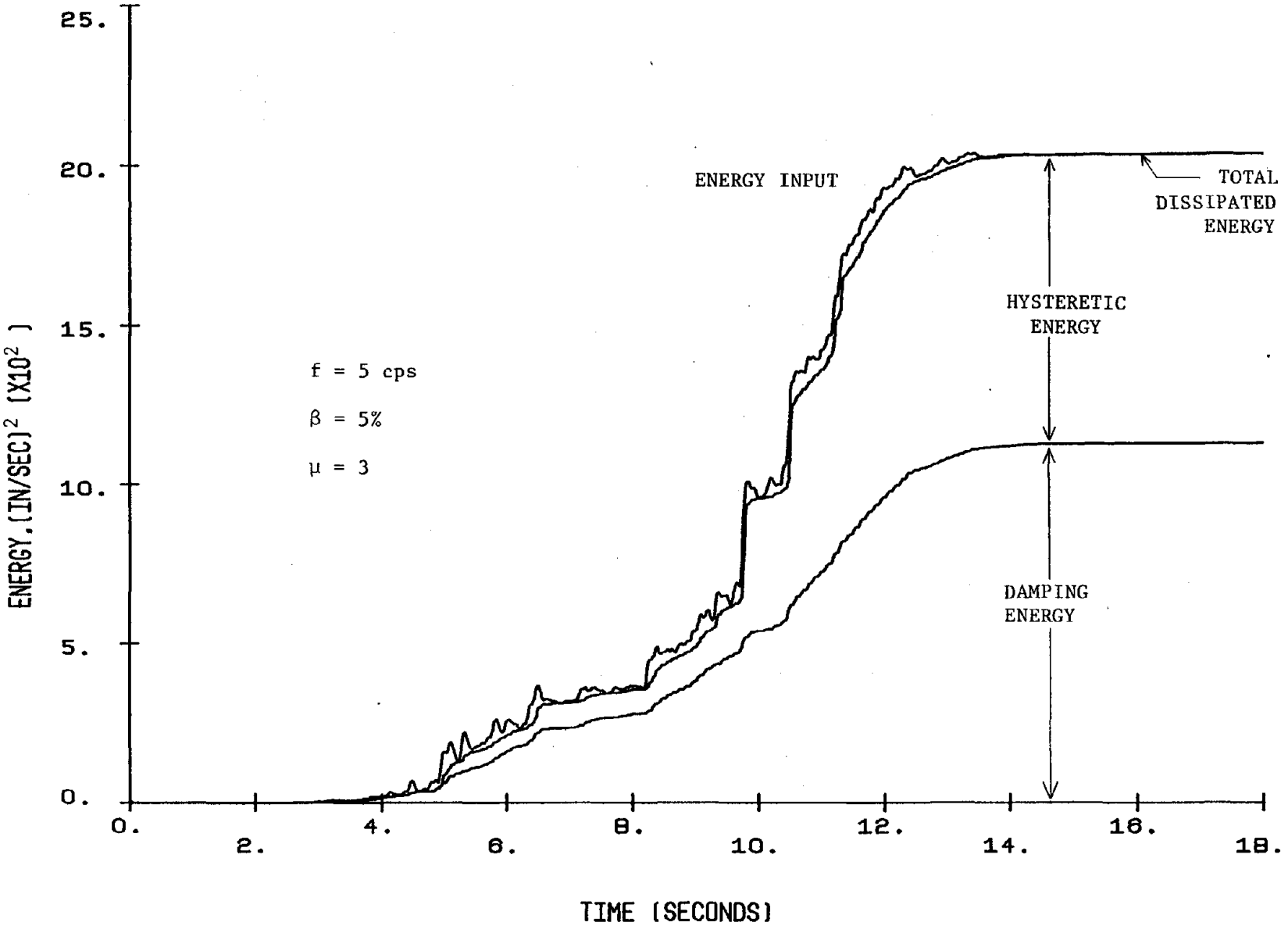

FIG. 4.16c ENERGY VS. TIME FOR A STRUCTURE SUBJECTED TO PACOIMA DAM

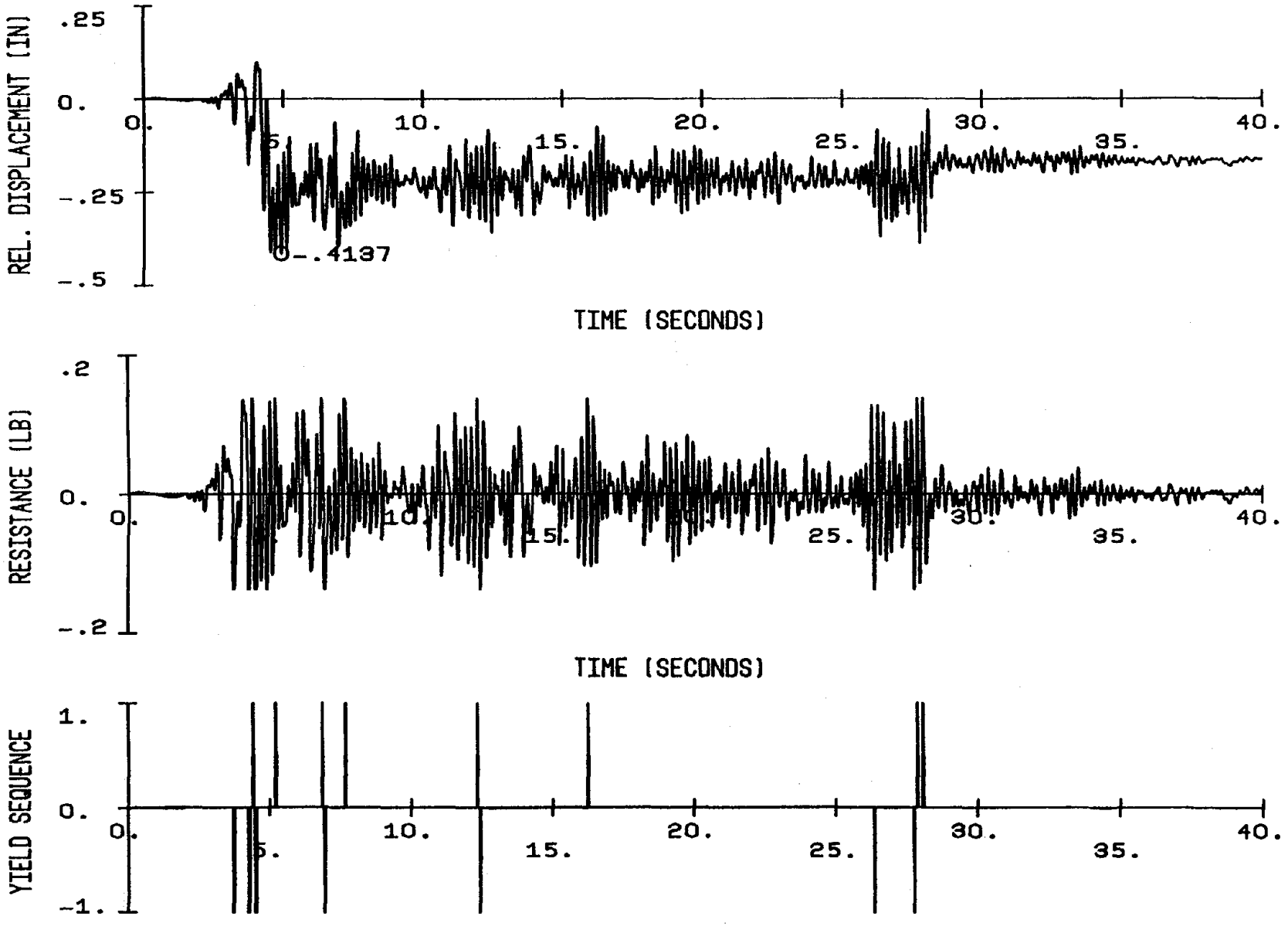

FIG. 4.17a RESPONSE TO EL-CENTRO FOR A STRUCTURE WITH f = 5 CPS, β = 5% AND μ = 3

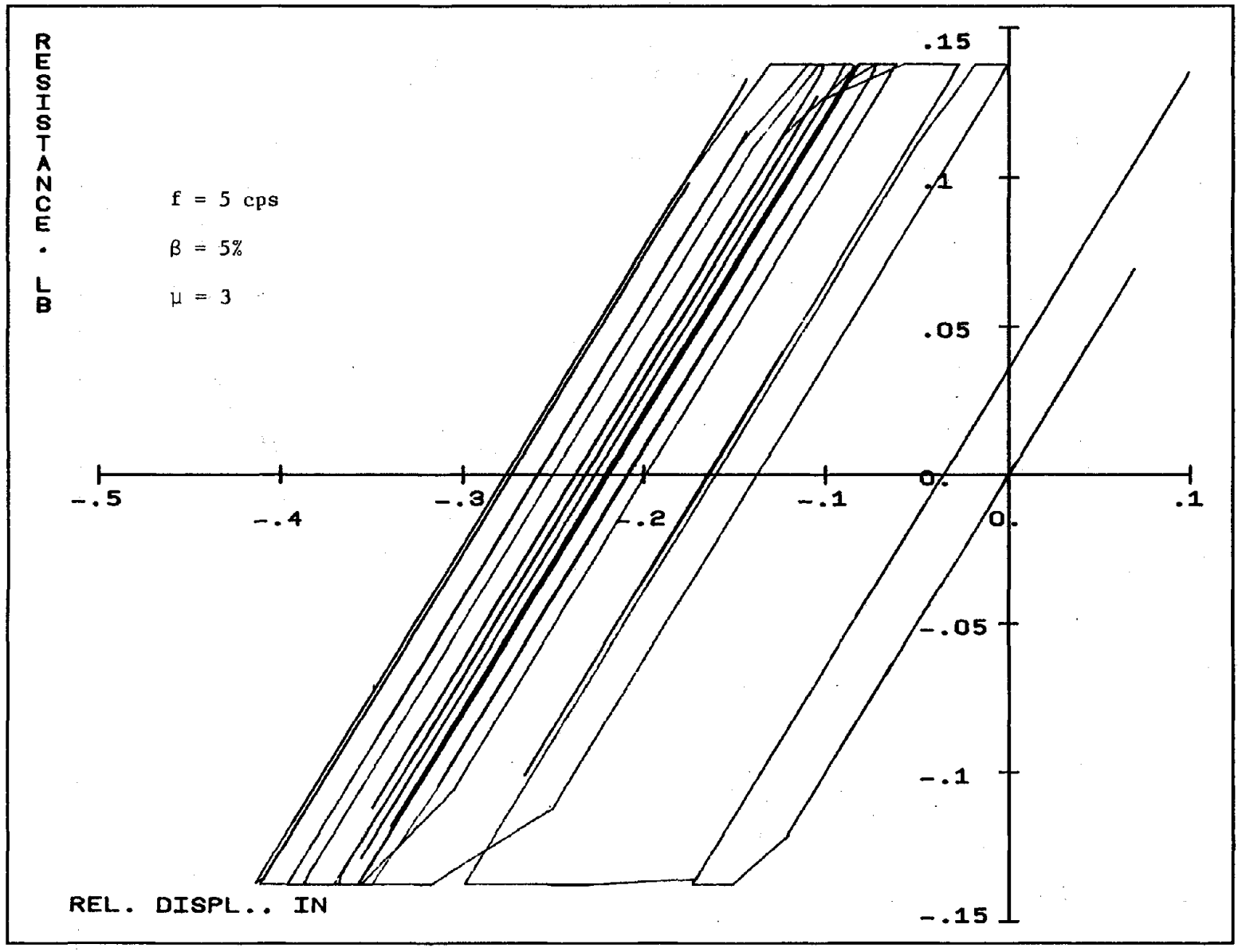

FIG. 4.17b INTERNAL FORCE VS. DEFORMATION FOR A STRUCTURE SUBJECTED TO EL-CENTRO

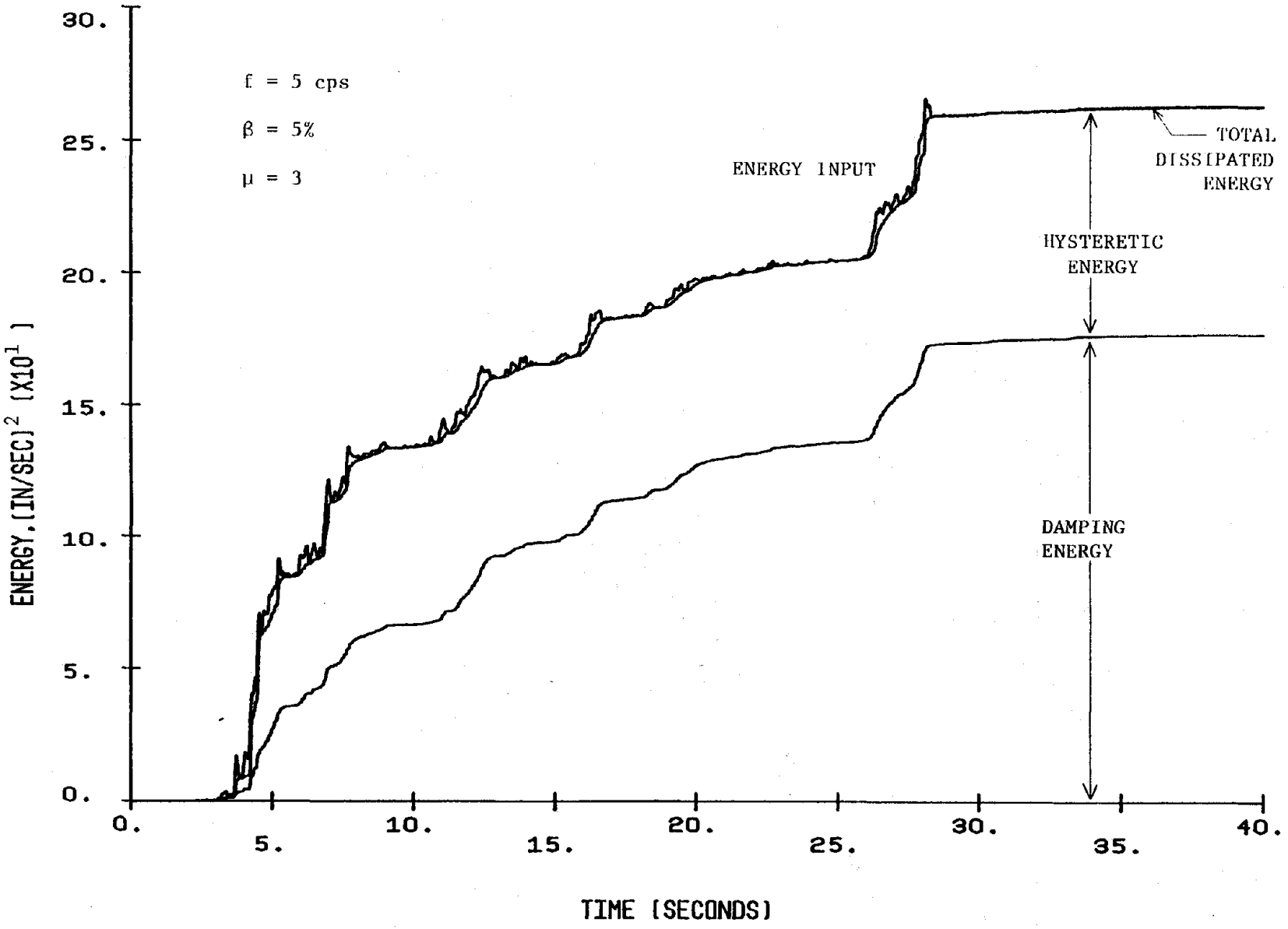

FIG. 4.17c ENERGY VS. TIME FOR A STRUCTURE SUBJECTED TO EL-CENTRO

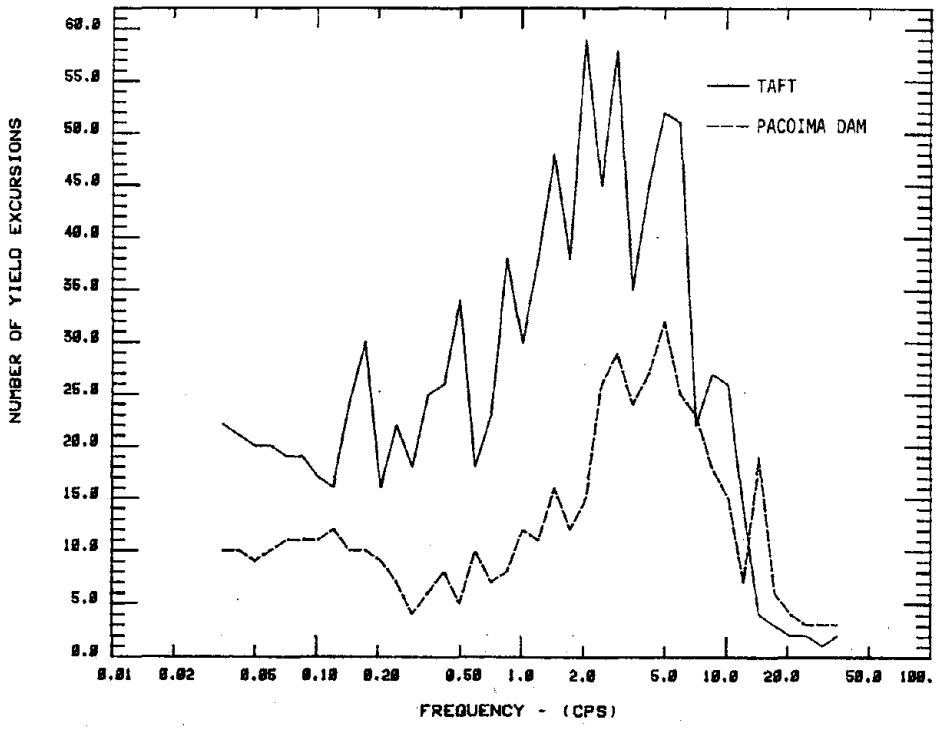

FIG. 4.18a COMPARISON OF THE NUMBER OF YIELD EXCURSIONS FOR STRUCTURES WITH β = 2% AND μ = 5 WHEN SUBJECTED TO TAFT AND PACOIMA DAM, RESPECTIVELY

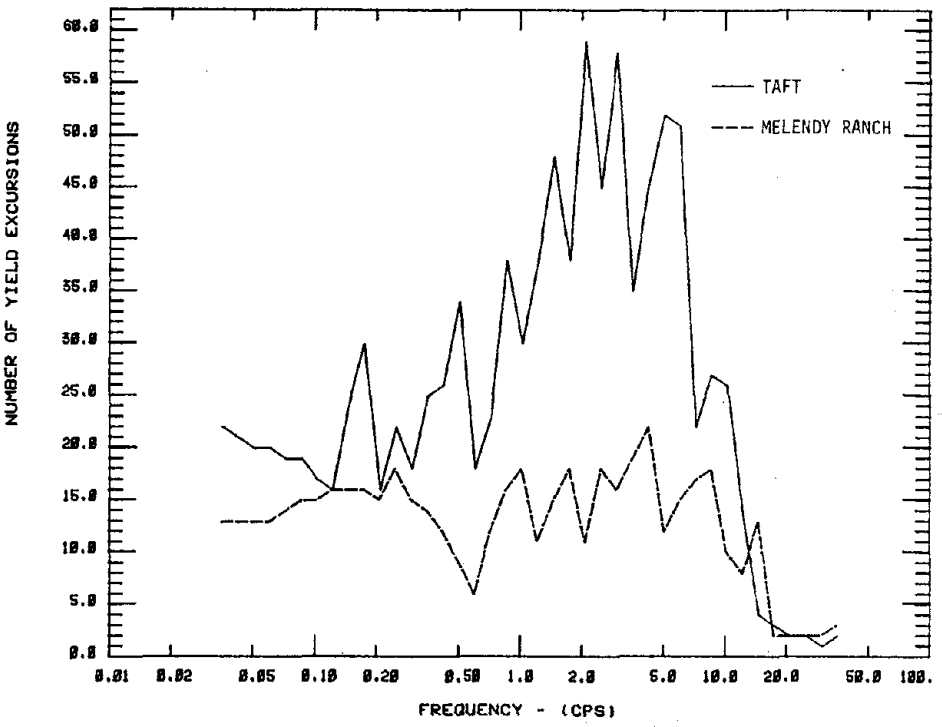

FIG. 4.18b COMPARISON OF THE NUMBER OF YIELD EXCURSIONS FOR STRUCTURES WITH β = 2% AND μ = 5 WHEN SUBJECTED TO TAFT AND MELENDY RANCH, RESPECTIVELY

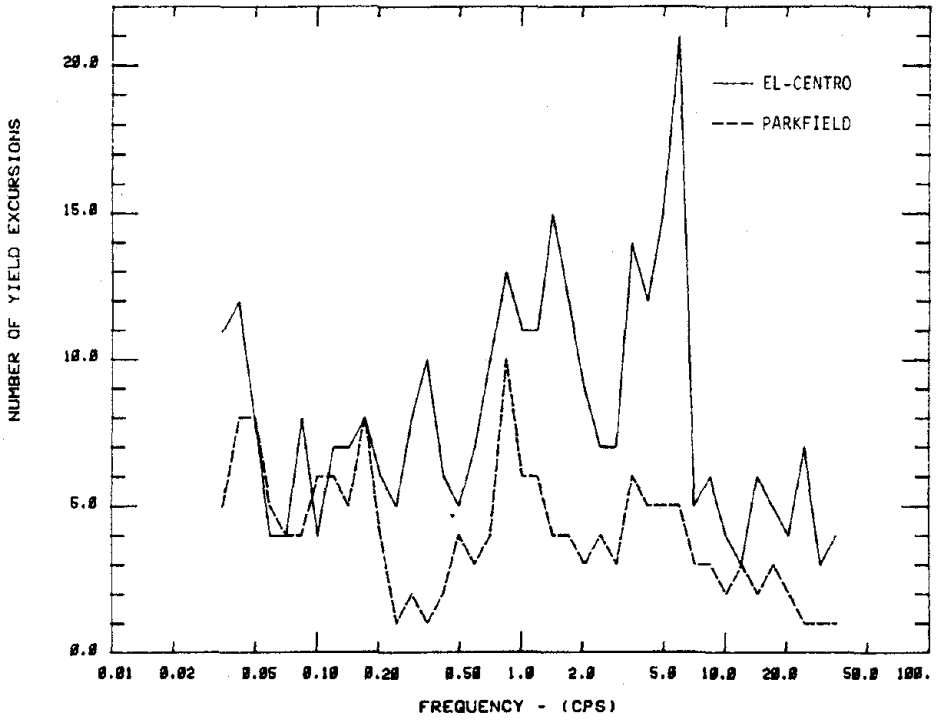

FIG. 4.19a COMPARISON OF THE NUMBER OF YIELD EXCURSIONS FOR STRUCTURES WITH $\beta = 2\%$ AND $\mu = 2$ WHEN SUBJECTED TO EL-CENTRO AND PARKFIELD, RESPECTIVELY

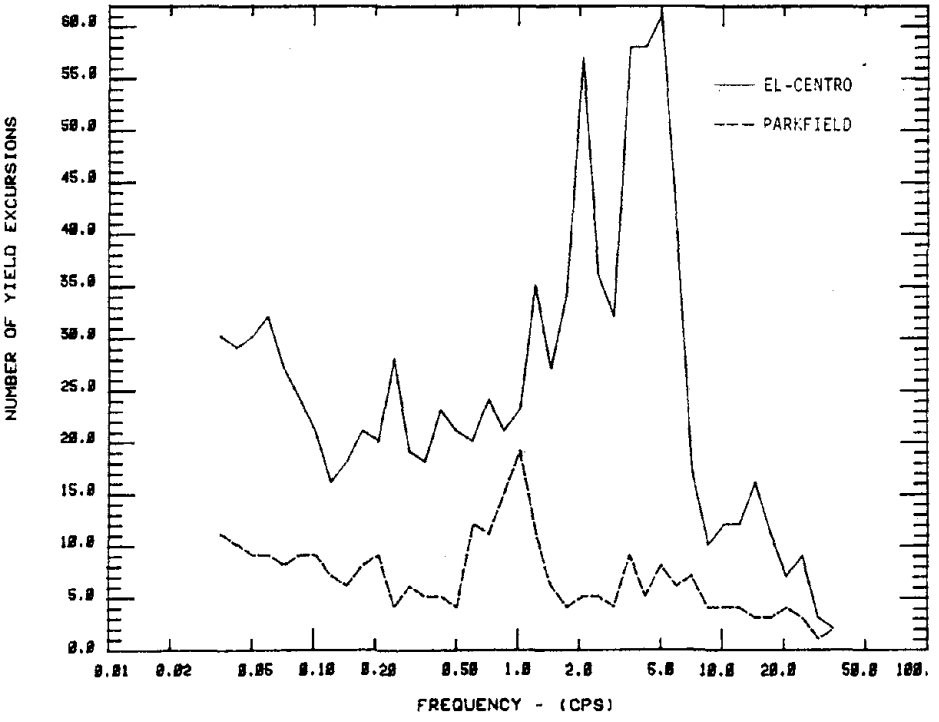

FIG. 4.19b COMPARISON OF THE NUMBER OF YIELD EXCURSIONS FOR STRUCTURES WITH $\beta = 2\%$ AND $\mu = 5$ WHEN SUBJECTED TO EL-CENTRO AND PARKFIELD, RESPECTIVELY

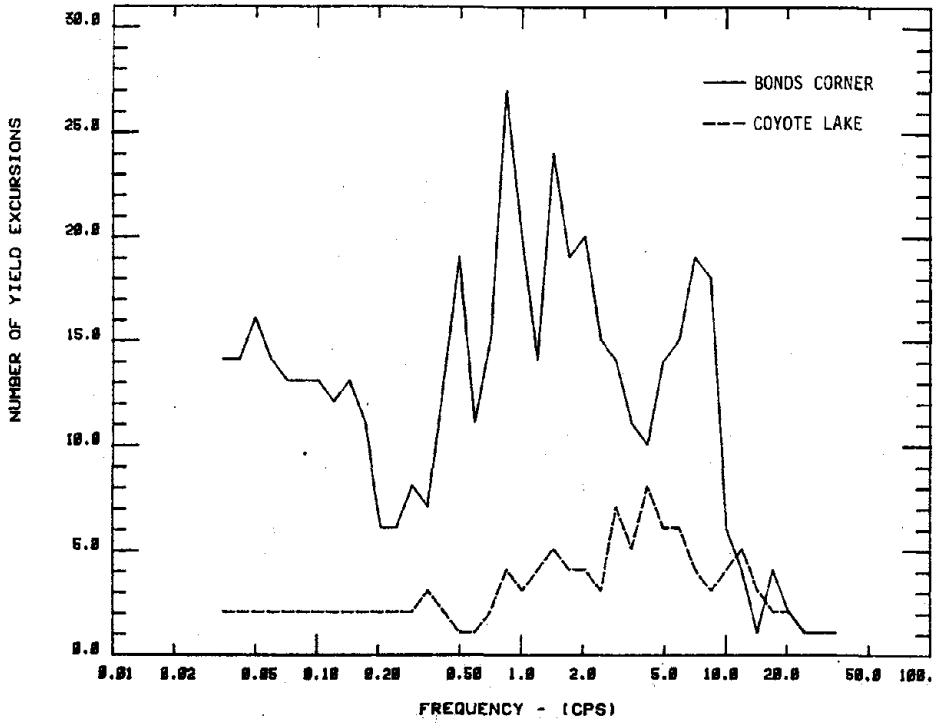

FIG. 4.20a COMPARISON OF THE NUMBER OF YIELD EXCURSIONS FOR STRUCTURES WITH $\beta = 5\%$ AND $\mu = 3$ WHEN SUBJECTED TO BONDS CORNER AND COYOTE LAKE, RESPECTIVELY

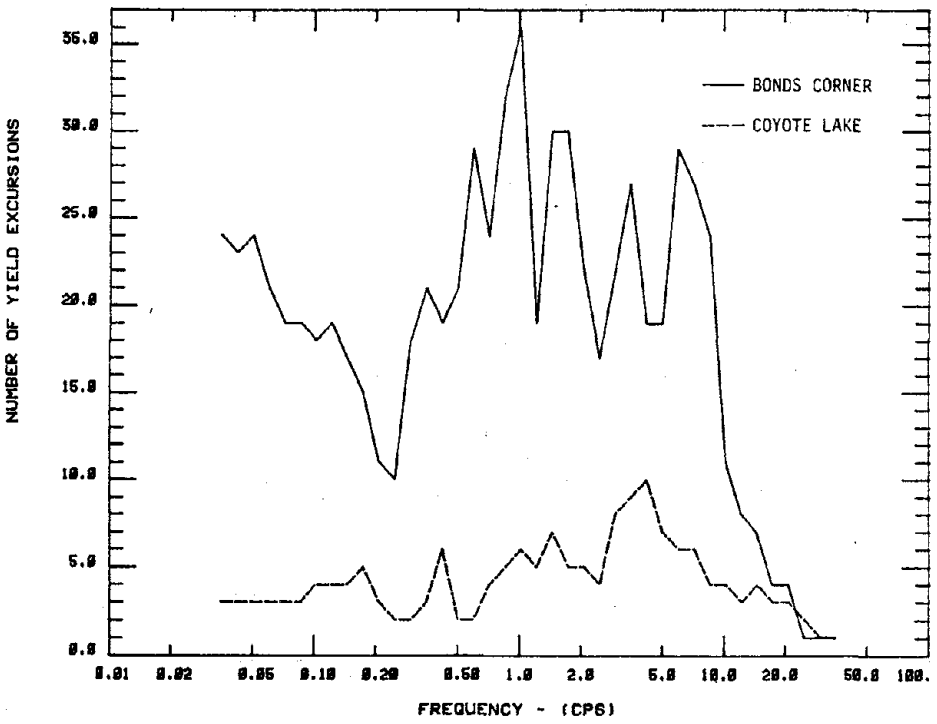

FIG. 4.20b COMPARISON OF THE NUMBER OF YIELD EXCURSIONS FOR STRUCTURES WITH $\beta = 5\%$ AND $\mu = 5$ WHEN SUBJECTED TO BONDS CORNER AND COYOTE LAKE, RESPECTIVELY

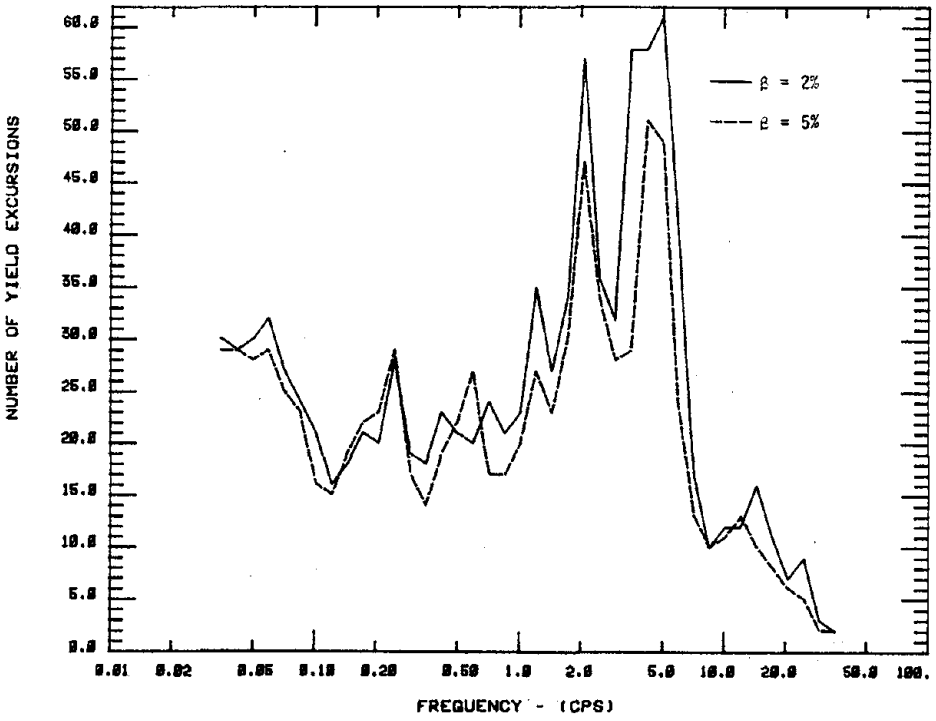

FIG. 4.21a COMPARISON OF THE NUMBER OF YIELD EXCURSIONS FOR STRUCTURES WITH β = 2 AND 5%, RESPECTIVELY, AND μ = 5 WHEN SUBJECTED TO EL-CENTRO

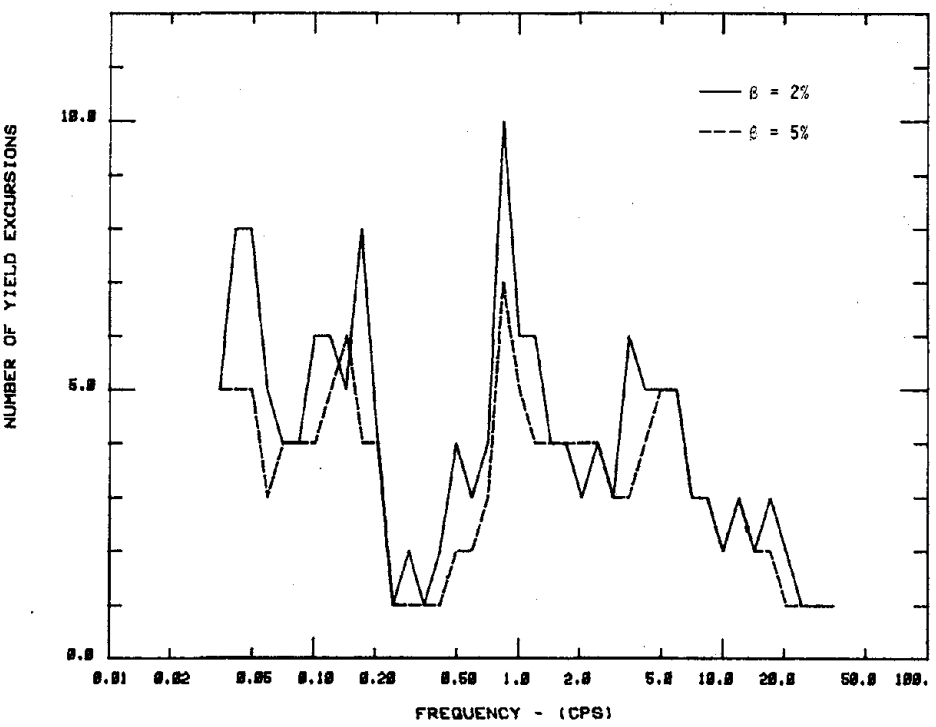

FIG. 4.21b COMPARISON OF THE NUMBER OF YIELD EXCURSIONS FOR STRUCTURES WITH β = 2 AND 5%, RESPECTIVELY, AND μ = 2 WHEN SUBJECTED TO PARKFIELD

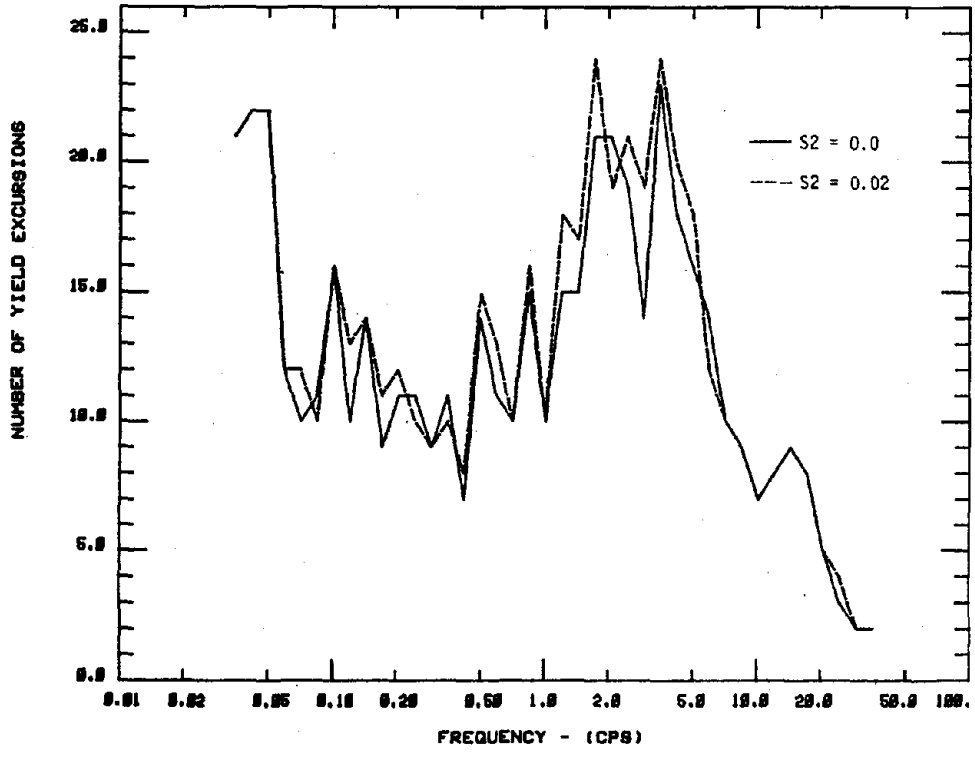

FIG. 4.22a COMPARISON OF NUMBER OF YIELD EXCURSIONS FOR ELASTOPLASTIC AND BILINEAR SYSTEMS WITH β = 5% AND μ = 3 WHEN SUBJECTED TO EL-CENTRO

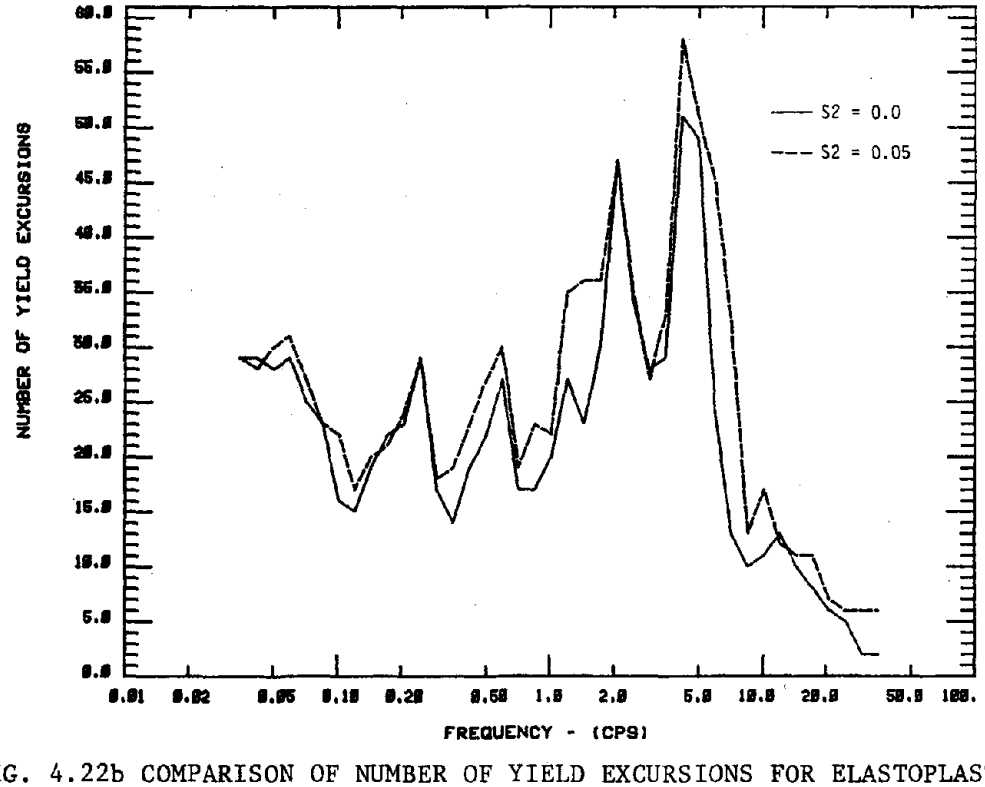

FIG. 4.22b COMPARISON OF NUMBER OF YIELD EXCURSIONS FOR ELASTOPLASTIC AND BILINEAR SYSTEMS WITH β = 5% AND μ = 5 WHEN SUBJECTED TO EL-CENTRO

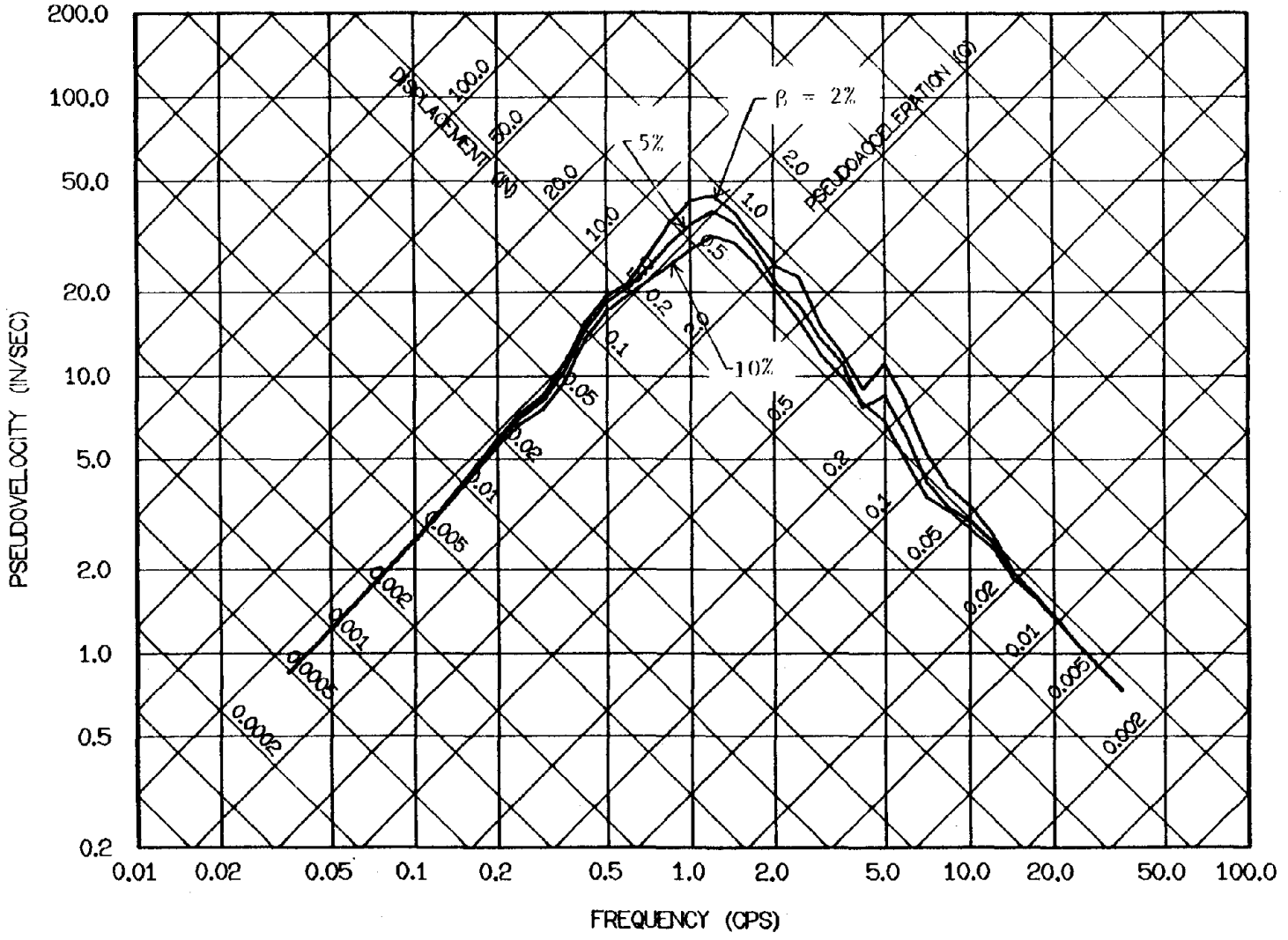

FIG. 4.23a ELASTIC RESPONSE SPECTRA FOR SYSTEMS WITH 2, 5 AND 10% DAMPING SUBJECTED TO THE COYOTE LAKE EARTHQUAKE OF AUG. 6, 1979, GILROY ARRAY NO. 6, COMPONENT 230°

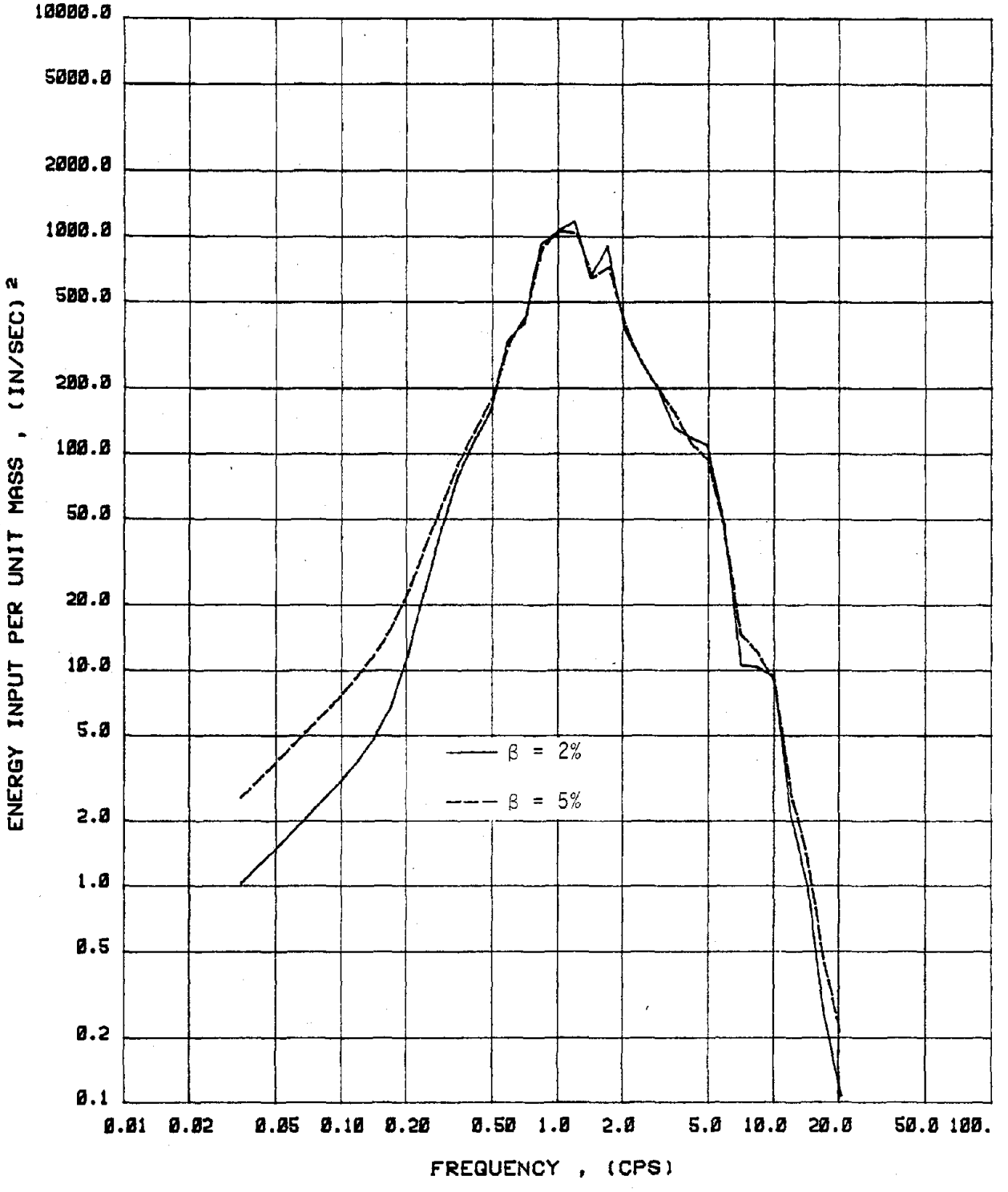

FIG. 4.23b ENERGY INPUT SPECTRA FOR ELASTIC SYSTEMS WITH 2 AND 5% DAMPING SUBJECTED TO THE COYOTE LAKE EARTHQUAKE OF AUG. 6, 1979, GILROY ARRAY NO. 6, COMPONENT 230°

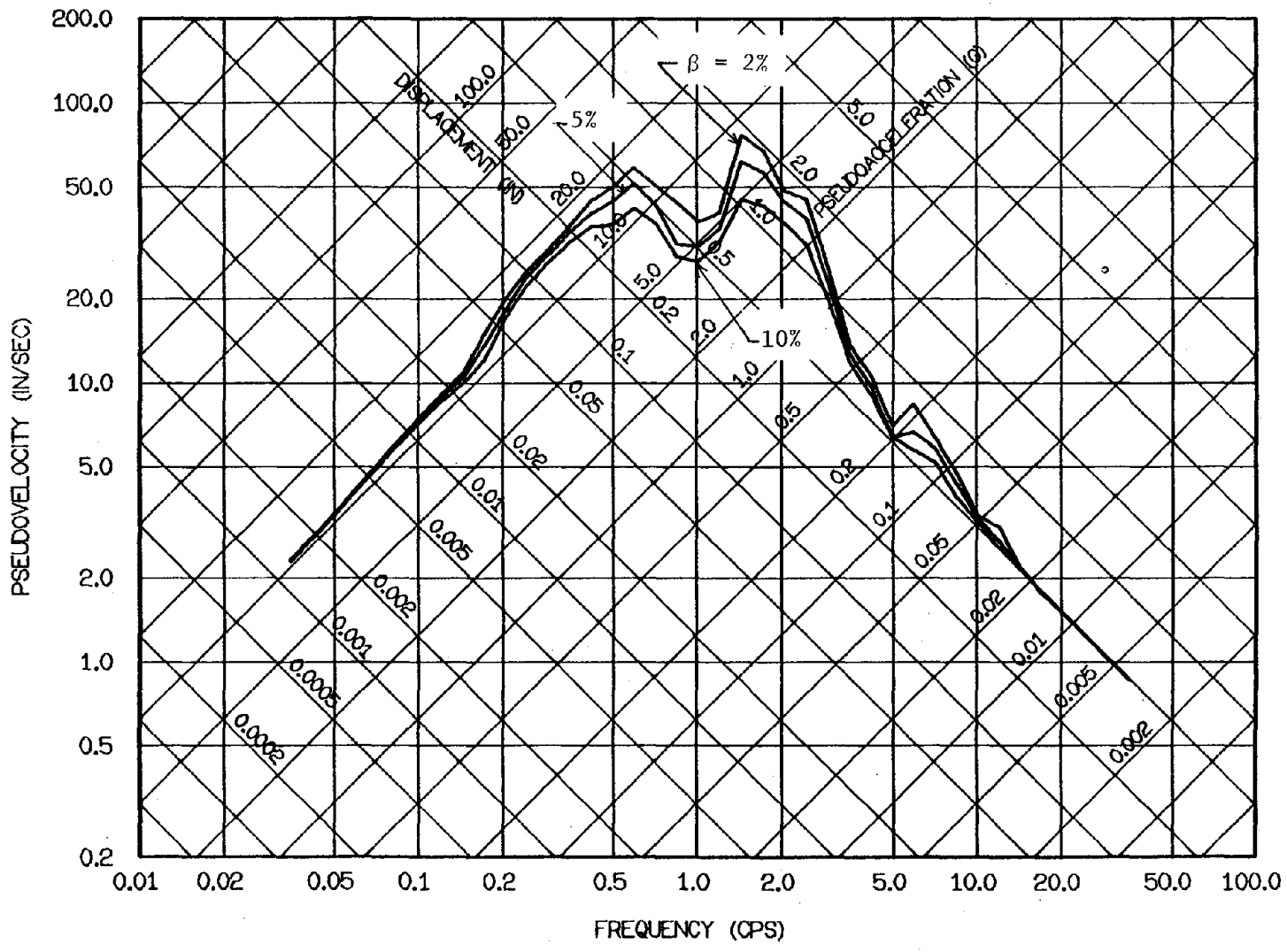

FIG. 4.24a ELASTIC RESPONSE SPECTRA FOR SYSTEMS WITH 2, 5 AND 10% DAMPING SUBJECTED TO THE PARKFIELD EARTHQUAKE OF JUNE 27, 1966, CHOLANE-SHANDON, CALIFORNIA ARRAY NO. 2, COMPONENT N65E

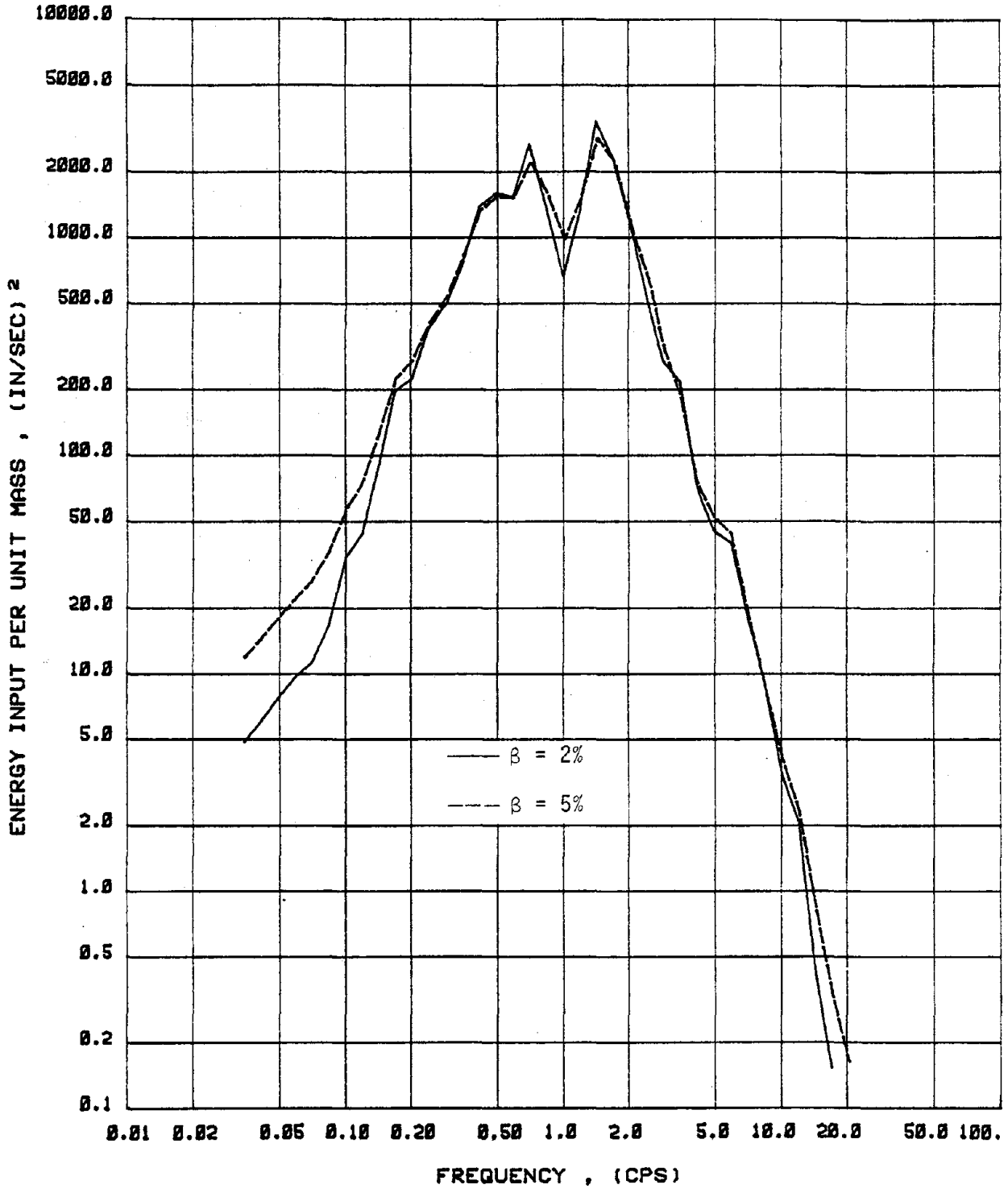

FIG. 4.24b ENERGY INPUT SPECTRA FOR ELASTIC SYSTEMS WITH 2 AND 5% DAMPING SUBJECTED TO THE PARKFIELD EARTHQUAKE OF JUNE 27, 1966, CHOLANE-SHANDON, CALIFORNIA ARRAY NO. 2, COMPONENT N65E

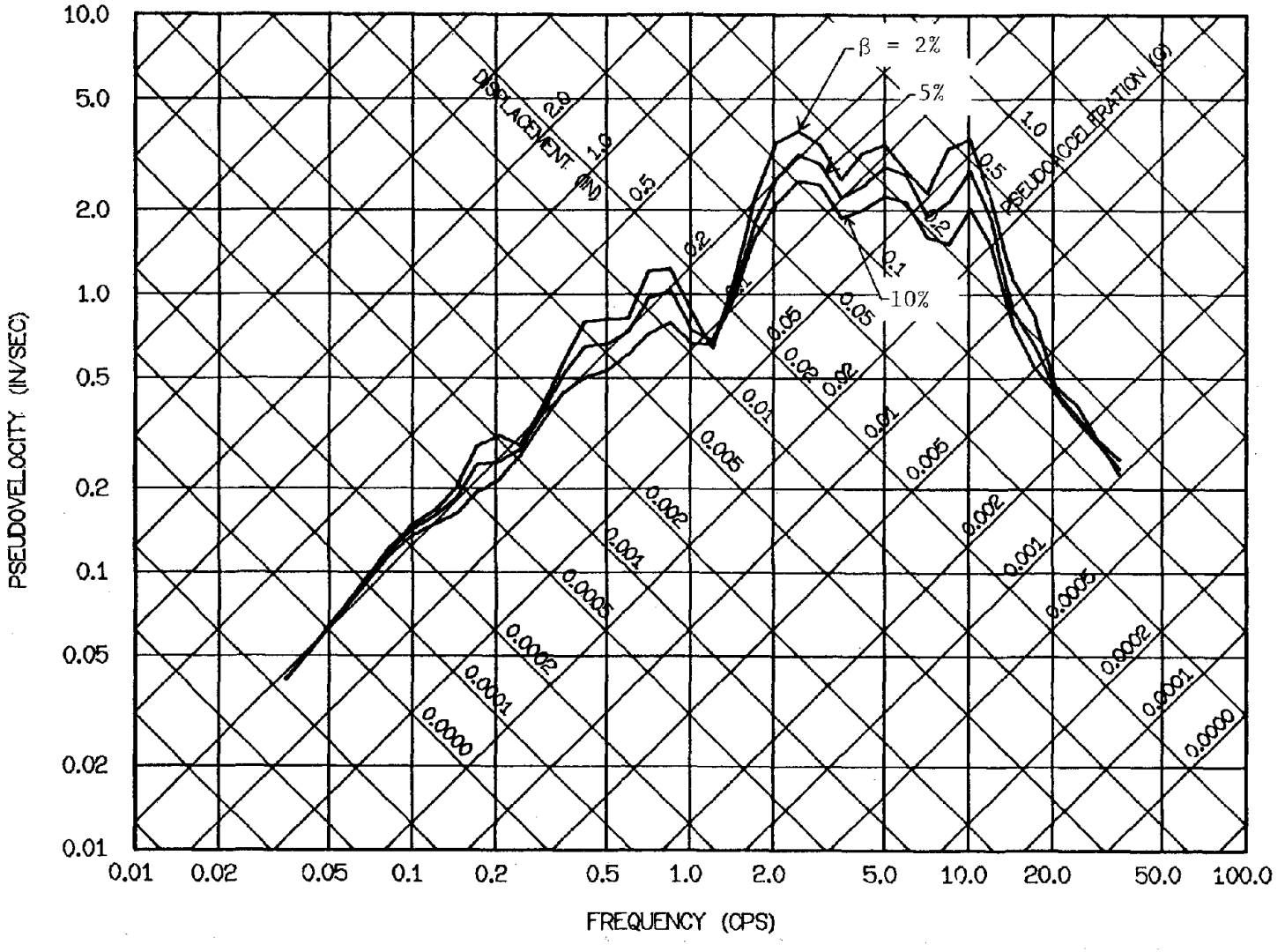

FIG. 4.25a ELASTIC RESPONSE SPECTRA FOR SYSTEMS WITH 2, 5 AND 10% DAMPING SUBJECTED TO THE HOLLISTER EARTHQUAKE OF NOV. 28, 1974, GAVILAN COLLEGE RECORD, COMPONENT S67W

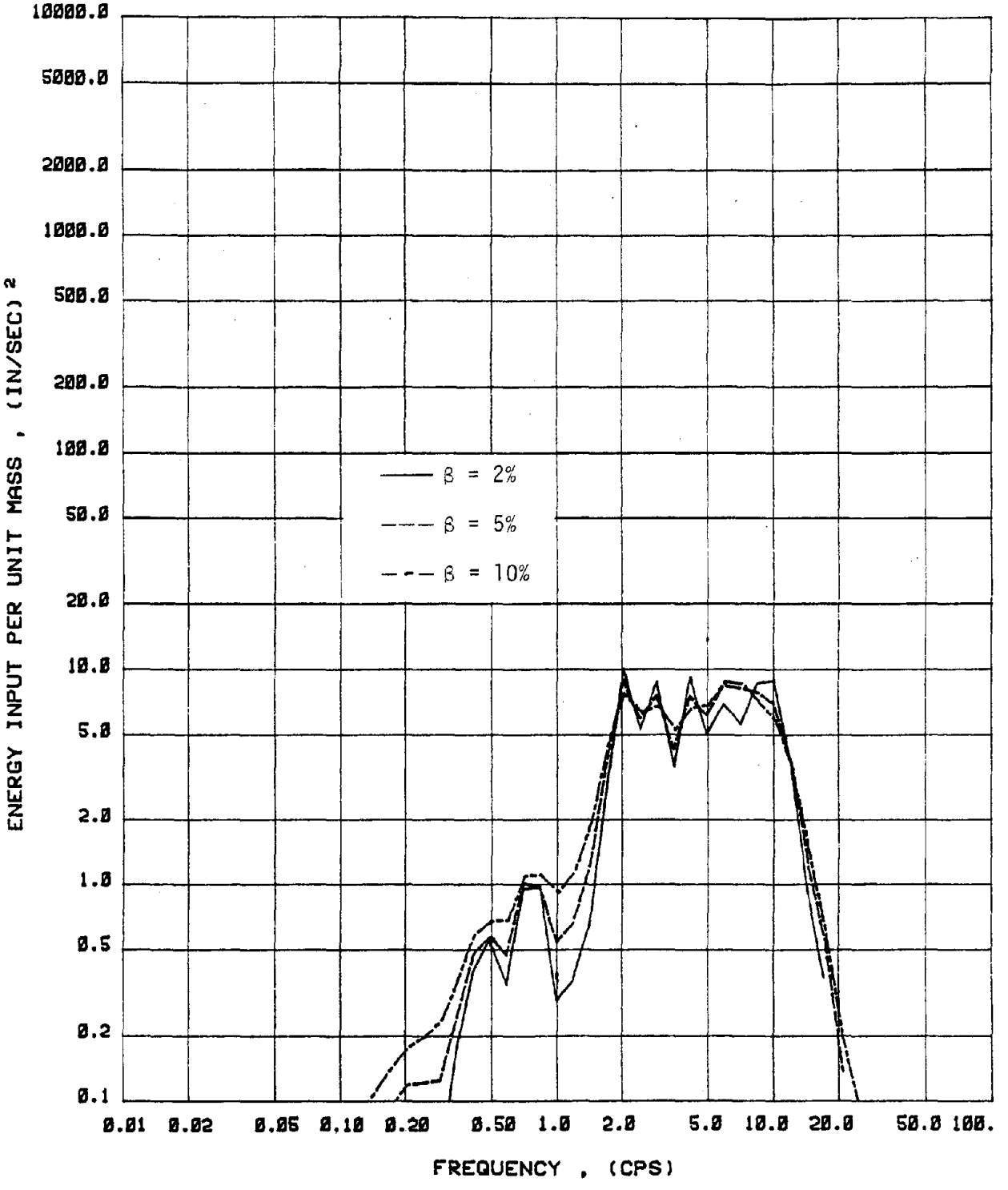

FIG. 4.25b ENERGY INPUT SPECTRA FOR ELASTIC SYSTEMS WITH 2, 5 AND 10% DAMPING SUBJECTED TO THE HOLLISTER EARTHQUAKE OF NOV. 28, 1974, GAVILAN COLLEGE RECORD, COMPONENT S67W

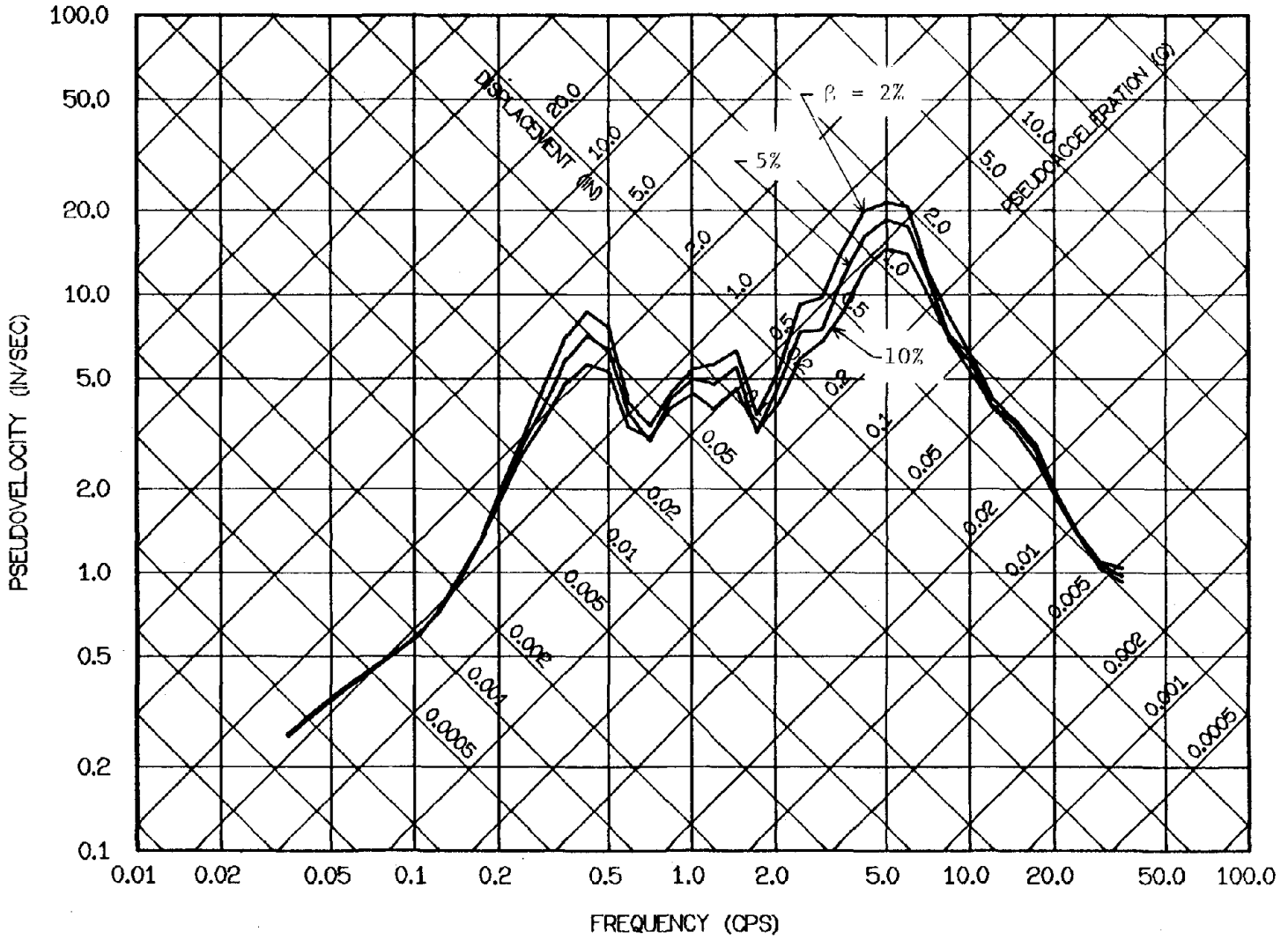

FIG. 4.26a ELASTIC RESPONSE SPECTRA FOR SYSTEMS WITH 2, 5 AND 10% DAMPING SUBJECTED TO THE BEAR VALLEY EARTHQUAKE OF SEPT. 4, 1972, MELENDY RANCH RECORD, COMPONENT N29W

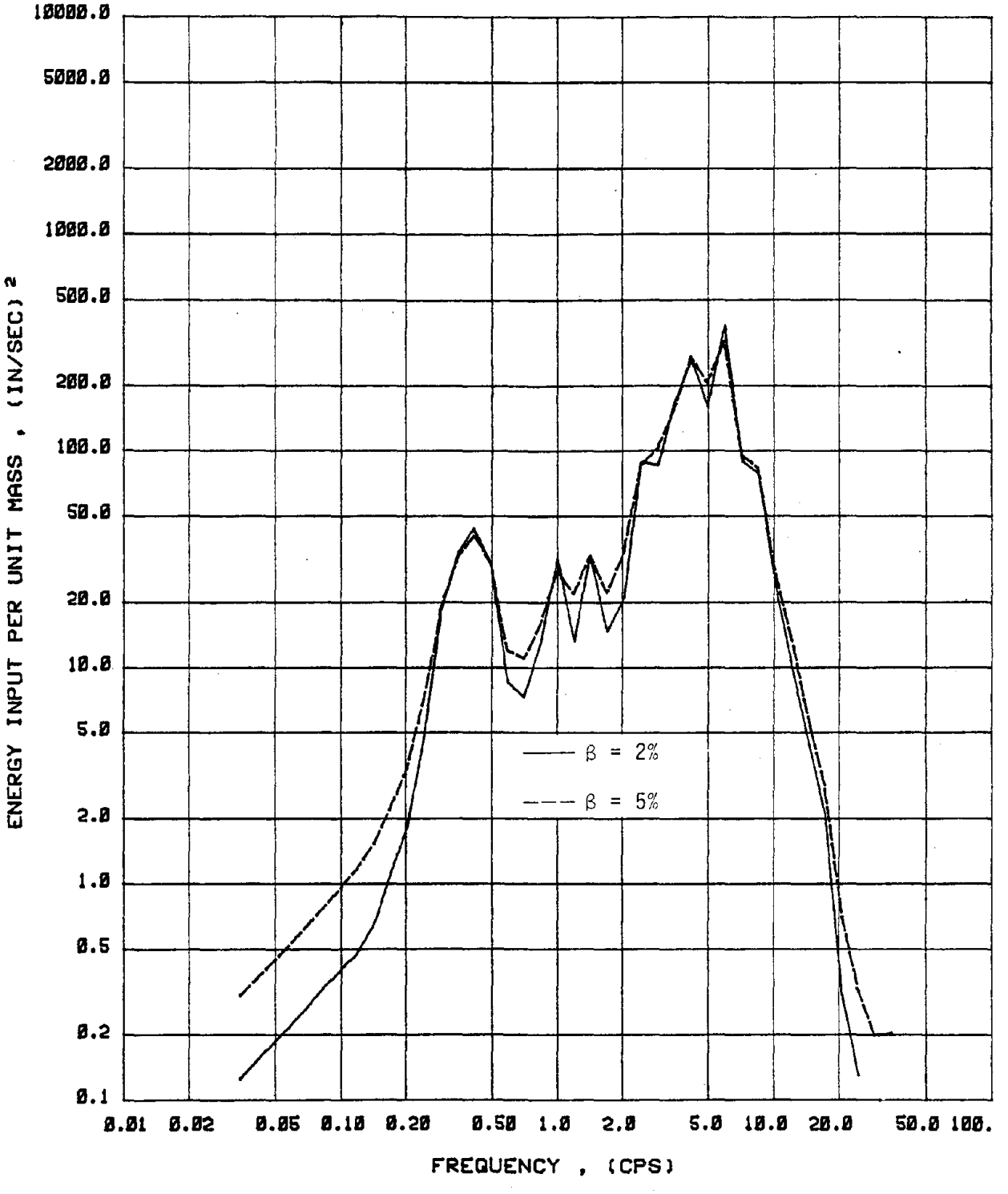

FIG. 4.26b ENERGY INPUT SPECTRA FOR ELASTIC SYSTEMS WITH 2 AND 5% DAMPING SUBJECTED TO THE BEAR VALLEY EARTHQUAKE OF SEPT. 4, 1972, MELENDY RANCH RECORD, COMPONENT N29W

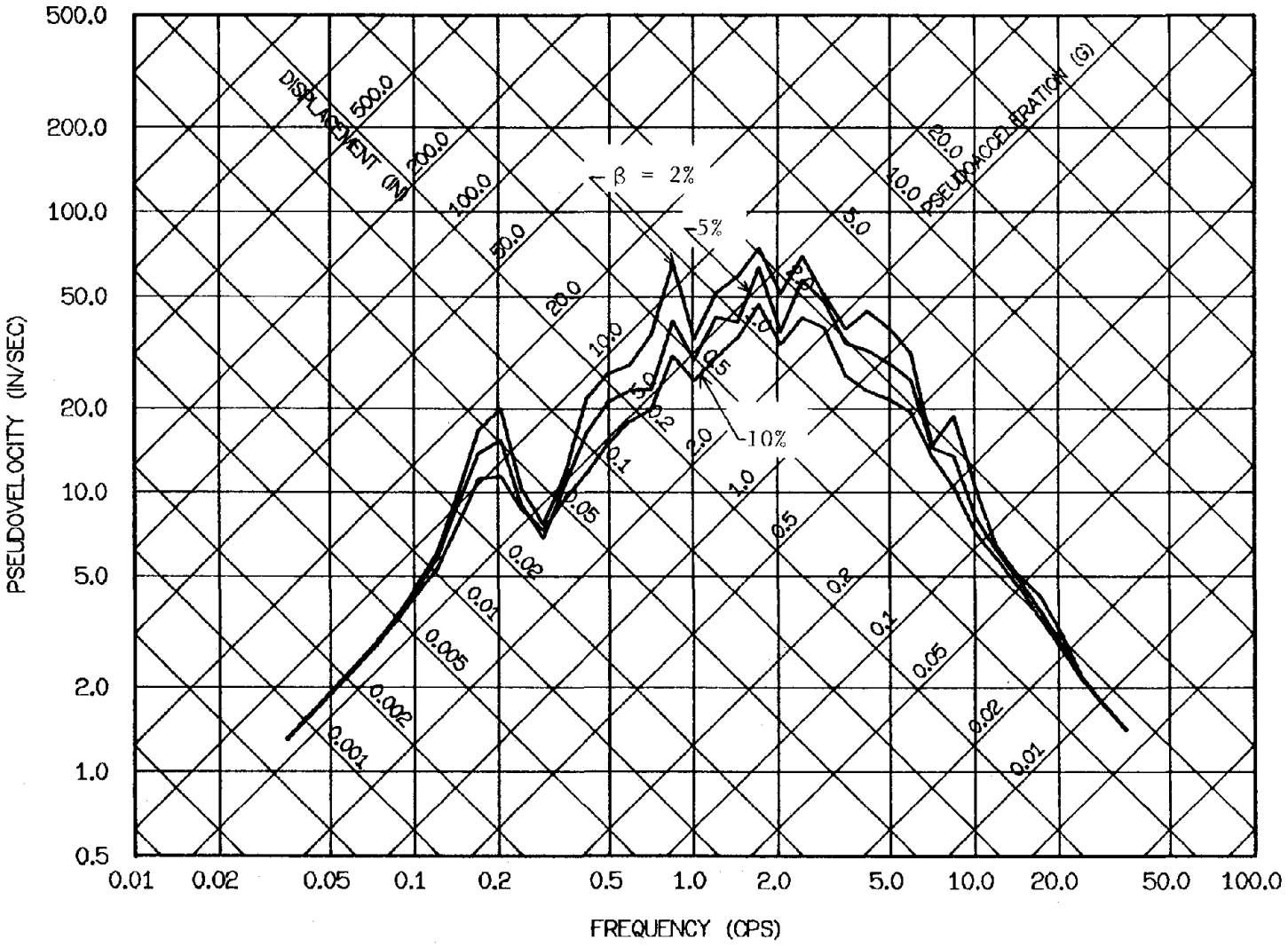

FIG. 4.27a ELASTIC RESPONSE SPECTRA FOR SYSTEMS WITH 2, 5 AND 10% DAMPING SUBJECTED TO THE IMPERIAL VALLEY EARTHQUAKE OF OCT. 15, 1979, BONDS CORNER RECORD, COMPONENT 230°

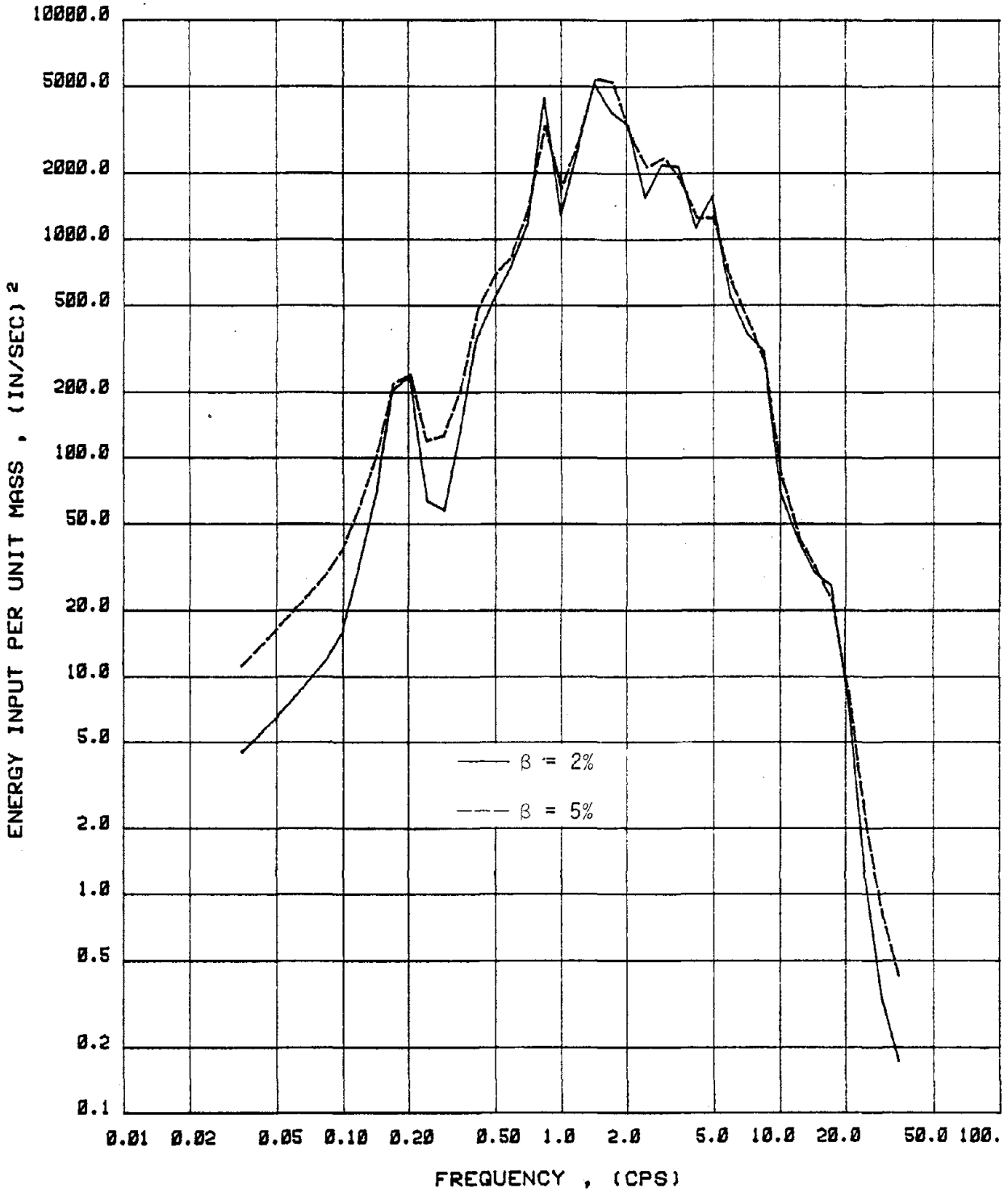

FIG. 4.27b ENERGY INPUT SPECTRA FOR ELASTIC SYSTEMS WITH 2 AND 5% DAMPING SUBJECTED TO THE IMPERIAL VALLEY EARTHQUAKE OF OCT. 15, 1979, BONDS CORNER RECORD, COMPONENT 230°

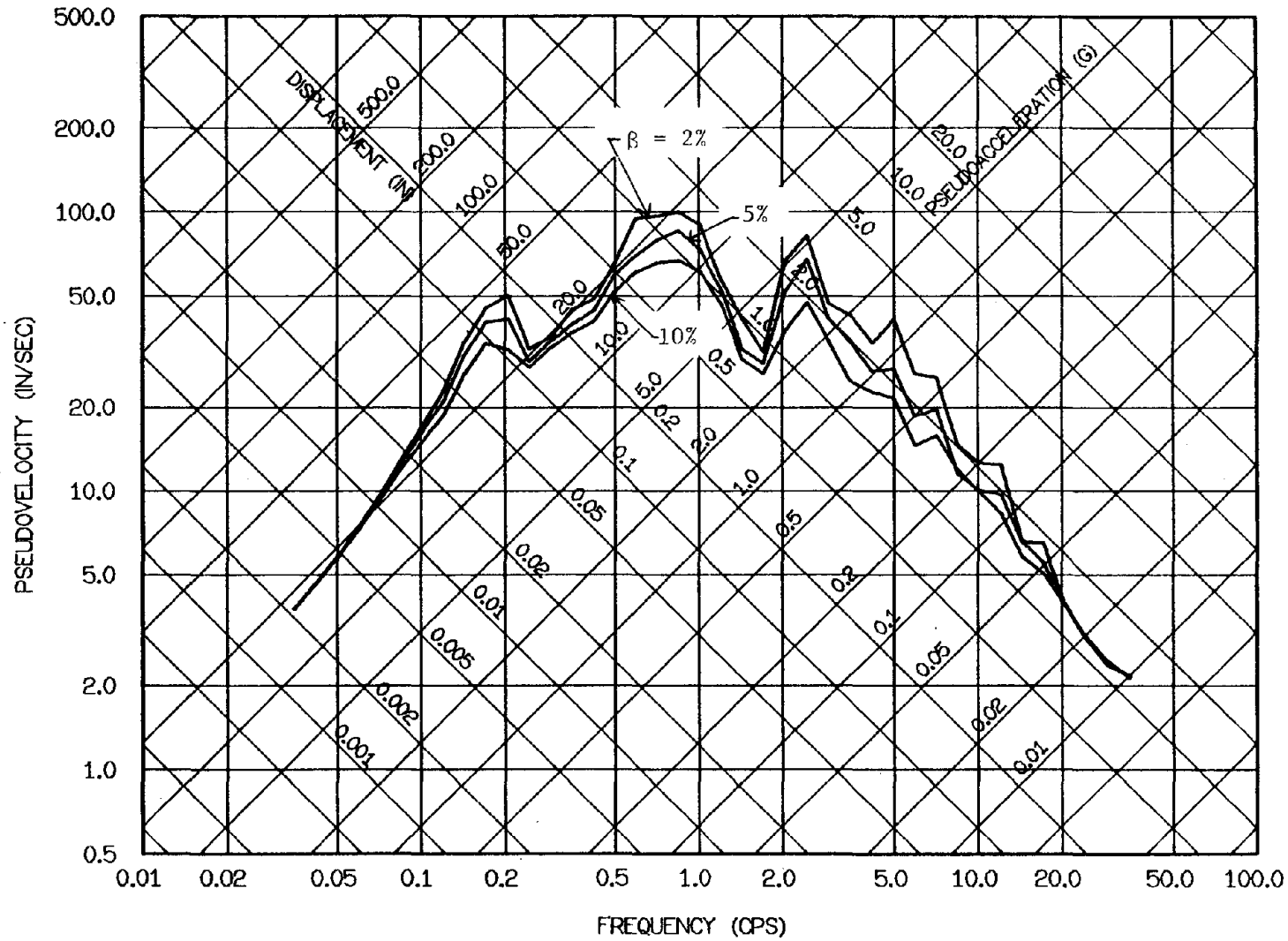

FIG. 4.28a ELASTIC RESPONSE SPECTRA FOR SYSTEMS WITH 2, 5 AND 10% DAMPING SUBJECTED TO THE SAN FERNANDO EARTHQUAKE OF FEB. 9, 1971, PACOIMA DAM RECORD, COMPONENT S16E

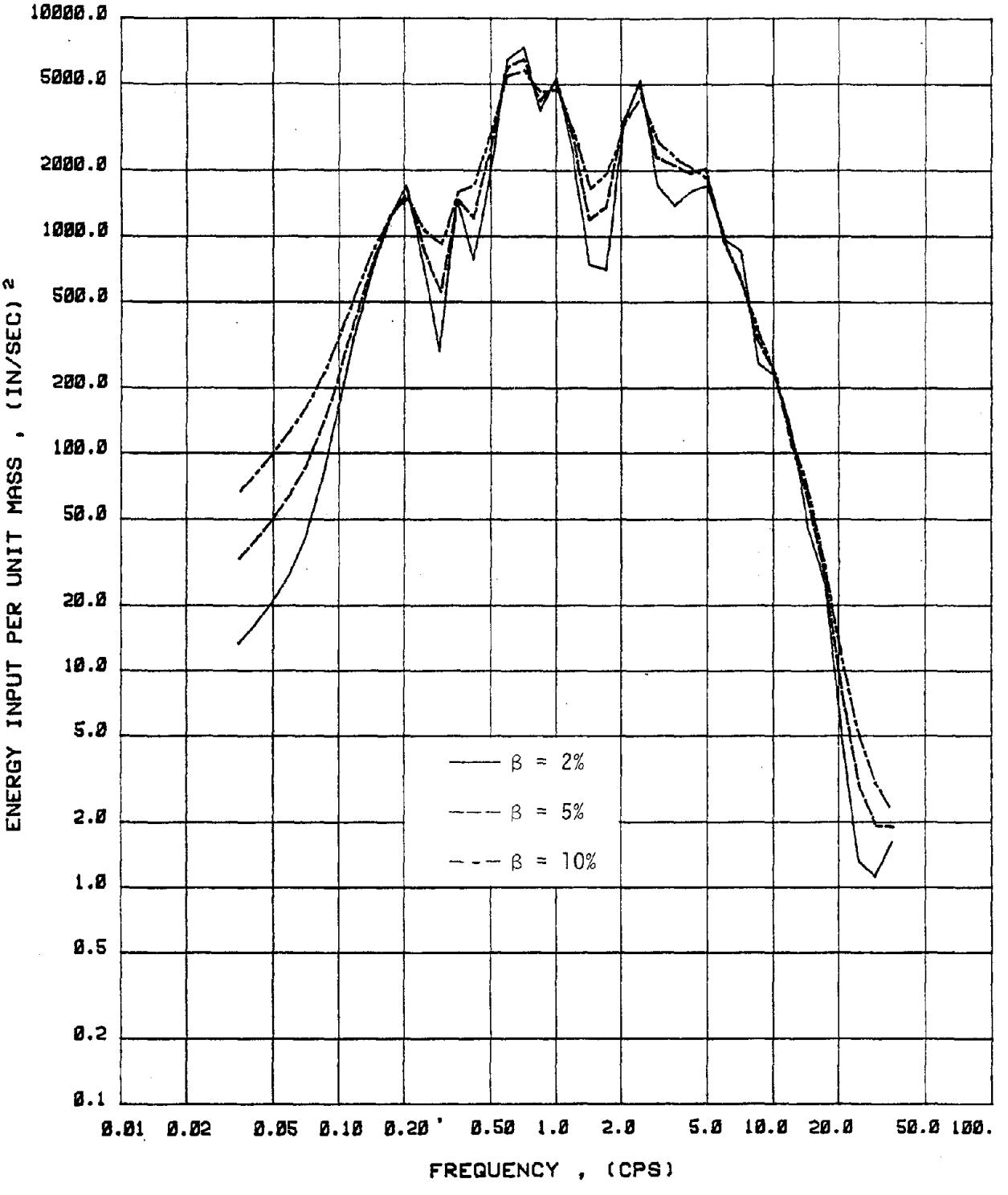

FIG. 4.28b ENERGY INPUT SPECTRA FOR ELASTIC SYSTEMS WITH 2, 5 AND 10% DAMPING SUBJECTED TO THE SAN FERNANDO EARTHQUAKE OF FEB. 9, 1971, PACOIMA DAM RECORD, COMPONENT S16E

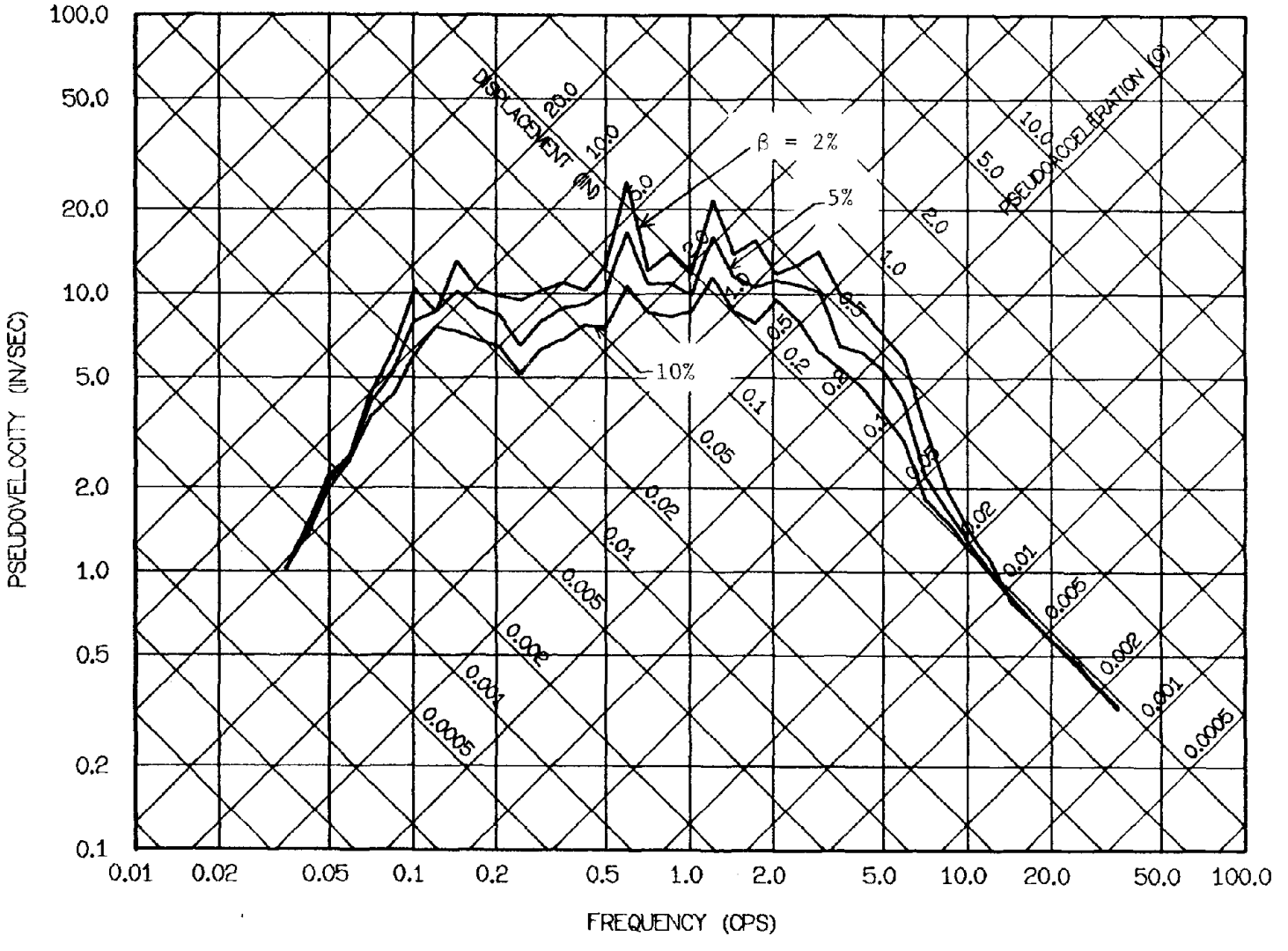

FIG. 4.29a ELASTIC RESPONSE SPECTRA FOR SYSTEMS WITH 2, 5 AND 10% DAMPING SUBJECTED TO THE KERN COUNTY EARTHQUAKE OF JULY 21, 1952, TAFT-LINCOLN SCHOOL RECORD, COMPONENT S69E

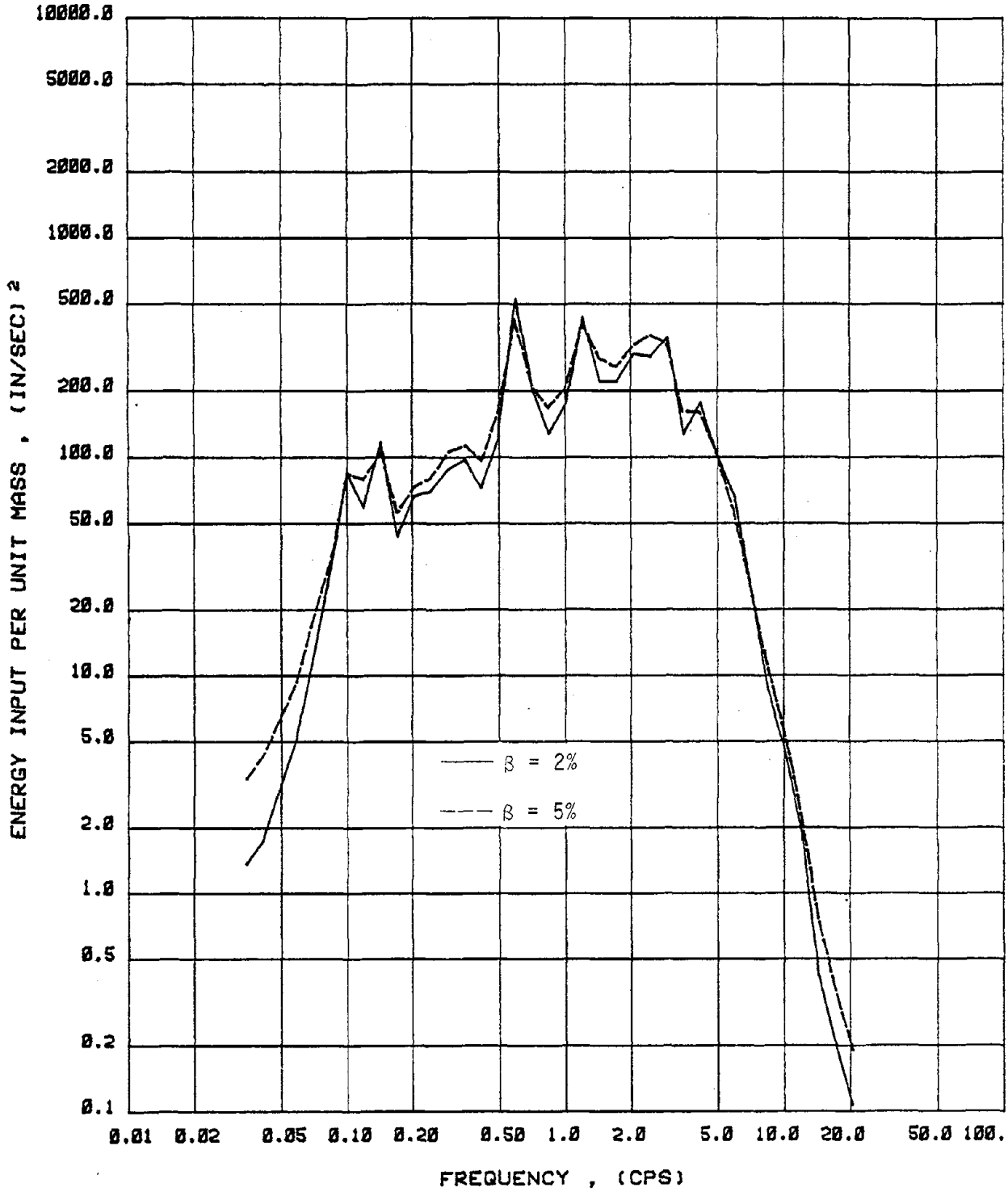

FIG. 4.29b ENERGY INPUT SPECTRA FOR ELASTIC SYSTEMS WITH 2 AND 5% DAMPING SUBJECTED TO THE KERN COUNTY EARTHQUAKE OF JULY 21, 1952, TAFT-LINCOLN SCHOOL RECORD, COMPONENT S69E

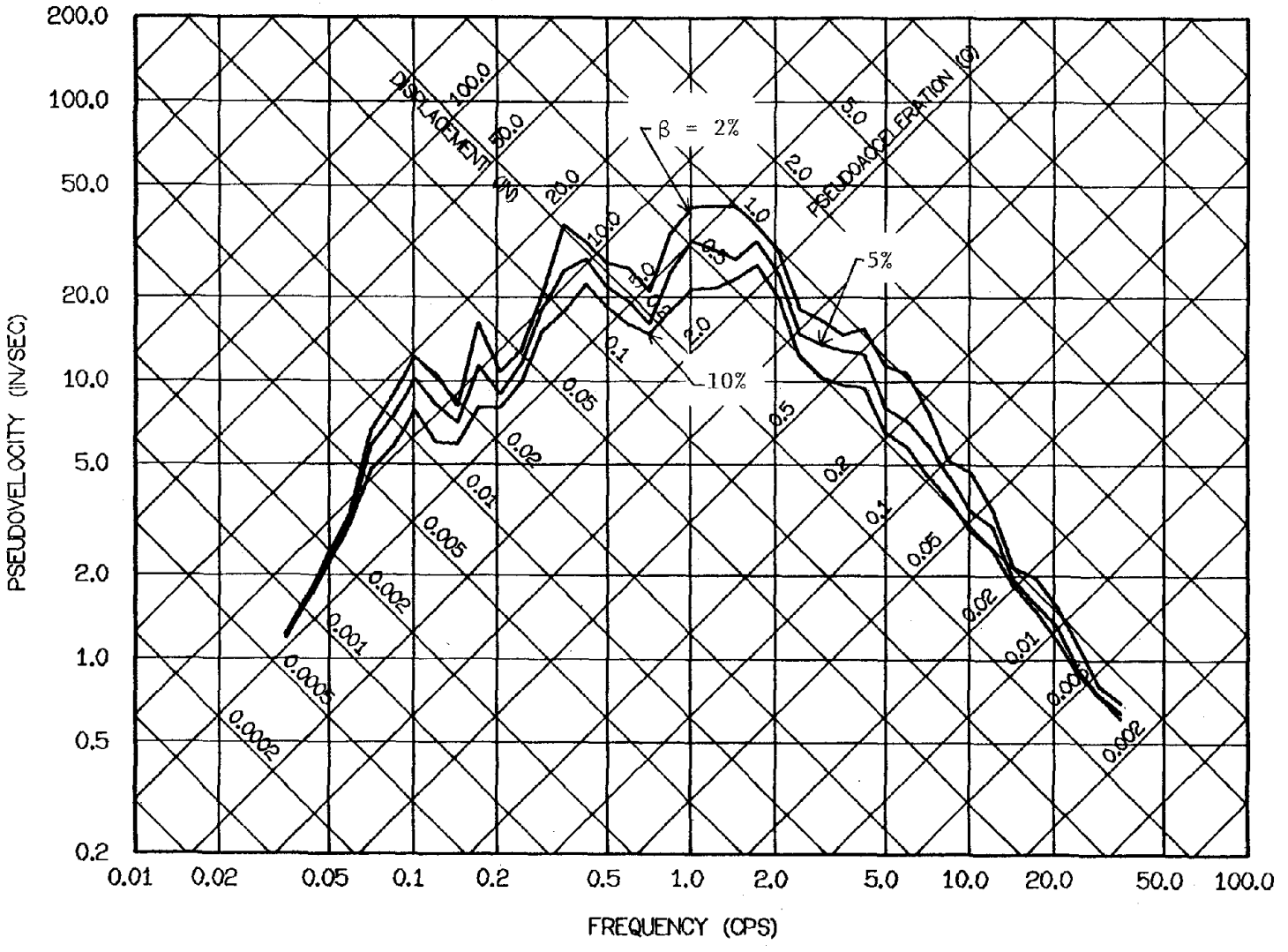

FIG. 4.30a ELASTIC RESPONSE SPECTRA FOR SYSTEMS WITH 2, 5 AND 10% DAMPING SUBJECTED TO THE IMPERIAL VALLEY EARTHQUAKE OF MAY 18, 1940, EL-CENTRO RECORD, COMPONENT S00E

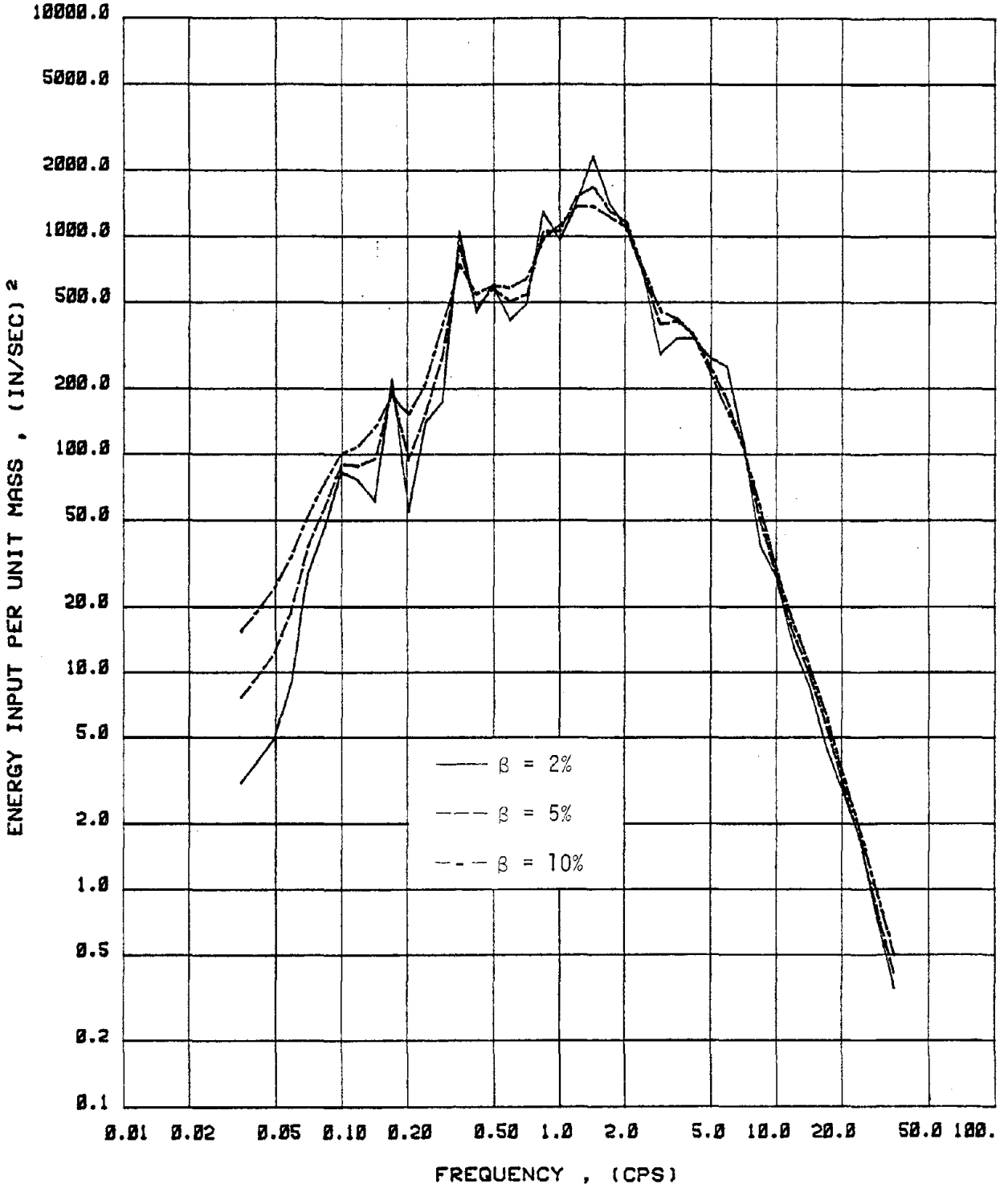

FIG. 4.30b ENERGY INPUT SPECTRA FOR ELASTIC SYSTEMS WITH 2, 5 AND 10% DAMPING SUBJECTED TO THE IMPERIAL VALLEY EARTHQUAKE OF MAY 18, 1940, EL-CENTRO RECORD, COMPONENT S00E

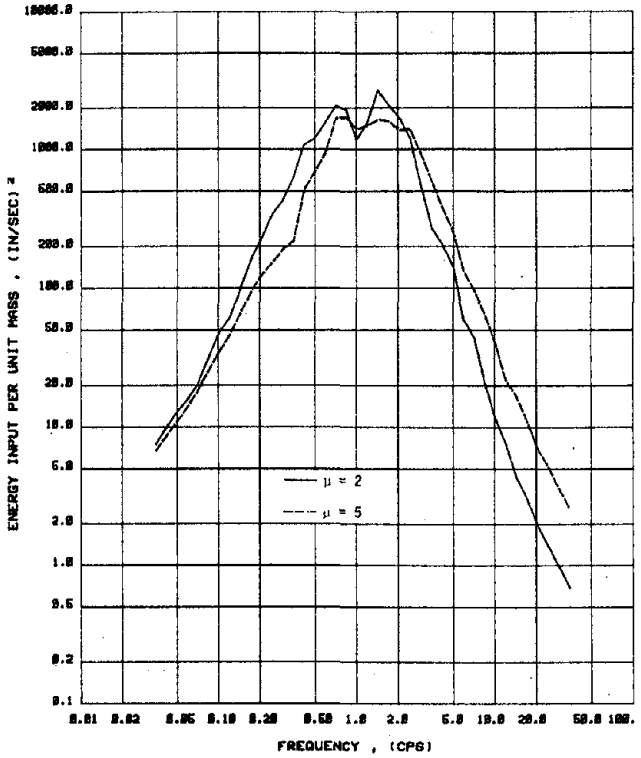

FIG. 4.35 ENERGY INPUT SPECTRA FOR ELASTOPLASTIC SYSTEMS WITH $\beta = 2\%$ AND $\mu = 2$ AND 5 WHEN SUBJECTED TO PARKFIELD

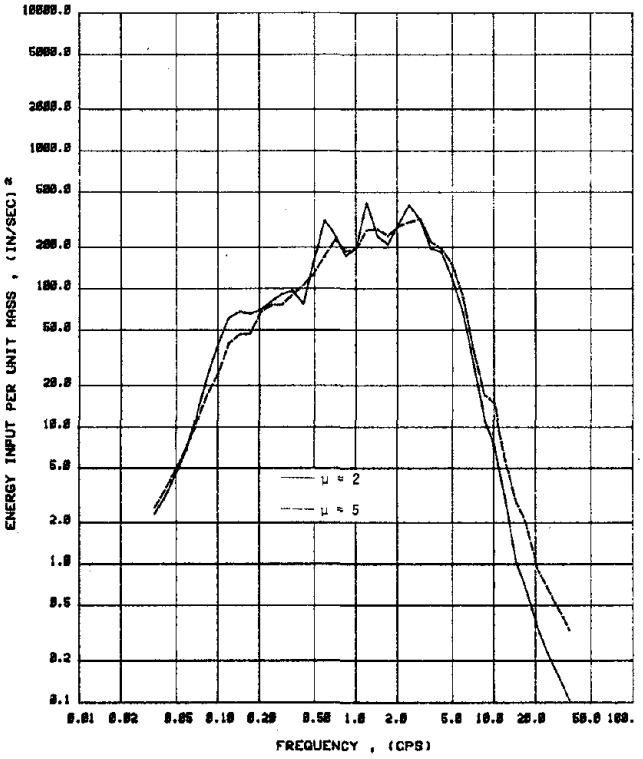

FIG. 4.36 ENERGY INPUT SPECTRA FOR ELASTOPLASTIC SYSTEMS WITH $\beta = 2\%$ AND $\mu = 2$ AND 5 WHEN SUBJECTED TO TAFT

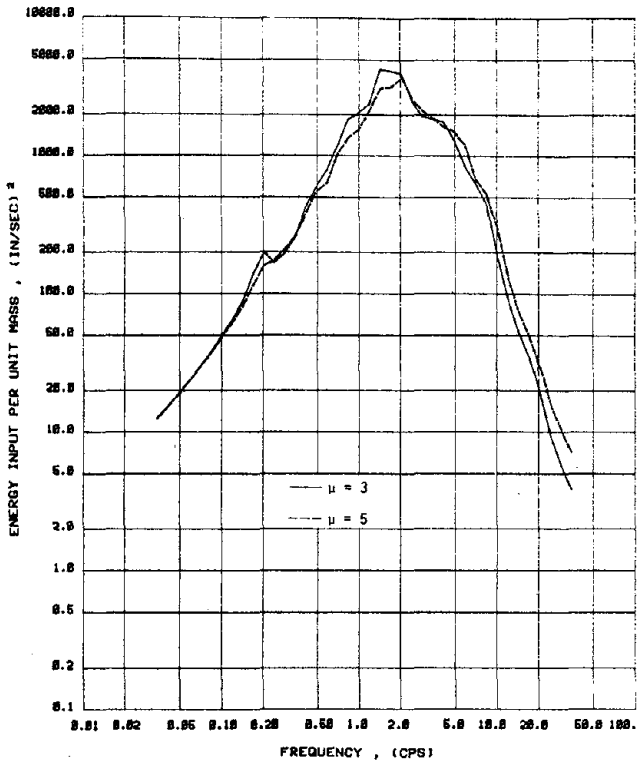

FIG. 4.37 ENERGY INPUT SPECTRA FOR ELASTOPLASTIC SYSTEMS WITH $\beta = 2\%$ AND $\mu = 3$ AND 5 WHEN SUBJECTED TO BONDS CORNER

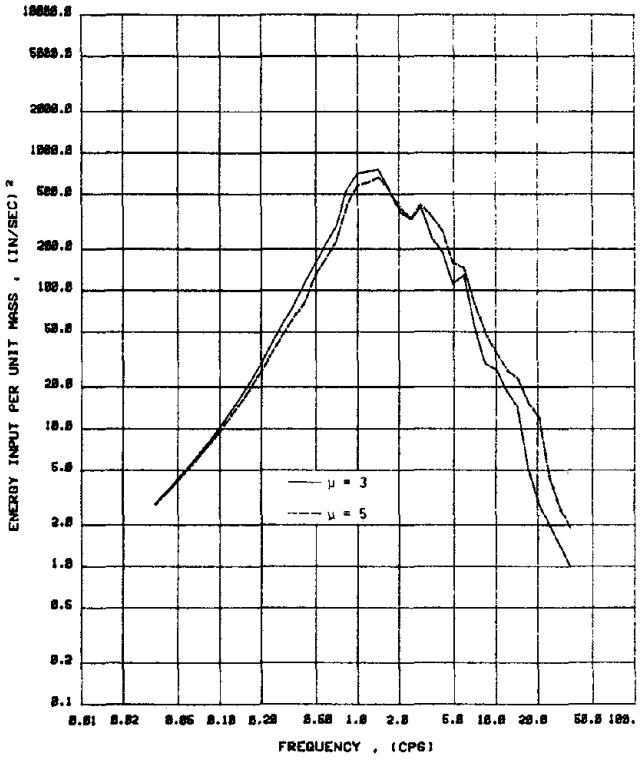

FIG. 4.38 ENERGY INPUT SPECTRA FOR ELASTOPLASTIC SYSTEMS WITH $\beta = 5\%$ AND $\mu = 3$ AND 5 WHEN SUBJECTED TO BONDS CORNER

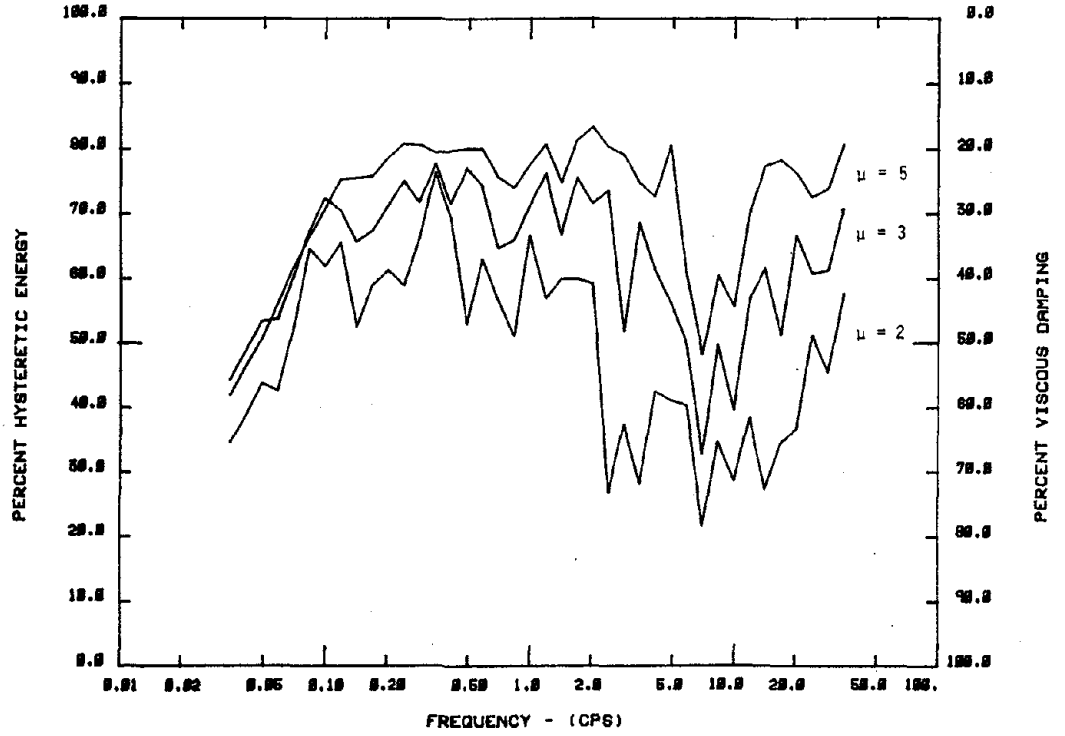

FIG. 4.39a PERCENT OF ENERGY INPUT DISSIPATED BY YIELDING AND DAMPING FOR ELASTOPLASTIC SYSTEMS WITH β = 2% AND μ = 2, 3, 5 WHEN SUBJECTED TO EL-CENTRO

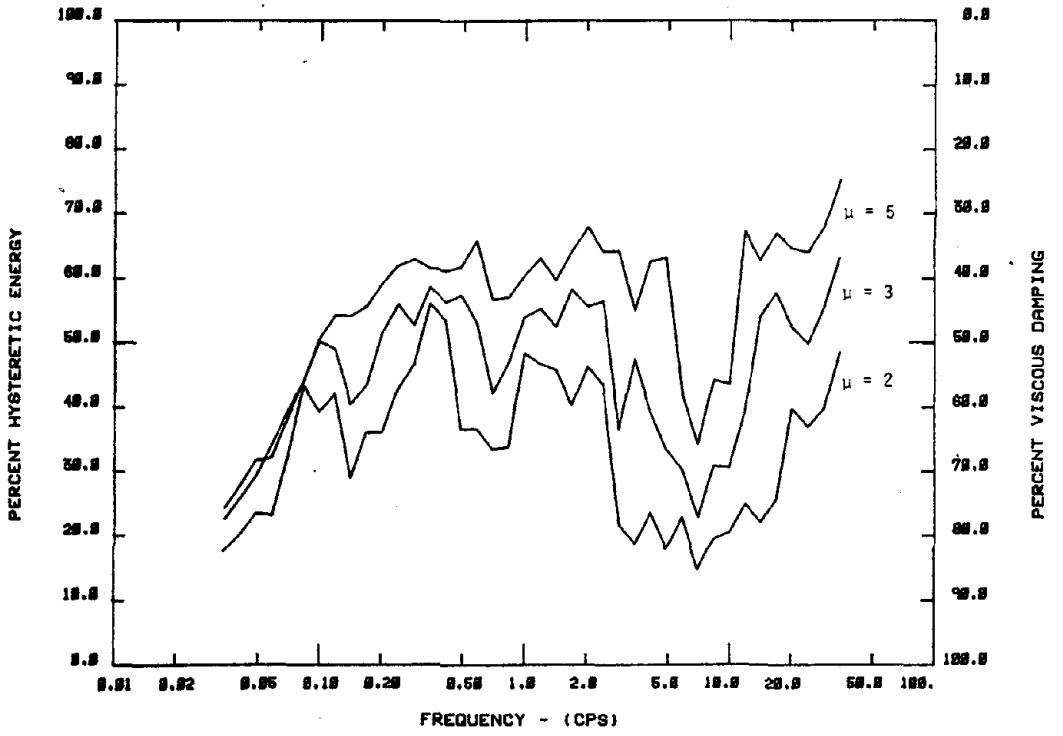

FIG. 4.39b PERCENT OF ENERGY INPUT DISSIPATED BY YIELDING AND DAMPING FOR ELASTOPLASTIC SYSTEMS WITH β = 5% AND μ = 2, 3, 5 WHEN SUBJECTED TO EL-CENTRO

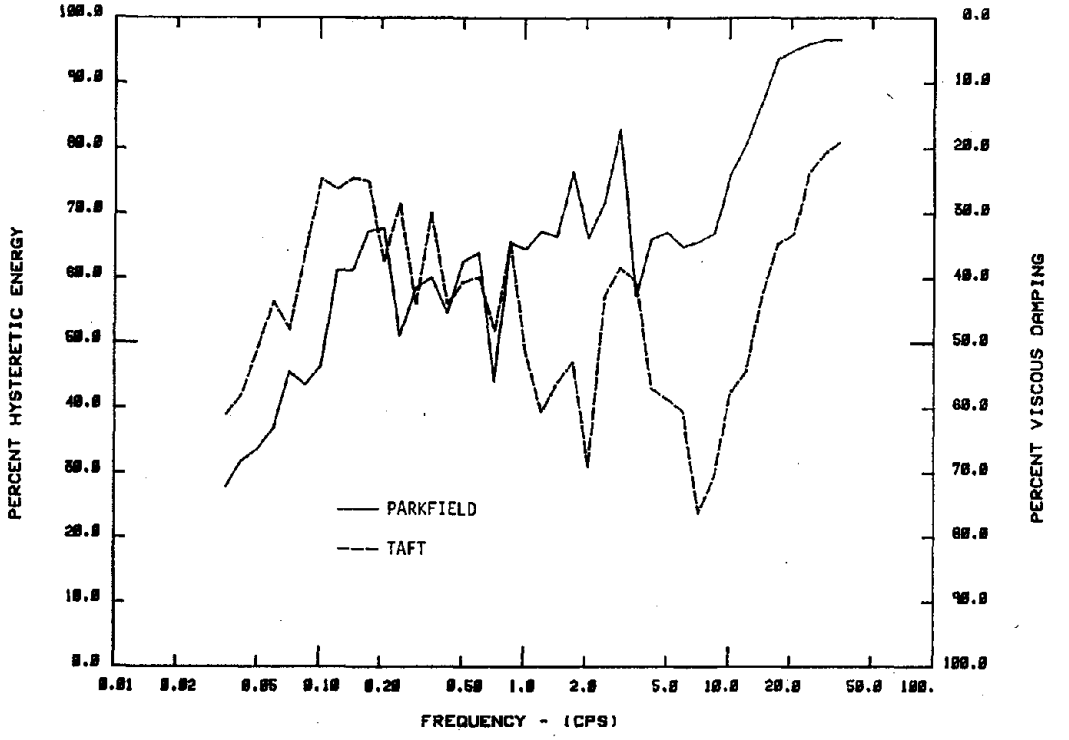

FIG. 4.40a PERCENT OF ENERGY INPUT DISSIPATED BY YIELDING AND DAMPING FOR ELASTOPLASTIC SYSTEMS WITH β = 2% AND μ = 2 WHEN SUBJECTED TO PARKFIELD AND TAFT, RESPECTIVELY

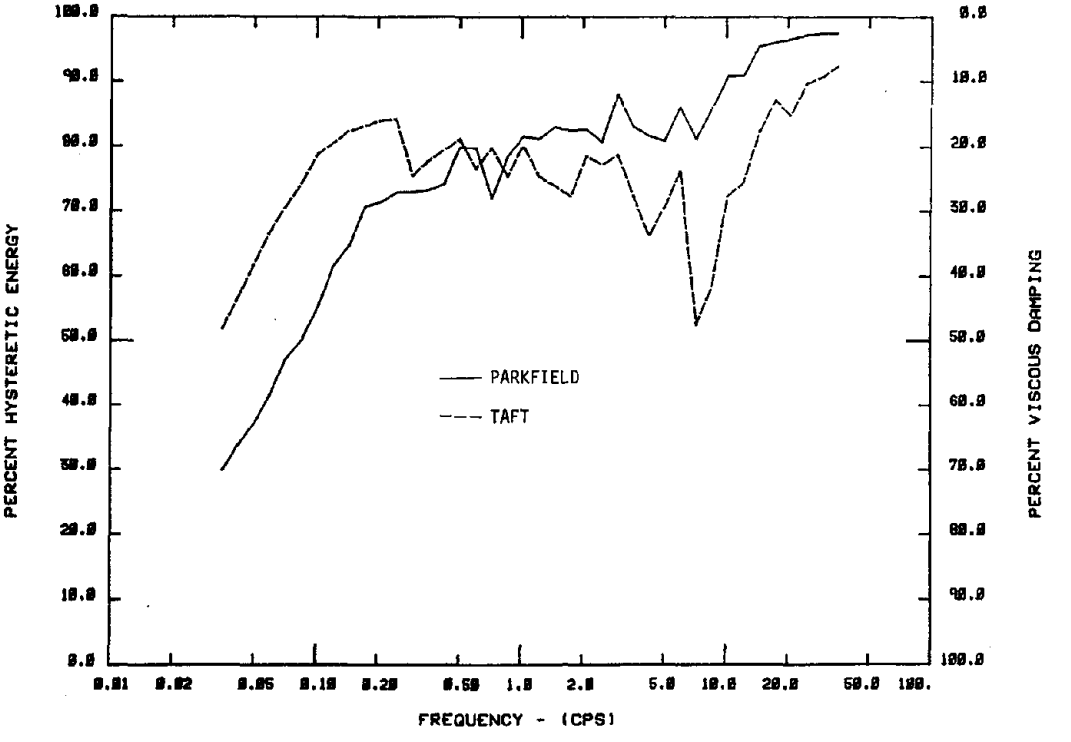

FIG. 4.40b PERCENT OF ENERGY INPUT DISSIPATED BY YIELDING AND DAMPING FOR ELASTOPLASTIC SYSTEMS WITH β = 2% AND μ = 5 WHEN SUBJECTED TO PARKFIELD AND TAFT, RESPECTIVELY

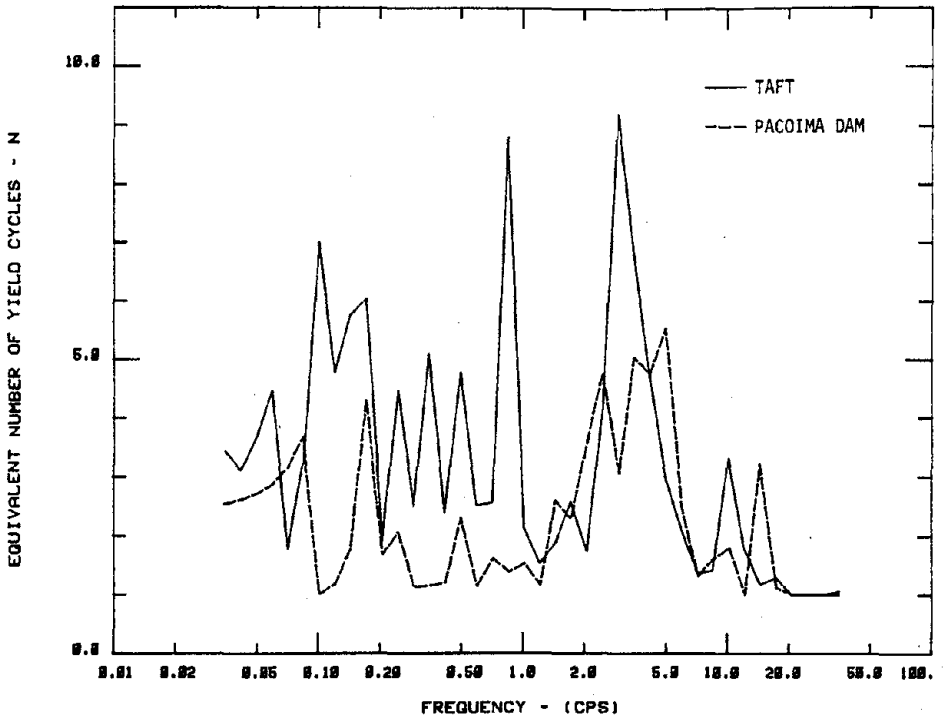

FIG. 4.45a COMPARISON OF EQUIVALENT NUMBER OF YIELD CYCLES FOR ELASTOPLASTIC SYSTEMS WITH $\beta = 2\%$ AND $\mu = 2$ WHEN SUBJECTED TO TAFT AND PACOIMA DAM, RESPECTIVELY

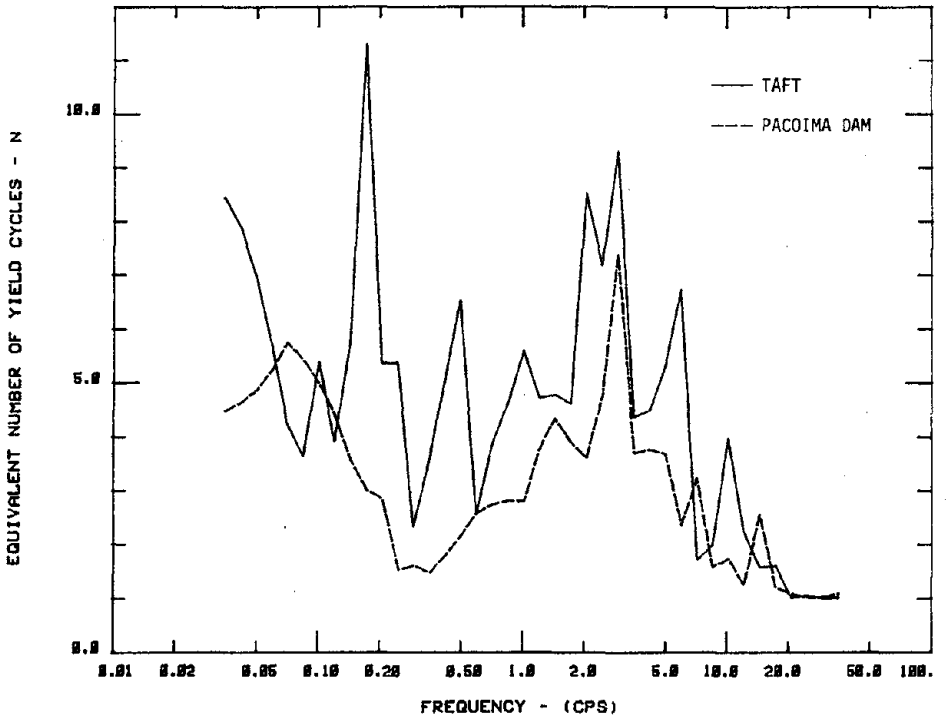

FIG. 4.45b COMPARISON OF EQUIVALENT NUMBER OF YIELD CYCLES FOR ELASTOPLASTIC SYSTEMS WITH $\beta = 2\%$ AND $\mu = 5$ WHEN SUBJECTED TO TAFT AND PACOIMA DAM. RESPECTIVELY

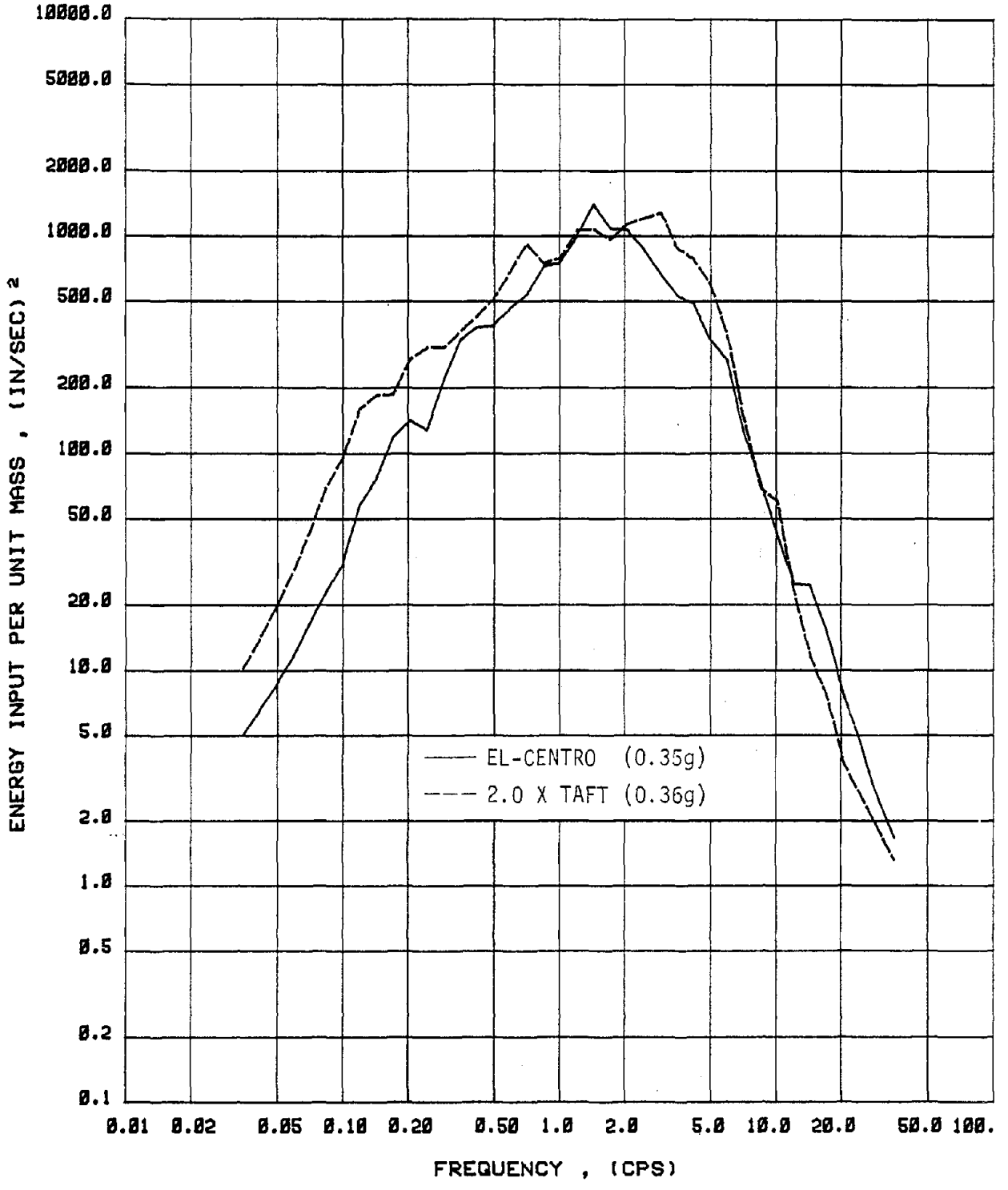

FIG. 4.46a COMPARISON OF ENERGY INPUT SPECTRA FOR ELASTOPLASTIC SYSTEMS WITH β = 2% AND μ = 5 WHEN SUBJECTED TO EL-CENTRO AND 2 X TAFT RECORDS, RESPECTIVELY

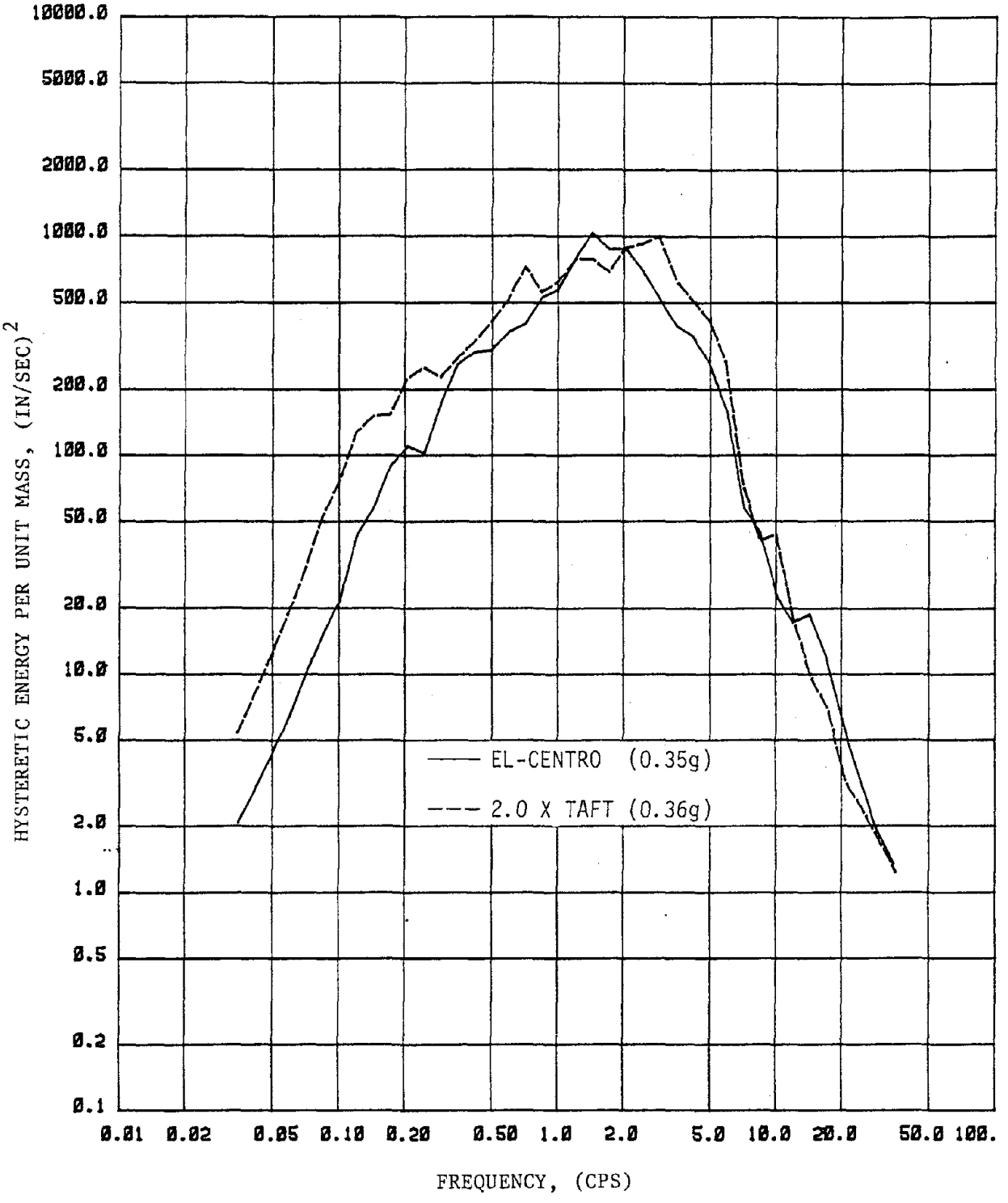

FIG. 4.46b COMPARISON OF HYSTERETIC ENERGY SPECTRA FOR ELASTOPLASTIC SYSTEMS WITH β = 2% AND μ = 5 WHEN SUBJECTED TO EL-CENTRO AND 2 X TAFT RECORDS, RESPECTIVELY

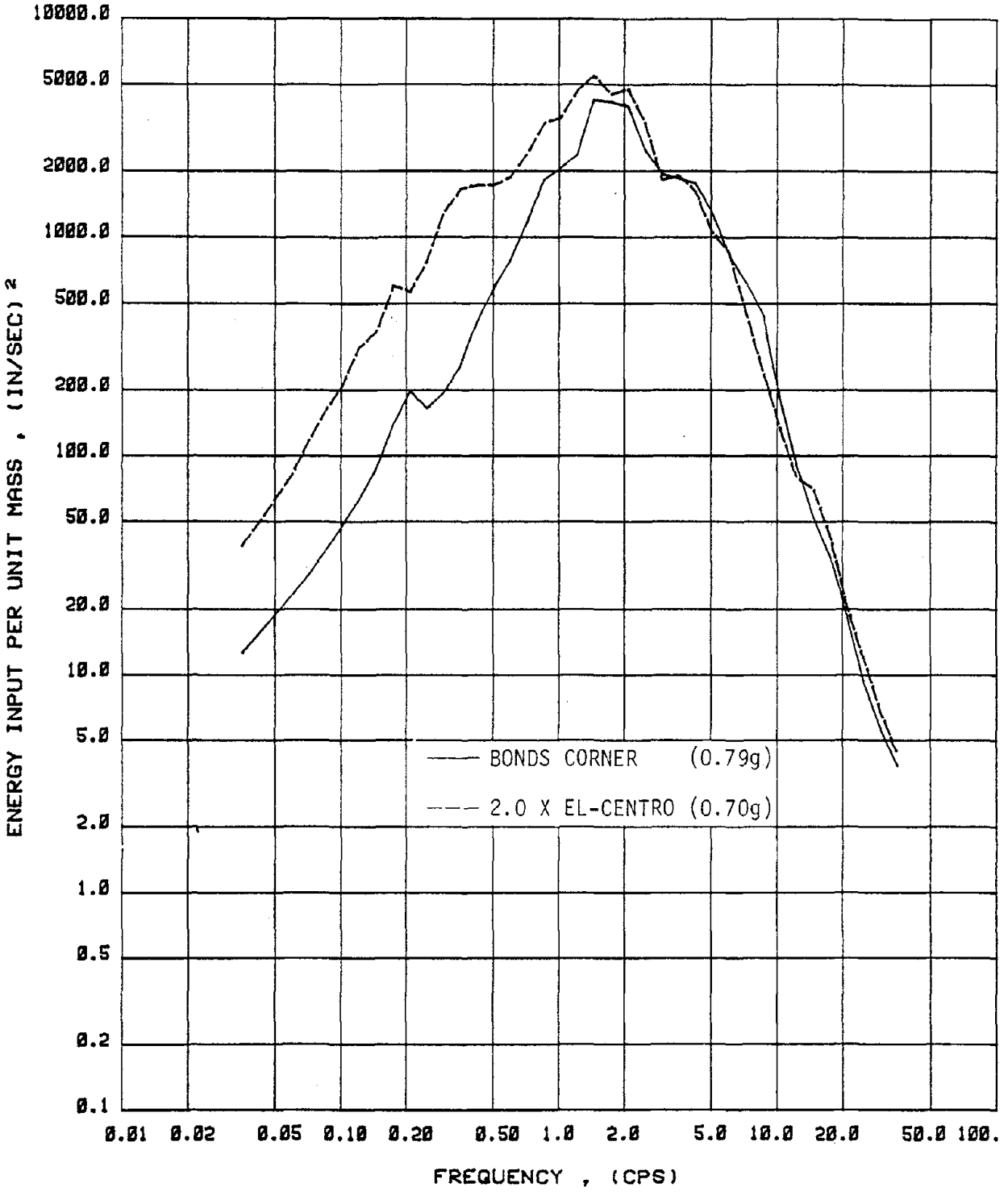

FIG. 4.47 COMPARISON OF ENERGY INPUT SPECTRA FOR ELASTOPLASTIC SYSTEMS WITH β = 5% AND μ = 3 WHEN SUBJECTED TO BONDS CORNER AND 2 X EL-CENTRO RECORDS, RESPECTIVELY

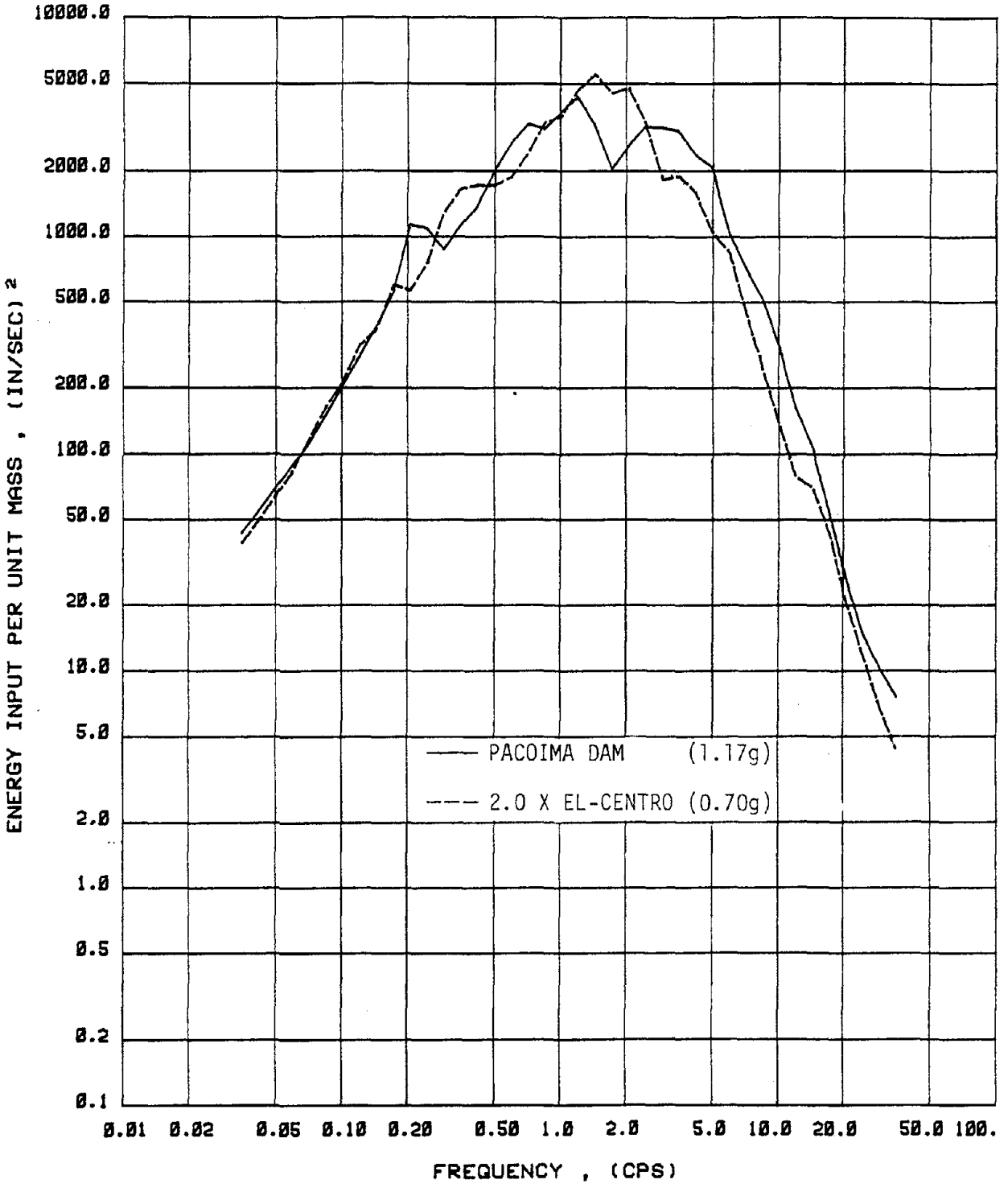

FIG. 4.48a COMPARISON OF ENERGY INPUT SPECTRA FOR ELASTOPLASTIC SYSTEMS WITH β = 5% AND μ = 3 WHEN SUBJECTED TO PACOIMA DAM AND 2 X EL-CENTRO RECORDS, RESPECTIVELY

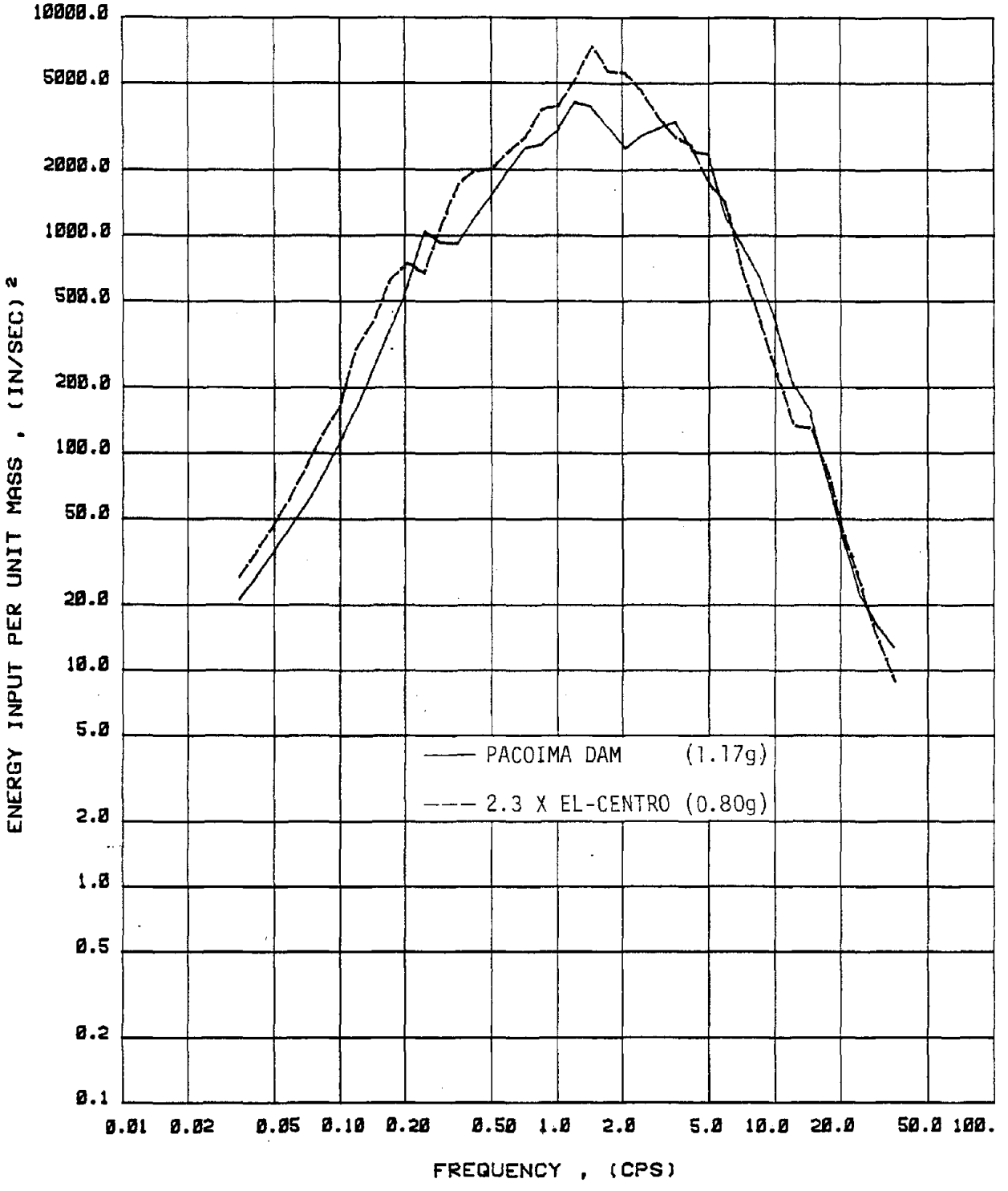

FIG. 4.48b COMPARISON OF ENERGY INPUT SPECTRA FOR ELASTOPLASTIC SYSTEMS WITH β = 5% AND μ = 5 WHEN SUBJECTED TO PACOIMA DAM AND 2.3 X EL-CENTRO RECORDS, RESPECTIVELY

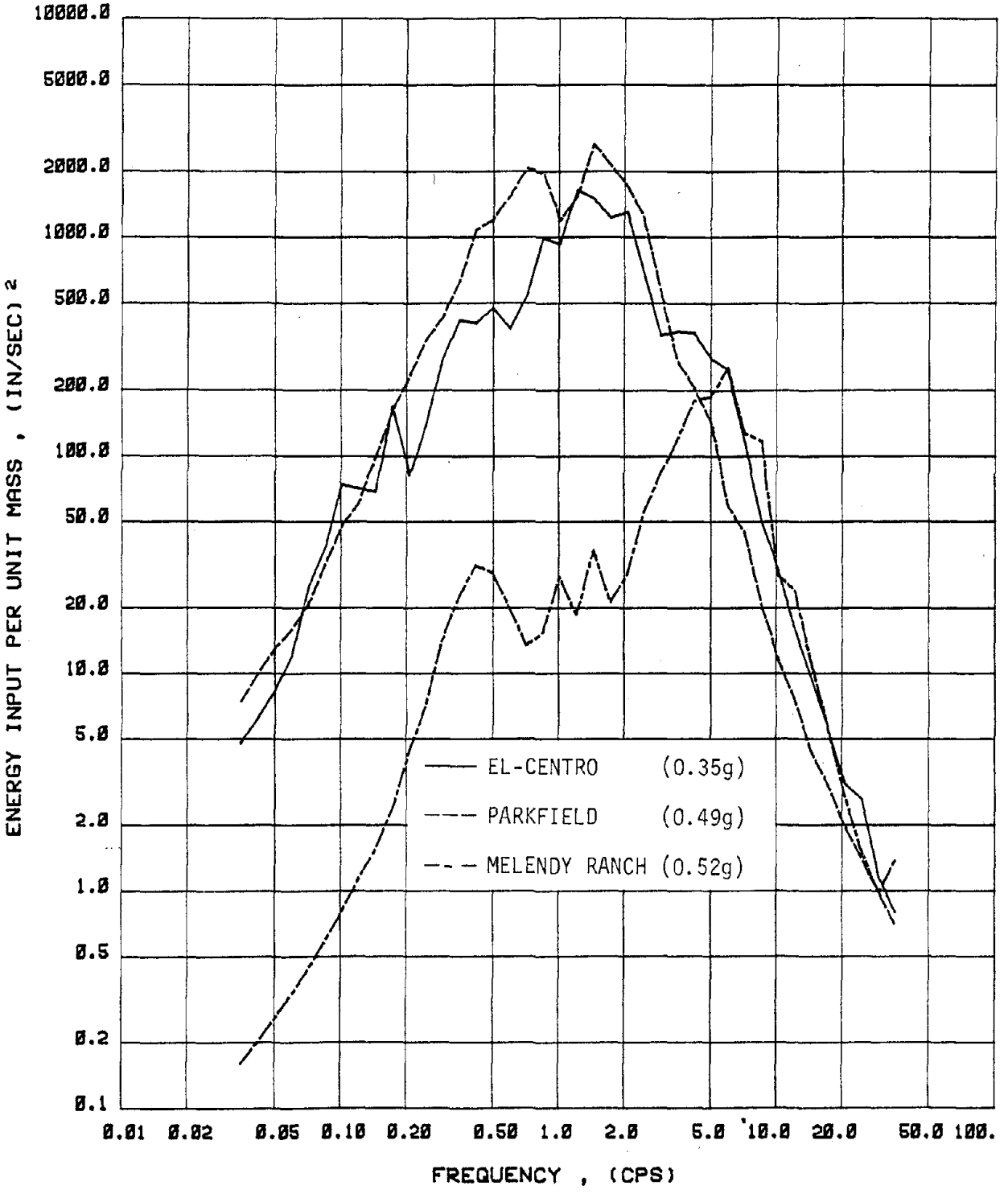

FIG. 4.49 COMPARISON OF ENERGY INPUT SPECTRA FOR ELASTOPLASTIC SYSTEMS WITH β = 2% AND μ = 2 WHEN SUBJECTED TO EL-CENTRO, PARKFIELD AND MELENDY RANCH RECORDS, RESPECTIVELY

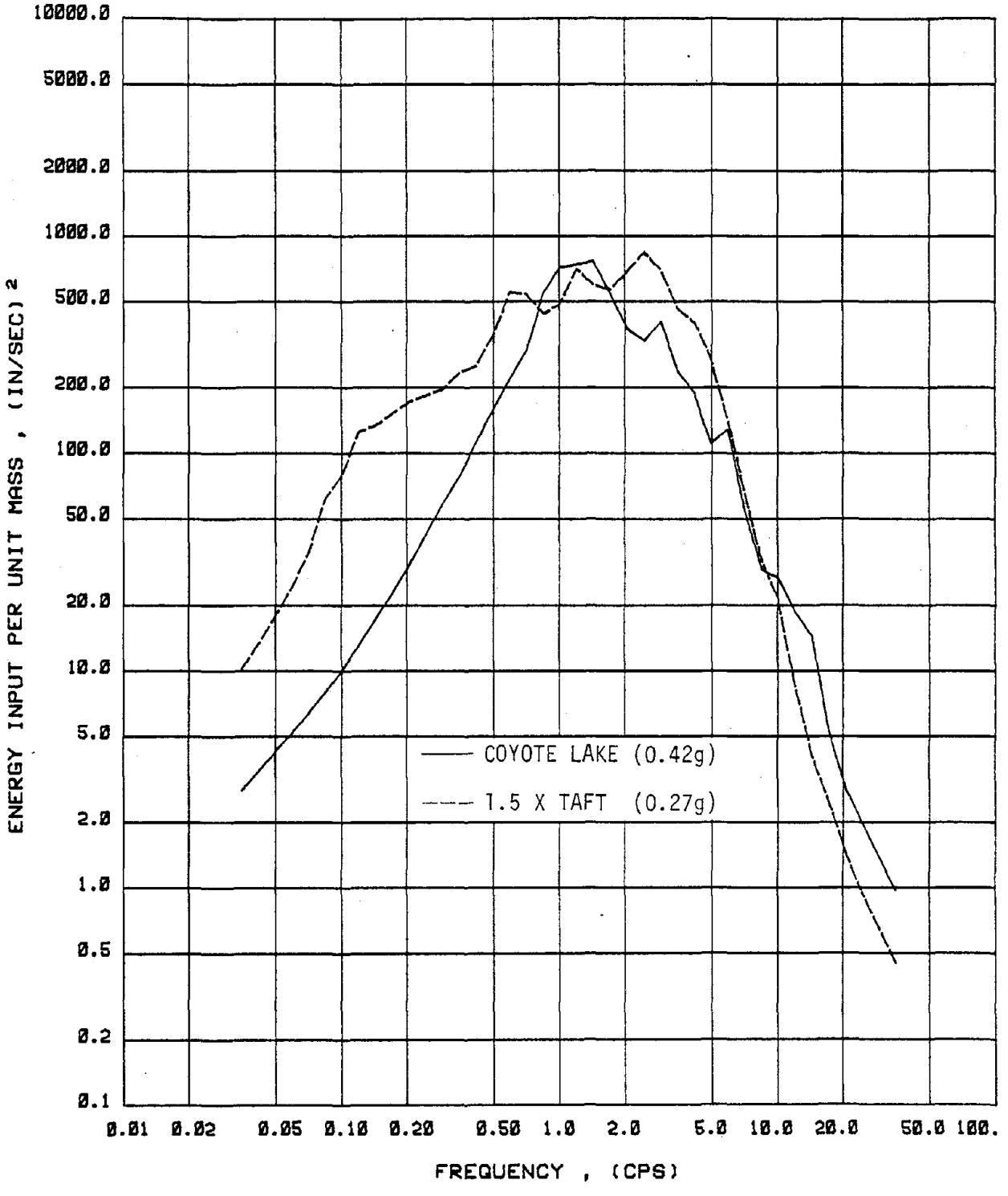

FIG. 4.50 COMPARISON OF ENERGY INPUT SPECTRA FOR ELASTOPLASTIC SYSTEMS WITH β = 5% AND μ = 3 WHEN SUBJECTED TO COYOTE LAKE AND 1.5 X TAFT RECORDS, RESPECTIVELY

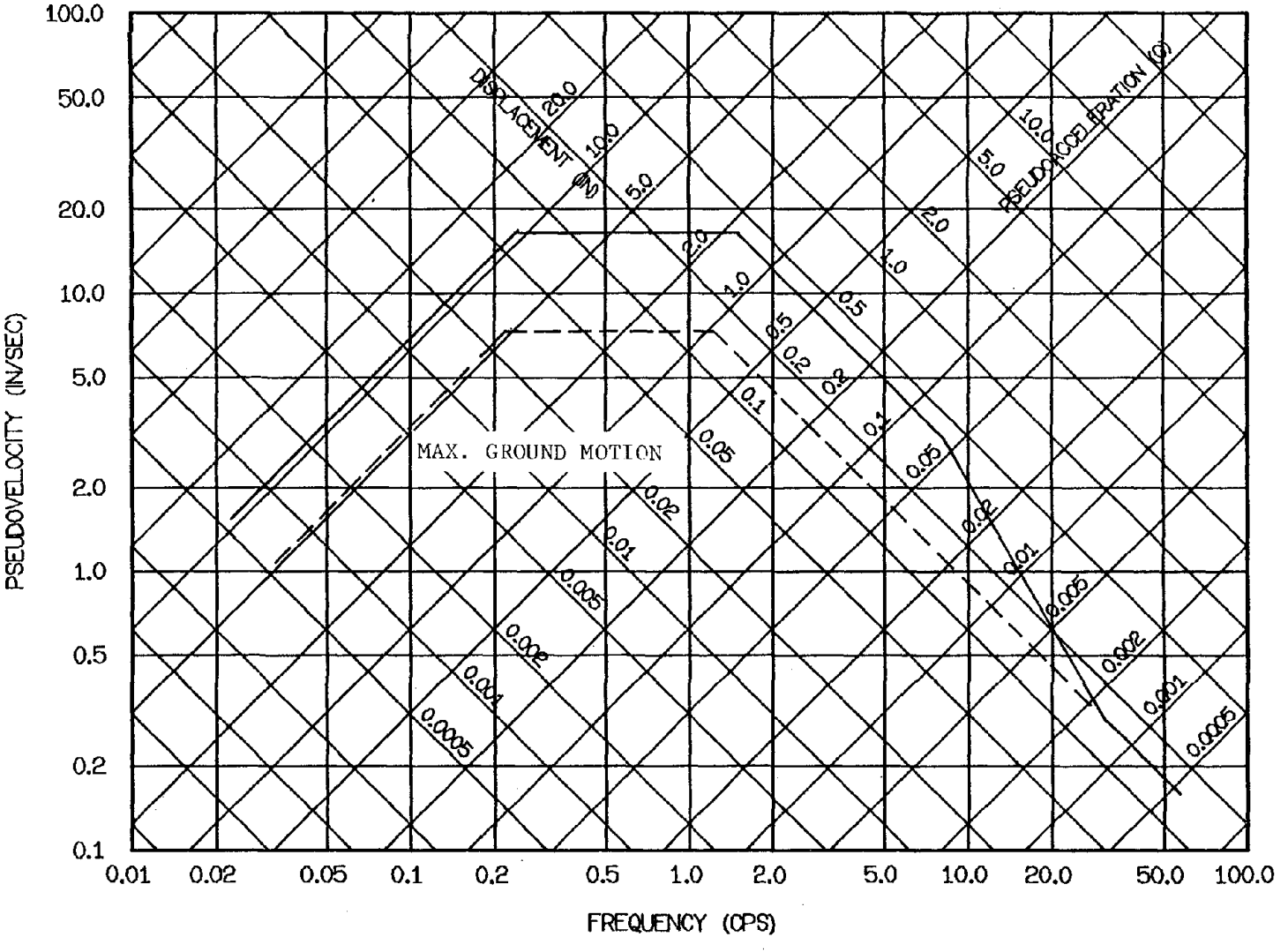

FIG. 5.1 ELASTIC RESPONSE SPECTRUM FOR SYSTEMS WITH 5% DAMPING AND ANCHORED TO 0.15g MAXIMUM ACCELERATION. AFTER NEWMARK AND HALL (41)

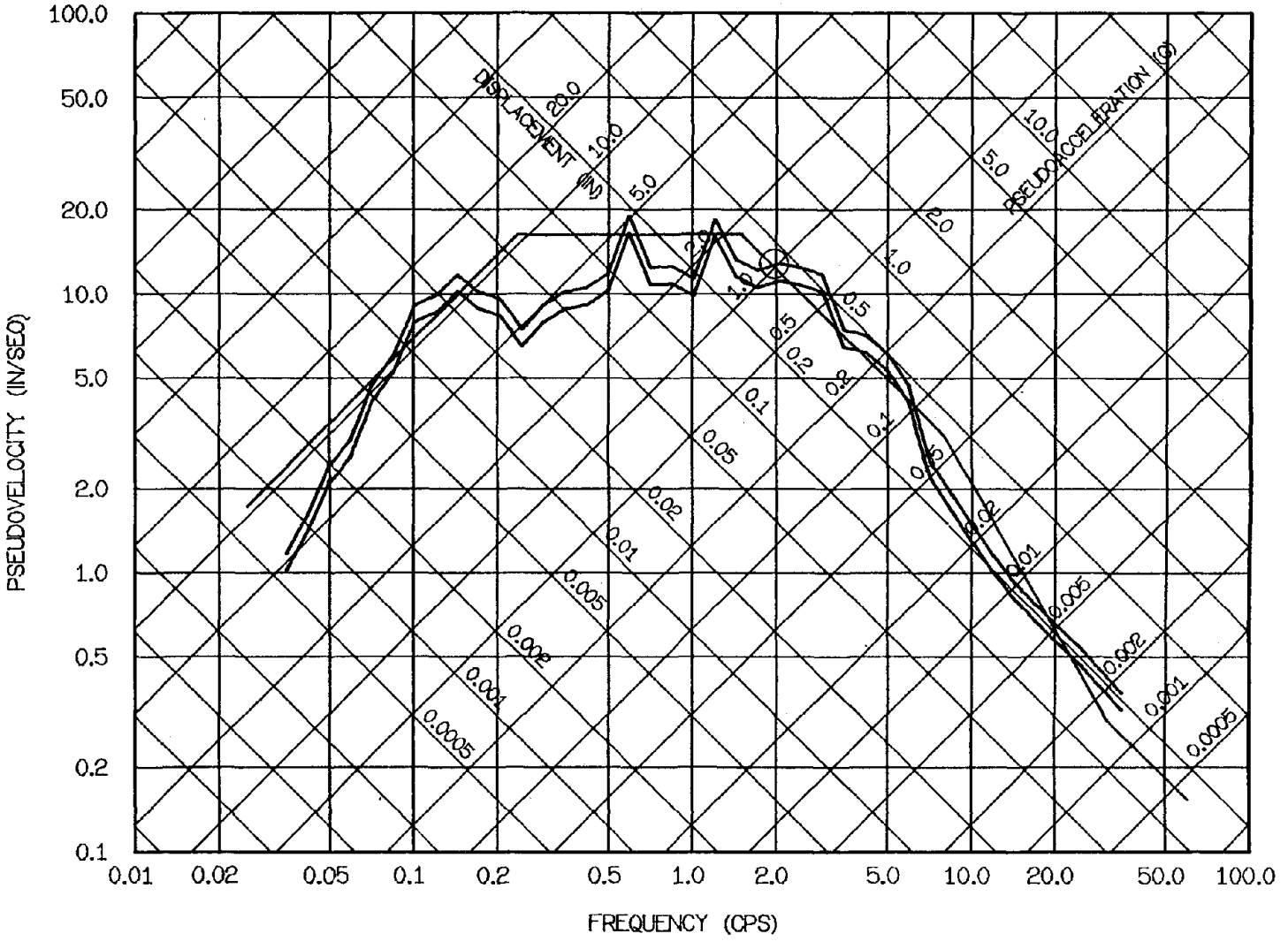

FIG. 5.2 ELASTIC RESPONSE SPECTRA FOR SYSTEMS WITH 5% DAMPING AND SUBJECTED TO TAFT AND 1.15 X TAFT

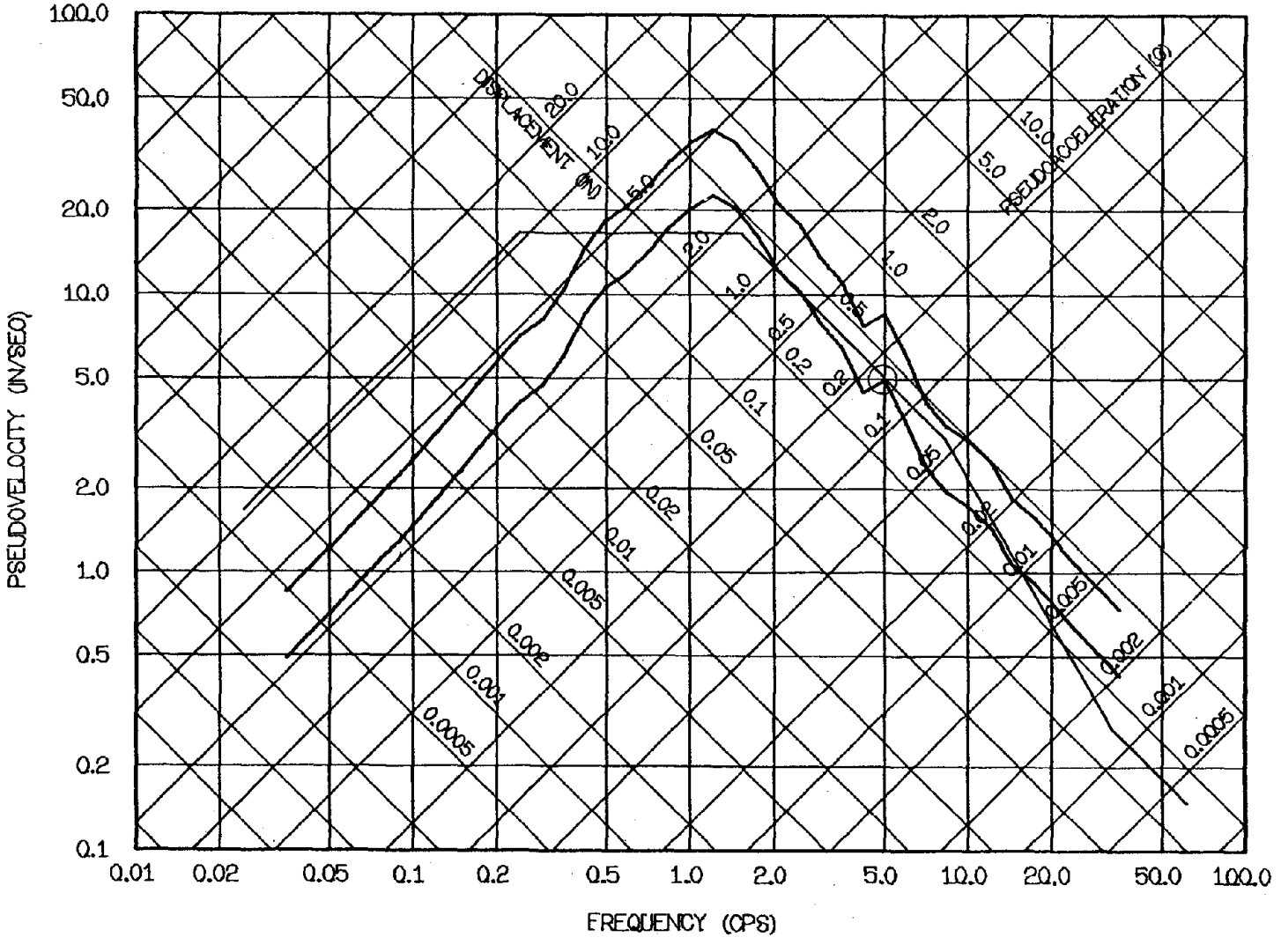

FIG. 5.3 ELASTIC RESPONSE SPECTRA FOR SYSTEMS WITH 5% DAMPING AND SUBJECTED TO COYOTE LAKE AND 0.58 X COYOTE LAKE

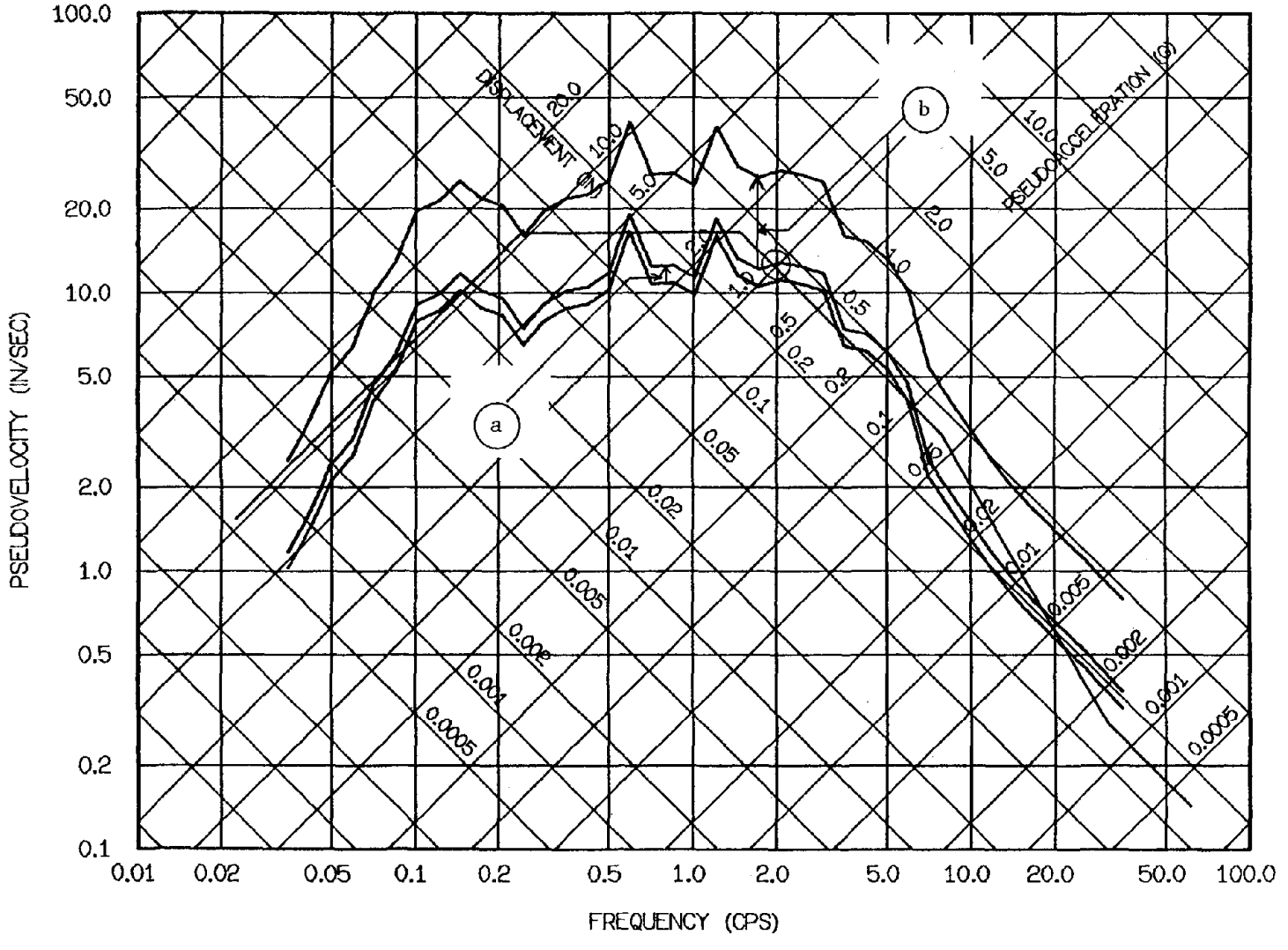

FIG. 5.4 ILLUSTRATION OF THE TWO MAIN STEPS (a) AND (b) OF SCALING TAFT RECORD AT A FREQUENCY EQUAL TO 2 CPS

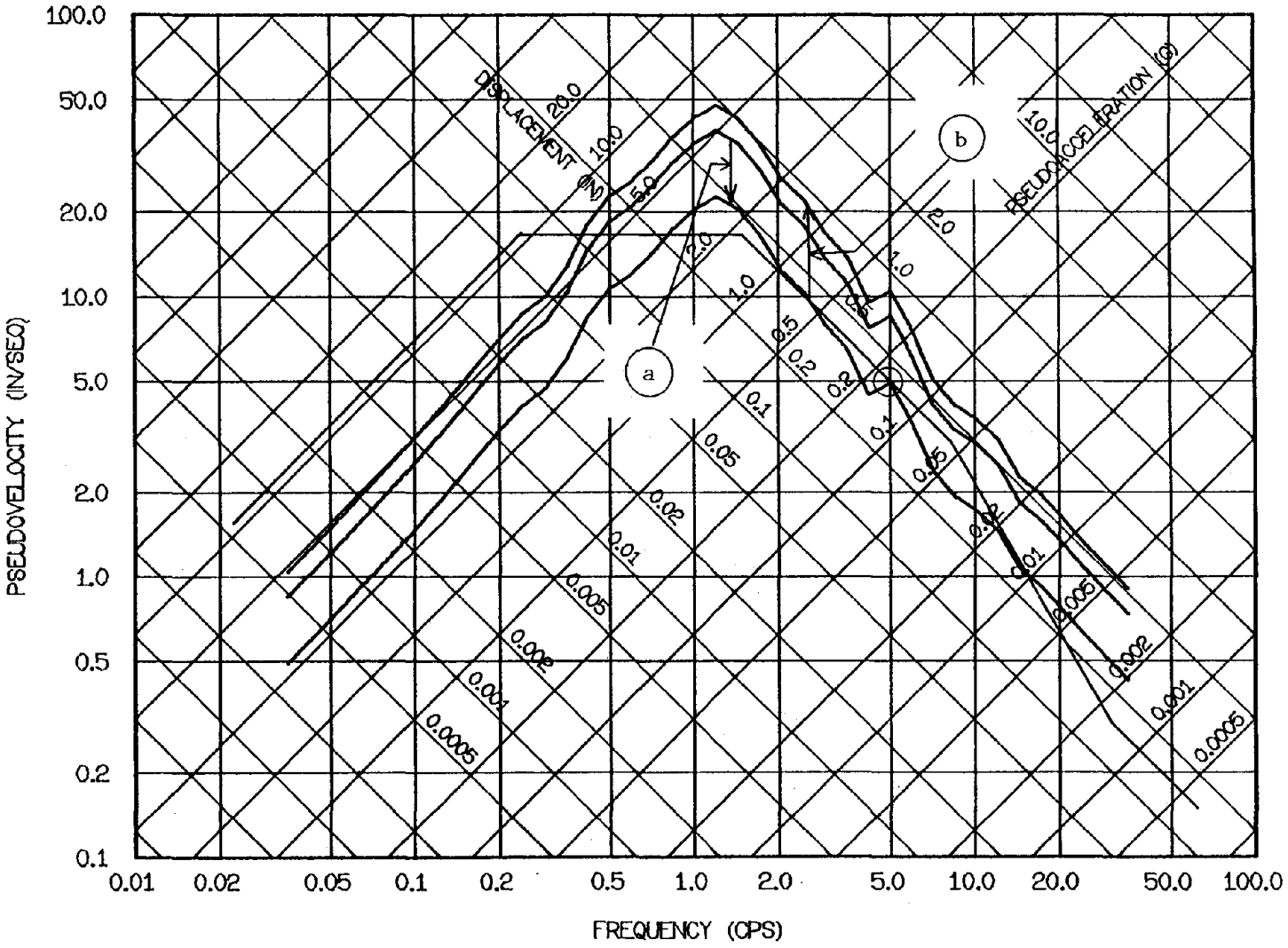

FIG. 5.5 ILLUSTRATION OF THE TWO MAIN STEPS (a) AND (b) OF SCALING COYOTE LAKE RECORD AT A FREQUENCY EQUAL TO 5 CPS

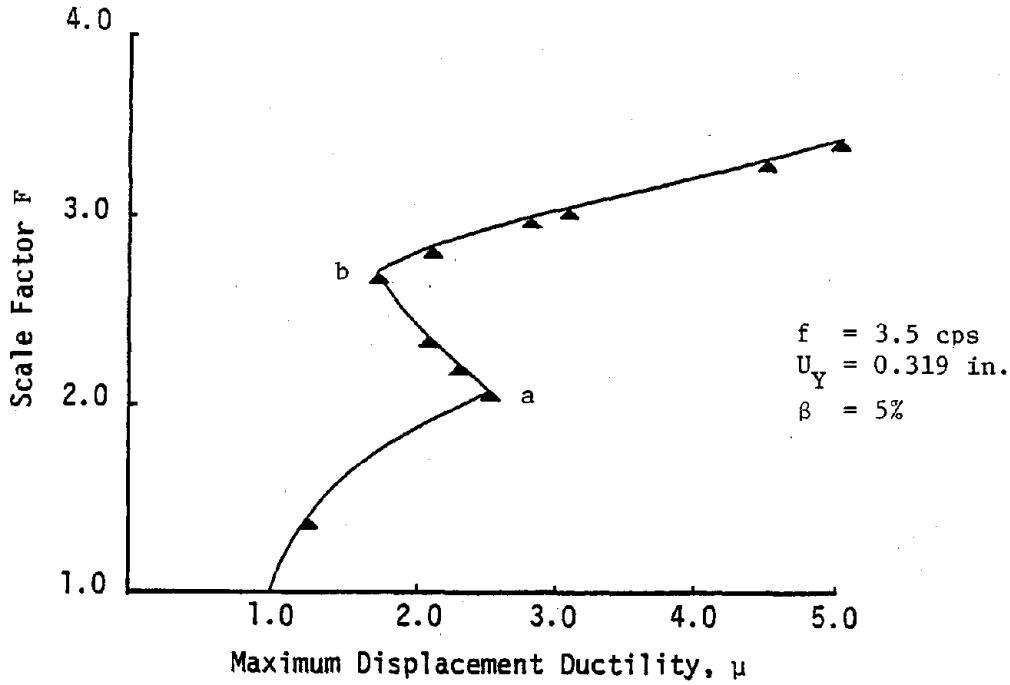

FIG. 5.6a SCALE FACTOR VS. DISPLACEMENT DUCTILITY FOR STRUCTURE SUBJECTED TO EL-CENTRO

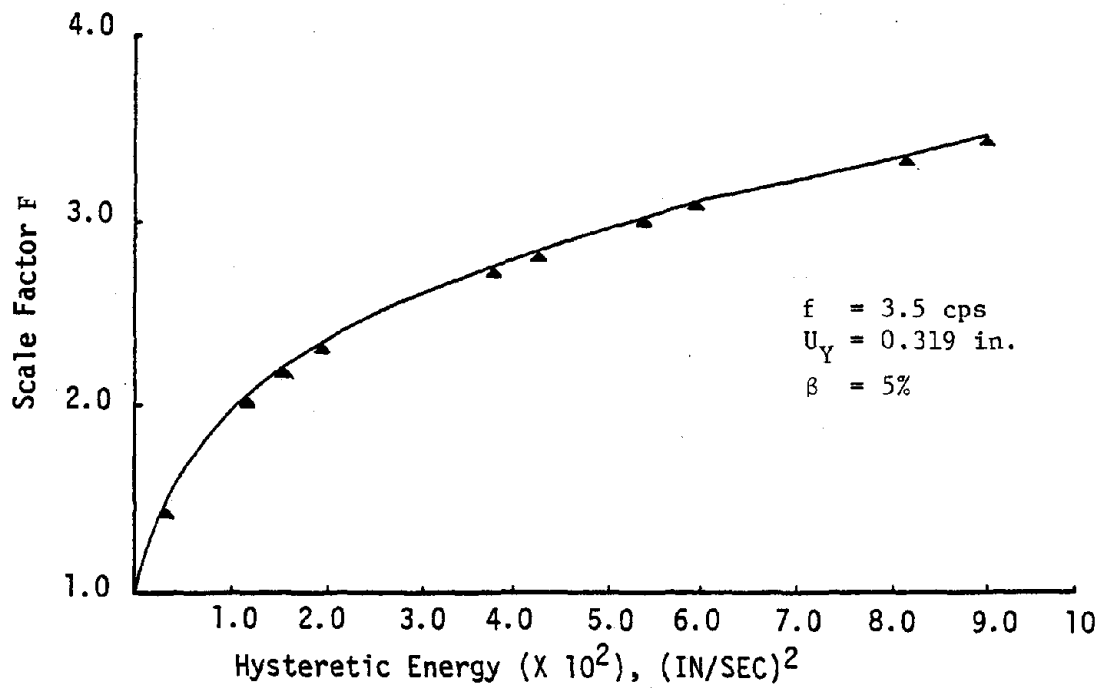

FIG. 5.6b SCALE FACTOR VS. HYSTERETIC ENERGY FOR STRUCTURE SUBJECTED TO EL-CENTRO

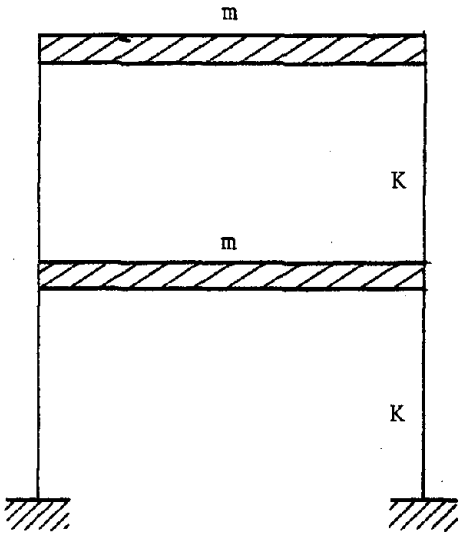

TYPE I

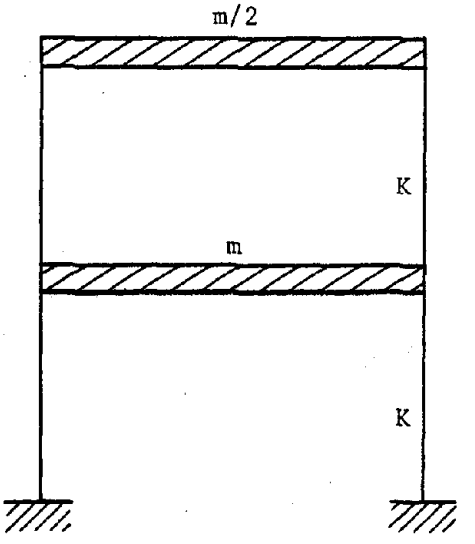

TYPE II

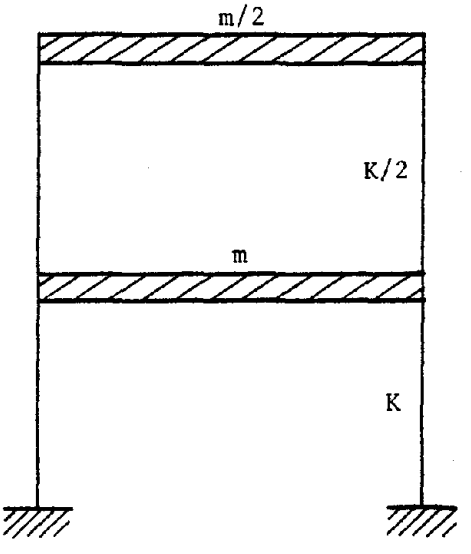

TYPE III

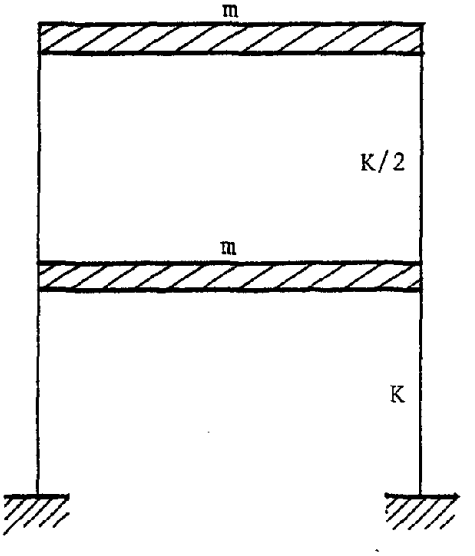

TYPE IV

FIG. 6.1 STRUCTURAL MODELS USED IN THE ANALYSIS

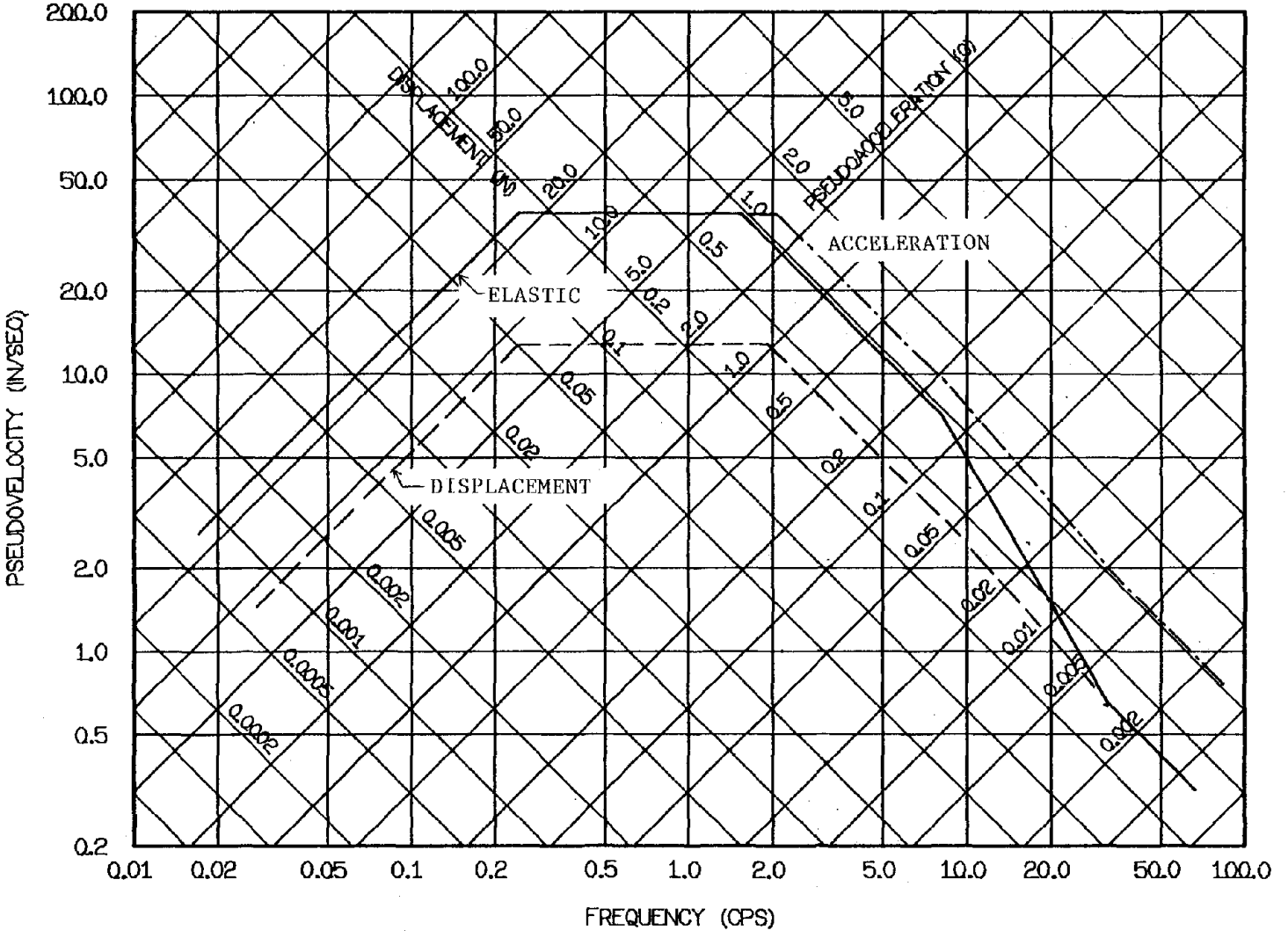

FIG. 6.2 DESIGN SPECTRA (ELASTIC AND INELASTIC FOR μ = 3) FOR SYSTEMS WITH 5% DAMPING AND ANCHORED TO 0.35g MAXIMUM ACCELERATION. AFTER NEWMARK AND HALL (41)

LIST OF REFERENCES

1. Aktan, A. E., Pecknold, D. A., and Sozen, M. A., "R/C Column Earthquake Response in Two-Dimensions," Journal of the Structural Division, ASCE, Vol. 100, No. ST10, Oct. 1974, pp. 1999-2015.

2. Almuti, A. M., and Hanson, R. D., "Static and Dynamic Cyclic Yielding of Steel Beams," Journal of the Structural Division, ASCE, Vol. 99, No. ST6, June 1973, pp. 1273-1285.

3. Applied Technology Council, Tentative Provisions for the Development of Seismic Regulations for Buildings, ATC 3-06, NSF Publication 78-8, June 1978.

4. Arias, A., "A Measure of Earthquake Intensity," Seismic Design for Nuclear Power Plants, R. Hansen, editor, MIT , Press, Cambridge, 1969.

5. Benfer, N. A., and Coffman, J. L., editors, San Fernando, California, Earthquake of February 9, 1971, U. S. Department of Commerce, National Oceanic and Atmospheric Administration, Washington, D.C., 1973.

6. Berg, G. V., "Inelastic Deformation in Earthquake Engineering," Proceedings of the 30th Annual Convention, Structural Engineers Association of California, Yosemite, California, Oct. 1963, pp. 30-40.

7. Berg, G. V., and Thomaides, S. S., "Energy Consumption by Sturctures in Strong-Motion Earthquakes," The University of Michigan Research Institute, Ann Arbor, Michigan, Mar. 1960.

8. Blume, J. A., "A Reserve Energy Technique for the Earthquake Design and Rating of Structures in the Inelastic Range," Proceedings of the Second World Conference on Earthquake Engineering, Tokyo and Kyoto, Japan, 1960, Vol. II, pp. 1061-1084.

9. Blume, J. A., Newmark, N. M., and Corning, L. H, Design of Multistory Reinforced Concrete Buildings for Earthquake Motions, Portland Cement Association, Skokie, Illinois, 1961.

10. Bolt, B. A., "State-of-the-Art for Assessing Earthquake Hazards in the United States, Report 17, Interpretation of Strong Ground Motion Records," U. S. Army Engineer Waterways Experiment Station, Vicksburg, Miss., Oct. 1981.

11. Brady, A. G., and Perez, V., "Seismic Engineering Data Report, 1972 Records, Strong-Motion Earthquake Accelerograms, Digitization and Analysis," Open File Report No. 78-941, U.S. Geological Survey, Menlo Park, California, Oct. 1978.

12. Brady, A. G., and Perez, V., "Seismic Engineering Data Report, 1974-75 Records, Strong-Motion Earthquake Accelerograms, Digitization and Analysis," Open File Report No. 79-929, U.S. Geological Survey, Menlo Park, California, May 1979.

13. Carpenter, L. D., and Lu, L.W., "Repeated and Reversed Load Tests on Full-Scale Steel Frames," Proceedings of the Fourth World Conference on Earthquake Engineering, Santiago, Chile, 1969, Vol. I, pp. B2, 125-136.

14. Chang, F. K., "State-of-the Art for Assessing Earthquake Hazards in the United States, Report 9, Catalogue of Strong Motion Earthquake Records, Volume 1, Western United States, 1933-1971," Misc. Paper S-73-1, U. S. Army Waterways Experiment Station Station, Vicksburg, Miss., Apr. 1978.

15. Cloud, W. K., "Intensity Map and Structural Damage, Parkfield, California, Earthquake of June 27, 1966," Bulletin of the Seismological Society of America, Vol. 57, No. 6, Dec. 1967, pp. 1161-1178.

16. Clough, R. W., and Penzien, J., Dynamics of Structures, McGraw-Hill Inc., New York, New York, 1975.

17. Earthquake Engineering Research Laboratory, "Strong Motion Earthquake Accelerograms, Index Volume," Report No. EERL 76-02, California Institute of Technology, Pasadena, California, Aug. 1976.

18. Ellsworth, W. L., "Bear Valley, California, Earthquake Sequence of February-March 1972," Bulletin of the Seismological Society of America, V. 65, No. 2, Apr. 1975, pp. 483-506.

19. Giberson, M. F., Two Nonlinear Beams with Definitions of Ductility," Journal of the Structural Division, ASCE, Vol. 95, No. ST2, Feb. 1969, pp. 137-157.

20. Goel, S. C., "Inelastic Behavior of Multistory Building Frames Subjected to Earthquake Motion," The University of Michigan, Ann Arbor, Michigan, Dec. 1967.

21. Goel, S. C., and Hanson, R. D., "Seismic Behavior of Multistory Braced Steel Frames," American Iron and Steel Institute, Steel Research for Construction, Bulletin No. 22, Apr. 1972.

22. Hart, G. C., et al., "Damping in Nuclear Reactors," Proceedings of the Fifth World Conference on Earthquake Engineering, Rome, Italy, June 1974, pp. 2029-2037.

23. Hart, G. C., and Vasudevan, R., "Earthquake Design of Building: Damping," Journal of the Structural Division, ASCE, Vol. 101, No. ST1, Jan. 1975, pp. 11-30.

24. Housner, G. W., "Limit Design of Structures to Resist Earthquakes," Proceedings of the First World Conference on Earthquake Engineering, California, U.S.A., 1956, pp. 5-1 to 5-13.

25. Housner, G. W., "Earthquake Research Needs for Nuclear Power Plants," Journal of the Power Division, ASCE, Vol. 97, No. PO1, Jan. 1971, pp. 77-91.

26. Housner, G. W., "Measures of Severity of Earthquake Ground Shaking," Proceedings of the U. S. National Conference on Earthquake Engineering, EERI, Ann Arbor, Michigan, June 1975, pp. 25-33.

27. Housner, G. W., and Jennings, P. C., "Generation of Artificial Earthquakes," Journal of the Engineering Mechanics Division, ASCE, Vol. 90, No. EM1, Feb. 1964, pp. 113-150.

28. Hudson, D. E., editor, "Strong-Motion Instrumental Data on the San Fernando Earthquake of Feb. 9, 1971," Earthquake Engineering Research Laboratory, California Institute of Technology and Seismological Field Survey, U. S. Department of Commerce, Sep. 1971.

29. Jennings, P. C., "Earthquake Response of a Yielding Structure," Journal of the Engineering Mechanics Division, ASCE, Vol. 90, No. EM4, Aug. 1965, pp. 41-68.

30. Kennedy, R. P., "Peak Acceleration as a Measure of Damage," presented at the Fourth International Seminar on Extreme-load Design of Nuclear Power Power Facilities, France, Aug. 1981.

31. Leeds, D. J., editor, Newsletter, Earthquake Engineering Research Institute, Vol. 13, No. 6, Nov. 1979.

32. Leeds, D. J., editor, "Reconnaissance Report, Imperial County, California, Earthquake, October 15, 1979," Earthquake Engineering Research Institute, Berkeley, California, Feb. 1980.

33. Maison, B. F., and Popov, E. P., "Cyclic Response Prediction for Braced Steel Frames," Journal of the Structural Division, ASCE, Vol. 106, No. ST7, July 1980, pp. 1401-1416.

34. McKevitt, W. E., Anderson, D. L., Nathan, N. D., and Cherry, S., "Towards a Simple Energy Method for Seismic Design of Structures," Proceedings of the Second U. S. National Conference on Earthquake Engineering, EERI, 1979, pp. 383-392.

35. Montgomery, C. J. and Hall, W. J., "Studies on the Seismic Design of Low-Rise Steel Buildings," Civil Engineering Studies, Structural Research Series No. 442, University of Illinois, Urbana, Illinois, July 1977.

36. Morris, L., Smookler, and Glover, D., "Catalog of Seismograms and Strong-Motion Records," Report SE-6, World Data Center A for Solid Earth Geophysics, NOAA, Boulder, Colorado, May 1977.

37. Nagahashi, S., "Effects of Ground Motion Duration upon Earthquake Response of Structure," Proceedings of the Seventh World Conference on Earthquake Engineering, Turkey, 1980, pp. 357-364.

38. Newmark, N. M., "A Method of Computation for Structural Dynamics," Transactions, ASCE, Vol. 127, 1962, pp. 1406-1435.

39. Newmark, N. M., "A Rationale for Development of Design Spectra for Diablo Canyon Reactor Facility," Report to the U. S. Nuclear Regulatory Commission, N. M. Newmark Consulting Services, 1211 Newmark Civil Engineering Laboratory, Urbana, Illinois, Sept. 1976.

40. Newmark, N. M., and Hall, W. J., "Vibration of Structures Induced by Ground Motion," Shock and Vibration Handbook, Second Edition, McGraw-Hill Inc., 1976, pp. 29-1 through 29-19.

41. Newmark, N. M., and Hall, W. J., "Development of Criteria for Seismic Review of Selected Nuclear Power Plants," U. S. Nuclear Regulatory Commission, Report NUREG-CR 0098, 1978.

42. Newmark, N. M., and Hall, W. J., Earthquake Spectra and Design, Earthquake Engineering Research Institute Monograph Series, Vol. 3, 1982, pp. 103.

43. Page, R. A., et al., "Ground Motion Values for Use in the Seismic Design of the Trans-Alaska Pipeline System," U. S. Geological Survey Circular 672, 1972.

44. Pecknold, D. A., and Riddell, R., "Effect of Initial Base Motion on Response Spectra," Journal of the Engineering Mechanics Division, ASCE, Vol. 104, No. EM2, Apr. 1978., pp. 485-491.

45. Penzien, J., "Elasto-Plastic Response of Idealized Multi-Story Structures Subjected to a Strong Motion Earthquake," Proceedings of the Second World Conference on Earthquake Engineering, Tokyo and Kyoto, Japan, 1960, Vol. II, pp. 739-760.

46. Person, W. J., "Seismological Notes-September-December 1979," Bulletin of the Seismological Society of America, Vol. 70, No. 6, Dec. 1980, pp. 2317-2325.

47. Popov, E. P., and Peterson, H., "Cyclic Metal Plasticity: Experiments and Theory," Journal of the Engineering Mechanics Division, ASCE, Vol. 104, No. EM6, Dec. 1978, pp. 1371-1388.

48. Popov, E. P., and Pinkney, R. B., "Cyclic Yield Reversal in Steel Building connections," Journal of the Structural Division, ASCE, Vol. 95, No. ST3, Mar. 1969, pp. 327-353.

49. Popov, E. P., and Stephen, R. M., "Cyclic Loading of Full-Size Steel Connections," Report EERC 70-3, University of California, Berkeley, California, July 1970.

50. Portillo, M., and Ang, A. H-S., "Evaluation of Safety of Reinforced Concrete Buildings to Earthquakes," Civil Engineering Studies, Structural Research Series No. 433, University of Illinois, Urbana, Illinois, Oct. 1976.

51. Riddell, R., and Newmark, N. M., "Statistical Analysis of the Response of Nonlinear Systems Subjected to Earthquake," Civil Engineering Studies, Structural Research Series No. 468, University of Illinois, Urbana, Illinois, Aug. 1979.

52. Roeder, C. W., and Popov, E. P., "Eccentrically Braced Steel Frames for Earthquakes," Journal of the Structural Division, ASCE, Vol. 104, No. ST3, Mar. 1978, pp. 391-412.

53. Shannon and Wilson, Inc., and Agbabian Associates, "Geotechnical and Strong-Motion Earthquake Data from U. S. Accelerograph Stations," prepared for U.S. Nuclear Regulatory Commission, June 1978.

54. Structural Mechanics Associates, "Engineering Characterization of Ground Motion: Free-Field Motion," prepared for Woodward-Clyde Consultants for a research project sponsored by the U. S. Nuclear Regulatory Commission, SMA 12702.01, Feb. 1982.

55. Takeda, T., Sozen, M. A., and Nielsen, N. N., "Reinforced Concrete Response to Simulated Earthquakes," Journal of the Structural Division, ASCE, Vol. 96, No. ST12, Dec. 1970, pp. 2557-2573.

56. Timoshenko, S., Young, D. H., and Weaver, W., Vibration Problems in Engineering, Fourth Edition, John Wiley β Sons Inc., New York, New York, 1974.

57. Trifunac, M. D., and Brady, A. G., "On the Correlation of Seismic Intensity Scales with the Peaks of Recorded Strong Ground Motion," Bulletin of the Seismological Society of America, Vol. 65, No. 1, 1975, pp. 139-162.

58. U. S. Coast and Geodetic Survey, U. S. Department of Commerce, United States Earthquakes, issues corresponding to the years 1936 to 1940, 1952, 1966, 1972 and 1974, U. S. Government Printing Office, Washington, D. C.

59. U. S. Geological Survey, "Compilation of Strong-Motion Records from the August 6, 1979 Coyote Lake Earthquake," Open File Report No. 79-385, Menlo Park, California, Oct. 1979.

60. U. S. Geological Survey, "Stong-Motion Accelerograph Station List-1980," Open File Report No. 81-664, Menlo Park, California, Jan. 1981.

61. Uniform Building Code 1979 Edition, International Conference of Building Officials, Whittier, California.

62. Veletsos, A. S., and Newmark, N. M., "Effect of Inelastic Behavior on the Response of Simple Systems to Earthquake Motions," Proceedings of the Second World Conference on Earthquake Engineering, Tokyo and Kyoto, Japan, 1960, Vol. II, pp. 895-912.

63. Veletsos, A. S., and Vann, W. P., "Response of Ground Excited Elastoplastic Systems," Journal of the Structural Mechanics Division, ASCE, Vol. 97, No. ST4, 1971, pp. 1257-1281.

64. Wakabayaski, M., et al., "Hysteretic Behavior of Steel Braces Subjected to Horizontal Load due to Earthquakes," Proceedings of the Sixth World Conference on Earthquake Engineering, New Delhi, India, Jan. 1977, Vol. III, pp. 3188-3193.

65. Workman, G. H., "The Inelastic Behavior of Multistory Braced Frame Structures Subjected to Earthquake Excitation," University of Michigan, Ann Arbor, Michigan, 1969.

66. Zienkiewicz, O. C., The Finite ELement Method, Third Edition, McGraw-Hill Inc., London, England, 1977.